Molecular Characterization of Induced Systemic Tolerance by PGPR in Wheat (*Triticum aestivum* L.) under Drought Stress

THESIS

Submitted in partial fulfillment of the requirements for the degree of

DOCTOR OF PHILOSOPHY

by

SAUMYA ARORA

Under the Supervision of

Prof. Prabhat Nath Jha

BIRLA INSTITUTE OF TECHNOLOGY AND SCIENCE

PILANI, RAJASTHAN- 333031

INDIA

2024

BIRLA INSTITUTE OF TECHNOLOGY AND SCIENCE

PILANI, RAJASTHAN, INDIA

CERTIFICATE

This is to certify that the thesis entitled "**Molecular Characterization of Induced Systemic Tolerance by PGPR in Wheat (*Triticum aestivum* L.) under Drought Stress"** submitted by **Ms. Saumya Arora**, ID No. **2017PHXF0439P** for the award of Ph.D. Degree of the Institute, embodies original work done by her under my supervision.

Signature in full of the Supervisor

Name: **PRABHAT NATH JHA**

Designation: Professor

Date:

॥ वक्रतुंड महाकाय
सूर्यकोटिसमप्रभ
निर्विघ्नं कुरुमेदव
सर्वकार्येषुसर्वदा ॥

Acknowledgement

This thesis consumed huge amount of work, research, and dedication. Still, implementation would not be possible without the guidance and support of many individuals who, in one way or another, contributed and extended their valuable assistance in the preparation and completion of this study; it is a pleasure to extend my sincere gratitude to all of them.

I am indebted to my supervisor, Prof. Prabhat Nath Jha, whose guidance, support, and expertise have enabled me to complete my Ph.D. His continuous support, patience, motivation, valuable comments, suggestions, and immense knowledge and advice made this research meaningful. I could not have imagined having a better advisor and mentor for my Doctorate study. His untiring efforts to guide me at every step and to sort out my difficulties throughout my research period are of great value.

I would like to express my deepest gratitude to our collaborator, Dr. Piyoosh Babele, Rani Lakshmi Bai Central Agricultural University, Jhansi, for his careful and precious guidance during my research work.

I also could not have undertaken this journey without my Doctoral Advisory committee members, Prof. Jitendra Panwar and Prof. Pankaj Sharma, Department of Biological Sciences, BITS Pilani, who generously provided knowledge, expertise, constructive feedback, and valuable comments and suggestions in developing this research. I must also acknowledge all the faculty members of the Department of Biological Sciences, BITS Pilani, for their support and direction. I thank all the non-teaching staff for assisting me with department-related issues.

I sincerely thank Vice Chancellor Prof. V Ramgopal Rao and Director Prof. Sudhir Kumar Barai of BITS Pilani, Pilani campus, Prof. Rajdeep Chowdhary, HOD, Department of Biological Sciences for providing laboratory facilities for conducting my research.

I would like to extend my sincere thanks to DST-INSPIRE, the government of India, for providing a research fellowship. I would also like to thank AIRF-JNU (Advanced Instrumental Research Facility- Jawahar Lal Nehru University), New Delhi and Proteomics Characterization Facility, C-CAMP (Centre for Cellular and Molecular Platforms), Bengaluru for processing and analysing of my research samples to generate the valuable data. I'd like to acknowledge Indian Institute of Wheat and Barley Research, Karnal for providing wheat variety for my research work.

I am also grateful to my seniors: Dr Monika Jangir, Dr Vidushi, Dr Shradha, Dr Vikram, Dr Poonam, Dr Sandeep, Dr Monica Sandhu, Dr Shahid, and Dr Tripti and juniors: Simran, Shobham, Garima, Sumit, Tripti Joshi, Sonakshi, Mamta, Ankita Das, Shreya, and Sonali for their cooperation and help during my study. I duly acknowledge my friends Aastha, Nidhi, Harshita, Nandita, Abhilasha, Sonia, and Sumukh, who inspired me to put in my best efforts for the research study. I especially want to thank Aastha and Nidhi who have made my doctoral experience a wonderful experience.

Lastly, I would be remiss in not mentioning my family, especially my parents, spouse, and my daughter for their endless support. Their belief in me has kept my spirits and motivation high during this process. I thank them for their patience and understanding they have shown me, particularly during the last few months while I was writing up.

Finally, I would like to thank God, for letting me through all the difficulties, and for providing me the grace and privilege to successfully completing the Doctorate program.

Sincerely,

Saumya Arora

Abstract

Introduction: Plant growth and productivity are highly affected by several abiotic stress like drought. Drought alone causes more annual loss in crop yield than the sum of all other environmental stressors. Some plant growth-promoting rhizobacteria (PGPR) can ameliorate drought stress and promote plant growth. PGPR contribute to plant growth through various direct and indirect mechanisms, including nitrogen fixation, synthesizing phytohormones, and solubilizing mineral nutrients, and can ameliorate abiotic stressors by inducing systemic tolerance in the host plant. IST is induced by PGPR-derived elicitors such as phytohormones, volatile organic compounds (VOCs), enzymes such as ACC deaminase, antioxidants, and exopolysaccharides. Although the role of PGPR in ameliorating drought stress has been demonstrated in earlier work, the application of these bacteria at the field level still needs the exploration of efficient inoculants and optimization of appropriate formulation to attain optimal growth under drought conditions. Despite several reports of drought-tolerant bacteria, there is a lack of information about the efficient bacteria recovered from the Shekhawati region of Rajasthan (India). With an annual rainfall of just about 600 mm, high summer temperatures, and sandy soils, agriculture in the Shekhawati region suffers from severe water scarcity. Therefore, we hypothesised that the bacteria recovered from the Shekhawati region might have the ability to survive under less water availability. Therefore, the present work aimed to characterize the efficient drought-tolerant bacteria from the rhizosphere of wheat plants growing in Rajasthan, India, and characterize their effect on plant growth under drought stress through functional studies following transcriptomic, proteomic, and metabolomic analysis. Moreover, there is growing interest in harnessing the potential of stress-resilient PGPR in conferring plant resistance and enhancing crop productivity in drought-affected agroecosystems. A detailed understanding of the complex physiological and biochemical responses will open the avenues to stress adaptation mechanisms of PGPR communities under drought. It will pave the way for rhizosphere engineering through metabolically engineered PGPR. Therefore, to reveal the physiological and metabolic networks in response to drought-mediated osmotic stress, the current study focused on investigating the stress adaptation mechanisms of a selected PGPR. Major objectives of the present study were: (i) isolation of drought-tolerant bacteria and their characterization for plant growth-promoting effects on wheat plants under drought stress, (ii) characterization of stress-responsive mechanism(s) under drought stress in selected isolate employing metabolomics analysis, (iii) to study the effect of selected PGPR on the expression of stress-related genes and metabolites in host plants under drought stress, and (iv) to test the effect of selected strain on the proteomic profile of plants grown under drought stress.

Methodology: Drought-tolerant rhizospheric bacteria were isolated on selective media containing polyethylene glycol (PEG). Recovered isolates were subjected to basic biochemical tests following standard protocol and identified based on partial 16S rRNA gene sequence analysis. Bacterial isolates were further tested for plant growth-promoting properties such as phosphate solubilization, indole acetic acid (IAA) production, siderophore production, ACC deaminase activity, nitrogen fixation, ammonia production, and antagonistic activity following standard protocols. Bacterial consortia constituting two or more compatible bacteria with different plant growth-promoting properties were formed to study their synergistic or additive effect for ameliorating drought. Further, the effect of individual bacterial isolates and microbial consortia on the growth of wheat crops under drought stress was assayed. For bacterial treatment, surface sterilized seeds were bacterized, germinated, and grown under standard laboratory conditions. To impose drought stress, plants were not watered after 15 days of germination (plants grown up to the three-leaf stage). Based on the results of bacteria-inoculated plant growth under drought stress, *Enterobacter bugandensis* WRS7 (*Eb* WRS7) was further tested for its ability to ameliorate drought stress in wheat plants employing biochemical and molecular following appropriate protocols. Moreover, to reveal the physiological and metabolic networks in response to drought-mediated osmotic stress, we performed biochemical analyses (including Reactive Oxygen Species (ROS) detection, Malondialdehyde (MDA) Assay, estimation of intracellular ion concentration, quantification of phytohormone and exopolysaccharide production, and estimation of proline and protein content), and applied untargeted metabolomics to investigate the stress adaptation mechanisms of a PGPR *Eb* WRS7. To discover the underlying metabolic signatures and their role in stress tolerance mechanisms in bacteria, we employed untargeted gas chromatography-mass spectrometry (GC-MS) based metabolomics to profile the deregulated metabolite (central and secondary) pool and identify core metabolic pathways under stress. In addition, the ability of *Eb* WRS7 to colonize wheat plants was tested by CFU count of bacteria recovered from plants after treatment and ERIC-PCR-based DNA fingerprinting approach. Furthermore, the abilities of *Eb* WRS7 to ameliorate drought stress in wheat plants were characterized by employing biochemical and molecular approaches. After the stress period, plants were harvested and analyzed for biochemical assays such as proline content, total soluble sugar estimation, lipid peroxidation estimation, and CAT and SOD enzyme activity following standard protocols. Further, the expression of different genes contributing to drought stress amelioration was investigated to understand the plant response to PGPR inoculation. Gene expression analysis was done using relative quantification by the $2^{-\Delta\Delta CT}$ method. Polar and non-polar metabolites were extracted from the control and *Eb* WRS7-treated wheat plants grown under normal and drought stress, followed by their analysis through GC-MS. Finally, differential abundance of proteins under drought stress in bacteria-inoculated wheat plants

was studied. For this, proteins were extracted using the TCA- acetone precipitation method from treated and control plants, and peptides were analyzed using Orbitrap Fusion Tribrid Mass Spectrometer coupled to a Thermo EASY nanoLC 1200 chromatographic system. All the experiments were carried out in triplicates unless otherwise stated, repeated in three different experimental sets, and plotted as mean ± SD using Prism 8 (Graph Pad software). Statistical analysis was performed using an unpaired student's t-test. Statistical significance: *P ≤ 0.05, **P ≤ 0.01, ***P ≤ 0.001, and ****P < 0.0001, ns = not significant.

Result and Discussion: Based on the ability to grow efficiently on PEG-containing media, 9 bacterial isolates having different morphotypes (8 rhizospheric and 1 endophytic) were selected for the test of plant growth-promoting properties and basic biochemical and molecular characterization. Based on the 16S rRNA sequence similarity, the test isolates were identified as members of different genera, including *Enterobacter, Pseudomonas, Kosakonia, Siccibacter, Acinetobacter,* and *Stenotrophomonas.* Bacterial isolates showed different plant growth-promoting properties, including nitrogen fixation, phosphate solubilization, siderophore production, phytohormone (indole acetic acid and gibberellic acid) production, exopolysaccharide secretion, and ACC deaminase activity. Based on their PGP activities, different consortia were also formulated. Further to test the efficacy of bacterial isolates/consortia as biofertilizers, plant growth studies under drought stress conditions under laboratory conditions were conducted. Results of the plant growth promotion test showed that bacterial inoculation leads to increase in plant growth in terms of root/shoot length, biomass, and photosynthetic pigments under drought stress. Among the tested isolates and consortia, *Eb* WRS7 was most effective for increasing the growth parameters of the wheat plant as well as for protecting them from the deleterious effects of drought stress. Therefore, *Eb* WRS7 was further characterized for stress-responsive mechanism(s) under drought stress employing metabolomics analysis. Drought caused oxidative stress and resulted in slower growth rates in *Eb* WRS7. However, *Eb* WRS7 could tolerate drought stress and did not show changes in cell morphology under stress conditions. Overproduction of ROS caused lipid peroxidation (increment in MDA) and eventually activated antioxidant systems and cell signalling cascades, which led to the accumulation of ions (Na^+, K^+, and Ca^{2+}), osmolytes (proline, exopolysaccharides, betaine, and trehalose), and modulated lipid dynamics of the plasma membranes for osmosensing and osmoregulation, suggesting an osmotic stress adaption mechanism in PGPR *Eb* WRS7. Further, GC–MS-based metabolite profiling and deregulated metabolic responses highlighted the role of osmolytes, ions, and intracellular metabolites in regulating *Eb* WRS7 metabolism. Our results suggest that understanding the role of metabolites and metabolic pathways can be exploited for future metabolic engineering of PGPR and developing

bio inoculants for plant growth promotion under drought-affected agroecosystems. Further, the ability of *Eb* WRS7 to confer induced systemic tolerance (IST) in wheat plants was confirmed by pot assay, which demonstrated minimum damages to wheat plants in the presence of bacterial inoculum under drought stress conditions. *Eb* WRS7 inoculation in wheat plants exhibited drought stress ameliorating properties, including increased osmolyte content (proline and total soluble sugar), relative water content, catalase, and superoxide dismutase activity, and decreased lipid peroxidation compared to non-inoculated plants. Our biochemical data were coherent with gene expression analysis of WRS7-treated plants, which showed altered expression of genes encoding antioxidant enzymes (*CAT,* APX, and *GPX*), osmolyte synthesis (*P5CS*, *P5CR*, and *TPS1*), biosynthesis of stress hormone genes (*NCED, WZE, SAMS, ACS1*, and *ACO* encoding proteins for the biosynthesis of abscisic acid and ethylene), and calcium transporter (*TPC1*) in the wheat plant. The regulation of the ethylene biosynthesis gene and modulation of TPC1 gene expression by PGPR *Eb* WRS7 in wheat plants highlights its additional role in alleviating drought stress. Interestingly, in our study, we found a decrease in the expression of enzymes required for ethylene biosynthesis supported by a decreased level of enzymes required for ethylene biosynthesis at the protein level. The colonization study demonstrated the successful colonization of *Eb* WRS7 in wheat plants. Metabolite profile patterns of wheat plants inoculated with *Eb* WRS7 provide a holistic biochemical phenotype of wheat plants under drought conditions. PGPR-induced amendments in amino acids, organic acids, lipids, and phytohormones levels, suggesting their role in the amelioration of drought tolerance through complex cellular changes characterized by altered metabolism in wheat plants. Further, the effect of *Eb* WRS7 on the proteomic profile of wheat plants under drought stress was investigated, which showed that the bacterial inoculation positively upregulated the abundance of various proteins responsible for drought tolerance and defense response. The observed drought-responsive proteins belong to antioxidant enzymes, phytohormone-related proteins, metabolism- and photosynthesis-related proteins, transporters proteins, osmotic homeostasis-related proteins, and secondary metabolism-related proteins. Overall, the present study indicates that *Eb* WRS7 alleviates drought stress in wheat plants by differentially regulating various metabolic pathways in treated plants, and hence, can be used as a potential biofertilizer. However, its pathogenicity must be evaluated before its application at the field level.

Contents

LIST OF FIGURES

LIST OF TABLES

Abbreviation

ABA	Abscisic Acid
ACC	1-Aminocyclopropane-1-carboxylate
ACCD	ACC Deaminase
ANOVA	Analysis of ariance
APX	Ascorbate Peroxidase
ATP	Adenosine Triphosphate
BLAST	Basic Local Alignment Search Tool
BSA	Bovine Serum Albumin
CAS	Chrome-Azurol-S
CAT	Catalase
CFU	Colony Forming Unit
CTAB	N-cetyl trimethyl ammonium bromide
DAPs	Differentially Abundant Proteins
DDW	Double Distilled Water
DF	Dworkin and Foster
DNA	Deoxyribonucleic Acid
EDTA	Ethylenediamine Tetraacetic Acid
EPS	Exopolysaccharides
FAME	Fatty Acid Methyl Ester
FAO	Food and Agriculture Organization
FESEM	Field Emission Scanning Electron Microscopy
GA	Gibberellic Acid
GC	Gas Chromatography
GC-MS	Gas Chromatography-Mass Spectroscopy
GO	Gene Ontology
GPX	Glutathione Peroxidase
GST	Glutathione S-transferase
HPLC	High-Performance Liquid Chromatography
HRMS	High Resolution Mass Spectrometry
HSP	Heat Shock Proteins
IAA	Indole-3-Acetic Acid
IMViC	Indole, Methyl red test, Voges-Proskauer test
ICP-OES	Inductively Coupled Plasma-Optical Emission Spectroscopy
ISR	Induced Systemic Resistance
IST	Induced Systemic Tolerance
JA	Jasmonic acid
LB	Luria Broth
LC	Liquid chromatography
LC-MS	Liquid Chromatography-Tandem Mass Spectrometry
LEA	Late Embryogenesis Abundant
MAPK	Mitogen-Activated Protein Kinase
MDA	Malondialdehyde

MUC	4-methylumbelliferyl-cellobioside
MUG	4-methyllumbelliferyl-β-D-glucoside
mRNA	Messenger Ribonucleic Acid
MS	Mass Spectrometry
NB	Nutrient Broth
NBRIP	National Botanical Research Institute's Phosphate
NBT	Nitro Blue Tetrazolium
NCBI	National Center for Biotechnology Information
NIST	National Institute of Standards and Technology
OD	Optical Density
PBS	Phosphate Buffer Saline
PCA	Principal Component Analysis
PCR	Polymerase Chain Reaction
PEG	Polyethylene Glycol
PGPR	Plant Growth Promoting Rhizobacteria
PMSF	Phenylmethylsulfonyl Fluoride
POD	Peroxidase
ROS	Reactive Oxygen Species
Rubisco	Ribulose-1,5-bisphosphate carboxylase/oxygenase
RWC	Relative Water Content
SA	Salicylic Acid
SOD	Superoxide Dismutase
TBA	Thiobarbituric Acid
TBARS	Thiobarbituric Acid-Reactive Substance
TCA	Trichloroacetic acid
TSS	Total Soluble Sugar
VIP	Variable Importance in Projection
VOCs	Volatile Organic Compounds

CHAPTER I

General Introduction

1.1 Wheat: An Important Cereal Crop

Wheat (*Triticum aestivum* L) is an important cereal and staple crop grown worldwide, contributing around 20% of total dietary calories and more than 25% of protein consumed. It occupies around 217 million hectares of land globally to achieve an annual production of approximately 731 million tonnes [1–3]. Wheat has been cultivated as a winter and spring crop across the world. Winter wheat is grown in cold countries like the USA, Europe, etc., whereas spring wheat is grown in Asia, including India [3]. Wheat demand has increased in recent years as wheat provides an extensive variety of end products at lower prices in comparison to other cereal crops [4]. According to the Food and Agriculture Organization (FAO) estimate, the current global annual wheat production is about 680 million tons, and the world will require around 840 million tonnes by the year 2050. Still, the production amount is not enough to meet the ever-growing demand of the growing population (FAO, 2017). This must be achieved through sustainable agriculture and agronomic interventions. Although wheat production is likely to increase by 60%, world agriculture faces severe challenges in meeting the demands of the increasing population and health safety concerns due to adverse environmental conditions, particularly high temperatures, and changes in rainfall distribution (Figure 1.1) [4].

The impact of climate change on food production is complex and widespread across the globe and is also influenced by socio-economic conditions. The loss in yield of cereal crops, including wheat, will threaten the food security of people in the Asia-Pacific region the most. The projected rise in temperature by 0.5 °C in every 10 years will affect the distribution and frequency of rainfall and, hence, will be the major cause of grain yield reduction [4].

Figure 1.1. Challenges faced in the Production of wheat at large scale.

Wheat, grown in the Rabi season (November- April), is the second most cultivated crop in India after rice. India is the second largest producer of wheat in the world, contributing to around 13% of the global wheat supply [5]. The land under cultivation is around 30.54 million hectares nationwide, producing around 94.57 million tonnes of wheat yearly [3]. To feed the increasing population, it requires more cultivable land, water, and energy for irrigation. However, intensive cropping has resulted in the irrational use of resources, pesticides, and chemical fertilizers causing a reduction in natural resources and a consequent decline in total production and yield of the crop. In addition to the above challenges, wheat production is vulnerable to changes in climatic conditions [3]. It has been predicted that in India, with every rise in 1 °C temperature, there will be a decline in rain-fed wheat production by 4- 6 million tonnes [3]. According to global estimates, abiotic factors like high or low temperature, salinity, and drought cause an average loss of 50% to agricultural crops [6]. Moreover, abiotic stressors can alter the interaction of crops with pests, making wheat more susceptible to pathogenic organisms. Also, a weakened immune system of plants reduces their competing ability with weeds.

1.2 Abiotic Stress: Major Challenge to Wheat Production

The natural environment for plants experiences a complex set of abiotic stresses and biotic stresses. Abiotic stress is defined as environmental conditions that reduce growth and yield below optimum levels. Major abiotic stresses faced by plants are salinity, drought, mineral toxicity, and extreme temperature (Figure 1.2). These stresses negatively affect the survival,

yield, and biomass production of crops by as much as 70% and threaten food safety worldwide [6]. Plant responses to these stresses are dynamic and complex. These responses can be either reversible or irreversible. The plant responses to stress are dependent on the tissue or organ affected by the stress as well as the level and duration of stress (acute vs chronic). Stress resistance/tolerance includes both stress avoidance and stress tolerance. Stress avoidance means that plants try to maintain unstressed conditions at cellular and tissue levels, whereas, in stress tolerance, plants respond to altered environmental conditions. The plant responses at a physiological level to abiotic stressors depend on the tissue or organ which are exposed or affected directly by the stress. The earliest metabolic responses to abiotic stress include growth inhibition, a decrease in protein synthesis, and an increase in protein folding and processing. The energy metabolic pathways are affected under severe stress conditions [7].

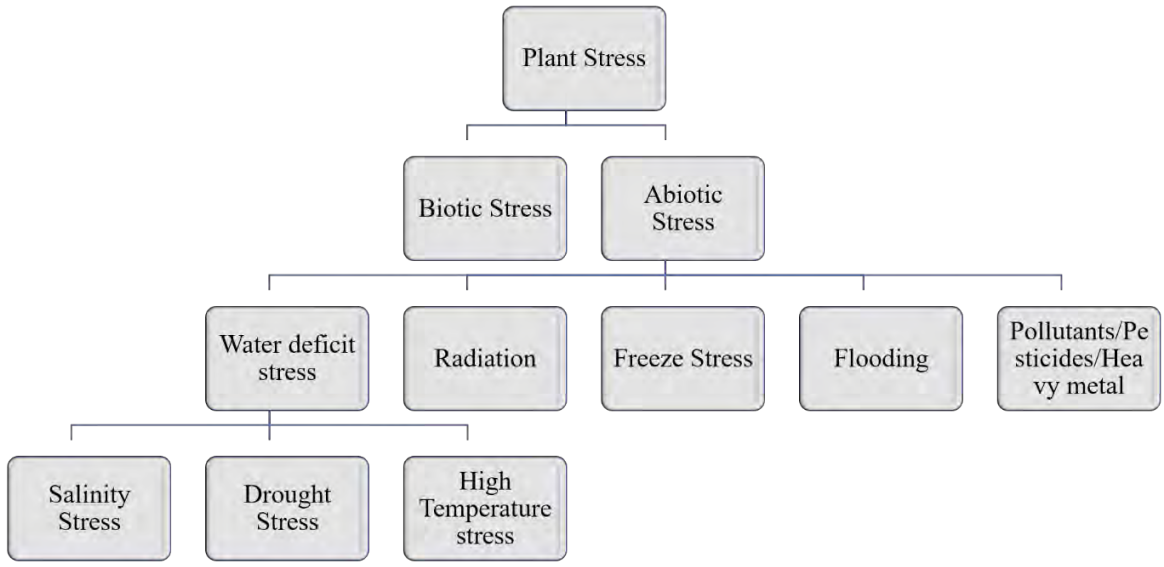

Figure 1.2. Different types of stress experienced by the plants in its lifetime.

1.3 Drought Stress

Out of the different abiotic stressors mentioned above, drought has negative impacts on wheat yield and growth worldwide, causing up to 40% yield losses [8]. Drought stress reduces plant growth by decreasing water uptake, modifying biochemical and physiological processes in plants ultimately decreasing the plant yield [2, 9]. Irregular rainfall is common in India, especially at the time of maturity of wheat, causing pre-harvest sprouting. Consequently, it decreases the quality of grains due to early activation of α- amylase enzyme.

Since wheat is a water-intensive crop, drought stress negatively impacts its yield and grain quality [1, 10]. Drought stress causes damage during all the stages of wheat crop growth. If it occurs at the early growth stage, less number of tillers per unit area are developed due to poor seed establishment. During mid-stage growth, drought causes reduced dry matter production and grains per plant. However, drought incidence at the terminal growth stage reduces carbon assimilates production, fertility, and grain weight [2]. In addition to osmotic stress, drought affects soil biota, increases soil heterogeneity, limits nutrient accessibility and mobility, and increases soil oxygen, often promoting a strong decline in microbial biomass [11]. The drought response cascade in plants comprises the activation of complex signalling networks. Initially, it includes an increase in cytosolic H^+ and Ca^{2+} ions, generation of reactive oxygen intermediates, and the signalling cross-talk between hormones like abscisic acid (ABA), ethylene, jasmonic acid (JA) and salicylic acid (SA). This further triggers various physiological responses like loss of turgor pressure, stomatal closure, and leaf area reduction, which decreases the photosynthetic capacity of the host plant, which negatively affects plant biomass and yield; if persists for a longer duration, it ultimately leads to leaf senescence and plant death [12].

Drought tolerance is a complex phenomenon. Plants adapt to various physiological and biochemical mechanisms to generate tolerance against drought, which include increased stomatal resistance to prevent water loss, development of deep root system, accumulation of osmoprotectant and compatible solutes, biosynthesis of secondary metabolites, and phytohormone modulation (Figure 1.3) [13]. Wheat plants respond to drought stress through various molecular mechanisms, including sensing the stress signal, activating multiple signaling pathways, translation, and post-translational modification, governed by genetic and epigenetic factors [14]. At the molecular level, several stress-related proteins and enzymes are produced, including dehydrins, late embryogenic abundant (LEA) proteins, and glutathione S-transferase (GST).

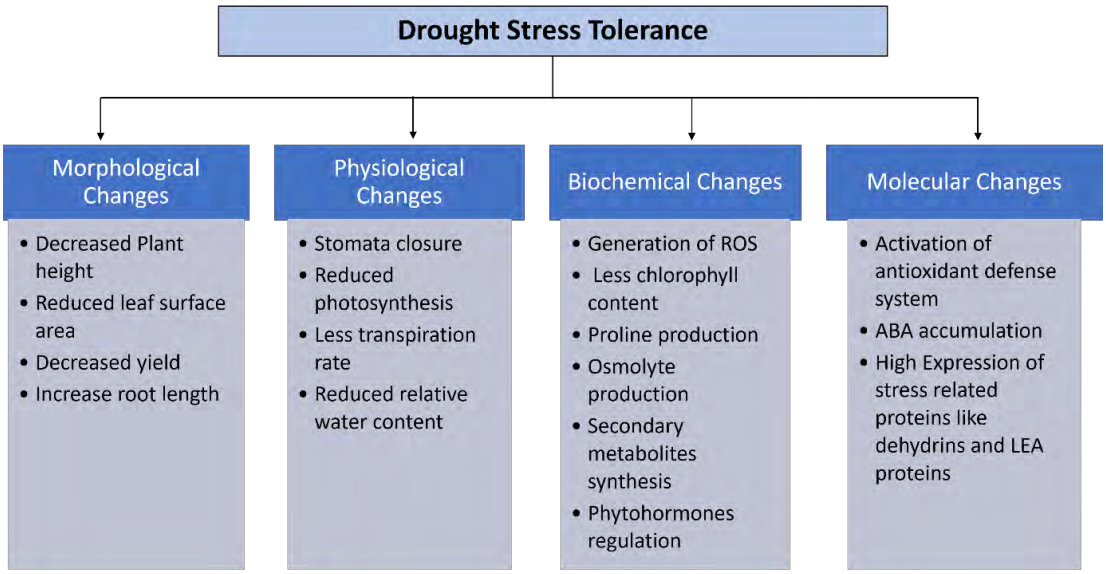

Figure 1.3. Drought stress tolerance in plants. Plants protect themselves against drought stress through various physical, biochemical, and molecular modifications. (Abbreviations: ROS- Reactive Oxygen Species; ABA- Abscisic Acid; LEA- Late Embryogenic Abundant proteins).

There are various practices that can improve plant growth under abiotic stress conditions. One of them is the application of chemical fertilizers, which promote plant growth under such environmental conditions [15]. However, chemical fertilizers have health and environmental concerns. The chemical fertilizer can substantially cause soil, water, and air pollution. The excessive use of chemical fertilizer has also impacted soil microorganisms and soil fertility and deteriorated the biological and physicochemical health of the arable soil [16, 17]. Secondly, breeding programs have been designed to architect a genotype enabling increased water and nutrient efficiency. However, it is a slow process and requires proper genetic variability detection between plant genotypes or sexually compatible cultivars [18]. Also, it is labor-intensive, requires skilled people, and is economically unsuitable. Moreover, generating genetically modified drought-stress-resistant crops can be an appropriate solution to enhance agricultural productivity and modify the genetic composition of a plant [4]. However, its health and environmental impacts are not fully known. Also, there are ethical concerns with the use of genetically modified crops. Therefore, taking account of the present scenario, biofertilizers are suitable alternative to counter the adverse effect of abiotic stress, facilitating the overall growth and yield of wheat crops in an eco-friendly manner and promoting sustainable agriculture [16]. The biofertilizers are the preparation of efficient soil microorganism or microbial communities, mainly isolated from plant rhizosphere or endosphere, when applied to soil, seed, or plant surface, colonize, and promote the growth of host plants. The biofertilizer provides major limiting nutrients, stimulates plant growth by modulating the level of

phytohormones, and ameliorates several biotic and abiotic stress conditions in host plants [16, 17]. One of the most potential biofertilizers is based on applying Plant Growth Promoting Rhizobacteria (PGPR).

1.4 Plant Growth Promoting Rhizobacteria —The Phyto-Friendly Soil Microbes

PGPR are free-living, beneficial, aggressively root-colonizing bacteria that thrive in the plant rhizosphere, thus promoting plant growth through various mechanisms [16, 17]. The term PGPR was introduced by Kloepper and Schroth in 1978. The ideal PGPR are characterized by the following inherent distinctiveness: (i) they must be rhizosphere-competent and proficient to colonize the root surface; (ii) they must survive and multiply upon inoculation; (iii) they must promote plant growth; and (iv) they must be compatible with other bacteria in the rhizosphere [16, 19]. PGPR are known to produce and secrete various regulatory chemicals near the rhizosphere, influencing plant growth, health, and productivity. They contribute to plant growth through nitrogen fixation, synthesizing phytohormones, solubilizing mineral nutrients, decomposing organic matter, recycling essential elements, degrading organic pollutants, and stimulating root growth. They also make various metals bioavailable to the plants by altering the pH of the soil, producing chelator molecules such as siderophores, organic acids, and biosurfactants, adsorbing metal ions directly on the root surface, or performing various biochemical reactions [17]. They also protect the host plant against phytopathogens and promote resistance to various abiotic stresses [16, 17, 20]. Several PGPR belonging to the genera *Acinetobacter*, *Aeromonas*, *Agrobacterium, Allorhizobium*, *Arthrobacter*, *Azoarcus*, *Azorhizobium*, *Azospirillum*, *Azotobacter*, *Bacillus*, *Bradyrhizobium*, *Burkholderia*, *Caulobacter, Chromobacterium, Delftia*, *Enterobacter*, *Flavobacterium*, *Frankia*, *Gluconacetobacter*, *Klebsiella*, *Mesorhizobium*, *Micrococcus*, *Paenibacillus*, *Pantoea*, *Pseudomonas*, *Rhizobium*, *Serratia*, *Streptomyces*, *Thiobacillus*, and others have been used as soil inoculums, either alone or in combination, to improve plant growth in various studies [16, 17, 20–23]. Many researchers have reported and reviewed the application of PGPR and their contribution to promoting plant growth across the plant kingdom [16, 17, 19, 21–23].

In addition to promoting plant growth by providing nutrients, some PGPR also ameliorates different abiotic stressors, including drought stress. For instance, PGPR-mediated stress-amelioration and plant growth stimulation have been reported in various crop plants, such as maize [24], cucumber [25], mung bean [26], and wheat [27–29]. The capacity of PGPR to combat abiotic stressors through 1-aminocyclopropane-1- carboxylate (ACC) deaminase and

other mechanisms is known as induced systemic tolerance (IST) in plants [20]. The PGPR-induced abiotic stress tolerance in plants is critically important in mitigating the negative impact of climate change on crop production. Therefore, a systematic study to understand the role of PGPR in managing abiotic stressors is essential for sustainable agriculture.

1.5 Induced Systemic Tolerance (IST)

PGPR-mediated enhancement of plants' tolerance to unfriendly environmental conditions, such as salinity stress, drought stress, heavy metals stress, high and low temperature, and flooding, through elicitation of a so-called process called Induced Systemic Tolerance (IST). IST results from PGPR-induced interaction that leads to various physiological and biochemical changes that protect host plants from the deleterious effects of abiotic stresses. Several research groups have reported the role of PGPR in abiotic stress amelioration (Table 1.1) [2, 30]. IST is induced by PGPR-derived elicitors such as phytohormones, volatile organic compounds (VOCs), enzymes such as ACC deaminase, antioxidants, and exopolysaccharides (Figure 1.4 and Figure 1.5) [12]. IST leads to the foundation of an eco-friendly stress management strategy.

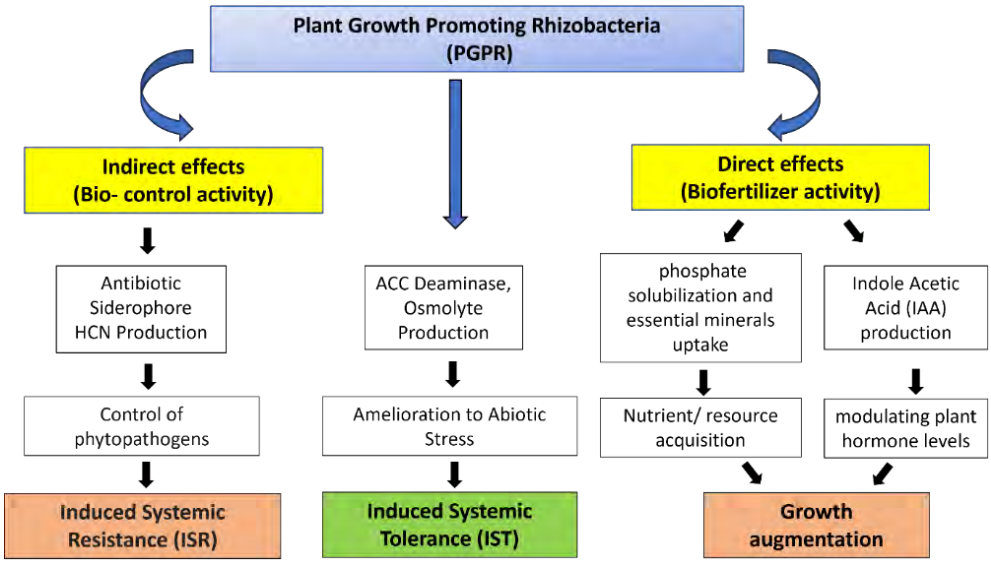

Figure 1.4. Overview of mechanisms exhibited by rhizobacteria (PGPR). PGPR directly promotes plant growth by improving nutrient acquisition (such as nitrogen fixation, phosphate solubilization) and growth augmentation by regulating phytohormone levels. They also make various metals bioavailable to the plants by altering the pH of the soil, producing chelator molecules such as siderophores, organic acids, and biosurfactants, and adsorption of metal ions directly on the root surface. They enhance stress tolerance in plants by osmolyte production, ACC deaminase activity, and inducing systemic tolerance in plants. The indirect effects of PGPR include the suppression of phytopathogens and the induction of systemic resistance in plants against a wide range of pathogenic microbes.

Table 1.1. Induced Systemic Tolerance (IST) by PGPR against various abiotic stress.

Bacteria	**Host Plant**	**Stress Protection**	**Mechanism/ tolerance strategy**	**Reference**
Bacillus amyloliquefaciens, Azospirillum brasilence	Wheat	Heat	Reduced regeneration of reactive oxygen species, reactivation of heat shock transcription factors, changes in metabolome	Abd El-Daim *et al.*, 2014 [46]
Pseudomonas sp.	Tomato	Salinity	ACC deaminase, Higher chlorophyll content	Ali *et al.*, 2014 [44]
Bacillus amylolequifaciens, Bacillus insolitus Microbacterium sp., *Pseudomonas syringa*	Wheat	Salinity	Restricted Na+ influx due to rhizo-sheath formation by EPS	Ashraf *et al.*, 2004 [39]
Bacillus amyloliquefaciens SQR9	Maize	Salinity	Enhanced Chlorophyll content, improved peroxidase/catalase activity and glutathione content	Chen *et al.*, 2016 [36]
Bacillus subtilis Rhizo SF 48	Tomato	Drought	ACC deaminase. Increased proline, SOD and APX activity.	Gowtham *et al.*, 2020 [35]
Pseudomonas pseudoalcaligenes, Bacillus pumilus	Rice	Salinity	Increased concentration of glycine betaine (compatible solute) Decrease in APX, Increase in nitrate reductase activity	Jha *et al.*, 2011 [41]
Bacillus sp. and *Enterobacter* sp.	Wheat and Maize	Drought	IAA and Salicylic Production	Jochum *et al.*, 2019 [34]

Enterobacter sp.	Tomato, Arabidopsis	Salinity	IAA, Increased expression of salt stress responsive genes such as DREB2b, RD29A, RD29B, RAB18 Higher APX activities	Kim *et al.*, 2014 [43]
Kocuria rhizophila	Maize	Salinity	Regulating phytohormones (IAA and ABA) and improving nutrient acquisition. Higher transcript level genes GR1 and APX1, and genes involved in salt tolerance (DREB2A, NHX1, NHX2)	Li *et al.*, 2020 [33]
Pseudomonas putida, Enterobacter cloacae, Serratia ficaria, Pseudomonas fluorescens	Wheat	Salinity	Improved nutrition	Nadeem *et al.*, 2013 [42]
Pseudomonas sp.	Maize	Drought	EPS increased soil aggregation and water uptake	Naseem & Bano, 2014 [38]
Pseudomonas fluorescens DR7	Foxtail millet	Drought	ACC deaminase, EPS production, increase soil moisture, and enhance the root adhering soil/root tissue ratio	Niu *et al.*, 2018 [31]
Cupriavidus necator 1C2 (B1) and *Pseudomonas fluorescens* S3X (B2)	Maize	Drought	Increase nitrogen (N) and phosphorous (P) use efficiency, accumulation of compatible solutes	Pereira *et al.*, 2020 [32]
Priestia megaterium	Wheat	Drought	ACC deaminase, IAA, antagonistic activities	Rashid *et al.*, 2021 [27]

			against plant pathogens. Increased chlorophyll and proline content	
Pseudomonas aeruginosa	Mung bean	Drought	IAA, Up regulation of DREB2A, CAT1, DHN, Increased activity of SOD, peroxidase (POX), CAT	Sarma & Saikia, 2014 [26]
Bacillus thuringiensis	Wheat	Drought	Production of volatile organic compounds. Increased activity of glutathione reductase (G.R.), catalase (CAT), superoxide dismutase (SOD), Alginate, IAA, Reduced emissions of stress volatiles	Timmusk *et al.*, 2014 [37]
Pseudomonas simiae	Glycine max (Soybean)	Salinity	4-nitroguaiacol and quinoline promote soybean seed germination	Vaishnav *et al.*, 2016 [45]
Bacillus cereus, Bacillus subtilis, Serratia sp.	Cucumber	Drought	Expression of genes cAPX, rbcL, rbcS, Increased chlorophyll content	Wang *et al.*, 2012 [25]
Bacillus subtilis	*Arabidopsis thaliana*	Salinity	VOCs regulates HKT1 expression	Zhang *et al.*, 2008 [40]

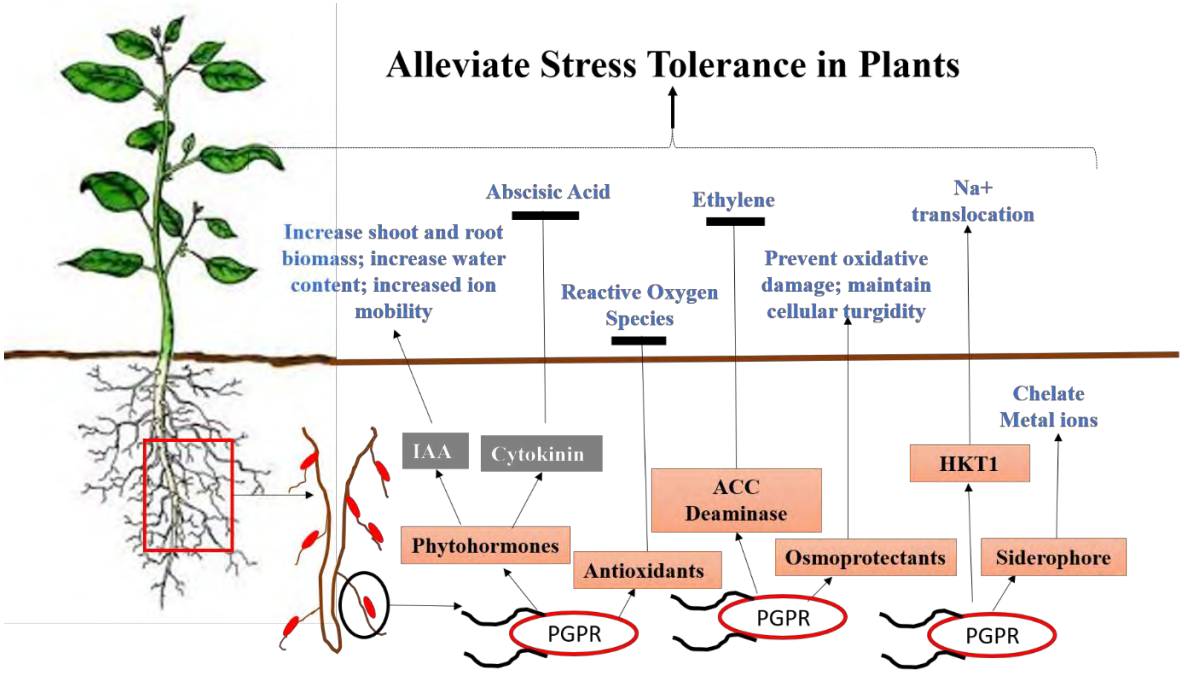

Figure 1.5. Microbe-mediated induced systemic tolerance in the plants. Bacteria residing in the rhizospheric region promote plant growth and alleviate stress tolerance in plants by synthesizing certain chemicals or modifying different biochemical pathways. (PGPR- Plant Growth-Promoting Bacteria; IAA- Indole Acetic Acid; ACC deaminase- 1-aminocyclopropane-1-carboxylate deaminase; HKT1- high-affinity K^+ transporters).

1.5.1 ACC Deaminase Activity

Ethylene is a gaseous phytohormone that directs several developmental processes in plants, such as promoting fruit ripening, leaf senescence and wilting, abscission, germination, root architecture, and flowering [47]. At low concentrations, ethylene impacts several benefits to the plants, but its higher concentration is detrimental and induces defoliation and other cellular processes that may deteriorate plant growth. The elevated ethylene level causes root growth inhibition, abnormalities in the development of hypocotyl and its elongation, and defoliation and growth retardation. These phenomena are collectively called a triple response. Increased ethylene biosynthesis is a characteristic phenomenon of plants during environmental stress conditions which accelerates senescence and ultimately results in plant growth retardation [47].

Many PGPR employ ACC deaminase activity to suppress the stress-induced ethylene level in host plants, thereby ameliorating plant stress and promoting plant growth. The ACC deaminase-producing bacteria sequester and degrade ACC, an immediate precursor to ethylene, to ammonia and α-ketobutyrate, which in turn provide nitrogen and carbon sources respectively to them [20, 48]. The ACC deaminase-producing rhizobacteria have been identified in a wide range of genera, such as *Acinetobacter, Bacillus, Burkholderia, Enterobacter, Pseudomonas* etc. [20, 35]. Previous studies have reported the efficiency of ACC deaminase-producing PGPR in upregulating antioxidant machinery, improving the functioning of photosynthetic apparatus that eventually leads to enhanced plant biomass and increased stress tolerance [49, 50]. Maxton *et al.* (2018) reported that inoculation of *Burkholderia cepacia* mitigated the adverse effects of salinity and drought by the proliferation of root system and increasing plant biomass in *Capsicum annuum* [51]. In another study, Murali *et al.* demonstrated the potential of ACC deaminase producing PGPR, *Bacillus amyloliquefaciens* MMRO4, to alleviate drought stress in pearl millets. They found that MMR04 enhanced enzymatic and non-enzymatic antioxidants and decreased expression of *DREB-1E* and *ERF-1B* genes, encoding transcription factors dehydration responsive element binding protein-1E and ethylene response factor-1B respectively, in pearl millet upon drought stress imposition. Also, APX1 and SOD1 gene expression was increased in MMR04-treated plants upon drought stress [52]. ACC deaminase-producing PGPR *Pseudomonas* sp. MRBP4, *Pseudomonas* sp. MRBP13 and *Bacillus* sp. MRBP10 isolated from maize rhizosphere ameliorates the effect of drought stress in maize by significantly affecting total soluble sugar, soil moisture content, and relative water content [53]. Therefore, the growth enhancement of plants by ACC deaminase

bacteria has motivated scientists to transfer ACC deaminase gene (*AcdS*) into plants as a future approach to minimize the harmful effects of ethylene in plants subjected to adverse environmental conditions [20].

1.5.2 Exopolysaccharide Production

Many PGPR produce exopolysaccharides (EPS), which help their attachment to plant roots and biofilm formation and enhance their mobility under drought and salinity stress [54, 55]. EPS formation protects bacteria from oxidative cell death. It also confers resistance to plants against drought stress as EPS can act as an emulsifier that quenches ROS and protects biomolecules. EPS-producing PGPR can ameliorate osmotic stress caused by drought and salinity and promote plant growth in different ways. EPS causes aggregation of soil particles, which increases root adhering of soil (RAS) by forming a hydrophilic biofilm around plants' roots. Consequently, it increases nutrient acquisition and water availability by the plants, promoting plant growth and biomass under drought stress [56]. Also, EPS prevents soil erosion, increases stability of the rhizosphere region, and maintains soil structure under drought conditions [54]. For instance, EPS-producing *Enterobacter cloacae* and *Bacillus drentensis* enhanced nutrient availability and water uptake in mung bean plants through the formation of biofilm in the root zone [54, 55]. Bashan *et al.* (2004) reported that EPS-producing *Azospirillum* bacteria enhance osmotic stress resistance in plants due to changes in the soil structure and aggregation properties [57]. Kaci *et al.* (2005) also observed improvements in soil aggregation properties of wheat rhizosphere due to EPS production by rhizobia, thus enhancing plant growth under stress [58]. Moreover, some EPS-producing rhizobacteria, such as *Bacillus subtilis* GB03, can also minimize ion toxicity by reducing Na^+ influx through the expression of HKT1/K^+ transporter under salt stress [40, 55]. Few EPS-producing PGPR, for example, *Bacillus amyloliquefaciens, Bacillus insolitus, Microbacterium* sp., and *Pseudomonas syringae* have been reported to improve wheat crop growth by inhibition of Na^+ influx during salinity stress [29, 38, 39, 59]. Wheat plants inoculated with EPS-producing rhizobacteria could overcome salinity stress as rhizo-sheaths formed around plant roots due to EPS-restricted Na^+ influx into the stele [39].

1.5.3 Production of Volatile Organic Compounds (VOCs)

PGPR-produced volatile organic compounds, like 2, 3-butanediol, and acetoin, constitute an important mechanism of plant growth elicitation by PGPRs. These compounds act as signaling molecules to mediate plant-microorganism interaction and regulate osmolyte and

phytohormone biosynthesis [22, 55, 56]. For instance, as reported by Ryu (2003), VOCs secreted by *Bacillus amyloliquefaciens* IN937a and *Bacillus subtilis* GB03 enhance *Arabidopsis* plant growth by modulating the expression of genes involved in cell wall structure [60]. VOCs produced by *Bacillus subtilis* GB03 caused the upregulation of transcripts involved in auxin homeostasis. They stimulated the biosynthesis of osmolytes, such as choline and glycine betaine, thus improving osmotic stress tolerance in *Arabidopsis* plants [40, 61]. VOCs, like 2R and 3R-butanediol, produced by *Pseudomonas chlororaphis* O6 cause stomatal closure in *Arabidopsis* plants, thus imparting IST to drought. However, various phytohormone signalling pathways comprising SA, ethylene, and JA are also involved [62]. Since VOCs are species-specific, they are often used as a marker for specific microbial species detection and in accessing the nature of interaction among microbial communities [55].

1.5.4 Phytohormone Production

IAA secreted by rhizobacteria interferes with plant developmental processes by changing the plant auxin pool. Bacterial IAA provides the plant greater access to soil nutrients by increasing root length and surface area. Also, rhizobacterial IAA is an effector molecule in plant-microbe interaction as it loosens plant cell walls, hence facilitating more root exudate secretion that provides additional nutrients to rhizobia bacteria [19]. Primarily using tryptophan as a precursor molecule, at least five different pathways have been described for IAA synthesis in bacteria. IAA formation is found in the majority of bacteria belonging to different genera like *Pseudomonas, Agrobacterium, Enterobacter, klebsiella,* etc. [63–67]. Numerous studies report that phytohormone-producing soil microbes can help in alleviating abiotic stress in plants. For instance, Marulanda *et al.* (2009) reported that plants inoculated with IAA-producing *Pseudomonas putida* survive drought stress, as there was an increase in root surface area and number of root tips, thus enhancing the uptake of nutrients and water [68]. Similarly, *Azospirillum* inoculation in wheat plants enhanced plant growth under water stress through changes in the root architecture, increased leaf water content, and water potential [69]. Ghosh *et al.* (2019) have shown the ability of bacterial strains, *Pseudomonas aeruginosa* PM389, *Pseudomonas aeruginosa* ZNP1, *Bacillus endophyticus* J13 and *Bacillus tequilensis* J12, to secrete phytohormones under drought stress, suggests their possible contribution to ameliorating the adverse effects of osmotic stress in plants [59].

Mechanisms involved in PGPR-induced abiotic stress tolerance include changes in root and shoot morphology, augmented phytohormones content, increased relative water content,

improved antioxidant metabolism, osmotic adjustment, and enrichment of nutrient uptake by the plants [2, 12]. Therefore, a better understanding of molecular crosstalk between these beneficial microorganisms and plants can be exploited to alter plant metabolism and provide resistance to abiotic stresses.

1.6 Understanding the Role of PGPR-Plant Interactions in Drought-Stress Amelioration Employing Omics Studies.

Understanding the role of plant-microbe interactions is important to improve crop resilience to abiotic stresses and maximize crop productivity. Also, studying the complex nature of plant-microbe interactions in terms of protection against abiotic stresses can offer several strategies to increase the productivity of plants in an eco-friendly manner by providing better insights into the stress-mitigating mechanisms. Different techniques and approaches incorporating genomics, metabolomics, transcriptomics, and proteomics can be used to elucidate plant-microbe abiotic stress frameworks and generate multi-layered information that can answer what is happening in real time within the cells (Figure 1.6). The data generated and analysed by these multi-omics technologies is possible through advancement in high-end instrumentation and computational integration, which helped in the identification of signal molecules, proteins, genes, and gene cascades that connect them to the gene network or pathway to describe their function [70]. These molecular techniques will help assess the effects of agitations caused by abiotic stress on soil microbiome and plant-microbial interaction [70, 71]. Culture-neutral molecular techniques are mostly used for deciphering the microbial diversity and rhizosphere microenvironments and to get more insight into the molecular basis of the plant-microbe associations and microbe-mediated mitigation strategies of abiotic stresses in plants.

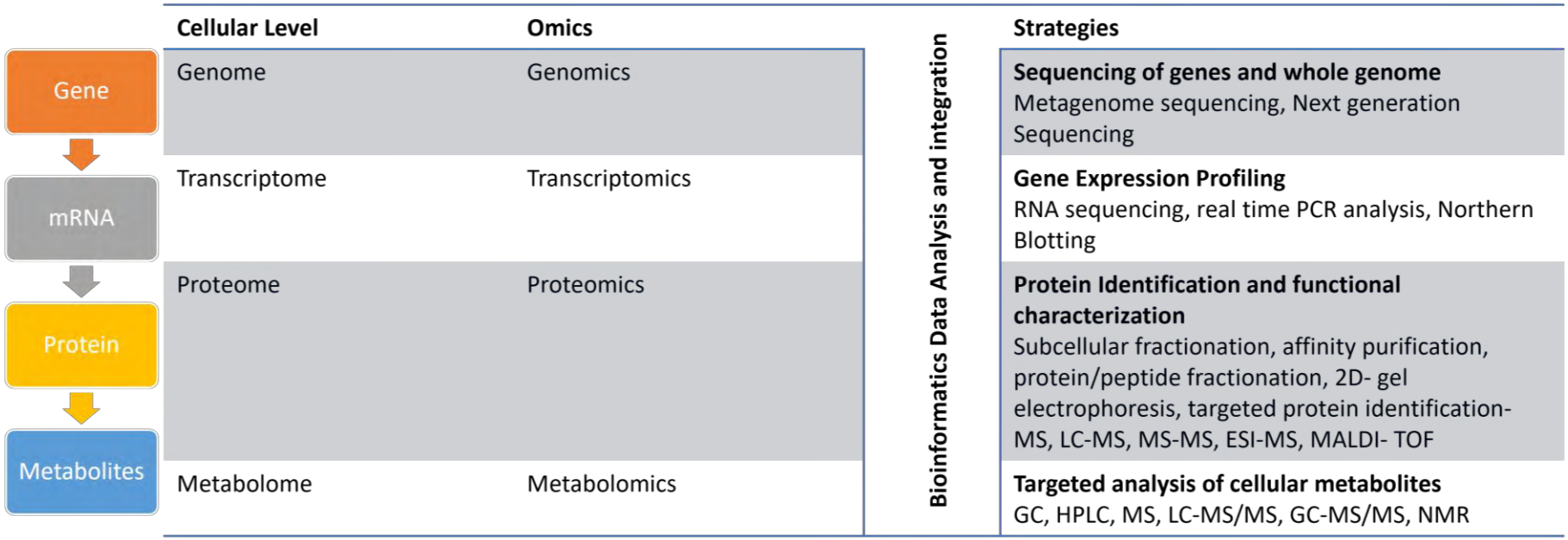

Figure 1.6. Multi-omics approaches and strategies for deciphering Plant-Microbe interactions. These approaches help in the identification, characterization, and detection of genes, proteins, and metabolites in response to stress/ microbial interactions. New functions to genes, proteins, and metabolites, as well as new metabolic pathways, can also be identified using these approaches. (Abbreviation: ESI- Electrospray ionization; MALDI- Matrix-assisted laser desorption/ ionization; G.C.- Gas chromatography; HPLC- High-Performance Liquid Chromatography; L.C.- Liquid chromatography; M.S.- Mass Spectrometry; NMR- Nuclear Magnetic Resonance; PCR- Polymerase Chain Reaction; TOF- Time of Flight).

Genomics: A large amount of genomic data in the form of sequenced genomes and expression profiles is important to know gene loci responsible for abiotic stress tolerance and, thus, for breeding for stress alleviation. Therefore, genomics-based technologies are essential for crop improvement programs. The genomic study helps in the identification of stress tolerance genes and their regulation in plants as well as in rhizobacteria. It helps breeders generate better varieties for stress tolerance [70].

Whole genome sequencing of PGPR has been widely used for their characterization, such as plant growth promotion capability or resistance/tolerance to abiotic stresses [72]. For instance, the whole genome of *Brevibacterium frigoritolerans* ZB201705, isolated from the rhizosphere of Maize under salinity and drought stress, was analysed. It revealed that this strain can synthesize many proteins, such as histidine-protein kinase/phosphatase DegS, sodium/proline symporter, superoxide dismutase (SOD), catalase (CAT), and glutathione peroxidase (GPX), involved in the cell response to drought and salt stress [73]. Similarly, Singh *et al.* (2017) analyzed the genome sequence of *Enterobacter cloacae* SBP-8, a PGPR isolated from the rhizosphere of *Sorghum bicolor* L, and identified genes potentially involved in plant growth-promoting properties such as those encoding for 1-aminocyclopropane-1-carboxylate deaminase (*AcdS*), phosphate solubilisation, siderophore, and IAA (indole acetic acid) production [74]. In another study, whole genome sequencing of three PGPR (*Enterobacter asburiae* CPCRI-1, *Pseudomonas putida* CPCRI-2, *Enterobacter cloacae* CPCRI-3) isolated from the rhizosphere of plantation crops' coconut, cocoa, and arecanut respectively. Functional annotation of the genes predicted that all three bacteria-encoded genes potentially needed for promoting plant growth such as ACC deaminase, siderophores, mineral phosphate solubilization, acetoin, butanediol, chitinase, phenazine, 4-hydroxybenzoate, trehalose, hydrogen sulfide (H_2S) production and quorum sensing molecules. Other identified genes were peroxidases, catalases, and superoxide dismutases. Also, genes involved in heat shock tolerance, cold shock tolerance, and glycine-betaine production were also identified [75]. Similarly, Aloo *et al.* (2020) analyzed the complete sequence of three PGPR *Klebsiella* sp. strain MPUS7, *Serratia* sp. strain NGAS9, and *Citrobacter* sp. strain LUTT5 isolated from *Solanum tuberosum* L. rhizosphere in Tanzania. Their protein-encoding genes were involved in potassium, nitrogen, phosphorus, and iron metabolism [76]. Also, Noori *et al.* (2021) presented the assembly of the whole genome of salinity and drought-resistant bacterium *Pantoea agglomerans* ANP8 isolated from root nodules of alfalfa. They identified genes involved in IAA production, multiple copies of the *gcd* gene involved in phosphate

solubilization, and genes involved in regulating potassium concentrations, such as the *nhaA* gene [77].

Transcriptomics: Transcriptomic study of plants in response to PGPR plays an important role in the identification of bacterial stimuli transduced to enhance plant growth and stress resistance. Transcriptomic studies reveal key gene expression patterns in the host during plant-microbe interactions. The main purpose of transcriptomic analysis of plants associated with bacteria, using gene expression microarray or RNA sequencing (RNA-seq.) approaches, is to identify differentially expressed genes under specific environmental conditions [72]. Transcriptomic investigation helps in detecting the regulation of actively transcribed genes under certain environmental conditions, thus posing an advantage over genomic analysis. For instance, Alavi *et al.* (2013) identified a novel plant growth regulator, spermidine, by transcriptome analysis of rapeseed and its symbiont *Stenotrophomonas rhizophila* during abiotic stress [78]. Mellidou *et al.* (2021) studied the effect of *Pseudomonas oryzihabitan* AXSa06 inoculation on the growth of tomato plants under salinity stress through transcriptomic and metabolomic profiling of the host. Different transcript levels upon bacterial inoculation have shown salt adaption in plants by efficiently activating antioxidant metabolism, reducing stress signals, detoxifying Na^+ ions, and effectively assimilating carbon and nitrogen [79]. Likewise, Morcillo *et al.* (2021) showed that *Priestia megaterium* TG1-E1 mitigates drought stress in tomato plants through comparative transcriptomics analysis. Comparison between the transcriptomes of drought-stressed plants with and without TG1-E1 inoculation revealed bacteria-induced transcriptome reprogramming, which highlights the role of differentially expressed genes belonging to the functional categories, including transcription factors, signal transduction, and cell wall biogenesis and organization [80]. In another study, a transcriptomic study reveals salt stress alleviation in cotton plants upon inoculation of salt-tolerant PGPR *Bacillus subtilis* and *Bacillus pumilus*. Their finding revealed that plant hormone signal pathways were expressed upon PGPR inoculation along with other metabolic pathways [81].

PGPR inoculation also regulates gene expression of stress-responsive genes in host plants. For instance, inoculation of PGPR strains *Klebsiella* sp. IG 3, *Enterobacter ludwigii* IG 10, and *Flavobacterium* sp. IG 15 up-regulated stress-related genes *DREB2A* and *CAT1* in wheat plants exposed to drought stress [28]. Similarly, Barnwal *et al.* (2017) reported that PGPR *Arthrobacter protophormiae* (SA3) and *Dietzia natronolimnaea* (STR1) enhance salt and drought tolerance in wheat crops by altering endogenous phytohormone levels and modulating

the expression of *TaCTR1/ TaDREB2* [82]. The *CAT1* gene encodes a catalase responsible for the elimination of H_2O_2 and ascorbate peroxidases, whereas the *DREB2* gene encodes for a transcription factor that interacts with promoter regions of genes involved in drought stress responses, regulating their expression and thus enhancing plant tolerance. Furthermore, Ali and the group did transcriptomic profiling of maize (*Zea mays* L.) seedlings in response to *Pseudomonas putida* stain FBKV2 inoculation under drought stress, and they found that the genes involved in ethylene biosynthesis, abscisic acid, and auxin signaling, catalase, superoxide dismutase, and peroxidase were downregulated whereas genes involved in β-alanine and choline biosynthesis, heat shock proteins, and late embryogenesis abundant (LEA) proteins were upregulated in FBKV2-inoculated seedlings [83].

Proteomics: Proteins play a vital role in shaping the phenotypic trait during plant stress response. Proteins are directly involved in plant stress response both as structural and regulatory proteins as they regulate plant epigenome, transcriptome, and metabolome. Moreover, protein function depends not only on its molecular structure but also on its cellular localization, post-translational modifications, and interacting partners. At the proteome level, drought is known to induce impairment in cellular metabolism, including photosynthesis, resulting in alterations of several photosynthesis-related proteins (RuBisCo large subunit, FBP aldolase), leading to an establishment of new homeostasis [84–86]. Also, drought induces differential expression of proteins involved in redox regulation, oxidative defense system, amino acid metabolism, carbon metabolism, and molecular chaperone [87]. Moreover, ABA-responsive marker proteins, such as LEA proteins and PP2C family phosphatases, are strongly augmented in different plant species in response to ABA and drought stress and constitute the core proteins of ABA signalling pathways. In addition, numerous proteins involved in secondary metabolism, including those related to jasmonic acid, are increased in response to ABA treatment under drought stress [88].

Proteomic analysis helps identify proteins, which reveal quantitative or qualitative differences between control and stress treatments. These proteins might play an important role in plant stress response [85]. Also, proteomics is a widely used technique to decipher plant-microbe interactions which are based on the knowledge of isolation, characterization, and identification of complete sets of proteins taking part in the process inside a cell at a given time under specific conditions. Proteomic study also helps explore various physiological processes and protein-protein interactions in plants and microbes. The structure and function of proteins involved in plant-microbe interactions are investigated through large-scale proteomics technology

involving liquid chromatography-tandem mass spectrometry (LC-MS) in a complex biological sample [89]. Implication of proteomics studies in host-microbe interaction led to the generation of a deeper understanding of how a biological system is regulated. Proteomic studies help in the identification of several proteins that act as signal molecules to physiological changes occurring due to stress as well as to a factor that is responsible for stress alleviation. Therefore, a comparative proteomic analysis in non-stressed, stressed, and microbe-associated/inoculated plants can help to identify protein targets and networks [70]. The various approaches for proteomic analysis include protein/peptide separation and identification and can also provide quantification and the characterization of post-translational modifications [72, 90]. Proteomic studies for abiotic stress responses have been studied extensively in plants including Arabidopsis (*Arabidopsis thaliana*), rice (Oryza *sativa*), wheat (*Triticum aestivum*), barley (*Hordeum vulgare*), Maize (*Zea mays*), soybean (*Soybean max*), common bean (*Phaseolus vulgaris*), pea (*Pisum sativum*), oilseed rape (*Brassica napus*), potato (*Solanum tuberosum*) and tomato (*Lycopersicon esculentum*) and have reflected dynamic alteration in protein metabolism, proteins of various signalling and regulator pathways, transcription factors, and structural and functional proteins (as reviewed by [70]).

Proteomic studies involve gel-based and gel-free separation techniques. The gel-based separation technique involves the separation of proteins based on their molecular weight and isoelectric point (p*I*) using two-dimensional electrophoresis (2DE), followed by identification and characterization of resolved proteins by mass spectrometry (M.S.). Although a significant amount of information has been gained from the classical gel-based separation technique, it has some limitations like visualization of proteins in 2DE is difficult, multiple protein spots with similar isoelectric point (p*I*) renders comparative quantification rather inaccurate. Other limitations include reproducibility, extreme pH, or hydrophobic proteins, and automation [89].

While gel-based separation is still frequently used for its simplicity, gel-free separation techniques have become standard for large-scale proteomics. Most gel-free methods utilize multidimensional protein identification technology of liquid chromatography (L.C.) for peptide separation, as extensive prefractionation of peptide mixtures significantly increases proteome coverage with MS-based peptide sequencing. Strong cation exchange (SCX) combined with reversed-phase (RP) chromatography is the most used LC technique, but other complementary forms of peptide separation also exist [90].

For unbiased protein identification, Mass Spectrometry (MS) is the most common and widely used technique for plant-microbe proteomics, with matrix-assisted laser desorption/ionization (MALDI) and electrospray ionization (ESI) as major protein/peptide ionization techniques whereas time-of-flight (TOF), quadrupole, ion trap, orbitrap, and Fourier transform ion cyclotron resonance (FT-ICR) as mass analysers. Further, quantification of proteomes can be performed either through stable isotope labelling or label-free methods. Labelling methods include the isotope-coded affinity tag (ICAT) and isobaric tag for relative and absolute quantification (iTRAQ). Other labelling techniques include Stable isotope labelling of amino acids in cell culture (SILAC) and metabolic labelling through stable isotope of nitrogen (^{15}N inorganic salts). Since the cost is an important factor, quantification labelling techniques are less preferred being costlier in comparison to label-free methods, which are time-consuming. MS/MS-based label-free quantification strategy includes sequential windowed acquisition of all theoretical fragment ion mass spectra (SWATH). SWATH™ permits the differentiation of isobaric peptides, followed by data mining of unpredicted species [71].

Proteomic studies in different plant species under drought stress are well documented by many researchers [91–94], including in wheat [95–100]. To investigate the mechanism of the plant-PGPR interaction proteomic approach was conducted by several researchers. Also, a proteomic approach was used to study how PGPR helps plants to mitigate environmental stress (Table 1.2). The proteomic analysis revealed that PGPR influences the expression levels of diverse proteins involved in plant growth promotion, plant pathogen inhibition, photosynthesis, and antioxidative processes, and transportation across membranes [101]. Banaei-Asl *et al.* (2015) have reported that *Pseudomonas fluorescens* helped the canola plant (*Brassica* sp.) to tolerate salinity stress through the enrichment of proteins related to energy metabolism and cell division [102]. Singh *et al.* (2017) reported that the wheat plant inoculated with the *Klebsiella* sp. SBP-8 under salinity stress had expressed proteins that govern osmotic homeostasis, defense activation, cell wall strengthening, ion transportation, and photosynthesis functioning to confer stress resistance [103]. To the best of our knowledge, comparative proteomic approach to study plant-microbe interaction under environmental stress is not well explored, especially in wheat under drought stress (Table 1.2).

Table 1.2. Proteomic study to investigate plant- PGPR interaction.

Plant	Bacteria	Abiotic Stress	Methodology	Reference
Wheat (*Triticum aestivum)*	*Bacillus velezensis* 5113	Heat, cold/freezing and Drought	2D PAGE-MS	Abd El-Daim *et al.*, 2019 [114]
Rice (*Oryza sativa)*	*Azotobacter chroococcum* W5 and A41	No stress	LC-MS/MS	Bandyopadhyay *et al.*, 2022 [109]
Canola (*Brassica napus)*	*Pseudomonas fluorescens* FY32	Salinity	Nano-liquid chromatograph by MS	Banaei-Asl *et al.*, 2015 [102]
Canola (*Brassica napus)*	*Pseudomonas putida* UW4	Salinity	2-DE MS	Cheng *et al.*, 2012 [115]
Sorghum bicolor	*Pseudomonas* sp.	No stress	LC-MS/MS	Dhawi, 2020 [113]
Nicotiana tabacum	*Bacillus* sp. JS	No stress	2-DE MALDI-TOF	Kim *et al.*, 2018 [112]
Maize **(***Zea mays)* and Tomato (*Solanum lycopersicum)*	*Azospirillum brasilense* sp7	No stress	2D-PAGE MALDI-TOF MALDI-TOF/TOF	Lade *et al.*, 2018 [105]
Arabidopsis thaliana	*Herbaspirillum seropedicae*	No stress	ESI-LC-MS/MS	Leandro *et al.*, 2019 [107]
Pepper (*Capsicum annuum* L.)	*Bacillus licheniformis* K11	Drought	2D-PAGE MALDI-TOF	Lim & Kim, 2013 [116]
Rice (*Oryza sativa)*	*Stenotrophomonas maltophilla* and *Bacillus* sp.	No stress	2D PAGE-MS	Naher *et al.*, 2018 [106]
Soyabean (Glycine max)	*Bradyrhizobium japonicum*	No stress	iTRAQ nanoRPLC-MS/MS (Phosphoproteome analysis)	Nguyen *et al.*, 2012 [111]
Maize (*Zea mays)*	*Herbaspirillum seropedicae*	No stress	Nano LTQ-Orbitrap	Nunes *et al.*, 2021 [110]
Wheat (*Triticum aestivum)*	*Enterobacter cloacae* SBP-8	Salinity	MS/MS analysis	Singh *et al.*, 2017 [103]
Wheat (*Triticum aestivum)*	*Ralstonia eutropha* Q2-8	Heavy metal (Cadmium and Arsenic)	iTRAQ nanoLC-MSMS	Wang *et al.*, 2018 [117]
Arabidopsis thaliana	*Kosakonia radicincitans* DSM 16656	No stress	2-DE nanoLC-ESI-MS/MS	Witzel *et al.*, 2017 [108]
Wheat (*Triticum aestivum)*	*Bacillus subtilis*	No stress	Nano-liquid chromatograph by MS	Yadav *et al.*, 2022 [104]

Metabolomics: The metabolome of an organism directly correlates with diverse pathways operating in the cell, which in turn reflects the availability of corresponding genetic information. The metabolome varies largely with alterations in the surrounding environment that induce direct physiological changes in a plant. Therefore, differential metabolomics is important to acquire detailed knowledge of the metabolome of an organism both in normal and under stress, which helps identify typical signature metabolites required for stress tolerance. This will help identify alterations induced within the pathways and induction of typical stress-inducible genes. Plant metabolome study will help in the identification of various signal molecules secreted by plants to attract and induce important biochemical pathways in colonizing microbial populations [70].

Targeted or untargeted metabolomics can be used to measure changes in specific metabolite levels in response to a given treatment. Mass spectrometry (MS) and nuclear magnetic resonance (NMR) are major approaches to study metabolites in a plant in response to different environmental conditions [72]. The high-throughput mass spectrometric profiling of cellular metabolites of plant-associated microbes under the influence of stressors could reveal the level of interference by the stressor in the overall cellular homeostasis. For instance, Kalozoumis *et al.* (2021) did a metabolomics analysis of tomato leaf upon inoculation with PGPR *Enterobacter mori* strain C3.1 under water and nutrient stress and revealed that combined stress affects several stress-related metabolites, including trehalose, myoinositol, and mono palmitin [118].

1.7 Role of Microbiome in Stress Amelioration

The plant microbiomes (rhizospheric, endophytic, and phyllospheric) and microbiomes of extreme habitat (halophilic, acidophilic, alkaliphilic, psychrophilic, thermophilic, and xerophilic) with plant growth promoting (PGP) attributes, are natural bioresource, which play crucial roles in the maintaining global nutrient balance and ecosystem functions. They have emerged as an important and promising tool to enhance plant growth, crop yield, and soil fertility [119]. The complex microbiome in the rhizosphere is influenced by various climatic conditions such as drought, temperature, salinity, etc., of soil and biotic factors, and physical factors, including the presence of metal ions and organic compounds. Host plants' exudates also influence the microbial diversity in the rhizosphere. Hence, exploring both cultivable and uncultivable plant microbiomes can enrich our understanding of plant-microbial ecology and their interaction within the community under changes in environmental conditions.

Metagenomics has enabled researchers to understand microbial ecology and functional genetic diversity of various microbes and their interaction with the environment [120].

Metagenomics helps in the real-time characterization of complex microbial communities in environmental samples through nucleotide sequencing. The Metagenomics approach has enabled one to acquire data related to the habitat-specific distribution of microbial communities with their PGP, biocontrol, antibiotic-producing, and xenobiotic degrading characteristics. For metagenomics analysis, targeted or shotgun sequencing are the two main approaches: using one or the other approach largely depends on the type of environmental studies to be performed. This technique helps discover new species along with their taxonomic profile. DNA sequence data generated through Next generation sequencing (NGS) helps to study plants with respect to their taxonomy, ecological function, and interactome involving genomics, transcriptomics, and metabolomics studies of microbes, which will eventually lead to the identification of the mechanism for their survival and interactions [71, 72]. For instance, Xu *et al.* (2021) used genome-resolved metagenomics to explore microbial properties associated with drought enrichment phenotypes in the sorghum rhizosphere. They identified carbohydrate and secondary metabolite transport and metabolism as pathways related to bacterial enrichment under drought [121]. They also revealed that bacterial iron transport and metabolism functionality is highly associated with drought enrichment. They have demonstrated that drought stress impacted the iron homeostasis within the root and that the loss of a plant phytosiderophore iron transporter affected microbial community composition, leading to significant increases in Actinobacteria. Finally, they revealed that application of iron exogenously, disrupts the drought-induced enrichment of Actinobacteria, as well as their improvement in host phenotype during drought stress. Another metagenomic study revealed the soil microbiome's drought tolerance and found that they promote plant growth through higher production of phytohormone, IAA [122]. Their findings suggested that there was a reliable link between the phenotype and genotype of the soil microbiome that could explain mechanisms of plant growth promotion under drought. Methe *et al.* (2020) used short-read metagenomic sequencing to study maize phyllosphere microbiomes under drought stress across three physically different locations. They revealed a wide variety of metabolic and regulatory processes that differed in drought and normal water conditions and provided key baseline information for future selective breeding [123]. Although several studies have been conducted on soil microbiomes under different environmental stress conditions, different farming conditions, and on different plant species, yet the information is varied depending on degree of

stress experienced as well as soil type. Moreover, further studies are required to study the entire microbe-microbe, plant-microbe and microbe-environment interactions that are highly complicated and complex. Further, the collective effect of the different parameters or stressors conditions on the soil microbiome is still lacking. Identification of microorganisms that are effective against biotic and abiotic stresses can be used as a consortium to improve host plant growth, development, productivity, and tolerance/resistance, which in turn helps in understanding the array of processes and genes turned on in response to induced systemic resistance (ISR) and systemic acquired resistance (SAR) in plants [124].

1.8 Gaps in Existing Research

Although the role of PGPR in ameliorating abiotic stresses, including drought stress, has been demonstrated in earlier work, the application of these bacteria at the field level still needs exploration of efficient inoculants and optimization of appropriate formulation to attain optimal growth under drought conditions. Moreover, PGPR is known to promote plant growth and mitigate deleterious effects of abiotic stressors through different mechanisms described in earlier sections. To ameliorate abiotic stressors like drought stress, PGPR must modulate their physiological status through changes in stress-related genes and metabolites. They can also induce molecular and metabolic changes in the host cells to protect from stress-induced damage and influence plant growth under abiotic stress. However, only a few studies have been carried out to track changes at molecular and metabolite levels in PGPR interacting with plants under drought stress to improve plant growth. Therefore, the present work aimed to characterize the efficient drought-tolerant bacteria from the rhizosphere of wheat plants growing in Rajasthan, India, and characterize their effect on plant growth under drought stress through functional studies following transcriptomic, proteomic, and metabolomic analysis. Based on the literature survey, the following gaps were identified in the present study.

- Despite several reports of drought-tolerant bacteria, there is a lack of information about the efficient bacteria recovered from the Shekhawati region of Rajasthan (India). The bacteria recovered from this region might have the ability to survive under less water availability. Therefore, in the present study, selected drought-tolerant bacteria were tested for the plant growth-promoting test on the wheat plant under controlled conditions. The ability to enhance plant growth under drought stress can be useful to exploit them as suitable biofertilizer agents.

- There is growing interest in harnessing the potential of stress-resilient PGPR in conferring plant resistance and enhancing crop productivity in drought-affected agroecosystem. A detailed understanding of the complex physiological and biochemical responses will open the avenues to stress adaptation mechanisms of PGPR communities under drought. It will pave the way for rhizosphere engineering through metabolically engineered PGPR. Therefore, to reveal the physiological and metabolic networks in response to drought-mediated osmotic stress, the current study focused on investigating the stress adaptation mechanisms of a selected PGPR.

- As the PGPR are known to modulate the physiological responses of plants to stressors, analysing changes in proteomic profiles driven by PGPR under stress conditions will highlight the mechanistic insights of how PGPR helps in mitigating the effects of drought stress. Proteomic approaches can elucidate a better discretion of interactions occurring between the host plant, PGPR, and environmental stress at the molecular level. Applying proteomic techniques will unravel stress-related and antioxidant proteins expressed amid plant-microbe interactions under drought stress. Though the changes in proteomic profiles have been investigated in plants growing under drought stress, to the best of our knowledge, it has not been well explored in response to PGPR inoculation under drought stress.

Anticipating the gap of knowledge in current research, our present work aimed to isolate efficient PGPR from plants growing in drought soil of western Rajasthan, India followed by their plant growth-stimulating effect on wheat plants in pots under drought stress conditions. We also intended to carry out an in-depth analysis (both qualitative and quantitative) of osmolytes and other metabolites produced in response to PGPR application in wheat plants grown under drought stress. Further, we studied proteome of wheat crop in response to drought stress and their alteration by PGPR, which has not been well-explored to the best of our knowledge. Regulation of physio- biochemical response of wheat crop under drought stress in the presence of efficient PGPR can be used as a suitable stress marker for the selection process.

1.9 Objective of the Proposed Research:

This research addresses the role of different mechanisms like phytohormones, ACC deaminase enzyme activity, and osmolyte synthesis in the isolated bacterial strains that strongly affect the competitiveness of organisms in the environment and plant growth promotion activity. Moreover, experimental evidence supports that bacteria with drought-tolerant ability might be

a good biofertilizer for plants growing under stress conditions. Thus, the objectives of this research work were as follows:

1. Isolation of drought-tolerant bacteria from wheat rhizosphere and their characterization for plant growth promoting effects on wheat plants under drought stress.

2. Characterization of stress-responsive mechanism(s) under drought stress in selected isolate employing metabolomics analysis.

3. Studying the effect of PGPR on gene expression of stress-related genes and metabolites in host plants under drought stress.

4. Investigating the effect of PGPR on the physiology of host plants employing proteomic approaches.

CHAPTER II

Isolation of Drought-tolerant Bacteria from Wheat Rhizosphere and their Characterization for Plant Growth Promoting Effects on Wheat Plant under Drought Stress

Part of this study has been published as – "**Arora, S**., Jha, P.N. Drought-Tolerant *Enterobacter bugandensis* WRS7 Induces Systemic Tolerance in *Triticum aestivum* L. (Wheat) Under Drought Conditions. J Plant Growth Regul (2023). https://doi.org/10.1007/s00344-023-11044-6"

2.1 Introduction

Expanding industrialization, urbanization, and increasing human population have a direct impact on the environment as well as on arable land that can be used for different agricultural practices [125]. Moreover, both biotic and abiotic stressors, including drought, salinity, flooding, heavy metals, temperature, and organic contaminants, adversely affect plant health, thus decreasing the yield of crops at large scale. Drought, as an extreme condition, severely affects plant growth and food production globally. Fundamental changes to the water cycle, particularly the patterns of rainfall and periods of drought, have enhanced drought risk and forced farmers to make adjustments in rainfed and irrigated crop production [126]. According to FAO, over 34% of crop and livestock production loss incurred due to drought between 2008 and 2018 in least-developed countries (LDCs) and low to middle-income countries (LMICs). Owing to deviated monsoon rains, depleted groundwater, and increasing population, India is at higher risk. Being an agricultural country, it can affect a large number of agricultural commodities. Further, an increase in temperature is expected to reduce the soil water level, leading to an increase in drought occurrence. India contributes around 109.59 million tons of wheat globally but as per the agriculture ministry data, wheat production declined by almost 3% to 106.84 million tonnes due to environmental factors during the 2021-22 crop year.

Wheat (*Triticum aestivum* L) is an important cereal and staple crop globally, consumed daily by the human population as a main source of protein and carbohydrates. Since wheat is a water-intensive crop, drought stress negatively impacts its production, including overall yield and grain quality, causing huge economic losses worldwide [1, 10, 28]. It reduces plant growth by decreasing water uptake and interrupting many physio-biochemical processes, including photosynthesis, carbon assimilation, nutrient uptake, plant growth, and development. Drought adversely affects CO_2 assimilation and transpiration rate, stomata closure, and relative water content (RWC), affecting wheat growth and productivity [127]. Therefore, measures to overcome drought stress must be addressed.

The most feasible and cost-effective approach to overcome drought-mediated crop loss is the application of PGPR, which is capable of ameliorating drought stress in plants. Such PGPR can alleviate abiotic stress in addition to plant growth through properties like phytohormone production and macronutrient supplementation and protect plants from the deleterious effects of environmental stresses, including drought [27, 28]. The application of PGPR is a promising, eco-friendly, and cost-effective alternative to developing productive and sustainable

agriculture despite environmental stress [31]. As mentioned in chapter 1, section 1.5, rhizobacteria can induce drought endurance and resilience through various direct and indirect mechanisms.

The importance of several PGPR to withstand drought have been reported by several researchers in the past few decades. For instance, *Priestia megaterium* MU2 isolated from semi-arid conditions promotes wheat plant growth under drought conditions [27]. Exopolysaccharide secreting PGPR and plant growth hormone, salicylic acid can improve wheat plant growth under drought stress [29]. Therefore, the understanding of plant growth-promoting bacteria with drought-tolerant ability can be utilized to ameliorate the stress conditions as well as to enhance the growth and yield of the plant. Many drought-tolerant bacterial strains have been isolated from different plant crops by different research groups (Table 1.1) [27, 31, 37, 128]. Though there are studies reporting the PGPR-mediated drought stress amelioration in wheat plants, exploration of more efficient PGPR is still required, which can be used as efficient and suitable bioinoculants for protecting plants from adverse effects of drought and as a better approach towards sustainable agriculture to a certain extent. Therefore, the present work aimed to isolate efficient drought-tolerant bacteria from wheat crops grown in the Shekhawati region of Rajasthan, India, and to characterize them for their plant growth-promoting activities. Also, the optimization of appropriate bio-formulation has been tested to attain optimal wheat growth under drought conditions.

2.2 Materials and Methods

2.2.1 Isolation of water-stress tolerant rhizobacteria/ endophytic bacteria from wheat rhizosphere

Healthy wheat plants (*Triticum aestiv*um L.) were carefully uprooted from cultivated fields of Pilani (28.37°N 75.6°E), Rajasthan, India, in January 2019. To isolate rhizospheric bacteria, 10 g of rhizospheric soil adhered to roots was weighed, added to 50 ml of 0.85% sodium saline, and kept on a shaker for mixing. The soil was allowed to settle, and 1 ml aliquot was inoculated to nutrient broth (NB) media containing 10% of polyethylene glycol (PEG-6000) and incubated at 30°C for 24 h on a shaker at 200 rpm to enrich water stress-tolerant bacteria. PEG was added to the medium to induce drought stress [129]. One ml of the above culture was re-inoculated in NB media containing 10% PEG and incubated as above-stated culture conditions. The culture suspension was serial diluted up to 10^{-6} dilution, and 100 µl of the final dilution was

plated onto a solid NB-agar medium containing 10% PEG. The inoculated plates were incubated at 30 °C for 72 h. Bacterial colonies growing on the above selective medium were aseptically picked, sub-cultured, and maintained for further use.

For isolation of endophytic bacteria, plant roots were rinsed with tap water for 2-3 h, followed by surface sterilization with tween-20 and 0.1% $HgCl_2$ for 1 min [130]. Roots were crushed in saline with a sterile motor and pestle. The process for enrichment, isolation, and selection of endophytic bacteria was followed as per the method described above.

2.2.2 Molecular characterization of water-stress tolerant rhizobacteria/ endophytic bacteria from wheat rhizosphere

For molecular identification, the genomic DNA of the bacterial isolate was extracted using a genomic DNA extraction kit (Qiagen, USA) as per the manufacturer's instructions. 16S rRNA gene was amplified by PCR using a standard method [17]. The rRNA gene was sequenced by Sanger Sequencing at Delhi University, South Campus India. The nucleotide sequence was compared against the GenBank database using the NCBI-BLAST algorithm and deposited in the NCBI database (http://www.ncbi.nlm.nih.gov/BLAST). A phylogenetic tree was constructed using the Neighbour-Joining (NJ) method with a bootstrap value 500 in MEGA 6.0 [131].

2.2.3 Biochemical characterization and antibiotic-resistant profile of isolated strains

Biochemical assays, including Gram staining, IMViC (Indole, Methyl Red, Voges Proskauer, Citrate utilization) test, and enzyme assays such as catalase, chitinase, lipase, and amylase were performed following standard protocols [132]. Further, antibiotic sensitivity against standard antibiotics such as streptomycin (10 µg), tetracycline (10 µg), kanamycin (30 µg), ampicillin (10 µg), chloramphenicol (10 µg), and gentamycin (30 µg) were tested using antibiotic discs (HTM 002, Hi-media). Briefly, the bacterial culture was spread onto Nutrient Agar media plates. The standard antibiotic disc (6 mm) was placed on the surface of the media, and the plates were incubated at 37 °C for 24 h. All the experiments were performed in triplicate. The results were interpreted by measuring the zone of inhibition diameter using a zone size interpretative chart provided by the manufacturer (Himedia).

An ability of the isolates to utilize different carbohydrates such as xylose, maltose, fructose, dextrose, galactose, raffinose, trehalose, sucrose, L-arabinose, mannose, glycerol, salicin,

inositol, sorbitol, mannitol, adonitol, α-Methyl-D-glucoside, rhamnose, cellobiose, ONPG, esculin hydrolysis, D-arabinose, sorbose, inulin, and mannose was tested using carbohydrate utilization test kit (KB 009, Himedia) as per instruction of the manual.

2.2.4 Test of hydrolytic activity

Cellulolytic activity: The production of cellulase by the isolates was tested usg Gram's iodine method with slight modifications [133]. Bacterial cultures were point-inoculated onto minimal-agar medium supplemented with 0.2% carboxymethyl cellulose (CMC) and 0.3% tryptone and incubated at 30 °C for four days. Gram's Iodine solution was poured onto the bacterial growth and kept for 5 min at room temperature till the appearance of a clear halo zone. The result was interpreted based on the diameter of the clear zone. Further, to measure the cellobiohydrolase and glucosidase activity, bacterial culture in its log phase were spot inoculated on $JNFb^-$ agar plates containing 0.5 mM ammonium chloride and ethanol (6 ml l^{-1}) as nitrogen and carbon sources, respectively. The plates were incubated at 30 °C for 3 days. Overlay containing 8 ml of 0.05 M potassium phosphate (pH 7.0), 0.7% agarose, and 0.5 µg/ml 4-methylumbelliferyl-β-cellobioside (MUC) (for glucosidase activity instead of MUC 4-methyllumbelliferyl-β-D glucoside (MUG) was used) was applied on the plates and further incubated for 4 to 10 h. Then, the plates were illuminated to UV light (302 nm) on a UV-trans-illuminator, and the active colonies were identified by the appearance of violet fluorescence [134].

Test for pectinolytic activity: For the pectinase test, actively grown bacterial cultures were spot-inoculated on NA plates containing 0.5% pectin and incubated at 30 °C 72 h. Colonies appearing on plates were overlaid with 2% CTAB (N-cetyl-N, N, N trimethyl-ammonium bromide) and further incubated for 30 min at 30 °C, followed by washing with 1 N NaOH thrice. Plates were then screened for the appearance of clear zones around the colonies.

Test for lipase and amylase activity: Lipase activity was determined by streaking the bacterial isolates on LB agar plates containing 0.5% tributyrin. Plates were then incubated at 30 °C in an incubator shaker. The presence of a halo zone around the streaked colony was considered lipase-positive. For amylase assay, bacterial culture was spot-inoculated on 1% starch-agar plates and incubated at 28±2 °C for 48 h. Colonies surrounded by a clear halo upon adding iodine solution were considered positive for amylase production.

2.2.5 Test of Plant growth-promoting (PGP) activities

Phosphate Solubilization: For the Phosphate solubilization assay, freshly grown bacterial culture was point inoculated on NBRIP (National Botanical Research Institute's Phosphate) medium containing insoluble tricalcium phosphate as the sole phosphate source and incubated at 28 °C for 4 days. A clear zone formed around the inoculated culture was considered positive for phosphate solubilization activity [135]. For the quantification assay, 1.5 ml of a 3-day-old culture grown in NBRIP media was pelleted down to 10,000 g for 2 min. The supernatant was collected, and 3.5 ml of reagent C (mentioned below) was added to it, appropriately mixed, and incubated at room temperature for 1 h. Absorption of the resultant reaction mixture was measured at 660 nm against blank. A standard curve was prepared using varying concentrations (0-50 µg/ml) of K_2HPO_4 [136].

Reagents used for the quantification of phosphate:

Reagent A: 10% Ascorbic acid (stored at 4 °C)
Reagent B: 42% Ammonium molybdate in 1 N H_2SO_4
Reagent C: 1 part of Reagent A and 5 parts of Reagent B

Indole-3-acetic acid (IAA) production: The standard method of [137] was followed to determine the ability of bacterial isolates to produce IAA. Bacterial cultures were grown in Nutrient broth supplemented with 100 µg/ml of tryptophan for 72 h at 30 °C at 180 rpm. IAA production was then determined by the Salkowski Method [138]. Stationary phase culture (1.5 ml) was collected and centrifuged at 10,000 g for 2 min. To 1 ml of the supernatant, 2 ml of the freshly prepared Salkowski reagent was added and kept for 30 min at RT. The development of the cherry-red color was considered a positive test of IAA production. An absorbance of the resultant reaction mixture was measured at 530 nm for quantification of IAA. Different concentration (0- 100 µg/ml) of pure IAA was used for standard curve preparation.

Salkowski reagent preparation:
Solution A: 2 ml of 0.5M $FeCl_3$ in 49 ml of distilled water
Solution B: 49 ml of 70% perchloric acid
Prepared solutions A and B separately and mixed as per the requirement.

Siderophore Production: Siderophore production by the bacterial isolates was assayed using the standard chrome azurole S (CAS)-agar method [139, 140]. The bacterial culture was spot inoculated on the CAS-agar plates and incubated at 30 °C for 5-6 days. The development of a

yellow-orange halo zone around the bacterial growth was considered a positive test for siderophore production. The efficiency of siderophore production was measured by calculating the siderophore index using the formula (Ds-Dc)/Ds, where Ds and Dc refer to colony diameter (in mm) and clear zone diameter (in mm), respectively.

The composition of chrome azurole S (CAS) dye is as follow:
Solution 1: Dissolve 0.06 g of CAS in 50 ml of distilled water
Solution 2: Dissolve 1 mM of $FeCl_3.6H_2O$ in 10 ml of 10 mM HCl
Solution 3: Dissolve 0.073 g of CTAB in 40 ml of distilled water

Dye preparation: Firstly, above-prepared solution 1 and solution 2 were mixed. Then solution 3 was added for the appearance of a blue colour. Dye was autoclaved and stored in a plastic container.

ACC deaminase activity: ACC deaminase activity of the bacterial isolates was quantified following the method of [141]. Bacterial cells were grown in 15 ml of Tryptic soy broth up to the late-log phase in a shaking water bath at 200 rpm at 30 ℃. Bacterial cells were collected by centrifugation at 8000g for 10 min at 4 ℃. The supernatant was removed, and the cells were washed with Dworkin and Foster (DF) salt minimal media and then resuspended in 10 ml of DF salt minimal media. To induce ACC deaminase activity, 60 µl of 0.5 M ACC was added to cell suspension just before incubation and incubated in a shaking water bath at 200 rpm for 24 h at 30 ℃. The bacterial cells were harvested by centrifugation, washed twice with 0.1 M Tris-HCl (pH 7.6), and resuspended in 0.1 M Tris-HCl (pH 8.5). Bacterial cells were lysed with 30 µl of toluene and vortexed at high speed for 30 s, and toluenized cell suspension was used immediately for ACC deaminase assay.

For ACC deaminase assay, to the 200 µl of toluenized cells, 20 µl of 0.5 M ACC was added, briefly vortexed, and then incubated at 30 ℃ for 15 min. Further, 1 ml of 0.56 M HCl was added to the reaction mixture, mixed by vortexing, and centrifuged for 5 min at 8000 g at RT. One ml of the resulting supernatant was mixed with 800 µl of 0.56 M HCl. Thereupon, 300 µl of 2,4- dinitrophenylhydrazine (0.2% 2,4- dinitrophenylhydrazine in 2 M HCl) was added to the above mixture in a glass tube and incubated at 30 ℃ for 30 min. Following this, 2 ml of 2 N NaOH was added, and the absorbance was measured at 540 nm in a spectrophotometer. The number of µmol of α- ketobutyrate produced is determined by comparing the absorbance of the samples to the standard curve of α- ketobutyrate (0.1 to 1.0 µmol) at 540 nm. The quantified ACC deaminase was expressed in terms of µmol α-ketobutyrate/mg protein/h.

Preliminary screening for nitrogen fixation: Preliminary screening for nitrogen fixation of bacterial isolates was carried out by following the standard protocol of [142]. Bacterial isolates were streaked on JNFb$^-$ medium lacking any organic or inorganic form of combined nitrogen and incubated at 30 ℃ for 48 to 72 h and observed for the appearance of bacterial growth. The composition (g/litre) of JNFb- was as follows. $CaCO_3$ - 1.0, K_2HPO_4 - 1.0, $MgSO_4.7H_2O$ - 0.2, $FeSO_4.7H_2O$ - 0.1, $Na_2MoO_4.2H_2O$ - 0.005, and Sucrose – 5. The pH of the medium was maintained to pH 5.5.

Assay for HCN and ammonia production: Production of HCN and ammonia was determined as these traits show the ability of bacteria to suppress the proliferation of fungi in the soil [143]. To test ammonia production, a freshly grown culture of the bacterial isolates was inoculated into 10 ml peptone water and incubated at 37 ℃ for 48 h. following this, Nessler's reagent (0.5 ml) was added and the development of brown to yellow colour was observed as a positive test for ammonia production [144]. Assessment of HCN production by bacterial isolates was carried out using method of [145]. Each bacterial isolate was inoculated in LB broth amended with 4.4g/l glycine. The sterile filter paper strip was dipped in picric acid solution (0.5 % picric acid in 2% sodium carbonate) and attached to the neck of the flask. The flasks were plugged and sealed off tightly with parafilm and incubated at 30 ℃ for 4 days at 150 rpm. Non-inoculated flasks were used as a control. A change in colour of filter paper from yellow to brick red was considered a positive test for HCN production. No change in colour was recorded as a negative reaction.

2.2.6 Osmotic stress tolerance test

Since the selected bacterial isolates were to be used to test the effect on ameliorating drought stress, we tested the tolerance of different isolates to hyperosmotic stress. To test the ability of bacterial isolates to grow under a hyperosmotic environment, LB media was supplemented with 10 % polyethylene glycol (PEG-6000). Media without PEG act as a control. The cultures were grown at 30℃ with constant shaking at 150 rpm in an incubator shaker. Bacterial growth was measured by reading the optical density (OD) at 600 nm using a UV-visible spectrophotometer (BioSpectrometer, Eppendorf, Germany). OD_{600} was measured every hour, and then the growth curve was plotted to study its growth pattern.

2.2.7 Test of motility

Considering that motility is required for colonization, different types of motilities, such as swimming, swarming, and twitching of the isolates, were tested using a standard protocol [17, 146]. For the swimming assay, bacterial isolates were inoculated on tryptone swim plates (1% tryptone, 0.5% NaCl, 0.3% agar) with a sterile toothpick and incubated at 25 °C for 16 h. Motility was assessed qualitatively by examining the circular turbid zone formed away from the point of inoculation by the bacterial cells. For swarming assay, the bacterial isolates were spot inoculated on swarm plates (NB media containing 0.5% Bacto- agar and 0.5 % dextrose) and incubated at 30 °C for 24 h. The swarm plates were dried overnight at room temperature before use. To assess twitching motility, bacterial cells were stab-inoculated through a thin layer of (approximately 3 mm) LB agar (1% agar) to the bottom of the Petri dish with a toothpick and incubated at 30 °C for 24 to 48 h. The appearance of the hazy zone of growth at the interface between the agar and the polystyrene surface was observed.

2.2.8 Microbial consortia formation

Bacterial consortia constituting two or more compatible bacteria with different plant growth-promoting properties were formed to study their synergistic or additive effect for ameliorating drought (Table 2.1). To evaluate the compatibility of strains when formulating a bioinoculant for plant growth promotion, cross-streak test between co-inoculated strains were performed.

Table 2.1. Formation of Bacterial consortia based on their plant growth-promoting properties.

S. No.	Consortium	Bacterial Isolate Chosen
1	Consortium I	All the bacterial isolates
2	Consortium II	WRS3 (Phosphate Solubilization & ACC deaminase) + WRS4 (Phosphate Solubilization & Siderophore) + WRS6 (Siderophore)+ WRS7 (IAA)
3	Consortium III	WRS1 (Phosphate Solubilization & ACC deaminase) + WRS3 (Phosphate Solubilization & ACC deaminase) + WRS7 (IAA)
4	Consortium IV	WRS1 (Phosphate Solubilization & ACC deaminase) + WRS5 (Phosphate Solubilization & ACC deaminase) + WRS7 (IAA)

2.2.9 Effect of bacterial isolates on the growth of wheat crop under drought stress

For the experimental studies, healthy and uniform-sized seeds of wheat variety WH1142 were procured from the Indian Institute of Wheat and Barley Research, Karnal (India). For the plant growth-promoting test, the inocula of the individual bacterial isolates and microbial consortia were prepared. The bacterial culture of each isolate was grown in an LB media, and optical

density (OD) at 600 nm was maintained at 0.15 using 1X PBS. For consortia preparation, each bacterial isolate was grown separately, harvested by centrifugation at 8000g for 20 min, washed once, and resuspended in a sterile 1X phosphate buffer saline (PBS) solution. The culture OD was adjusted to attain 2.5×10^3 CFU mL^{-1} for use. Different consortia were prepared by mixing the respective bacterial cell suspensions in equal ratios by volume (Table 2.1).

Wheat seeds were surface sterilized by treating with 0.1% $HgCl_2$ for 1 min, followed by 70% ethanol for 1 min. The sterile seeds were washed five times with distilled water. Surface-sterilized seeds were treated with 2.5×10^3 CFU (colony-forming unit) of bacterial inoculum at room temperature (RT) for 2 h and dried under aseptic conditions. Five seeds were sown in each plastic pot (5″×5″) filled with sterile soil in triplicates and incubated in a plant growth chamber (LabTech, South Korea) with a 16:8 photoperiod at 28 ± 2 °C, the humidity of 70%, and light intensity of 140 µmol m^{-2} s^{-1}. Control seeds were incubated with PBS. Murashige and Skoog (MS) macronutrient solution was applied to soil as a nutrient solution on alternate days. To impose drought stress, plants were not watered after 15 days of germination (plants grown up to the three-leaf stage). After 15 days of stress, plants were harvested, and their growth was measured based on various parameters, such as percent germination, root and shoot length, fresh and dry weight of five randomly collected seedlings, and chlorophyll content. For the measurement of photosynthetic pigments, chlorophyll a/b, 1-g fresh leaf samples were homogenized in 80% acetone, and pigment was extracted and quantified as per the method of [147]. The relative water content (RWC) of wheat plant leaves was determined by following the standard protocol [148].

2.2.9 Statistical Analysis

All the experiments were conducted in triplicates, and results were expressed as mean ± Standard Error Mean (SEM) (n = 3). Data were analysed by analysis of variance (ANOVA) and subsequently by Duncan's multiple range test at $p < 0.05$.

2.3 Results

2.3.1 Isolation and molecular characterization of water-stress tolerant rhizobacteria/ endophytic bacteria from wheat rhizosphere

Bacterial colonies growing actively on NB media supplemented with 10% PEG were selected and sub-cultured several times to enrich water stress-tolerant bacteria. Based on the efficiency

of growing on PEG-containing media and the difference in morphological features, 9 bacterial isolates (8 rhizospheric and 1 endophytic) were selected for the test of plant growth-promoting properties and basic biochemical and molecular characterization. For molecular identification, 1.5 kb of the 16S rRNA gene of the isolates was amplified by PCR and sequenced. The nucleotide sequence was analyzed by comparing it with 16S rRNA genes available at the GenBank database of the National Centre for Biological Information (NCBI) using the BLAST algorithm (http://www.ncbi.nlm.nih.gov/BLAST) to find the closest match to type strain. Based on the sequence similarity, the test isolates were identified as members of different genera, including *Enterobacter, Pseudomonas, Kosakonia, Siccibacter, Acinetobacter,* and *Stenotrophomonas* and a phylogenetic tree was constructed to find diversity amongst them (Figure 2.1). The sequence of the resulting amplicon was submitted to the NCBI GenBank database for the accession number. The various bacterial species isolated in the present study with their accession number are listed in Table 2.2.

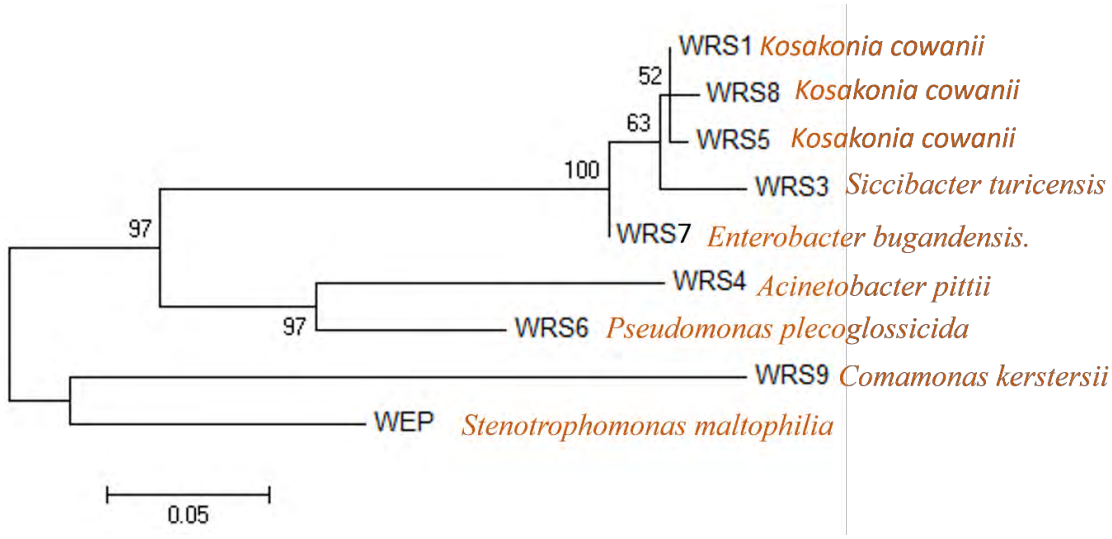

Figure 2.1. A phylogenetic tree was constructed using the Neighbour-Joining (NJ) method with a bootstrap value of 500 to find similarities amongst isolated bacterial species based on 16S rRNA gene sequences. Numbers at the branching points are bootstrap values >50% (percentages of 1000 re-samplings). The bar shows a sequence divergence of 0.05 nucleotides. Evolutionary analysis was conducted using Mega software version 6.0.

Table 2.2. The closest affiliations of the representative isolate in the GenBank according to the 16S rRNA gene sequences.

Isolates	Closest Match[#]	Query Coverage (%)	Percent Identity (%)	Accession Number
WRS1	*Kosakonia cowanii* strain QS24-21	100	99.09	MW453052
WRS3	*Siccibacter turicensis* strain WTB61	100	99.54	MW453053
WRS4	*Acinetobacter pittii* strain Bi	99	98.84	MW453054
WRS5	*Kosakonia cowanii* strain SP1	100	98.87	MW453055
WRS6	*Pseudomonas putida* strain SMB	100	99.73	MW453056
WRS7	*Enterobacter bugandensis* strain XM29	100	99.16	MW453057
WRS8	*Kosakonia cowanii* strain P4	100	98.86	MW453058
WRS9	*Comamonas kerstersii* strain 8943	100	98.82	MW453059
WEP	*Stenotrophomonas maltophilia* strain MGT19	100	99.17	MW453060

 # All closest matches were type strains

2.3.2 Biochemical characterization

All the isolates were screened for various biochemical characteristic features. Results of basic biochemical tests are given in Table 2.3. All the isolates were found to be gram-negative and catalase positive. With respect to the IMViC test, WRS3, WRS4, and WRS9 showed positive results for methyl red, whereas others showed negative results for indole and methyl-red test. Only isolates WRS1 and WRS7 were found to be positive for the Voges-Proskauer test. Isolates WRS3, WRS4, WRS5, and WRS6 were found to be positive for urease production. The Nitrate reductase test was used to determine the ability of an organism to reduce nitrate (NO^{3-}) to nitrite (NO^{2-}) using the enzyme nitrate reductase. Nitrate reductase test was positive for most isolates except for WRS5, WRS6, and WRS8.

Table 2.3 Biochemical characterization of various drought-tolerant bacteria

Isolate	Gram staining	Catalase	Indole	MR	VP	Urease	Nitrate reductase
WRS1	Negative	+	-	-	-	-	+
WRS3	Negative	+	-	+	-	+	+
WRS4	Negative	+	-	+	-	+	+
WRS5	Negative	+	-	-	-	-	+
WRS6	Negative	+	-	-	-	+	-
WRS7	Negative	+	-	-	+	-	+
WRS8	Negative	+	-	-	-	-	+
WRS9	Negative	+	-	+	-	-	+
WEP	Negative	+	-	-	-	-	+

Bacterial isolates were also characterized based on their ability to utilize different carbon sources. Therefore, the recovered isolates were subjected to carbohydrate and substrate utilization tests to evaluate their efficacy in utilizing various substrates. It is evident from Table 2.4 that all the isolates were found to utilize fructose, dextrose, galactose, trehalose, sucrose, mannose, and sorbose. The tested isolates except WEP were found to utilize the xylose and L-L-arabinose. Only WRS5 and WRS7 were able to utilize maltose as a carbon source. A negative result was observed for raffinose in WRS-3,6,8,9 and WEP and for melibiose in WRS8 and WEP. For the substrate utilization test, it is evident from Table 2.5 that all the isolates were found to utilize esculin hydrolysis, whereas none of them utilized adonitol. Except for WRS8, WRS9, and WEP, all showed positive tests for citrate. All tested isolates, but WRS8 showed negative results for phenylalanine deaminase. All tested isolates showed positive results for cellobiose except for WRS6, WRS8, and WEP.

On comparison of three strains of *Kosakonia*- WRS1, WRS5, and WRS8, we found that they are gram-negative and catalase-positive, whereas they showed negative results for Indole and MRVP test. All three isolates gave nitrate reductase test positive but gave urease test negative. Based on the carbon utilization test, all three strains can utilize xylose, fructose, dextrose, galactose, trehalose, sucrose, L-arabinose, mannose, and sorbose. In contrast, raffinose and melibiose were only utilized by WRS1 and WRS5. Also, they were able to utilize different substrates.

Among the antibiotic sensitivity test, most of the isolates were found to be sensitive to streptomycin, gentamycin, and kanamycin except WEP. WRS6 and WEP were resistant to

antibiotic tetracycline. For chloramphenicol, all were sensitive except WRS4 and WRS6, while all were resistant to ampicillin (Table 2.6).

Since hydrolytic activities such as cellulolytic and pectinolytic activities are required for endophytic colonization, the bacterial isolates were tested for the same. WRS3, WRS7, and WEP were found to be positive for cellulase activity. All isolates were cellobiohydrolase positive except for WRS-6, 7, 8, and WEP. Only WRS-1, 6, 8, and 9 showed β- glucosidase activity. WRS-4, 6, 9, and WEP were found to be pectinase positive. Since amylases are required to degrade organic matter in soil (starch), the production of amylase by bacteria is considered as an important plant growth-promoting property. The amylase test was shown by isolates WRS5, WRS6, WRS7 and WRS8. None of the isolates showed lipase activities (Table 2.7).

Table 2.4. Carbohydrate utilization efficacy of drought-tolerant bacterial isolates

Isolate	Xylose	Maltose	Fructose	Dextrose	Galactose	Raffinose	Trehalose	Melibiose	Sucrose	L-Arabinose	Mannose	Sorbose
WRS1	+	-	+	+	+	+	+	+	+	+	+	+
WRS3	+	-	+	+	+	-	+	+	+	+	+	+
WRS4	+	-	+	+	+	+	+	+	+	+	+	+
WRS5	+	+	+	+	+	+	+	+	+	+	+	+
WRS6	+	-	+	+	+	-	+	+	+	+	+	+
WRS7	+	+	+	+	+	+	+	+	+	+	+	+
WRS8	+	-	+	+	+	-	+	-	+	+	+	+
WRS9	+	-	+	+	+	-	+	+	+	+	+	+
WEP	-	-	+	+	+	-	+	-	+	-	+	+

Table 2.5. Substrate utilization efficacy of drought-tolerant bacterial isolates

Isolate	ONPG	Lysine utilization	Ornithine utilization	Phenylalanine deaminase	H_2S production	Citrate	Malonate utilization	Esculin hydrolysis	Adonitol	Rhamnose	Cellobiose	Saccharose
WRS1	+	-	-	-	-	+	-	+	-	+	+	+
WRS3	+	-	-	-	-	+	+	+	-	+	+	+
WRS4	-	-	-	-	-	+	+	+	-	+	+	+
WRS5	-	-	-	-	-	+	+	+	-	+	+	-
WRS6	-	+	-	-	-	+	+	+	-	-	-	+
WRS7	-	-	+	-	-	+	+	+	-	+	+	+
WRS8	-	-	-	+	-	-	+	+	-	-	-	-
WRS9	-	-	+	-	-	-	+	+	-	-	+	+
WEP	-	-	-	-	-	-	-	+	-		--	-

Table 2.6. Antibiotic sensitivity test of bacterial isolates

Isolate	Streptomycin	Tetracycline	Kanamycin	Ampicillin	Chloramphenicol	Gentamycin
WRS1	Sensitive	Moderately Sensitive	Moderately Sensitive	Resistant	Sensitive	Sensitive
WRS3	Sensitive	Moderately Sensitive	Moderately Sensitive	Resistant	Sensitive	Sensitive
WRS4	Sensitive	Sensitive	Moderately Sensitive	Resistant	Resistant	Sensitive
WRS5	Sensitive	Moderately Sensitive	Moderately Sensitive	Resistant	Sensitive	Sensitive
WRS6	Moderately Sensitive	Resistant	Moderately Sensitive	Resistant	Resistant	Sensitive
WRS7	Moderately Sensitive	Moderately Sensitive	Moderately Sensitive	Resistant	Sensitive	Sensitive
WRS8	Sensitive	Moderately Sensitive	Moderately Sensitive	Resistant	Sensitive	Sensitive
WRS9	Moderately Sensitive	Sensitive	Moderately Sensitive	Resistant	Sensitive	Sensitive
WEP	Resistant	Resistant	Resistant	Resistant	Moderately Sensitive	Resistant

Table 2.7. Test of hydrolytic enzymatic assay by drought tolerant bacteria

Isolate	Cellulase	Cellobiohydrolase	β-glucosidase	Pectinase	Amylase	Lipase
WRS1	-	+	+	-	-	-
WRS3	+	+	-	-	-	-
WRS4	-	+	-	+	-	-
WRS5	-	+	-	-	+	-
WRS6	-	-	+	+	+	-
WRS7	+	-	-	-	+	-
WRS8	-	-	+	-	+	-
WRS9	-	+	+	+	-	-
WEP	+	-	-	+	-	-

2.3.3 Test of plant growth promotion (PGP) activities

Bacterial isolates were screened qualitatively and/or quantitatively for their various PGP activities. The results of PGP properties have been summarized in Table 2.8. All the isolates were found to be positive for phosphate solubilization, indole acetic acid production, and ACC deaminase activity, while only WRS4, WRS6, WRS7, and WEP showed positive results for siderophore production. Nitrogen fixation tests were qualitatively evaluated by their growth on nitrogen-free JNFb$^-$ media. Most of the isolates showed dense growth on the JNFb, which indicated positive for nitrogen fixation. Based on the quantitative estimation, the highest

phosphate solubilization was observed in WRS3 (15.19 ± 1.15 µg/ml), followed by WRS1 (13.54 ± 2.25 µg/ml), and WRS7 (12.26 ± 1.72 µg/ml). Similarly, the highest production of indole acetic acid was recorded in WRS7 (1.42 ± 0.12 µg/ml), followed by WRS9 (0.38 ± 0.065 µg/ml) and WRS6 (0.28 ± 0.073 µg/ml). Since the ACC deaminase activity of PGPR appears to be important in inducing systemic tolerance in plants against drought stress, the efficiency of bacterial isolates to utilize ACC as a nitrogen and carbon source was determined quantitatively. WRS3 showed the highest ACCD activity of 1.32 ± 0.011 µmol/mg protein/h., followed by WRS5 (0.78 ± 0.003 µmol/mg protein/h) and WRS1 (0.74 ± 0.014 µmol/mg protein/h). All the isolates showed positive tests for ammonia production but negative results for HCN production. Hence, based on plant growth-promoting properties, WRS1, WRS3, WRS6, and WRS7 were identified as the most potential isolates to promote plant growth.

Table 2.8. Plant growth-promoting features of bacterial isolates.

	Nutrient Uptake			**Phytostimulants**	**Stress Tolerance**	**Biocontrol Activity**
Isolate	**Phosphate solubilization (µg/ml)**	**Siderophore Index**	**N_2 Fixation**	**IAA production (µg/ml)**	**ACC Deaminase activity (µmol/mg protein/h)**	**HCN Production**
WRS1	13.54±2.25	-	+	0.19±0.247	0.74±0.014	-
WRS3	15.19±1.15	-	+	0.14±1.87	1.32±0.011	-
WRS4	7.72±0.03	0.215	+	0.06±0.11	0.46±1.14	-
WRS5	12.77±1.08	-	+	0.16±1.04	0.78±0.003	-
WRS6	8.12±0.09	0.548	+	0.28±0.073	0.51±0.059	-
WRS7	12.26 ±1.72	0.447	+	1.42±0.12	0.46 ± 0.01	-
WRS8	11.62±1.23	-	+	0.15±0.009	0.59±2.14	-
WRS9	2.23±0.19	-	+	0.38±0.065	0.51±0.18	-
WEP	1.37±0.27	0.443	+	0.08±0.17	0.54±1.27	-

2.2.4 Osmotic stress tolerance test

All the bacterial isolates were able to grow in PEG-supplemented culture media, although growth was slower in comparison to the respective untreated control. Their growth pattern is represented in Figure 2.2. At 12 h, growth retardation was seen from 14.68% to 48.8%. WRS5 (14.68% decreased growth) was found to be the most tolerant isolate, followed by WRS4 (20.63%) and WRS7 (35.17%).

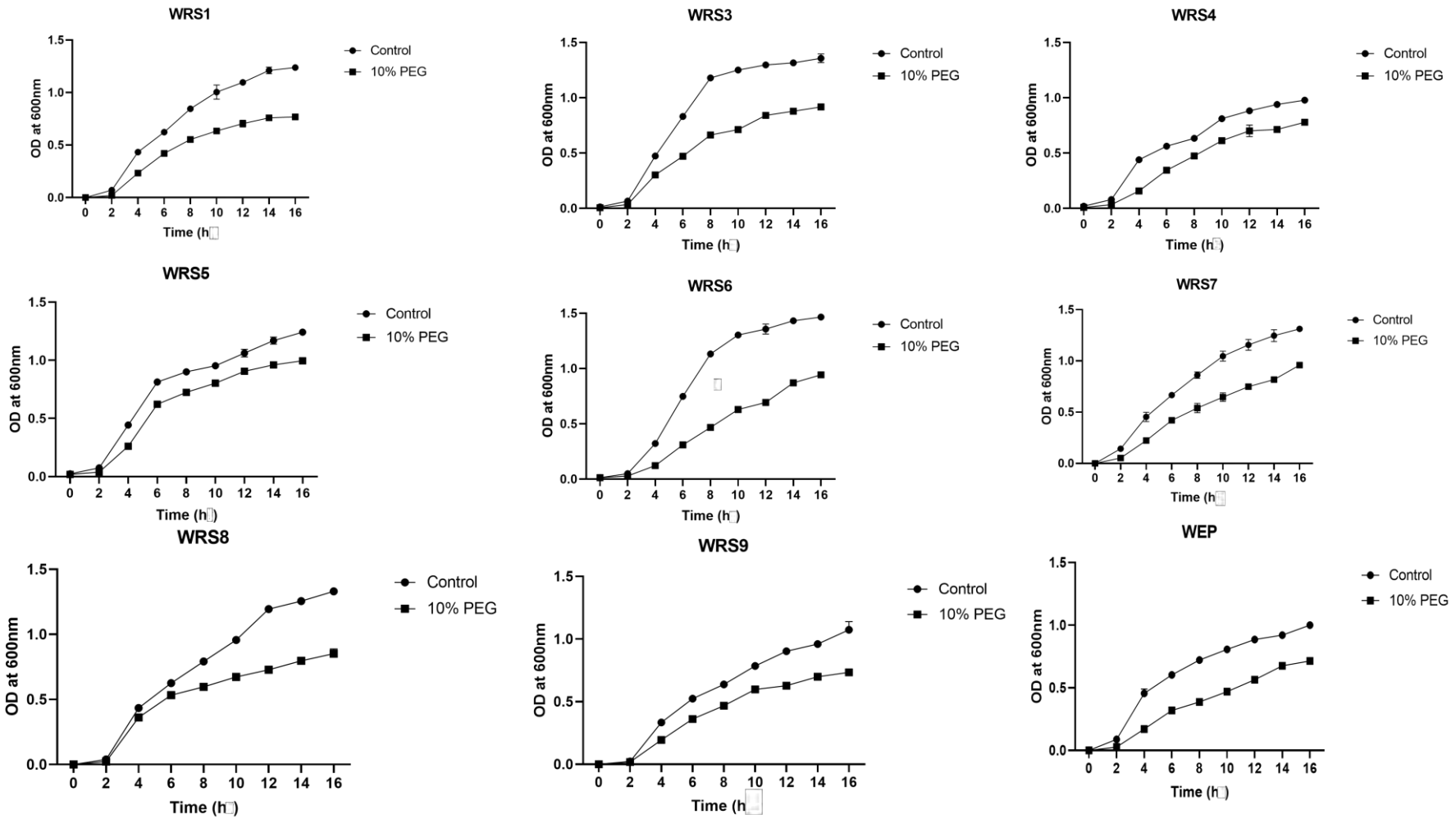

Figure 2.2. Osmotic stress tolerance of bacterial isolates. The ability of bacterial isolates to grow under a hyperosmotic environment was tested in LB media supplemented with 10 % polyethylene glycol (PEG-6000). Media without PEG was used as a control. Bacterial growth was measured by taking the optical density (OD_{600}) of the culture at every 2 h. Each value represents the mean ± SE of 4 replicate samples.

2.3.5 Test of motility

Bacterial motility is required by a microorganism for its successful colonization on or inside the host plant. Therefore, bacterial isolates were screened for three types of motility behaviours: swimming, swarming, and twitching. In the swimming test, bacterial cells formed the circular turbid zone; in swarming, they spread on the media plates, whereas in the case of twitching, the isolates were found to be attached to the media containing plastic plate surfaces. All the strains showed swimming and twitching motility, but strains WRS4, WRS6, WRS9, and WEP lack the swarming motility (Figure 2.3).

2.2.7 Effect of bacterial isolates on the growth of wheat crop under drought Stress

Pot-based plant growth studies were conducted to study the effect of bacterial isolates, individually or synergistically, on drought stress amelioration in the wheat plant. Inoculation with all the isolates significantly increased the growth of wheat plants in terms of various growth parameters tested. It is apparent from Table 2.9 A that the highest significant ($P<0.05$) growth in total length was observed for WRS7 (11.50%) followed by WRS5 (8.68%) as compared to uninoculated control under well-watered conditions. WRS7 was found to be the best isolate which enhanced the increase in all the growth parameters, such as root length (15.94%), shoot height (9.76%), fresh weight (16.46%), dry weight (20.83%), chlorophyll a (33.36%), and chlorophyll b (3.37%) content under well- watered conditions (Table 2.9 A). Similarly, an increase in root length (10.76%), fresh weight (24.49%), and dry weight (33.33%), was observed following inoculation of WRS5.

Following induction of drought stress, the reduction in shoot length (17.75%), root length (44.29%), fresh weight (27.71%), dry weight (25%), chlorophyll a (23.17%), and chlorophyll b (17.40%) was observed in control plants. Under drought stress, WRS7 was found to be the best isolate to promote plant growth, followed by WRS1, WRS5, and WRS4. As compared to uninoculated control plants, treatment of wheat seeds with WRS7 showed an enhanced increase in all the growth parameters, such as root length (96.29%), shoot height (16.54%), fresh weight (16.67%), dry weight (16.66%), chlorophyll a (33.53%), and chlorophyll b (29.89%) content, when tested under drought stress. (Table 2.9 B). WRS1-inoculated plants also showed enhanced growth under drought stress in terms of total length (49.38%), root length (97.53%), shoot length (14.23%), dry weight (27.78%), and chlorophyll a (10.51%).

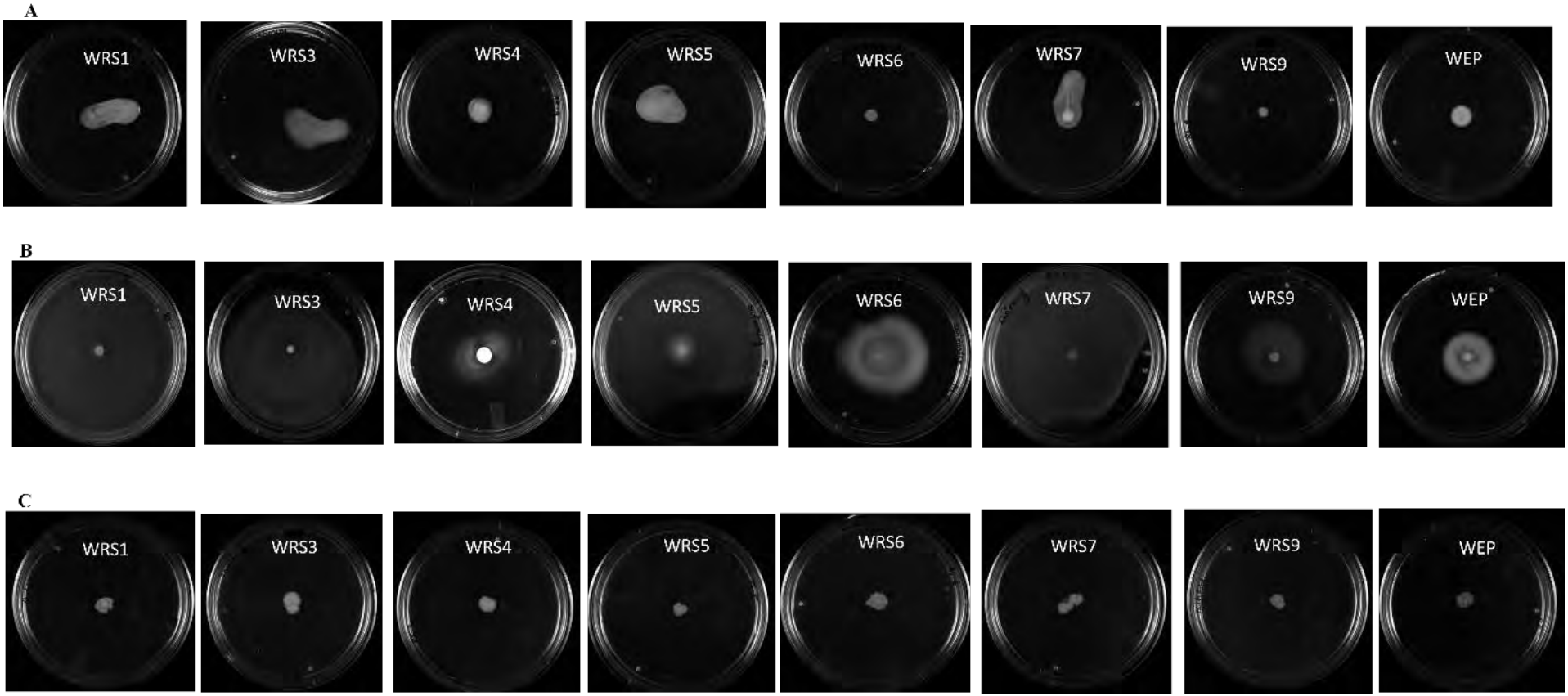

Figure 2.3. Test of motility shown by drought tolerant bacterial isolates: (A) swarming assay (B) swimming Assay, and (C) twitching Assay.

Table 2.9 (A). Plant growth promotion test following inoculation of isolates under non-stressed conditions.

Isolates	Shoot Length (cm)	Root Length (cm)	Total Length (cm)	Fresh wt.	Dry wt.	Chl. a (mg g^{-1}FW)	Chl. b (mg g^{-1}FW)
CONTROL	23.66±0.55	21.83±0.67	45.70±0.07	2.49±0.44	0.24±0.03	11.39±0.72	5.63±1.03
WRS1	24.13±0.21*	24.11±0.28**	48.65±0.87**	2.78±0.03**	0.28±0.02**	12.45±1.53*	5.34±0.32
WRS3	21.42±0.03	20.661.02	43.31±1.99	2.68±0.05	0.26±0.11	11.31±2.06	4.60±1.10
WRS4	24.27±0.05*	20.92±0.09	45.45±0.49	2.71±0.04**	0.27±0.02	10.92±2.83	4.65±0.60
WRS5	23.39±0.09	24.18±1.34***	48.67±1.15**	3.10±0.04**	0.32±0.01**	11.35±3.60	4.63±0.54
WRS6	21.81±0.11	21.12±1.20	43.61±1.98	2.78±0.04	0.28±0.02	13.59±1.83**	6.11±0.66*
WRS7	25.97±0.09*	25.31±0.19***	50.96±0.17***	2.90±0.02**	0.29±0.02**	15.19±1.65***	5.82±0.43
WRS9	23.06±0.50	13.78±0.22	37.15±0.67	2.81±0.02**	0.25±0.02	14.14±2.46**	5.60±1.22
WEP	23.65±0.58	18.28±0.22	43.06±0.28	2.63±0.04	0.27±0.02	14.65±1.09**	6.82±0.43*

'*' indicates statistical significance: *P ≤ 0.05, **P ≤ 0.01, ***P ≤ 0.001, and ****P < 0.0001

Table 2.9 (B). Plant growth promotion test following inoculation of isolates under drought- stressed conditions.

Isolates	Shoot Length (cm)	Root Length (cm)	Total Length (cm)	Fresh wt.	Dry wt.	Chl. a (mg g^{-1}FW)	Chl. b (mg g^{-1}FW)
Control	19.46±0.48	12.16±0.28	31.55±0.66	1.80±0.49	0.18±0.01	8.75±0.69	4.65±2.50
WRS1	22.23±0.22**	24.02±3.36****	47.13±5.05****	1.96±0.23**	0.23±0.01**	9.67±1.69*	3.76±1.97
WRS3	18.28±0.11	19.56±0.44***	38.06±1.12***	1.82±0.06	0.19±0.02	7.82±0.86	4.08±0.34
WRS4	20.24±0.08	24.13±1.00****	45.36±2.08****	1.98±0.07**	0.22±0.01**	9.20±0.19*	4.26±0.63
WRS5	20.19±0.13	24.54±1.65****	45.24±2.62****	1.91±0.65**	0.21±0.02**	11.14±3.38**	4.74±0.50
WRS6	20.17±0.28	15.70±0.42	36.24±1.08**	1.87±0.64	0.19±0.01	10.80±0.26**	4.84±0.08
WRS7	22.68±1.44***	23.87±0.47****	46.04±0.83****	2.10±0.09**	0.21±0.01**	15.59±1.50****	6.04±0.11***
WRS9	19.03±0.61	16.68±0.92	35.17±1.03**	1.86±0.05	0.17±0.02	9.52±2.97*	3.64±1.27
WEP	19.74±0.40	11.61±0.23	32.00±0.13	2.05±0.81**	0.21±0.65**	10.35±7.42*	4.95±4.32

'*' indicates statistical significance: *P ≤ 0.05, **P ≤ 0.01, ***P ≤ 0.001, and ****P < 0.0001.

Among the tested consortia, all could increase plant growth under well-watered conditions (Table 2.10 A), except consortium IV. The highest significant growth in total length was observed for Consortium I (29.96%), followed by Consortium III (22.89%) and Consortium II (18.68) as compared to uninoculated control under well-watered conditions. However, growth retardation was observed in consortium IV-treated plants (10.80%). A significant increase in shoot length of 41.81%, 41.34%, and 43.18% was observed in consortia I, II, and III-treated plants, respectively. Consortium I was found to be best for increasing root length (18.37%), whereas a decrease in root length (22.59%) was observed in Consortium IV. A decrease in chlorophyll content was observed in all the consortia under well-watered conditions. No significant increase was observed in fresh and dry weights in any consortia.

Almost all the consortia show the ability to ameliorate drought stress in wheat plants (Table 2.10 B). As compared to uninoculated control plants, treatment of wheat seeds with different consortia under drought stress showed an enhanced total plant growth with the highest significant difference with consortium II (64.29%), followed by consortium I (58.34%), III (44.59%) and consortium IV (14.50%). The highest increase in root length (74.59%) and shoot length (63.34%) was observed in Consortium II, followed by Consortium I. Compared to individual isolates, WRS7 and WRS1, none of the consortia showed improved plant growth under drought stress.

Table 2.10 (A). Plant growth promotion test following inoculation of consortia under non-stressed conditions.

Isolates	Shoot Length (cm)	Root Length (cm)	Total Length (cm)	Fresh wt. (g)	Dry wt. (g)	Chl. a (mg g^{-1}FW)	Chl. b (mg g^{-1}FW)
Control	21.77±0.30	22.13±0.37	44.32±0.29	2.53±0.44	0.56±0.29	10.55±0.23	5.18±0.36
Consortia I	30.87±0.50****	26.20±0.22***	57.60±0.40****	2.86±0.57*	0.72±0.16***	9.01±0.036*	4.31±0.18
Consortia II	30.77±0.03****	21.53±0.27	52.60±0.49****	2.97±0.15**	0.67±0.18**	6.78±0.19****	5.09±0.04
Consortia III	31.17±0.35****	23.40±0.32	54.47±0.31****	2.78±0.04*	0.63±0.71*	3.88±0.02****	3.42±0.23**
Consortia IV	22.20±0.31	17.13±0.44****	39.53±0.47*	2.10±0.04**	0.28±0.17***	4.14±0.06****	4.05±0.17

'*' indicates statistical significance: *P ≤ 0.05, **P ≤ 0.01, ***P ≤ 0.001, and ****P < 0.0001.

Table 2.10 (B). Plant growth promotion test following inoculation of consortia under drought- stressed conditions.

Isolates	Shoot Length (cm)	Root Length (cm)	Total Length (cm)	Fresh wt. (g)	Dry wt. (g)	Chl. a (mg g^{-1}FW)	Chl. b (mg g^{-1}FW)
Control	18.37±0.25	12.07±0.28	30.80±0.24	1.49±0.64	0.14±0.31	8.85±0.17	1.38±0.71
Consortia I	30.13±0.36****	18.79±0.54****	48.77±0.51****	1.78±0.13*	0.18±0.25**	4.20±0.14****	6.17±0.07****
Consortia II	30.00±0.49****	21.06±0.32****	50.60±0.40****	1.68±0.25	0.16±0.11*	9.28±0.13	5.95±0.28****
Consortia III	29.67±0.51****	14.93±0.54**	44.53±0.49****	1.71±0.14*	0.17±0.02*	4.80±0.13****	5.65±0.16****
Consortia IV	22.33±0.50**	12.77±0.22	35.27±0.42***	1.70±0.04**	0.12±0.11*	7.52±0.36**	3.89±0.33****

'*' indicates statistical significance: *P ≤ 0.05, **P ≤ 0.01, ***P ≤ 0.001, and ****P < 0.0001.

2.2.8 Effect of bacterial isolates on relative water content and seed germination of wheat crop under drought stress

Relative water content (RWC) is an important indicator of water status in plants and influences the ability of the plant to recover from stress, affecting its yield [149]. Therefore, RWC was measured in uninoculated and bacteria-inoculated plants under normal and drought-stressed conditions. RWC decreased by 33.24% in control plants (without bacteria) under drought stress, whereas bacteria inoculation increased RWC compared to non-stressed plants (bacteria inoculated well-watered plants). The maximum change was observed in WRS4 (11.07%), whereas the least change was observed in WRS9 (1.07%) and WEP (-0.19%) in comparison to bacteria-inoculated non-stressed plants. (Figure 2.4 A). However, in comparison to uninoculated drought-stressed plants (stressed control plants), inoculation with WRS1 (270%), WRS3 (137%), WRS4 (181%), WRS6 (92%), WRS7 (365%), and WRS9 (98%) showed increased relative water content (RWC). The highest increase in RWC was observed in plants inoculated with WRS7, which enhanced RWC under both normal (90.28%) and osmotic stress conditions (365.16%) with respect to un-inoculated plants (Figure 2.4 A). Further, wheat seeds were pre-treated with different isolates to see the effect of bacterial isolates on seed germination. However, seed germination was not found to be affected by bacterial inoculation as there was no significant change with respect to control (Figure 2.4 B).

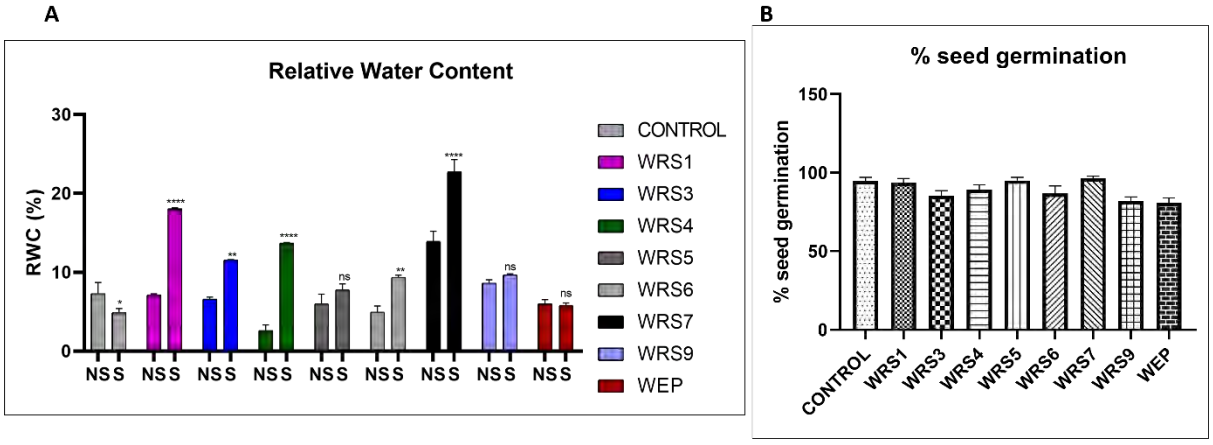

Figure 2.4. The impact of bacterial isolates on drought stress amelioration in wheat. **(A)** Relative water content (RWC) of the whole plant after 15 days of the drought treatment. Each bar represents mean ± SE (n = 30). **(B)** Seed germination percentage of 100 seeds with and without bacterial inoculation under standard conditions. Symbol '*' represents significant differences among different treatments ($p < 0.05$). (Abbreviations: NS- Non-Stressed; S-Stressed).

2.4 Discussion

Although, the role of PGPR in mitigating the adverse effects of drought stress has been exclusively studied by many researchers [150–154], the suitable bacteria or consortium is unavailable to promote plant growth at the field level under actual farming conditions, which necessitates further exploration of efficient drought-tolerant PGPR. Therefore, the present work aimed to isolate and characterize the efficient drought-tolerant bacteria from wheat plants growing in the Shekhawati region of Rajasthan. In the present study, we selectively isolated nine drought-tolerant bacteria and characterized them for their plant growth-promoting abilities under osmotic stress caused by drought. To the best of our knowledge, very few studies have been carried out to characterize drought-tolerant bacteria associated with wheat plants in this region. Therefore, the result of the current study is a valuable addition to understanding the properties of PGPR associated with plants growing in the stressed condition of the Shekhawati region of Rajasthan.

Most of the bacterial isolates recovered in the present study exhibited ACC deaminase activity, indole acetic acid (IAA) and siderophore production, solubilization of inorganic phosphate, fixation of atmospheric nitrogen, and HCN production. The bacterial isolates were also subjected to biochemical assessment, antibiotic sensitivity, and substrate utilization tests. The ability of the bacterial isolates to utilize various carbon sources helps them to survive under deficiency conditions of their conventional carbon sources. Their growth pattern under osmotic stress was also studied to monitor their survival so that they can further be used as inoculum for plant growth promotion tests under osmotic stress conditions. Their motility was also tested to evaluate their ability to colonize hosts efficiently. Based on their PGP activities, different consortia were also formulated and tested to promote wheat plant growth under drought stress. In the current study, *Kosakonia cowanii, Siccibacter turicensis,* and *Comamonas kerstersii* WRS9 showed plant growth properties and promoted wheat plant growth under drought stress. The above-mentioned bacterial species are not known to be established PGPR. Similar to our study, Rashid *et al.* (2021) isolated drought-resilient PGPR *Priestia megaterium* (MU2) and *Bacillus licheniformis* (MU8) from wheat plants [27]. Gontia-Mishra *et al.* (2017) isolated ACC deaminase-producing bacteria from the wheat rhizosphere and subsequently evaluated their effect on growth enhancement of wheat seedlings under drought and salinity stress [155]. They have also reported that isolated PGPR exhibit various plant growth-promoting properties and can ameliorate drought stress effects in the host plant.

As the ACC deaminase activity of PGPR is one of the important PGPs for inducing systemic tolerance to plants [20], we quantitatively analysed the ACC deaminase activity of bacterial isolates. In the current study, a wide range of ACC deaminase activity (µmol/mg protein/h) from 0.46 to 1.32 has been shown by bacterial isolates, falling in the range reported in earlier studies [17, 141, 156, 157]. *Siccibacter turicensis* WRS3 showed promising ACCD activity, followed by *Kosakonia cowanii* WRS5 and *K. cowanii* WRS1. Similar to our finding, Ojuederie and Babalola (2023) found ACCD-producing PGPR *Pseudomonas* sp. MRBP4 (0.41 ± 0.09 µmol/mg protein/h), *Pseudomonas* sp. MRBP13 (0.93 ± 0.23 µmol/mg protein/h) and *Bacillus* sp. MRBP10 (0.64 ± 0.33 µmol/mg protein/h) isolated from Maize rhizosphere ameliorate the effect of drought stress in Maize [157]. Out of different PGPs, phytohormones secreted as secondary metabolites by bacteria can act as phytostimulants and prominently impact plant growth and metabolism under stress and non-stress conditions [128]. In the present study, all the bacterial isolates were able to produce varying levels of IAA from 0.06 to 1.42 µg/ml. In the current study, maximum IAA production was shown by *Enterobacter bugandensis* WRS7 (1.42 µg/ml). Production of IAA by *E. bugandensis* TJ6 was also reported by Wang *et al.* (2020) [158]. Three strains of *Kosakonia cowanii* (WRS1, WRS5, and WRS8) produced almost similar levels of IAA (0.15-0.19 µg/ml), which was much lesser than *K. cowanii* MGR1 (26.17 µg/ml) and *K. cowanii* KAS 1 (9 µg/ml) as reported in earlier studies [158]. Similar to our observation, previous studies have shown the IAA production by many bacterial species, including *Pseudomonas fluorescens, P. putida, P. aeruginosa Bacillus subtilis, B. endophyticus, Serratia marcescens, Klebsiella pneumoniae,* and *Enterobacter cloacae* [17, 128, 159, 160].

We also tested for phosphate solubilisation properties in all the isolates. The presence of such activities increases the applicability of PGPR as a bioinoculant for facilitating plant growth The highest phosphate solubilisation ability was shown by PGPR strains *Siccibacter turicensis* WRS3 (15.19 µg/ml) followed by *Kosakonia cowanii* WRS1 (13.54 µg/ml) and *Enterobacter bugandensis WRS*7 (12.26 µg/ml). Phosphate solubilisation from the above species has been reported in a couple of studies. For instance, Panigrahi and Rath (2019) reported phosphate solubilization by *Kosakonia cowanii* MK834804 (7.200µg/ml) [161], whereas Kiprotich *et al.* (2023) reported phosphate solubilization by *Enterobacter bugandensis* KB2 (11.03 ± 9 µg/ml) [162]. Phosphate solubilization by *Siccibacter turicensis* has also been reported in earlier studies [153].

Rhizospheric bacteria were also characterized based on their ability to fix atmospheric nitrogen and make it bioavailable. The nitrogen-fixing bacteria, both free-living and symbiotically

associated with leguminous plants, convert the atmospheric nitrogen into ammonia with the help of the nitrogenase enzyme. Biological nitrogen fixation by these microbes can minimize the use of chemical nitrogen fertilizer and can be promising for sustainable agriculture in an eco-friendly manner. In the present study, all the isolates gave preliminary nitrogen test positive, but further experiments such as acetylene reduction assay and ^{15}N methods are required to confirm their ability to fix atmospheric nitrogen.

Ammonia production by the rhizobacteria is one of the important properties that can indirectly benefit plants, as accumulated ammonia in the soil can suppress the proliferation of fungus growth by inhibiting the growth of fungal spores[163]. Another important property of rhizobacteria that indirectly promotes plant growth is the production of small molecular weight compounds, known as siderophores, which can inhibit the growth of pathogens by competing for iron, thus augmenting induced systemic resistance (ISR) in plants against certain pathogenic diseases [164]. In the present study, *Acinetobacter pittii* WRS4, *Pseudomonas putida* WRS6, *Enterobacter bugandensis* WRS7 and *Stenotrophomonas maltophilia* WEP, were able to produce siderophore on CAS- agar plates. Previous studies have shown siderophore production by several bacterial species belonging to different genera like *Enterobacter bugandensis* [158, 165], *Siccibacter turicensis* C2 [153], *Pseudomonas* [166, 167], *Serratia* [168], *Klebsiella* [17], *Mesorrhizobium* [169]. Hydroxamate- and catechol-type siderophore is reported in *Acinetobacter* sp. isolated from the rhizosphere of *Pennisetum glaucum* [143]. Hydroxamate-type siderophores production was also reported in *E. bugandensis* isolated from mangrove sediments [165].

Bacteria can also restrict pathogen growth by secreting hydrolytic enzymes such as β-1,3-glucanase, protease, chitinase, and lipase, and hence can be exploited as biocontrol agents to overcome the infestation if several microbial diseases in plants [170]. Other than antagonistic behaviour, these hydrolytic enzymes by bacteria may be required for endophytic colonization inside the host plant. In the current study, the bacterial isolates have shown most of the hydrolytic activity, if not all. Like our observation, Sayahi *et al.* (2022) reported that PGPR S. turicensis C2 produces hydrolytic enzymes (proteases, cellulases, cellulase, and lipases). Chitinase, protease, cellulase, and endoglucanase activities were reported in endophytic bacteria *Kosakonia oryzae, K. pseudosacchari, K. oryziphila, K. arachidis, and K. radicincitans* [171]. Saxena *et al.* (2023) functionally characterized bacterial isolates isolated from Neem gum based on hydrolytic enzyme production and found that *E. bugandensis* PNGSC2 produces pectinase, whereas *E. bugandensis* PNGAIA7 showed cellulase activity.

Also, *Stenotrophomonas panacihumi* PN3N8 and *Acinetobacter vivianii* PN3DN6 showed lipase and pectinase activity [172].

Colonization of root surfaces by rhizobacteria is a crucial step for establishing plant-microbe interaction. Therefore, we investigated the colonization potential of test isolates as root colonization by PGPR is an important trait for plant growth stimulation and survival of bacteria under stress conditions [17]. All forms of motility shown by bacteria are required for chemotactic response and root colonization. In response to specific root exudates, bacteria induce flagellar motility that directs their colonization on the plant root surface [173]. This chemotaxis response is followed by attachment or invasion of these bacteria on the root surface or to the interior of plant tissue. In our study, most of the bacterial isolates showed the presence of all tested motility. However, these motilities can be required for different functions. For instance, twitching motility (mediated by type IV pili) is responsible for colonization inside the plants [174] and for biofilm development [175].

Drought stress disturbs the water use efficiency of a plant, reducing plant growth and rate of photosynthesis, causing membrane damage, and affecting the activity of various enzymes [176]. The role of PGPR in mitigating the adverse effects of drought stress has been exclusively studied [145, 150, 152]. To test the efficacy of bacterial isolates as biofertilizers, we conducted plant growth studies under drought-stress conditions and their amelioration under laboratory conditions. From the growth promotion results, *E. bugandensis* WRS7 emerged as the best isolate in terms of protecting plants from the deleterious effects of drought stress. It was evident from our results that *E. bugandensis* WRS7-inoculated plants showed better root and shoot length and increased RWC, FW, and DW under water-stressed conditions (Table 2.9 A), suggesting the ability of WRS7 to mitigate the negative effects of drought. Our results are also supported by previous studies on PGPR-mediated drought stress mitigation [24, 27, 28, 177]. However, this is the first study to report enhanced growth of wheat plants by *E. bugandesis* under drought-stress conditions. Increased root length increases root surface area, which in turn helps in more water absorption from the soil under drought stress. Our study found increased chlorophyll content in PGPR-primed plants, indirectly improving plant photosynthetic efficiency and energy metabolism. Earlier studies have also established increased photosynthetic efficiency and chlorophyll content in PGPR-inoculated plants [178, 179]. The effectiveness of these isolates opens the possibility of evaluating the performance at the field scale and even with different crop plants. The pot experiments suggest that inoculation of bacterial isolates protects the plants against adverse effects of drought stress. In brief, the

observed result in this study indicates that such multifarious PGPR holds great potential to be used as a biofertilizer in drought soil.

Different consortia of bacteria formulated in this study have also revealed their ability to confer IST to drought stress in the wheat plant, which is manifested by better plant growth in bacteria-treated plants than in control plants. Significantly higher chlorophyll content in consortia-treated plants suggests their ability to maintain photosynthesis efficiency under drought conditions. Consortium II worked best under drought-stressed conditions in the present study, but its efficacy was less than that of individual isolates. With respect to *E. bugandensis* WRS7, plant biomass and chlorophyll a decreased by 40% and 42%, respectively. These results suggest that although individual isolates are compatible to each other, they might not be working synergistically to promote plant growth. Few studies have been reported where attempts were made to enhance plant growth by using microbial consortium. For example, a consortium of *Streptomyces* species improved fruit quality in bell pepper, induced plant defence priming, and changed microbial communities of the rhizosphere [180]. PGPR microbial consortium formulated using *Paenibacillus* sp. strain B2 and *Arthrobacter* sp. strain AA have protected wheat plants against *Zymoseptoria tritici* and drought stress and provided effective and durable ISR [181].

Based on their plant growth-promoting attributes, the individual isolates and the consortia were tested for their effectiveness in improving the growth of wheat plants under drought stress under laboratory set-up. Inoculation of strain *E. bugandensis* WRS7 significantly enhanced plant growth for different morphological parameters, such as root length, shoot height, and fresh and dry weight, tested under drought stress compared to un-inoculated plants. Therefore, we further restricted our studies to *Enterobacter bugandensis* WRS7 and performed biochemical and molecular studies to understand whether selected PGPR assists plants' physiological changes and adaption mechanism under drought stress.

CHAPTER III

Characterization of Stress-responsive Mechanism(s) under Drought Stress in *Enterobacter bugandensis* WRS7 Employing Metabolomics Analysis

This chapter has been published as "**Arora, S**., Babele, P. K., & Jha, P. N. (2023). Biochemical and metabolic signatures are fundamental to drought adaptation in PGPR Enterobacter bugandensis WRS7. Molecular Omics, 19(8), 640-652. https://doi.org/10.1039/D3MO00051F"

3.1 Introduction

Drought is a major abiotic stress that undermines crop productivity and quality and may lead to plant death under prolonged conditions. Drought induces osmotic stress in plants and modulates a number of physiological and biochemical processes, including stomatal closure, decreased photosynthesis and respiration, altered root system architecture and root exudation, and the onset of oxidative stress [182]. Drought also substantially affects soil biota, as it increases soil heterogeneity, restricts nutrient mobility and accessibility, and increases soil oxygen, frequently resulting in a drastic decrease in microbial biomass [11]. During drought, plant systems actively trigger specific signalling and metabolic responses to maintain osmotic balance by promoting root elongation for water uptake from the soil, stomata closure to reduce water loss, adjusting osmotic and biochemical processes within tissues, activating phytohormones (e.g., abscisic acid) signalling, and producing and mobilizing antioxidant and metabolites [183]. Traditional breeding and genetic engineering approaches have continuously been applied to design drought-tolerant transgenic plants. Unfortunately, these methods are time-consuming, expensive, and difficult to apply in the field [184].

In an agroecosystem, plants are inhabited by a large number of microbiota. Interaction between plant roots, soil, and microbes forms a most complex zone known as the rhizosphere [185]. Plant root exudates mediate the interactions and selection of beneficial soil microbial communities or PGPR, thus playing a key role in plant-microbial communication, which is crucial for both counterparts [186, 187]. PGPR colonize the rhizosphere/endo-rhizosphere and confer specific functions to their hosts, such as ameliorating abiotic stress tolerance (e.g., drought) and triggering systemic resistance against biotic stress factors [188]. PGPR support plant growth, health, and productivity through various direct and indirect mechanisms, such as the facilitation of nutrient acquisition, the production of phytohormones and lytic enzymes, and the accumulation of osmolytes, antioxidants, and secondary metabolites [189, 190]. Climate change-driven environmental stresses alter the rhizosphere properties and functioning, thus having a direct impact on the plant-microbe interactions and eventually on crop growth and yield [184]. Sustainable and efficient crop production to feed a growing world population in the era of global climate change requires alternate and eco-friendly approaches. Rhizosphere engineering, by harnessing the potential of PGPR, is an alternative to traditional approaches to increase crop resilience against drought [191, 192]. Certain PGPR have unique metabolic capabilities and exhibit various tolerance and adaptation mechanisms to drought stress. It includes thickening of the cell wall, maintaining the dormant stage (spore

formation), accumulation of osmolyte/compatible solutes (proline, trehalose, glycine betaine), ions (Na^+, K^+), and exopolysaccharide (EPS) production to overcome reduced water potential for maintaining normal cell physiology [59, 193]. The drought-tolerant PGPR maintains the biologically active state of the plasma membrane in response to drought/osmotic stress by modifying the fatty acid composition and maintaining the ratio of unsaturated to saturated fatty acid, thereby ensuring the fluidity and rigidity of the plasma membrane [194].

There is growing interest in harnessing the potential of stress-resilient PGPR and its subsequent application to induce stress tolerance mechanisms in plants [184]. Rhizosphere engineering based on genetically/metabolically engineered PGPR with improved performance under stress is one of the most important strategies critically required to achieve sustainable crop production in drylands. Developing genetically modified PGPR is simpler and less time-consuming than plants with a higher level of genetic complexity.[191, 192] Hence, developing more effective PGPR strains with longer shelf lives and improved stress adaptation requires identifying and investigating useful metabolic pathways associated with the production of secondary metabolites and complex stress-responsive pathways modulated in response to specific stress environments [189, 195]. We hypothesize that plant-associated-PGPR undergo morphological and physiological reprogramming under abiotic stress and produces metabolites that protect bacteria and the associated plants from the harmful effects of a given stress. To date, little is known about the drought tolerance mechanisms of PGPR and how their biochemical and metabolic characteristics can influence plant performance under drought/osmotic stress. Therefore, it is necessary to comprehend the physiology and metabolism of stress-resistant PGPR and their interaction with plants before implementing them in intensive farming practices to enhance plant performance under drought stress.

Metabolomics holds the potential to identify and characterize metabolites and biochemical pathways and their dynamic responses to changes in the environment, e.g., stress [196, 197]. This information is utilized to manipulate novel metabolic pathways involved in drought/osmotic tolerance in PGPR. Therefore, to investigate the physiological and biochemical capabilities of stress-resilient PGPR, we studied the physicochemical parameters of *Enterobacter bugandensis* WRS7 (hereafter *Eb* WRS7). This bacterium showed its ability to grow under drought/osmotic stress and improved wheat plant growth under drought stress (Chapter II). Furthermore, to discover the underlying metabolic signatures and their role in stress tolerance mechanisms, we employed untargeted gas chromatography-mass spectrometry (GC-MS) based metabolomics to profile the deregulated metabolite (central and secondary) pool and identify core metabolic pathways under stress.

3.2 Materials and Methods

3.2.1 *Eb* WRS7 culture conditions and drought exposure

Eb WRS7, a PGPR isolated from wheat rhizospheric soil under drought stress conditions, was used in the present study. *Eb* WRS7 showed different plant growth-promoting properties, including nitrogen fixation, phosphate solubilisation, siderophore production, and ACC deaminase activity (Chapter II). A phylogenetic tree was constructed using the Neighbor-Joining (NJ) method with a bootstrap value 500 in MEGA 6.0 [131]. For all the experiments, *Eb* WRS7 was grown in LB media. To test the ability of *Eb* WRS7 to grow under a water stress-mediated hyperosmotic environment, LB media was supplemented with different concentrations (0 to 25 %) of polyethylene glycol (PEG-6000). The cultures were grown at 30°C with constant shaking at 150 rpm in an incubator shaker. Bacterial growth was measured by reading the optical density (OD) at 600 nm using a UV-visible spectrophotometer (BioSpectrometer, Eppendorf, Germany). OD_{600} was measured every hour, and then the growth curve was plotted to study its growth pattern.

3.2.2 Morphophysiological and biochemical analyses

Field Emission Scanning Electron Microscopy

To check the osmotic efficiency of *Eb* WRS7, its cellular morphology of non-stressed and osmotic-stressed cells (10% PEG) were studied through Field Emission Scanning Electron Microscopy (FESEM) following standard protocol. One ml of 24 h grown bacterial cells was pelleted down and washed with phosphate buffer saline (PBS) twice. Cells were then suspended in 2.5% glutaraldehyde solution and kept overnight incubated in the dark at 4 °C. Cell pellet was collected through centrifugation (5000 g for 5 min) and washed three times with PBS. The sample was then dehydrated with 30, 50, 70, 80, and 90% ethanol with 10 min incubation each. The cell pellet was dehydrated with 100% ethanol. Finally, SEM stubs were prepared by applying adhesive tape and adding bacterial samples. The fixed bacterial cells were sputter coated with gold and subjected to FE-SEM (FEI-APREO SEM, Thermo Fisher Scientific, USA) to investigate the morphological changes in bacterial cells under drought stress.

Reactive Oxygen Species (ROS) detection

To measure the level of intracellular ROS, a stress marker, in control and stressed bacterial cells of *Eb* WRS7, the cell-permeable free radical sensor 2',7'-dichlorodihydrofluorescein diacetate (H_2DCFDA) was used [198]. Briefly, 1 mL of bacterial culture grown in LB media

supplemented with (control) and without 10% PEG (stressed) was collected at 6, 12, and 24 h. Bacterial cells were harvested through centrifugation, washed with 1X PBS, and resuspended in PBS. H_2DCFDA (10 µM) was added to the cells and incubated in the dark for 30 min at room temperature (RT). The ROS generation was detected using a Fluorimeter (Fluoroskan Ascent, Thermo Scientific) at excitation/emission at 485 nm/ 535 nm, respectively.

Malondialdehyde (MDA) Assay

MDA is one of the final products of the peroxidation of polyunsaturated fatty acids in cells. An increase in free radicals causes the overproduction of MDA and is commonly known as a marker of oxidative stress and the antioxidant status of the cell. Lipid peroxidation was determined by observing the formation of a thiobarbituric acid-reactive substance (TBARS). Bacterial cells from non-stressed and stressed conditions were harvested at 6, 12, and 24 h, washed with 0.85 % NaCl once, and then suspended in 0.25 % SDS by gentle swirling, TBA buffer reagent was added, followed by 60 min incubation at 95 °C. Tubes were then allowed to cool to RT by incubating on ice for 10 min. Then, the reaction mixture was centrifuged at 3000 g, and the supernatant was collected. The adduct formation of MDA-thiobarbituric acid (TBA) was measured at 532 nm by using a spectrophotometer (BioSpectrometer Eppendorf, Germany). The concentration of MDA formed was calculated by comparing the absorbance obtained from experimental samples to the standard curve obtained using the malondialdehyde (MDA). The extent of lipid peroxidation was expressed in nanomoles of MDA.

Estimation of intracellular ion concentration

The inductively coupled plasma-optical emission spectroscopy (ICP-OES) method was performed to determine the concentrations of intracellular potassium (K^+), sodium (Na^+), and calcium (Ca^{+2}) ions in the bacterial cell under control and stress conditions as described previously [199]. Briefly, 10 mL bacterial culture was collected at 6, 12, and 24 h of growth under control and stress conditions and centrifuged at 3000 g for 15 min. The supernatant was decanted, and residual media was completely removed. The cell pellet was dried at RT for 24 h, followed by its digestion with 1 mL of 30% nitric acid, and incubated at RT for 48 h. Later, the solution was sonicated using a probe sonicator (ultrasonic cell disruptor, Microson, USA) at 10 Hz with 10-second pulses for 5 cycles. Samples were then centrifuged at 20,000 g for 20 min. The supernatant was filtered through 0.2 µm syringe filters, and the filtrate was diluted five times with sterilized, deionized water. Samples were then analyzed by ICP-OES (Optima 8000 PerkinElmer, USA). Standard curves for K^+, Na^+, and Ca^{+2} were prepared for quantitative estimation. Ion concentration was normalized using bacterial optical density at 600 nm.

Quantification of phytohormone production

For IAA and GA detection, the protocol of Ghosh *et al.* was followed with slight modifications [59]. Phytohormones secreted by bacterial isolate were extracted using an equal volume of ethyl acetate and kept for 48-h incubation at 150 rpm at 4 °C. The organic layer was separated and evaporated using a rotary evaporator under a vacuum. The residue was re-dissolved in methanol, filtered through a 0.22µ filter, and then subjected to HPLC analysis (HPLC 1260, Agilent Technology, USA) using a C-18 column (4.6 × 150 mm x 4 µm). The column was washed with 80% methanol and equilibrated with an isocratic flow of acetonitrile and 10 mM ammonium acetate buffer (pH 4.2) in a 70:30 (v/v) ratio at a flow rate of 2.0 mL/min [59, 200]. The same solvent system was used to separate phytohormones, and 20 µl of the sample was injected at a flow rate of 1 mL/min. Detection of peaks respective to phytohormones was done using a UV–visible detector (VWD detector) at a wavelength of 254 nm and 280 nm for GA and IAA, respectively. A standard curve (area under the curve vs. concentration) was prepared and extrapolated using different concentrations of commercially available phytohormones to quantify IAA and GA. Later, the samples were subjected to HRMS (Agilent Technologies 6545 Q-TOF LC/MS) to confirm the presence of IAA. The sample was prepared as stated above. The Solvent system used for HRMS analysis was a mixture of acetonitrile and water in a 40:60 (v/v) ratio at a 3.0 mL/min flow rate.

Quantification of exopolysaccharide production

Eb WRS7 was analyzed for its ability to produce EPS under no stress and osmotic stress according to the method of Sandhya *et al.* with slight modifications [201]. Briefly, a 3-day-old culture grown in LB (with and without 10% PEG) was centrifuged at high speed (13000 g) for 30 min at 4 °C, and the supernatant was collected. To the supernatant, two-volume of chilled absolute alcohol was added and kept overnight at 4°C. The precipitated EPS was harvested by centrifugation at 10,000 g for 20 min and suspended in water. Precipitated EPS was estimated for total carbohydrate content following the method of Dubois *et al.* (1956) [202]. Glucose standards for different concentrations were used for the standard curve preparation and carbohydrate quantification in EPS.

Protein content estimation

Total cellular protein in the bacterial cell was determined by lysing the cell pellet obtained from the 3-day-old culture under normal and osmotic stress conditions with 5 mL of lysis buffer [201]. The cell suspension was sonicated, cell lysate was collected through centrifugation at 13000 g for 10 min, and total protein was estimated using the standard Bradford method [203].

Proline content estimation

The free proline accumulated in bacterial cells under normal and osmotic-stress conditions was estimated as per a previously described method [204]. Cell pellets obtained from 72 h grown cultures were lysed. The supernatant (1 mL) obtained was treated with 2 mL of 3% aqueous sulphosalicylic acid, followed by incubation for 30 min. After incubation, the solution was centrifuged at 8000g for 20 min at 4°C, and the supernatant was collected. The obtained supernatant was treated with 2 mL glacial acetic acid and 2 mL acid ninhydrin and incubated at 100°C in a water bath for 1 h. The reaction was terminated by keeping the tubes in ice. Four ml of toluene was added to each reaction mixture and mixed well. The chromophore containing the toluene layer was collected, and the absorbance was measured spectrophotometrically at 520 nm against toluene as blank. The concentration of free proline was calculated from the standard curve prepared using different concentrations of L-proline.

3.2.3 Fatty Acid Methyl Ester analysis

In order to comprehend the fatty acid profile under osmotic stress, the fatty acid composition of PGPR *Eb* WRS7 was analysed in accordance with a standard protocol [205]. The bacterial cells were grown in only LB media (control) and LB media containing 10% PEG (stressed) for 24 h. Cells were harvested by centrifugation at 1000 g for 5 min and sonicated in lysis buffer containing 50 mM Tris-Cl (pH 7.6), 1.1 mM dithiothreitol, 1 mM PMSF, and 0.2% lysozyme. The resulting supernatant was extracted using a mixture of methanol and chloroform in a 1:2 ratio followed by centrifugation at 6000 g for 10 min. The supernatant was diluted with the same solvent system ten times and kept on a shaker at 160 rpm for 3 h for phase separation. The lower organic phase was collected and concentrated using a rotary evaporator, dissolved in toluene, and converted to fatty acid methyl ester (FAME) by the trans-esterification reaction. Later, samples were subjected to GC-MS analysis (GCMS-TQ8040, Shimadzu Corporation, Japan). GC was operated at split-less injector mode with the following conditions: initial oven temperature of 50°C held for 2 min and temperature ramping from 50 to 250°C at a rate of 10 °C per min. MetaBoAnalyst 5.0 was used for the Hierarchical heat map construction.

3.2.4 Metabolite extraction, derivatization, and GC-MS analysis

Polar and non-polar metabolites were extracted from the bacterial cells grown in only LB media (control) and LB media containing 10% PEG (stressed) for 24 h for GC-MS Analysis. Cell pellets were sonicated in lysis buffer using a sonicator probe using three cycles of 10 s pulses at 40 Hz on ice. Cells were centrifuged at 20,000 g for 5 min. Metabolites from the supernatant were extracted using a 2:1 ratio of chloroform and methanol. Then, 100 µl of each solvent layer

was collected and evaporated to dryness using a rotary vacuum concentrator. The dried supernatant was suspended in 1 mL methanol. As mentioned below, 200 µl was aliquoted in a fresh microcentrifuge tube, followed by evaporation to dryness and derivatization. To each 200 µl of the dried sample, 30 µl of methoxyamine hydrochloride was added, heated at 70 ℃ for 45 min, and then cooled at room temperature to derivatize the samples. After that, 50 µl of MSTFA was added and heated at 40 ℃ for 90 min. Later, derivatized samples were transferred to auto-sampler vials for analysis. 1 µl of the derivatized sample was loaded on Shimadzu capillary column SH-RXi-5SilMS (30 m × 0.32 mm × 0.25µm) through autosampler in splitless mode at 250 ℃. The constant flow rate of 1 mL/min of helium gas was maintained. Initially, the GC program was started at 60 ℃ for 1 min, followed by temperature ramping of 10 ℃/ min to 180 ℃ with a temperature hold of 2 min, followed by second ramping of 4 ℃/ min till the final temperature reached 300 ℃ and held constant for 10 minutes. Data acquisition involved a mass range of 50 to 650 m/z. Peaks were identified using the NIST 14 library. The metabolomics data were obtained in .qgd file format for analysis. MetaBoAnalyst 5.0 was used for the statistical analysis.

3.2.5 Statistical Analysis

All the experiments were carried out in triplicates unless otherwise stated, repeated in three different experimental sets, and plotted as mean ± SD using Prism 8 (Graph Pad software). Statistical analysis was performed using an unpaired student's t-test. Statistical significance: *P ≤ 0.05, **P ≤ 0.01, ***P ≤ 0.001, and ****P < 0.0001, ns = not significant. The experiment used four replicates of each control and stressed sample for GC-MS analysis. After data normalization, all significant metabolites were analyzed using unsupervised principal component analysis (PCA) to observe the overall distribution trend among samples. Differential metabolites were screened according to Variable importance in Projection (VIP) >1 and $p < 0.05$. Univariate analysis and metabolic pathway enrichment analyses were performed using the online tool MetaboAnalyst 5.0 (https://www.metaboanalyst.ca).

3.3 Result

3.3.1 Cell growth and morphological responses under osmotic stress

To identify bacterial isolate *Eb* WRS7, a 1.5 kb 16S rRNA gene of the isolate was amplified by PCR and sequenced. The sequence of the resulting amplicon was submitted to the NCBI GenBank under the accession number MW453057. Based on the sequence similarity, the isolate was identified as *Enterobacter bugandensis* with a close match to *E. bugandensis* strain

XM29, with 99.16% similarity (Chapter II). Phylogenetic analysis showed that the sequence of 16S rRNA of the same genus clustered together (Figure 3.1).

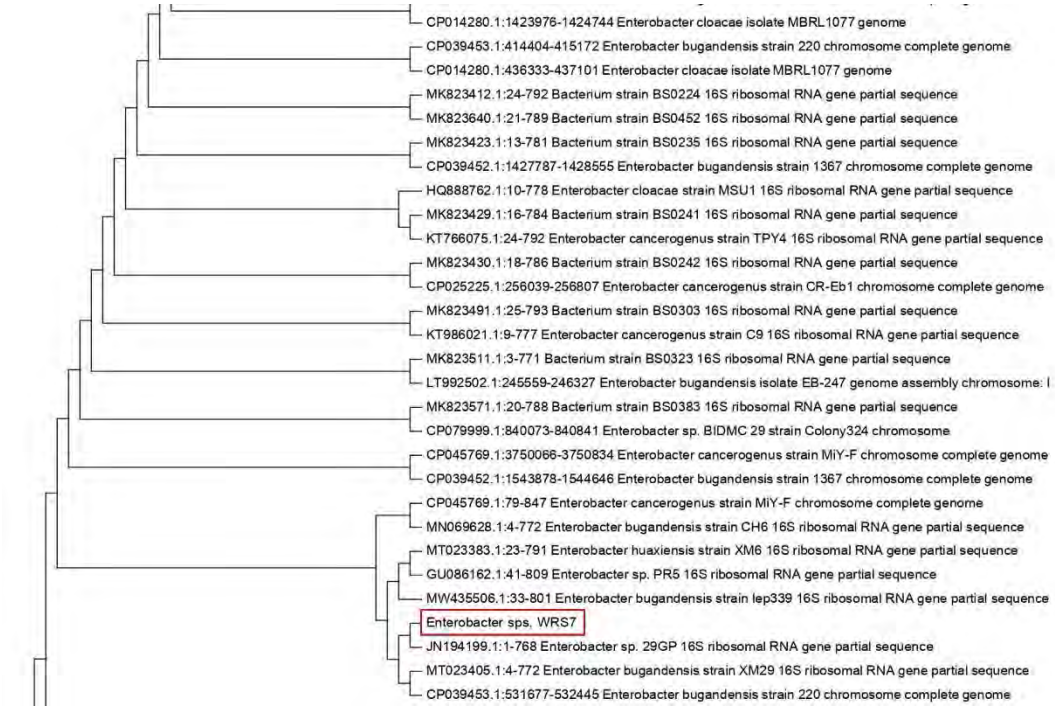

Figure 3.1. Phylogenetic tree constructed using the neighbour-joining method with bootstrap value 500 between isolate *Eb* WRS7 and reference bacterial sequences retrieved from GenBank database of National Centre for Biotechnology Information (NCBI) based on 16S rRNA gene sequences. Isolate WRS7 clustered among the genus *Enterobacter.* Evolutionary analysis was conducted using Mega software version 6.0.

First, we asked whether and to what extent the cells of *Eb* WRS7 could tolerate and survive the osmotic stress. To test this, we exposed cells to a range of PEG (5 to 25 %) concentrations and measured the optical density (600 nm). The growth curve showed maximum cell growth under control (no PEG exposure) conditions, while significant growth retardation was observed with increasing concentrations of PEG (Figure 3.2 A and B). Although cells can sustain up to 25% PEG, there was a significant loss in cell growth, whereas *E. coli* cells can sustain up to 20% PEG (Figure 3.2 C). In all the tested doses of PEG, *Eb* WRS7 could withstand 10% PEG concentration and showed about 50% survival of *Eb* WRS7 as compared to the control. Therefore, 10% PEG was selected to induce drought/osmotic stress in all the subsequent experiments to analyze the physiological, biochemical, and molecular responses. After testing the growth defect in *Eb* WRS7 in response to osmotic stress, we observed the changes in cellular morphology directly related to the osmotic tolerance efficiency. Small (100 nm to 250 nm in size) vesicle-like structures were also observed in PEG-exposed cells. FE-SEM analysis showed that *Eb* WRS7 maintained cellular integrity upon exposure to 10% PEG (Figure 3.3).

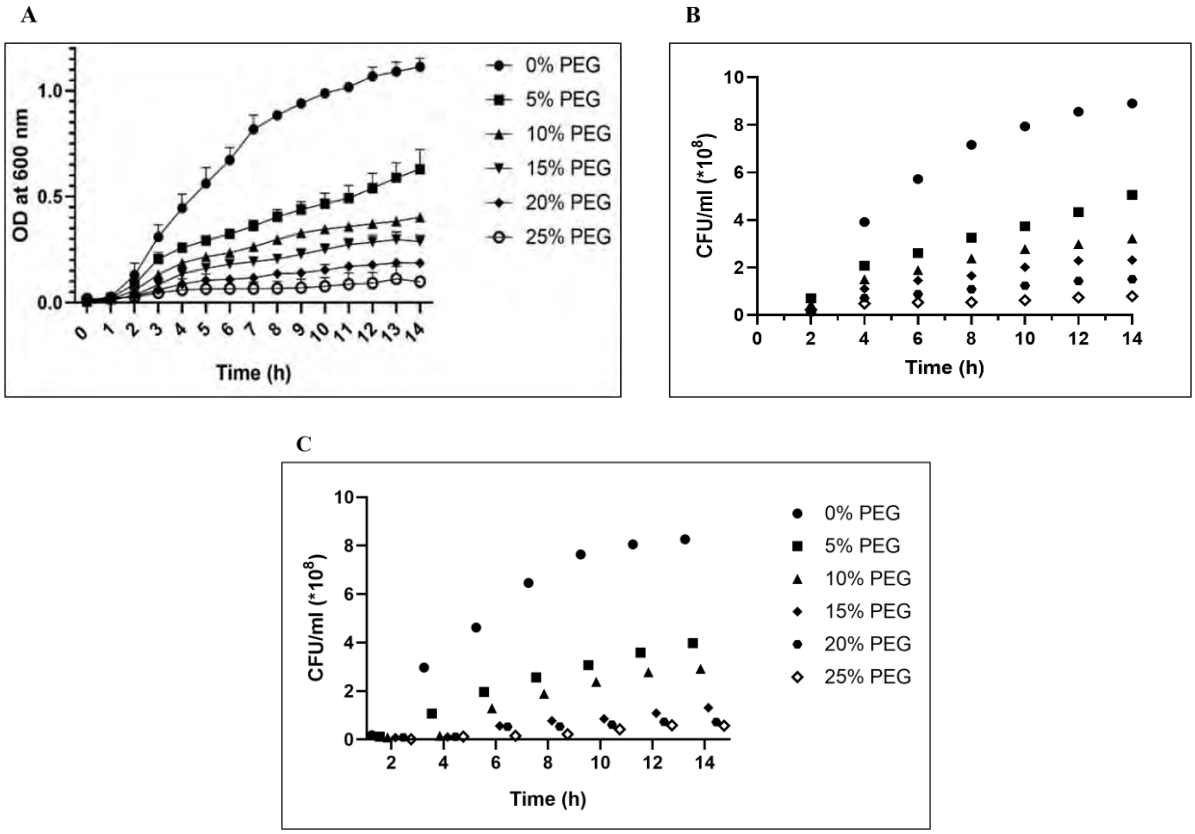

Figure 3.2. Effect of water stress on growth of *Eb* WRS7. **(A)** Growth curve of *Eb* WRS7 based on the OD at 600 nm and **(B)** CFU of *Eb* WRS7 based on the number of viable colonies (CFU) present on an agar plate, multiplied by the dilution factor of *Eb* WRS7 both under normal (0 % PEG) and osmotic- stressed (5 to 25 % PEG) conditions at an interval of 1 hour. **(C)** Growth curve of *E. coli* based on the number of viable colonies (CFU) present on an agar plate, multiplied by the dilution factor of *E. coli* under normal (0 % PEG) and osmotic stressed (5 to 25 % PEG) conditions at an interval of 1 hour. Each point represents mean ± SE of 4 replicate samples.

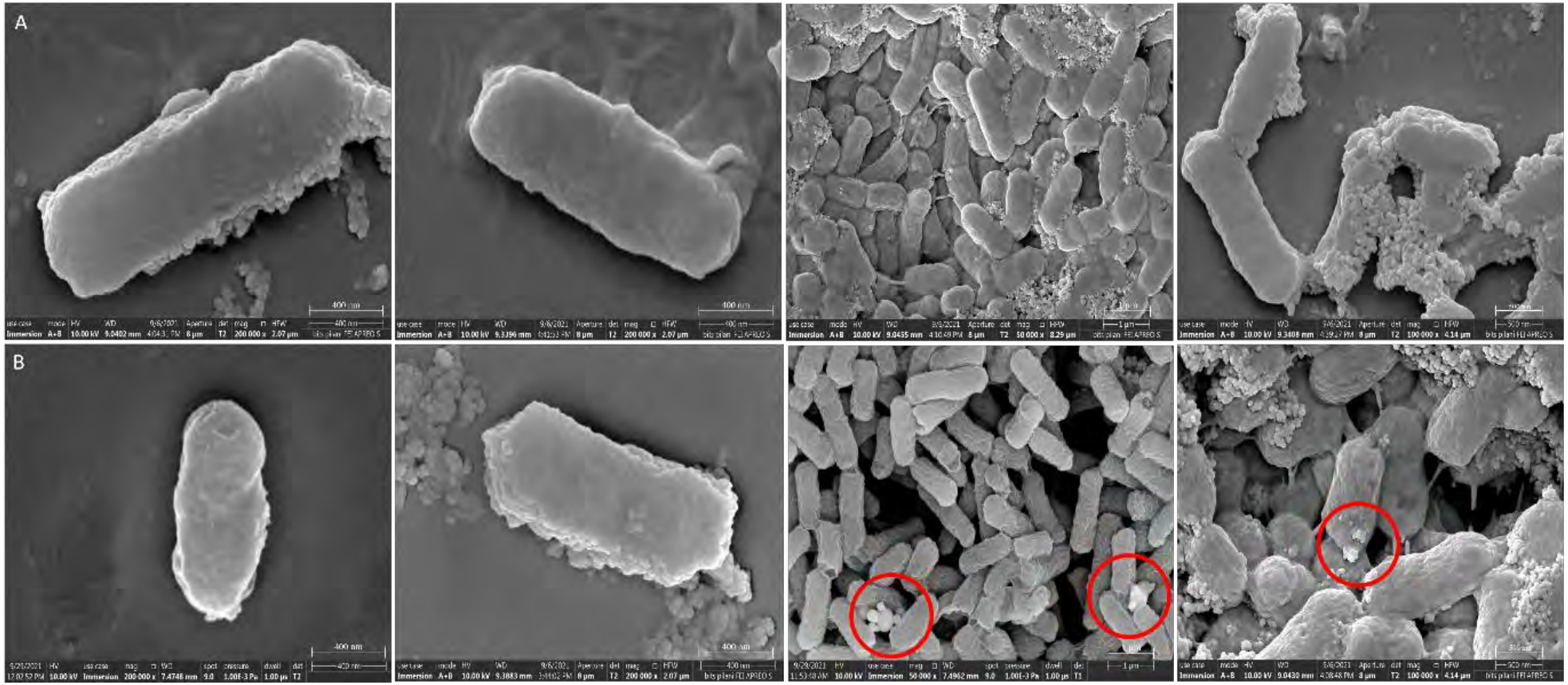

Figure 3.3. Scanning electron microscopic images of *Eb* WRS7 cells under **(A)** non-stressed and **(B)** osmotic (10% polyethylene glycol) stressed conditions. Osmotic stress-exposed cells do not show any significant morphological changes. Small vesicle-like structures (inside red circles) were seen. Similar appearances were found in separate experiments. Two left-side images (with single cell) were captured at 200,000X magnification (Bar-400nm). Two right-side images (with multiple cells) were captured at 50,000X (Bar-1µm) and 100,000X magnification (Bar-500nm).

3.3.2 Physiological and biochemical responses under osmotic stress

Cell growth and morphology analysis indicated that PEG-induced osmotic stress slowed down the growth of *Eb* WRS7. However, we did not observe significant morphological alterations in cells grown with 10% PEG. To determine whether decreased cell growth resulted from oxidative stress and membrane damage, we measured the accumulation of intracellular ROS and conducted lipid peroxidation assays in control and osmotically stressed cultures. At 6 h of growth of PEG-treated cells, there was a significantly high level of both ROS (81.33 %) and MDA (179.59 %) as compared to non-stressed cells (Figure 3.4). After that, a gradual decline in both ROS and MDA contents was observed at 12 and 24 h, suggesting the stress adaptation and tolerance of *Eb* WRS7 under osmotic stress.

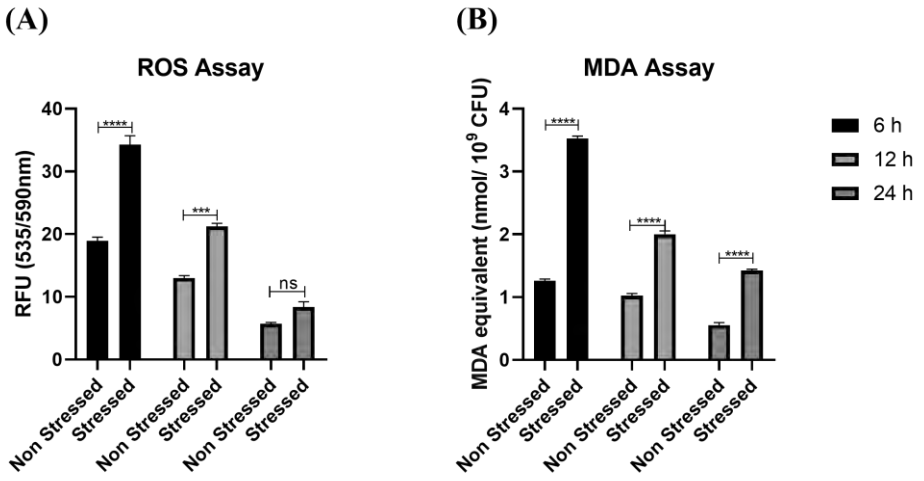

Figure 3.4. *Eb* WRS7 responses under osmotic-stressed conditions. **(A)** Reactive Oxygen Species (ROS) detection by H_2DCFDA and expressed as relative fluorescence unit (RFU) at 535/590 nm, **(B)** Membrane lipid peroxidation products were determined as TBARS (MDA-TBA adduct) and are reported as nmol MDA equivalents/10^9 cells. The error bars indicate standard deviations from three independent cultures assayed in triplicate. The error bar refers to the mean ± SD of three independent measurements. Horizontal bars with asterisks (*) indicate statistical significance between two values based on a student's t-test. Statistical significance: *$P \leq 0.05$, **$P \leq 0.01$, ***$P \leq 0.001$, and ****$P < 0.0001$, ns = not significant. Abbreviations: MDA- Malondialdehyde; TBA- thiobarbituric acid.

ROS and MDA analysis pointed out that osmotic stress triggers oxidative stress in the cells. We expected that stress exposure would activate the ROS-mediated signaling cascades and eventually promote stress-responsive pathways for cell survival in response to stress events. Since the uptake and release of ions, especially K^+, $Na^{+,}$ and Ca^{+2}, are involved in osmoregulation, we measured the intracellular concentration of K^+, Na^+, and Ca^{+2} to understand the mechanism of osmotic stress tolerance in *Eb* WRS7. The content of these ions significantly

increased at 6 h but decreased gradually at 12 and 24 h under osmotic stress. At 24 h, a significant difference in ionic concentration under stress and non-stress conditions was found only for Ca^{2+} (Figure 3.5). The Na^{+} concentrations were significantly different at 6, 12, and 24 h, showing 182.33 ± 4.426, 154.465 ± 5.933, and 27.22 ± 0.938 mM respectively under osmotic stress. In contrast, K^{+} was relatively low and measured to be 91.325 ± 0.148, 40.393 ± 0.061, and 4.557 ± 0.054 mM, respectively. Similarly, the level of Ca^{2+} decreased with an increase in time duration of stress, with a maximum of 14.825 ± 0.594 mM after 6 h of osmotic stress. We observed an increase of 75% in Na^{+} till 12 h of stress compared to control conditions, whereas K^{+} content first increased to 185.12% at the initial hour of stress, which further decreased to 47% after 24 h compared to control conditions. Interestingly, we observed a very high concentration (~15 mM) of Ca^{2+} during the initial hour of stress, which further decreased to ~5 mM after 24 h of stress condition (Figure 3.5c).

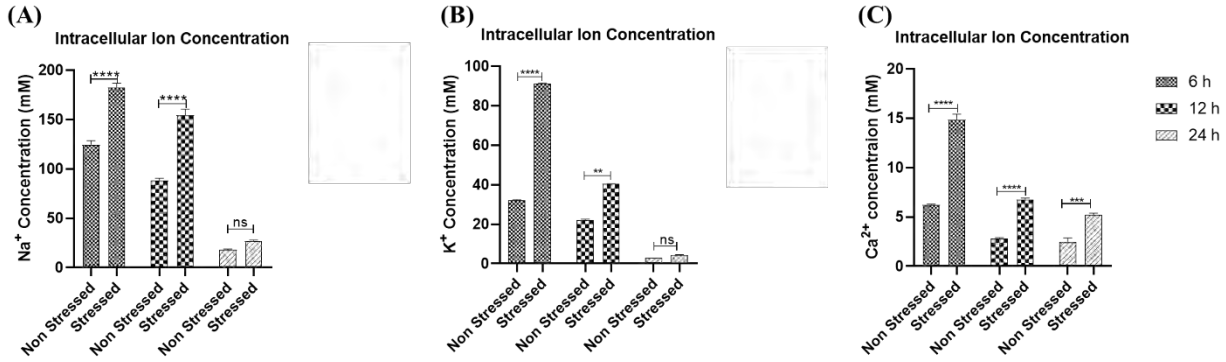

Figure 3.5. Intracellular ion concentration in *Eb* WRS7 **(A)** Sodium ion, **(B)** Potassium ion, and **(C)** Calcium ion. The error bar refers to the mean ± SD of three independent measurements. Horizontal bars with asterisks (*) indicate statistical significances between two values based on a student's t-test. Statistical significance: $*P \leq 0.05$, $**P \leq 0.01$, $***P \leq 0.001$, and $****P < 0.0001$, ns = not significant.

Both spectrometric and HPLC methods confirmed the production of phytohormones IAA and gibberellic acid (GA) by the given isolate. The water stress caused a significant increase of 23.11% and 119.31% in the level of the phytohormones IAA and GA, respectively (Figure 3.6), compared to non-stressed conditions. Further, the presence of IAA was confirmed by HRMS analysis. A mass peak of 175.066 was detected in mass spectra at 0.126-min retention time, which may correspond to IAA (Figure 3.7).

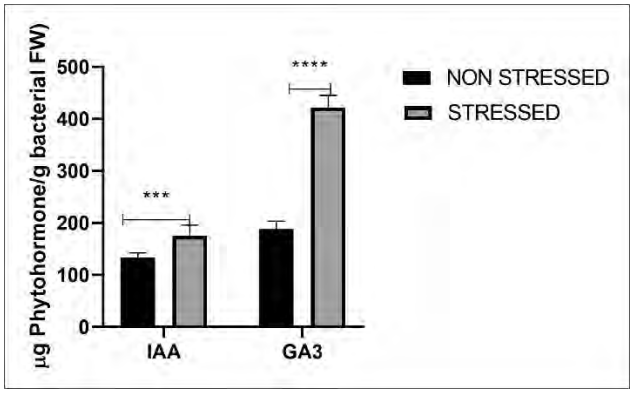

Figure 3.6. Quantification of secreted Indole Acetic Acid (IAA) and Gibberellic Acid (GA) of *Eb* WRS7 under osmotic-stress conditions. The concentration of the secreted phytohormones is expressed in µg/g bacterial fresh weight (FW). Each bar represents the mean ± SE of 5 biological replicates. Symbol '*' represents a significant difference between test samples.

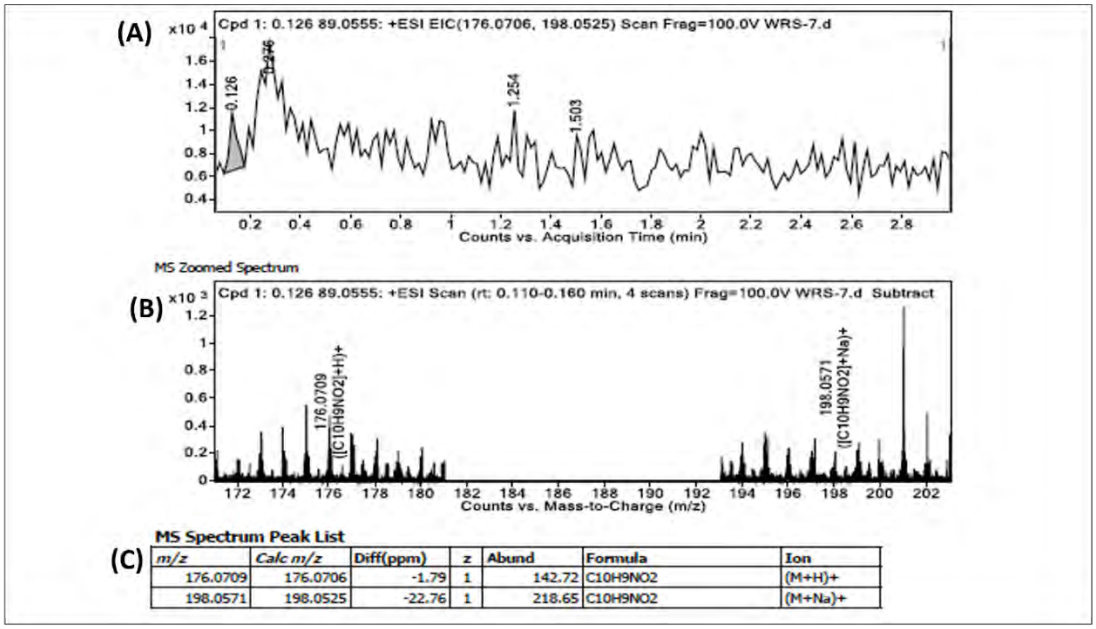

m/z	Calc m/z	Diff(ppm)	z	Abund	Formula	Ion
176.0709	176.0706	-1.79	1	142.72	C10H9NO2	(M+H)+
198.0571	198.0525	-22.76	1	218.65	C10H9NO2	(M+Na)+

Figure 3.7. HRMS spectra of secreted IAA by *Eb* WRS7. **(A)** chromatogram; **(B)** Mass Spectrum; and **(C)** Mass Spectrum Peak List.

We tested EPS production, along with the ability of *Eb* WRS7 to modulate endogenous proline and cellular protein under osmotic stress. In response to PEG-induced osmotic stress condition, there was an about 3-fold increase in EPS concentration. We also observed 1.8-fold higher free proline levels in stressed cells than in control cells. Finally, there was an increment in the total cellular protein content after 72 h under stress conditions (Figure 3.8).

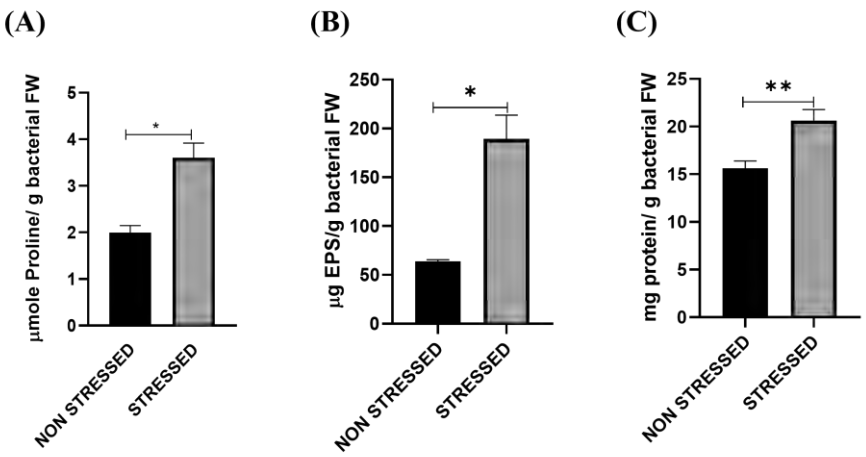

Figure 3.8. Quantification of **(A)** cell-free proline, **(B)** exopolysaccharide (EPS) production, and **(C)** total cellular protein in *Eb* WRS7 under non-stressed and osmotic-stressed (10% PEG) conditions. Each bar represents the mean± SE of three replicate samples. '*' represents the significant difference between osmotic-stressed versus non-stressed conditions based on a student's t-test. Statistical significance: *$P \leq 0.05$, **$P \leq 0.01$, ***$P \leq 0.001$, and ****$P <$ 0.0001, ns = not significant.

3.3.3 Plasma membrane lipid dynamics under osmotic stress

Since membrane lipids are crucial in protecting an organism from the adverse effects of osmotic stress, we analyzed the fatty acid profile of *Eb* WRS7 by GC-MS analysis. Saturated hydrocarbons such as triacontane, pentacosane, and tetradecane were detected at 0% PEG (non-stressed condition) along with unsaturated hydrocarbons such as heptadecene and nonadecene. At 10% PEG (osmotic stress), the hydrocarbon composition of the extract changed, showing the presence of saturated (hexadecane, heptadecane, triacontane, docosane, tetradecane) and unsaturated (9-eicosene, 1-dodecene, 1-heptadecene, 1-nonadecene, and 1-pentadecene) hydrocarbons (Figure 3.9a and Table 3.1). Some short-chain fatty acids like valeric acid were also detected under stressed conditions. Fatty alcohols like 1-dodecanol, 1-heptacosanol, and n-tetracosanol-1 were observed in both stressed and non-stressed conditions. The saturated fatty acids C16:0 and C18:0 and the monounsaturated fatty acid C18:1 were found as the predominant lipid components in non-stressed bacterial cells. A hierarchical heatmap was drawn using Metaboanalyst 5.0 software to represent the change in the fatty acid profile (Figure 3.9b), which showed the qualitative distribution of fatty acids under control and stress conditions. Heatmap clustering showed that saturated fatty acids like myristic and palmitic acids were less in stressed bacterial cells. In contrast, branched-chain fatty acids like isopalmitic acid were dominant in stressed bacterial cells.

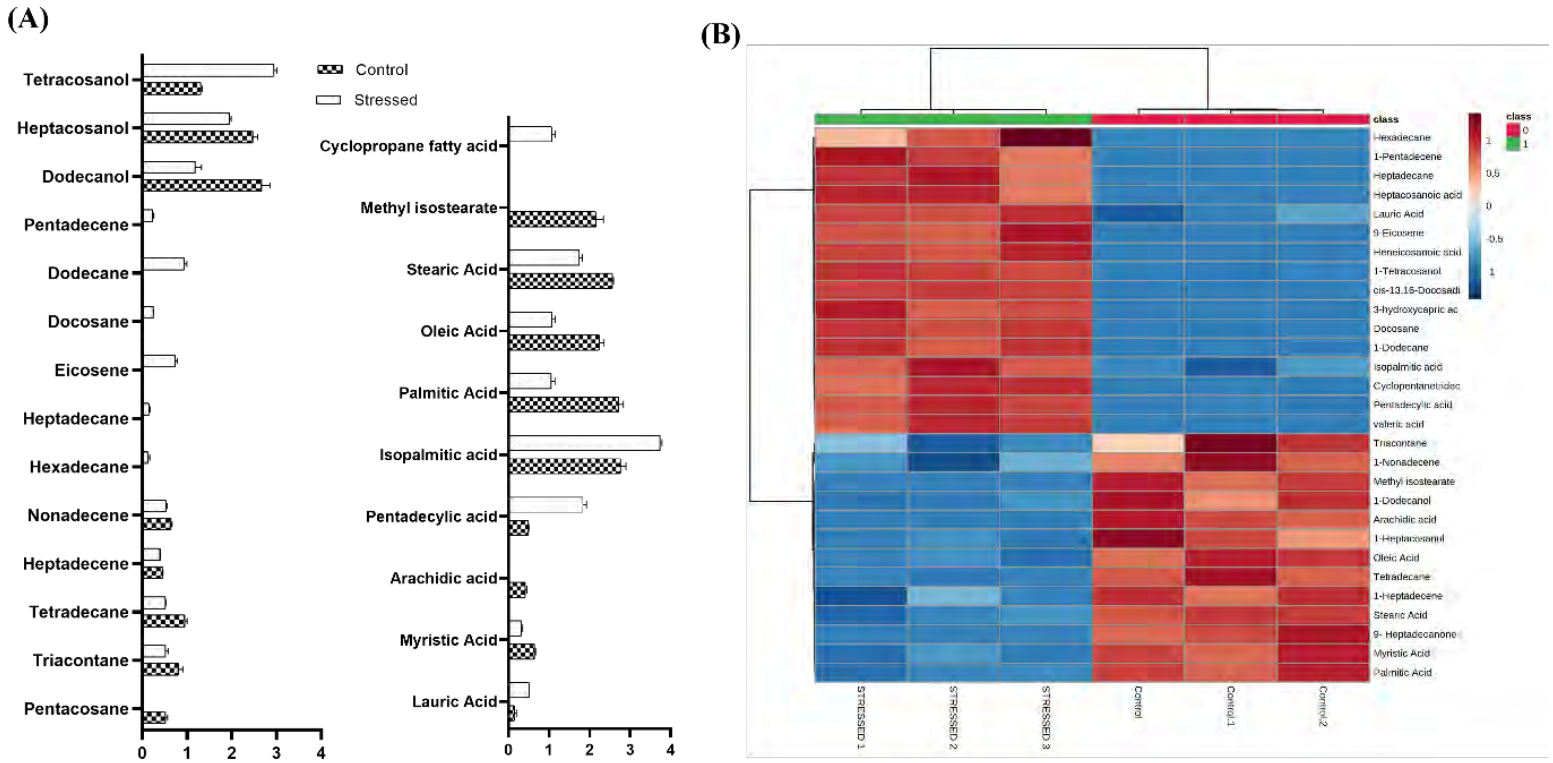

Figure 3.9. Change in fatty acids composition of *Eb* WRS7 cells exposed to osmotic stress. **(A)** Normalized abundance of saturated and unsaturated fatty acids and **(B)** Heatmap hierarchical clustering of detected fatty acids. A hierarchical tree was performed to detect fatty acids in control (non-stressed) and osmotic stress treatment using Metaboanalyst 5.0 software. Each colored cell on the map represents the peak intensity. Columns correspond to two conditions in replicates (n=3), while rows represent different metabolites detected. On the top of the heatmap, control samples are represented in red, while stressed samples are represented in green. A dark blue to dark red color gradient denotes lower to higher expression.

Table 3.1. The membrane fatty acid composition of Eb WRS7 was grown in normal (without PEG) and osmotic stressed (with 10% PEG) conditions.

S. No.	Formula	Compound (methyl ester/ Hydrocarbon)	Name of fatty acid	Corresponding Acid	Condition	FC*
1	$C_{13}H_{26}O_2$	Dodecanoic acid- methyl ester	Lauric Acid	C12:0	Both	1.779
2	$C_{15}H_{30}O_2$	Tetra decanoic acid- methyl ester	Myristic Acid	C14:0	Both	-0.985
3	$C_{21}H_{42}O_2$	Eicosanoic acid-methyl ester	Arachidic acid	C20:0	Non-stressed	-2.412
4	$C_{16}H_{32}O_2$	Pentadecanoic acid, methyl ester	Pentadecylic acid	C15:0	Both	1.897
5	$C_{16}H_{32}O_2$	Pentadecanoic acid, 14-methyl-, methyl ester	Isopalmitic acid	C16:0	Both	0.488
6	$C_{17}H_{32}O_2$	Hexadecanoic acid, methyl ester	Palmitic Acid	C16:0	Both	-1.357
7	$C_{19}H_{36}O_2$	8- octadecenoic acid, methyl Ester	Oleic Acid	C18:1	Both	-1.07
8	$C_{19}H_{38}O_2$	Octadecanoic acid, methyl ester	Stearic Acid	C18:0	Both	-0.550
9	$C_{19}H_{38}O_2$	Heptadecanoic acid, 16-methyl-, methyl ester	Methyl isostearate	C18:0	Non-stressed	-2.455
10	$C_{28}H_{56}O_2$	Heptacosanoic acid, methyl ester		C27:0	Stressed	2.497
11	$C_6H_{12}O_2$	Pentanoic acid, methyl ester	valeric acid	C5:0	Stressed	2.412
12	$C_{10}H_{20}O_3$	3-Hydroxydecanoic acid	3-hydroxycaproic acid	C10:0	Stressed	2.408
13	$C_{22}H_{44}O_2$	Heneicosanoic acid, methyl ester		C21:0	Stressed	2.392
14	$C_{19}H_{36}O_2$	Cyclopentanetridecanoic acid, methyl ester		C18:0	Stressed	2.459
15	$C_{17}H_{34}O$	9- Heptadecanone		C17:0	Non-stressed	-2.437
16	$C_{30}H_{62}$	Triacontane		C30:0	Both	-0.624
17	$C_{14}H_{30}$	Tetradecane		C14:0	Both	-0.875
18	$C_{16}H_{34}$	Hexadecane		C16:0	Stressed	2.737
19	$C_{17}H_{36}$	Heptadecane		C17:0	Stressed	2.484
20	$C_{22}H_{46}$	Docosane		C22:0	Stressed	2.361
21	$C_{12}H_{26}$	Dodecane		C12:0	Stressed	2.411
22	$C_{17}H_{34}$	1-Heptadecene		C17:1	Both	-0.191
23	$C_{19}H_{38}$	1-Nonadecene		C19:1	Both	-0.278
24	$C_{20}H_{40}$	9-Eicosene		C20:1	Stressed	2.410
25	$C_{15}H_{30}$	1-Pentadecene		C15:1	Stressed	2.494
26	$C_{12}H_{26}O$	1-Dodecanol		C12:0	Both	-1.502
27	$C_{27}H_{56}O$	1-Heptacosanol		C27:0	Both	-0.336
28	$C_{24}H_{50}O$	1-Tetracosanol		C24:0	Both	1.206

*FC= Fold change w. r. t. normal condition (n= 3).

3.3.4 Metabolic responses under osmotic stress

To study the role of metabolites and identify the metabolic pathways participating in osmotic stress tolerance, we extracted intracellular metabolites and performed GC-MS-based untargeted metabolomics of *Eb* WRS7 grown under normal and osmotic stress conditions (PEG-10%). We identified 33 significantly deregulated metabolites (fold change ≥ 1.9) in control vs. stress-exposed cells. Based on their chemical structure, functions, and associated metabolic pathways, annotated metabolites were categorized into different classes, such as organic acids (TCA cycle metabolites), sugar/carbohydrates, amino acids, polyamines, phytohormones, and osmolytes (Figure 3.10a). Metabolites of glycolysis, TCA cycle pathways, and sugar/carbohydrates are significantly higher in stress-exposed cells than in control cells. Similarly, polyamines (putrescine and cadaverine), phytohormones (indole acetic acid and gibberellic acid), and osmolytes (trehalose, proline, glycine betaine, and ethanolamine) were also over-accumulated in stress exposed cells. Osmotic stress also resulted in a higher level of some amino acids such as aspartate, proline, glutamate, and tryptophan, whereas amino acids like leucine, tyrosine, and lysine were significantly reduced (Figure 3.10a).

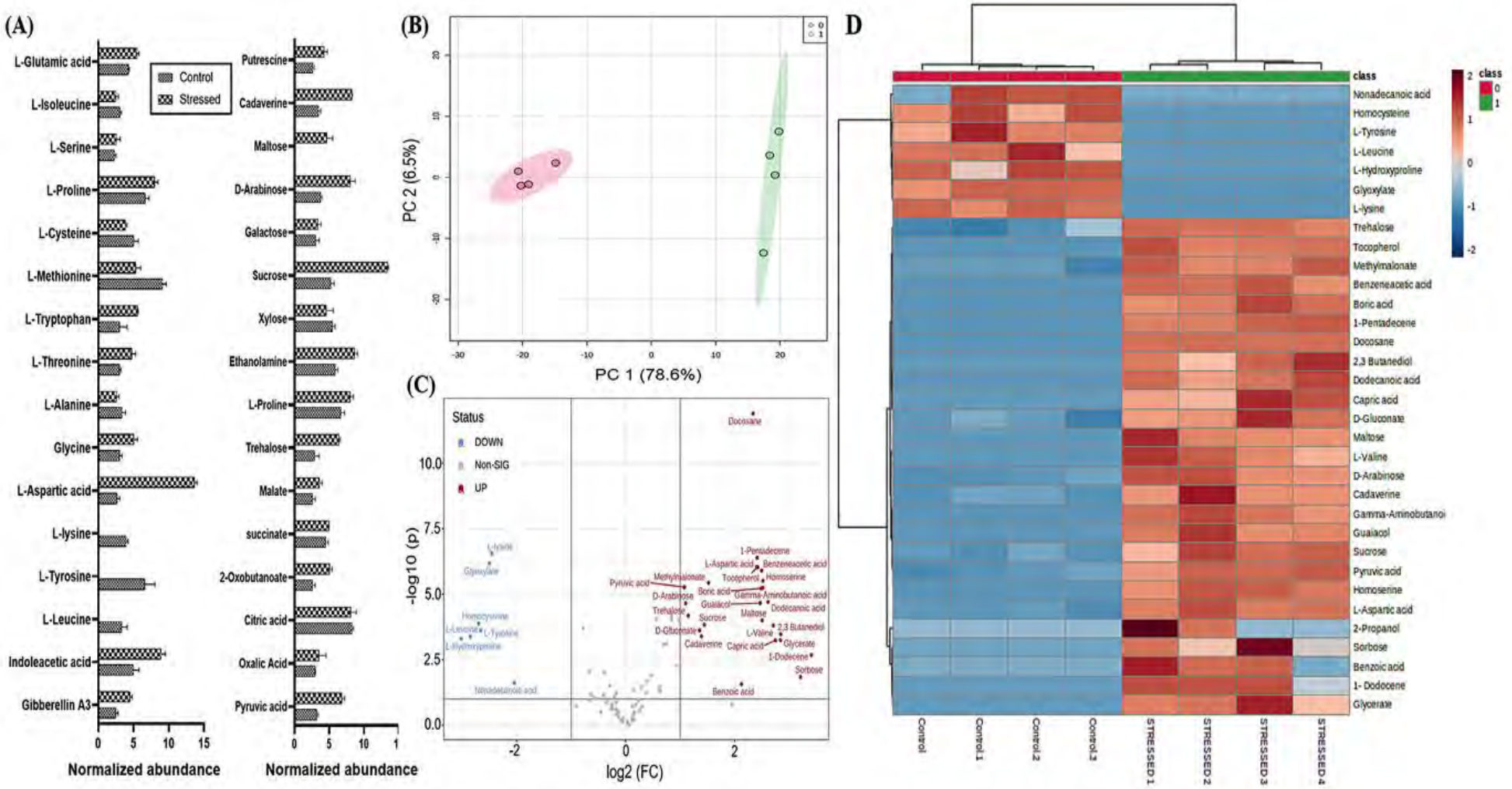
(A)
L-Glutamic acid
L-Isoleucine
L-Serine
L-Proline
L-Cysteine
L-Methionine
L-Tryptophan
L-Threonine
L-Alanine
Glycine
L-Aspartic acid
L-lysine
L-Tyrosine
L-Leucine
Indoleacetic acid
Gibberellin A3
Control
Stressed
0 5 10 15
Normalized abundance
Putrescine
Cadaverine
Maltose
D-Arabinose
Galactose
Sucrose
Xylose
Ethanolamine
L-Proline
Trehalose
Malate
succinate
2-Oxobutanoate
Citric acid
Oxalic Acid
Pyruvic acid
0 5 10 1
Normalized abundance
(B)
PC 2 (6.5%)
PC 1 (78.6%)
(C)
Status
DOWN
Non-SIG
UP
-log10 (p)
log2 (FC)
Docosane
1-Pentadecene
L-Aspartic acid
Benzeneacetic acid
Pyruvic acid
Methylmalonate
Tocopherol
Homoserine
D-Arabinose
Boric acid
Gamma-Aminobutanoic acid
Guaiacol
Dodecanoic acid
Trehalose
Sucrose
Maltose
D-Gluconate
L-Valine
2,3 Butanediol
Cadaverine
Capric acid
Glycerate
1-Dodecene
Sorbose
Benzoic acid
L-lysine
Glyoxylate
Homocysteine
L-Leucine
L-Tyrosine
L-Hydroxyproline
Nonadecanoic acid
D
class
Nonadecanoic acid
Homocysteine
L-Tyrosine
L-Leucine
L-Hydroxyproline
Glyoxylate
L-lysine
Trehalose
Tocopherol
Methylmalonate
Benzeneacetic acid
Boric acid
1-Pentadecene
Docosane
2,3 Butanediol
Dodecanoic acid
Capric acid
D-Gluconate
Maltose
L-Valine
D-Arabinose
Cadaverine
Gamma-Aminobutanoi
Guaiacol
Sucrose
Pyruvic acid
Homoserine
L-Asparticacid
2-Propanol
Sorbose
Benzoic acid
1- Dodecene
Glycerate
Control
Control1
Control2
Control3
STRESSED 1
STRESSED 2
STRESSED 3
STRESSED 4

Figure 3.10. Change in intracellular metabolites of *Eb* WRS7 cells exposed to osmotic stress (PEG- 10%). **(A)** Normalized abundance of different metabolites, **(B)** Scores Plot (PC1 vs. PC2) of partial least-squares- discriminant analysis (PLS-DA) of metabolites. Each ring represents the distribution of biological replicates. The pink color denotes control samples, whereas the green color represents stressed samples. **(C)** Volcano map depicting contributory metabolites to the differences in two conditions, with fold change threshold (x-axis) =2 and t-tests threshold (y-axis) =0.1. **(D)** Heatmap hierarchical clustering of detected intracellular metabolite pools. Hierarchical trees were drawn based on detected metabolites in control (non-stressed) and osmotic stress treatment. Columns correspond to two conditions in replicates, while rows represent different metabolites detected.

The biological replicates clustered together, whereas metabolites under normal and stressed conditions clustered differently. Principle component analysis (PCA) was used to visualize variance between the two conditions, which showed a similar clustering pattern. A total variance of 85.1% (PC 1= 78.6% and PC 2= 6.5%) was observed (Figure 3.10B). Considering the control (non-stressed) condition as a reference, 26 metabolites were significantly upregulated (shown in red), whereas 7 were significantly downregulated (shown in blue) in stress-exposed cells, as shown in the volcano plot (Table 3.2 and Figure 3.10C). Annotated metabolites were further processed by hierarchical clustering to provide an intuitive visualization of metabolite changes under tested conditions (Figure 3.10D). The heat map obtained from the selected metabolites indicates that some metabolites are upregulated while others are downregulated under osmotic stress (Figure 3.10D). Finally, metabolite enrichment analysis revealed the functions and involvement of these metabolites in various metabolic pathways. Based on this observation, we conclude that the TCA cycle, glyoxylate, dicarboxylate metabolism, alanine, aspartate and glutamate metabolism, and fatty acid biosynthesis metabolic pathways are significantly more active in response to osmotic stress in *Eb* WRS7 (Figure 3.11A, B).

Table 3.2. Significantly altered intracellular metabolites of *Eb* WRS7. The fold change shows metabolite levels from *Eb* WRS7 with osmotic stress (by PEG 10%) compared to the non-stressed condition.

S. No.	Metabolites	Log 2 (Fold Change)
1.	1-Dodecene	3.406
2.	Sorbose	3.2082
3.	L-Hydroxyproline	-3.0187
4.	L-Leucine	-2.8512
5.	2,3 Butanediol	2.844
6.	Glycerate	2.8413
7.	Capric acid	2.7461
8.	L-Valine	2.7076
9.	Homocysteine	-2.697
10.	L-Tyrosine	-2.6581
11.	Dodecanoic acid	2.6116
12.	Homoserine	2.5187
13.	Gamma-Aminobutanoic acid	2.517
14.	Maltose	2.5027
15.	Glyoxylate	-2.4979
16.	Benzeneacetic acid	2.4945
17.	Boric acid	2.4891
18.	Guaiacol	2.467
19.	L-lysine	-2.4569
20.	Tocopherol	2.4213
21.	1-Pentadecene	2.4108
22.	L-Aspartic acid	2.4041
23.	Docosane	2.3378
24.	Benzoic acid	2.1249
25.	Nonadecanoic acid	-2.0448
26.	2-Propanol	1.9509
27.	Methylmalonate	1.5216
28.	Sucrose	1.4431
29.	Cadaverine	1.3913
30.	D-Gluconate	1.3558
31.	Trehalose	1.1505
32.	D-Arabinose	1.1025
33.	Pyruvic acid	1.0769

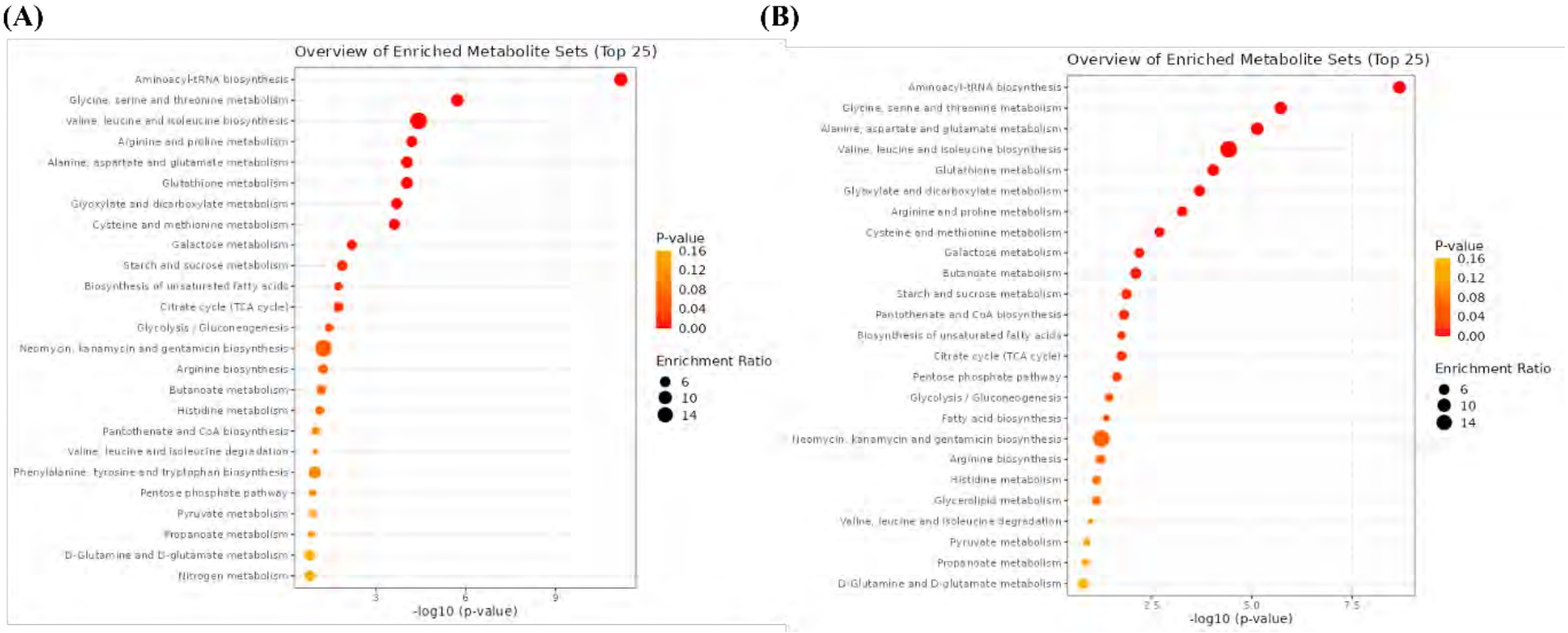

Figure 3.11. Dot plot of KEGG pathway enrichment of metabolites corresponding to **(A)** Non-stressed and **(B)** Osmotic stressed in *Eb* WRS7. The top 25 enriched pathway terms are displayed. The P-value indicates the enrichment level of the pathway term and ranges from 0 to 1.

3.3 Discussion

The rhizosphere microbiome is considered one of the effective and better alternative approaches for sustainable agriculture and a reasonable solution to meet the twin challenges of food security and environmental stability. This approach offers several advantages, including the capability of PGPR to confer abiotic stress tolerance through modulating plant physiological and biochemical traits [11]. Developing drought-tolerant PGPR (bioinoculant) seems a promising solution to improve crop productivity under drought-prone agroecosystems. However, despite an increased application of PGPR, our understanding of the stress adaptation mechanisms of PGPR communities under drought is still incomplete. In this study, we contend that a comprehensive understanding of the complex physiological and biochemical responses to drought will pave the way for rhizosphere engineering through PGPR and, ultimately, the exploitation of these responses to increase the drought resistance of crop production. Among all the isolates recovered in our study, PGPR *Eb* WRS7 showed plants' best growth-promoting and abiotic stress tolerance ability under drought stress (Chapter II). Being isolated from a drought-prone agroecosystem and considering its role in ameliorating plant growth under drought stress, we hypothesized that this PGPR might have unique stress adaptation abilities.

To prove our hypothesis, we initially assessed the growth and morphology of this bacterium upon drought exposure. Since dehydrating agents like PEG can reduce bacterial growth, *Eb* WRS7 growth was studied at different concentrations of PEG. It is evident from Figure 3.2A that *Eb* WRS7 showed better growth and survival under osmotic stress conditions than *E. coli,* used as control, at higher PEG concentration (Figure 3.2C). However, slower growth was observed than its non-stressed counterparts. Under stress conditions, bacterial cells might have directed their energy flow towards activating the protection mechanisms, which might have affected their growth [128, 206]. Previous reports also described the tolerance of PGPR *Pseudomonas* sp. and *Bacillus* sp. under osmotic stress [59, 206]. There were no significant morphological changes, but we observed the formation of vesicle-like structures in response to osmotic stress. Vesicle formation is influenced by bacterial growth stage and stress insults. These vesicles might serve some specialized function, such as nutrient acquisition or biofilm formation, and play an important role in host-microbe interactions, hence offering stress tolerance under stressful environmental conditions [207, 208]. McMillian *et al.* (2021) reported that outer membrane vesicles from *Pseudomonas syringae* and *P. fluorescens* activate plant immune response in *Arabidopsis thaliana* against pathogenic bacteria [209]. Membrane vesicles play an essential defense function in mitigating osmotic and oxidative stress [210]. The

latest study described the role of vesicles in mitigating the osmotic stress in *E. coli* when exposed to titanium dioxide nanoparticles, showing that osmotic stress and cell vesiculation are associated with nanoparticle resistance [211]. However, factors stimulating vesicle generation and their specialized functions in PGPR have not been well studied; therefore, specific experiments are required to know the exact function of this vesicle-like structure in future studies.

The primary signal caused by drought is hyperosmotic stress, which often induces complex secondary effects such as oxidative stress, damage to cellular macromolecules, and consequent metabolic dysfunction. Oxidative stress triggers over-accumulation of the cells' ROS. Excess ROS production induces lipid (polyunsaturated fatty acids) peroxidation in the cells, as evidenced by a high content of MDA, a common biomarker of oxidative stress, and determines the antioxidant status of the cell [212]. Lipid peroxidation alters the membrane structure, affecting its fluidity and damaging its integrity [213]. We observed an initial increase in ROS and MDA followed by a decline at 24 h, indicating adaptive responses of this bacteria against stress. ROS production is a normal physiological process and plays a vital role in cell signaling and homeostasis [214]. Over-accumulation of ROS is, however, kept under tight control by a versatile and cooperative antioxidant system. ROS functions as a secondary messenger that triggers adaptive responses by activating signal transduction pathways, limiting intracellular ROS concentration and hence maintaining the cell's redox homeostasis [214].

The common osmoadaptation mechanisms of bacteria include accumulating or releasing solutes such as inorganic ions (often K^+, Na^+, and Cl^-) and organic osmolytes to attenuate water fluxes (efflux/influx) to counter the variations in external osmotic pressure [215, 216]. In bacteria, K^+ is the most abundant inorganic ion in the cell cytosol and, therefore, is the most suitable candidate for osmotic adjustment purposes under stress conditions. The electrochemical gradients favor K^+ loss and accumulation of Na^+ into the cell via specific ion transport systems and play a significant role in maintaining normal cell turgor. The imbalance in the cytosolic K^+/Na^+ ratio dramatically impacts cell metabolism and may trigger programmed cell death [217]. In *E. coli*, it has been reported that osmotic shock causes an increase in intracellular Na^+ over K^+ concentration [218]. We also observed higher Na^+ concentrations than K^+ in stressed cultures, suggesting inorganic ions' role in maintaining osmotic balance in *Eb* WRS7. However, more experimental data are needed to support our hypothesis. It is well established that hyperosmotic stress induces a rapid rise in intracellular Ca^{2+} concentration in plants and may reflect the activities of biochemical and metabolic

components to counter osmotic stress [219]. Interestingly, we also observed higher Ca^{2+} concentration, suggesting the role of this secondary messenger in activating the osmo-adaptation mechanism in this PGPR. A previous report shows that Ca^{2+} affects several bacterial physiological processes, including chemotaxis, cell differentiation (spore development and heterocyst formation), and membrane transport [220]. We also recorded high Ca^{2+} under stress conditions, which might be involved in an osmotic stress signalling pathway.

Microorganisms preferentially accumulate organic solutes like glutamate, glycine betaine, proline, and trehalose, decreasing water potential without interfering with cellular metabolism. These osmolytes maintain osmotic potential and scavenge ROS, thus preventing cellular damage from oxidative stress without any adverse effects on cellular macromolecules [201, 217]. We observed around a two-fold increase in proline content under stress. Microorganisms can increase their function and survival in hostile environments by improving their local habitat.

Phytohormones secreted as secondary metabolites by bacteria can act as phytostimulants and prominently impact plant growth and metabolism under stress and non-stress conditions [59]. Bacteria-secreted phytohormones modulate plant hormone levels in a similar way as exogenous phytohormone application does. As previously reported, bacterial IAA stimulates primary root elongation and helps form lateral roots, affecting the root architecture and helping plants survive under stressful conditions [148, 221]. Gibberellic acid is a growth hormone involved in cell elongation and division and responds to abiotic stress. Also, GAs produced by PGPR improve plant growth and yield [222]. Similar to our observations regarding increased IAA and GA production under drought stress, some research groups also reported increased production of phytohormones by PGPR under drought stress. Ghosh *et al.* reported enhanced production of auxin and GA by *Bacillus* and *Pseudomonas* strains under osmotic stress [59], whereas Bhatt *et al.* reported the same for *Enterobacter* strain P-39 under osmotic stress [223].

Since drought limits substrate availability and reduces nutrient diffusion, bacteria preferably start synthesizing extracellular polymeric substance (EPS) as an effective drought adaptation method. EPS functions like a sponge, slowing the drying process and thus retaining water by allowing action at low water potential [224]. Our results also indicate increased EPS (predominantly containing polysaccharides, protein, and DNA) production and a significant increase in protein content after 72 h in stressed cells. This might be because of the enhanced production of bacterial extracellular protein to produce EPS, which protects them against

desiccation [224]. Bacterial cellular protein contributes to exopolysaccharide (EPS) production under stress conditions [59], which in turn forms a sheath around the bacterial colonies and protects them from osmotic stress by decreasing water loss [201]. EPS exhibits high antioxidant properties, protecting bacteria from ROS-dependent cell death [225]. EPS produced by bacteria not only helps them tolerate osmotic stress but also improves the quality and fertility of the soil, acts as a nutrient facilitator, reduces ion toxicity, and maintains plant health under abiotic stress [54].

Microbes tune their membrane lipid composition to maintain membrane fluidity and properties in response to environmental changes. Global patterns of lipid remodelling can provide insights into fundamental principles of membrane adaptation [226, 227]. Lipid determination by FAME analysis is an accurate reflection and can be used to quantify total lipids. Using FAME-based lipidomics, we examined the total lipid fraction of this PGPR to understand the role of fatty acids in regulating membrane dynamics. The change in fatty acid composition, especially carbon length and degree of saturation under stressed conditions, indicates the adaption of bacteria to tolerate osmotic stress, increasing the cytoplasmic membrane's fluidity. They also play an important role in membrane stability and permeability [228]. Under stressed conditions, there was an increase in cyclopropane fatty acids. The bacterial production of the cyclopropane ring is related to changes in the composition of the membrane fatty acids. It represents one of the most important adaptive microbial responses that favor the stress tolerance of several bacteria [229]. Cyclopropane membrane lipids have been associated with resistance to oxidative stress in *Mycobacterium tuberculosis*, organic solvent stress in *E. coli*, and acid stress in *E. coli* and *Salmonella* [230]. It has been reported that in the membrane of *Lactococcus lactis*, osmotic stress induces high levels of cyclopropane fatty acid (ΔC19:0) [231]. Although the mechanism is not yet known, researchers believe that a change in the fatty acid composition of the lipid membrane may regulate glycine betaine transporter activity [193]. Earlier studies showed a different profile of fatty acids under stress conditions, which might help bacterial cells survive the changing environment by maintaining the cell membrane as an iso-osmotic barrier [207]. Therefore, the present study highlighted that bacteria change their membrane composition in changing environments for survival.

To get a deeper insight into the stress adaption mechanism, we evaluated the metabolic responses of this PGPR (*Eb* WRS7) under drought. To better understand the mechanism of osmolarity and adaptability, we employed GC-MS-based untargeted metabolomics to determine the change in primary and secondary metabolites under drought stress. Deregulation

in these intracellular metabolites indicated the operation of central carbon and nitrogen metabolism in response to osmotic stress and provided deeper insights into the osmoadaptation mechanism of PGPR. Deregulated metabolites were subdivided into several classes based on their biochemical structure, functions, and involvement in different metabolic pathways. We recorded higher organic osmolyte content, including amino acids, polyamines, quaternary ammonium compounds, and sugars. The role of these metabolites in osmoprotection has been very well-established in many bacteria [215]. We observed a higher content of ethanolamine and polyamines. It has been reported that ethanolamine is a precursor of betaine and proline, and its supplementation promotes glycine biosynthesis [232]. Polyamines possess antioxidant properties and protect bacteria exposed to oxidative stress by decreasing ROS, binding and shielding negatively charged macromolecules, and modulating the expression of adaptive genes [233]. For instance, cadaverine can bind to porin proteins and lipopolysaccharides of the cell envelope, regulate transport through the outer membrane, and is involved in the adaptive responses to acid stress, redox-active compounds, and antibiotics. Putrescine primarily binds to nucleic acids, regulates gene expression by modulating transcription, protein stability, mRNA secondary structure, and functioning of the ribosome, stabilizes and protects DNA, and is involved in the adaptive responses to oxidative stress, osmotic shock, heat shock, etc [232].

In addition to the aforementioned organic molecules, volatile organic compounds (VOCs) were over-accumulated in stress-exposed cultures. Under stress exposure, PGPR produces VOCs to regulate osmolyte and phytohormone biosynthesis. These compounds also play a crucial role in plant-microbe interactions [223]. The ability of 2, 3-butanediol, and acetoin in plant growth promotion and induced systemic resistance against pathogenic fungi, bacteria, and viruses in plants has been reported in earlier studies [234, 235]. Also, 2, 3-butanediol secreted by bacteria is known to stimulate root development, leading to increased nutrients and water uptake by plants and hence improving plant growth [62]. In our study, 2, 3-butanediol was detected under osmotic stress known to be produced by various root-associated bacteria such as *Bacillus* sp., *Aerobacter* sp., and *Klebsiella* sp. [236]. To best of our knowledge, production of 2, 3-butanediol by *E. bugandensis* has not been reported earlier. Although VOCs regulate growth hormones and ion acquisition, a lot more can be explored regarding their direct role in the bacteria defense system and ameliorating abiotic stress in plants. Metabolomics data also highlighted increased levels of sugar molecules such as sucrose, maltose, and arabinose in *Eb* WRS7 under osmotic stress. It has been reported that the production of EPS required a higher amount of glucose, trehalose, mannose, and rhamnose for better water retention ability

[237]. Therefore, higher sugar content might contribute to EPS production, enhance water retention within the bacteria, and protect them from fluctuating water potential [238]. Higher sugars may also act as a carbon pool to fulfill the carbon demands of this PGPR under drought.

Finally, we observed a higher accumulation of the glycolytic pathway and TCA cycle metabolites such as pyruvate, α- ketoglutarate, succinate, malate, and oxaloacetate. Moreover, several amino acids, such as aspartate and glutamate, are over-accumulated in contrast to leucine, lysine, and tyrosine, showing lower concentrations under stress exposure. Since survival in high osmotic stress is an energy-demanding process, and the production of osmolytes demands high energy and carbon, the activation of glycolysis and the TCA cycle might be involved in fulfilling these demands [239]. Under osmotic stress, the glycolytic pathway may have contributed to the production of trehalose in plants and bacteria [240]. Also, increased levels of glycolysis and TCA cycle metabolites might provide energy in the form of ATP to the bacterial cell under stressed conditions [241, 242]. Glutamate is an important metabolite that plays a role in various metabolic processes and is involved in protein synthesis and other fundamental processes such as glycolysis, gluconeogenesis, and the TCA cycle. Glutamate metabolism plays a vital role in resistance to acid stress and multiple other stresses in *E. coli* [242]. Since the synthesis of glutamate and aspartate are energetically economical for the bacteria and act as a counter partner for K^+, which increases during the osmotic stress, this can be an adaptive strategy of bacteria to deal with hyperosmotic stress [242]. Similar to our findings, a previous study reported a decrease in aromatic (tyrosine) and branched chain (leucine and isoleucine) amino acids, which may be a result of increased energy demands for maintaining cell integrity and homeostasis under stress [242]. Moreover, the increased production of essential amino acids like threonine and serine during stress can produce the defense molecule glutathione [243]. Furthermore, there was an increase in intracellular tryptophan, IAA, and GA levels under osmotic stress conditions. These observations support the PGPR capability of *Eb* WRS7. However, to understand the specific role of phytohormones in bacterial physiology, further experiments are needed using mutant bacterial strains, compromising their ability to produce these phytohormones. The deregulation in metabolites indicates that *Eb* WRS7 can modulate their physiological and metabolic processes to combat stress. These metabolic responses and alterations in cellular metabolism might be related to certain stress signaling and adaptation mechanisms and provide a roadmap for the commercialization of bacterial metabolites for the development of bioinoculants, which can

combat abiotic stress and improve plant growth and yield in drought-prone agroecosystems in a sustainable manner.

In conclusion, this study provides a detailed understanding of the stress-responsive mechanism(s) in *Eb* WRS7 at a metabolic level under drought/osmotic stress conditions (Figure 3.12). Stress-tolerant abilities of PGPR strains and their detailed understanding of the osmo-adaptation mechanism could be translated into the engineering of efficient PGPR inocula (biofertilizer) with wide adaptability to the different agroecosystems with varying soil types and eventually can be harnessed for the betterment of dryland agriculture.

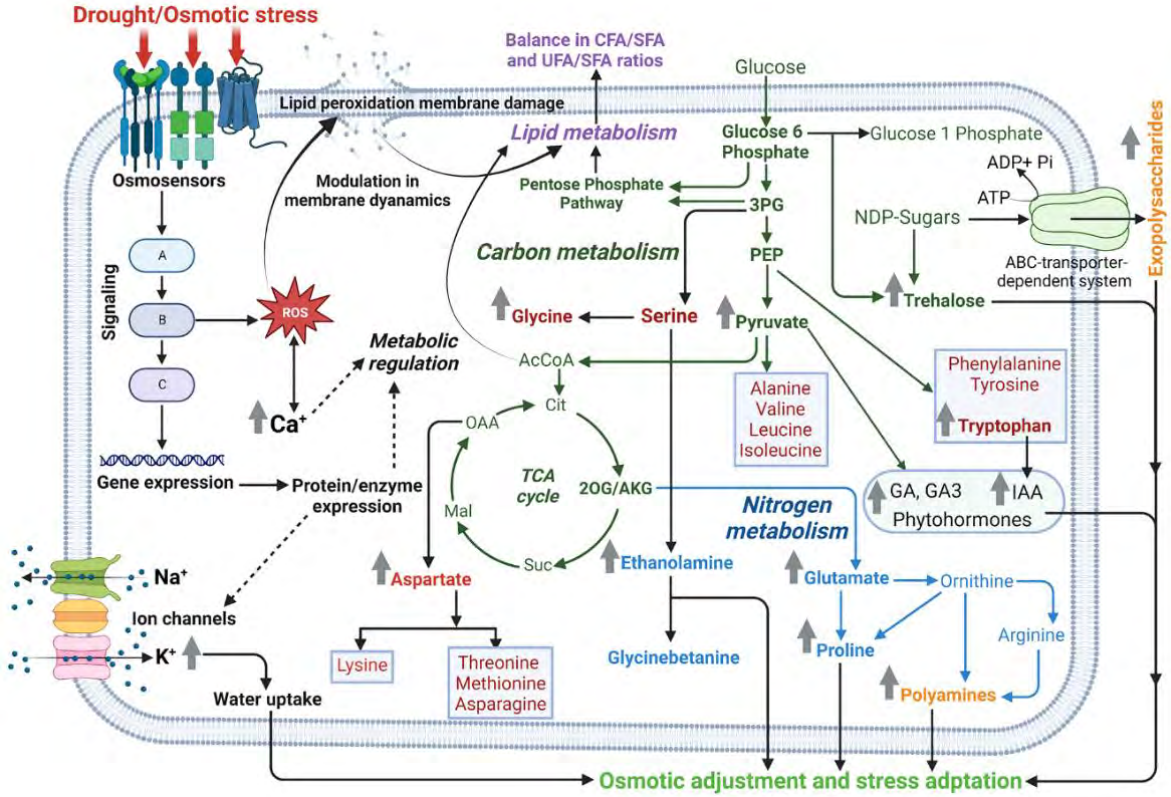

Figure 3.12. *Eb* WRS7 response to osmotic stress and tolerance mechanism. Drought/osmotic stress triggers osmosensors and induces oxidative stress through ROS accumulation. ROS causes lipid peroxidation and damage to the plasma membrane. ROS over accumulation activates cell signaling cascades and induces gene expression. Osmotic stress tolerance mechanisms are governed by maintaining the lipid dynamics (balance in membrane fatty acids) and ion transport systems. PGPR regulate their carbon and nitrogen metabolism to fulfill the energy demands, and biosynthesis of osmolytes and other secondary metabolites. Abbreviations: 2OG-2-oxoglutarate3PG-3-phosphoglycerate, AcCoA-acetyl coenzyme A, AKG-alpha ketoglutarate, Cit-Citrate, CFA-cyclo fatty acid, GA-gibberellic acid, IAA-indole acetic acid, Mal-malate, NDP-nucleotide diphosphates, OAA-oxaloacetic acid, PEP- phosphoenolpyruvate, ROS-reactive oxygen species, SFA-saturated fatty acid, Suc-succinate, UFA-unsaturated fatty acid.

CHAPTER IV

Role of PGPR *Enterobacter bugandensis* WRS7 in Modulating Gene Expression and Metabolites of Host Plants under Drought Stress.

Part of this study has been published as – "**Arora, S**., Jha, P.N. Drought-Tolerant *Enterobacter bugandensis* WRS7 Induces Systemic Tolerance in *Triticum aestivum* L. (Wheat) Under Drought Conditions. J Plant Growth Regul (2023). https://doi.org/10.1007/s00344-023-11044-6"

4.1 Introduction

Drought stress restricts the utilization of arable land and crop productivity worldwide. In response to drought stress, plants undergo hyperosmotic signal transduction, which leads to transcriptional and metabolomic reprogramming and repair stress-induced damage to maintain cellular homeostasis [80]. Various microorganisms including beneficial soil microbes inhabit plants and stimulate plant growth and plant tolerance to various environmental conditions including drought. *Eb* WRS7 was found to be an important plant growth-promoting rhizobacteria due to its ability to protect wheat plants from drought stress conditions and its ability to colonize plants efficiently. It has several plant-growth-promoting properties such as exopolysaccharide production, ACC deaminase activity, phytohormone production, phosphate solubilization, and siderophore production. Inoculation of this bacterium promotes wheat plant growth under stress (Chapter II). Moreover, *Eb* WRS7 has shown the ability to tolerate osmotic stress (Chapter III). Therefore, it can be exploited as a promising biofertilizer candidate to promote plant growth under drought-stress conditions.

Drought-stress response in plants is a complex mechanism involving various physiological and molecular regulation. The mechanism of drought tolerance includes ion homeostasis, osmolytes biosynthesis, and scavenging of harmful radicals. To tolerate drought stress, one of the most important strategies of plants is to accumulate solutes, known as osmolytes, of lower cellular water potential to maintain cellular turgor. PGPR confer drought stress tolerance in plants by increasing the plant's capacity to produce osmolytes [12]. Drought stress enhances the generation of ROS, which is responsible for cellular damage. To mitigate drought-induced oxidative damage, plant activates their antioxidant enzyme system, which protects plants from oxidative stress [244]. PGPR enhances plants' ability to produce antioxidant enzymes under oxidative stress generated from abiotic and biotic stress [12]. Drought-tolerant PGPR can tolerate osmotic stress and help plants ameliorate drought stress through several synergistic mechanisms, including increasing osmolyte accumulation, nutrient uptake, phytohormone signalling, and antioxidant capacity. Moreover, in response to PGPR, plant cells undergo transcriptional reprogramming, which may enhance plant growth and stress tolerance [80]. For instance, Gontia-Mishra (2016) and their group investigated the effect of PGPR *Enterobacter ludwigii* and *Flavobacterium* sp. in wheat at physiological and biochemical parameters. They studied gene expression of stress-responsive genes under drought stress. These PGPR can improve plant growth under drought stress by attributing plant growth directly influencing

plant physiology and regulating the expression of genes required to protect plants from abiotic stress-mediated alteration of plant functions. They also reported upregulation of some stress-related genes, such as *CAT1* and *DREB2A,* in uninoculated wheat plants under drought stress, whereas attenuated transcript levels were observed in PGPR-inoculated plants, indicating improved tolerance due to PGPR interaction [28]. Similarly, Barnawal *et al.* suggested that PGPR inoculation confers abiotic stress tolerance by modulating the expression of the *CTR1* gene, a regulatory component of the ethylene signalling pathway and *DREB2* in wheat [82]. These works suggest that the plant-microbe interaction can be a promising approach to improving plant growth and productivity in a drought environment through multiple mechanisms. Therefore, understanding plant–PGPR interaction at the biochemical and molecular level will be highly helpful in exploiting selective PGPR for sustainable agriculture. Therefore, the present study aimed to characterize their abilities to ameliorate drought stress in wheat plants by employing biochemical and molecular approaches. Only a few studies have highlighted the combinational impact of rhizobacteria and drought stress through gene expression analysis in different plants, including wheat. Therefore, the present work tried to investigate the abilities of *Eb* WRS7 to overcome the deleterious effects of drought stress and to characterize its ability to colonize wheat plants.

In addition to molecular changes, we aimed to study differentially produced plant metabolites in response to PGPR inoculation under drought stress. In response to environmental stress, PGPR-inoculated plants re-program their metabolic pathways by altering the biosynthesis of various compounds such as amino acids, sugars, and tricarboxylic acids [245]. Interrogating the metabolism of PGPR-treated plants could reveal the metabolic profile and key metabolomic signatures that define the effects of microbial inoculation on plant physiology. Such insights provide a framework for mechanistic prediction and understanding microbe-induced physiological changes in crop plants under drought conditions [246]. For example, Carlson *et al.* (2020) reported that PGPR inoculation in *Sorghum bicolor* induced differential metabolic reprogramming to ameliorate drought stress, which involved augmentation of the antioxidant system, production of the osmolytes, change in root architecture, and hence activation of induced systemic tolerance [12]. In another study, Lucini *et al.* (2019) reported that inoculation of *Rhizoglomus irregulare* or *Trichoderma atroviride* differentially modulates metabolite profiling of wheat root exudates as they observed differential changes in lipids, phenolic compounds, terpenoids, siderophores, chelating acids, derivatives of amino acids and phytohormones [247]. Recently, Zhao *et al.* (2022) did a metabolomics analysis to investigate

the changes in wheat seedlings under salinity stress upon inoculation with *Bacillus* sp. wp-6. They found that galactose, phenylalanine, and glutathione metabolism might play an important role in promoting wheat plant growth under salt stress after the inoculation with wp-6 [248]. Also, Vilchez *et al.* (2018) described the characterization of metabolic alteration during the interaction of pepper plants with *Microbacterium* sp. 3J1 under drought stress. They observed that plants change their carbon and nitrogen metabolism in response to bacteria contributing to major changes in the concentration of molecules, such as sugars and amino acids, to maintain osmotic balance [248]. There are very few metabolomics studies on the PGPR-plant interaction and even fewer on the PGPR-plant-abiotic stress interaction. Therefore, metabolite profile patterns of wheat plants inoculated with *Eb* WRS7 can provide a holistic biochemical phenotype of plants under drought conditions. Also, this study elaborates our understanding of bacteria-mediated IST in plants.

4.2 Material and Methods

4.2.1 Bacterial culture and growth conditions

The bacterium *Eb* WRS7 isolated from the rhizospheric soil of *Triticum aestivum* L. was used in this study. The growth condition and detailed characterization of plant growth-promoting properties have been reported earlier (Chapter III, Section 3.2.1).

4.2.2 Plant growth and experimental design

Surface sterilization of wheat seeds (*Triticum aestivum* L.), preparation of bacterial inoculum, soil sterilization, and seed treatment were performed as per the protocol mentioned in Chapter II, section 2.2.8).

4.2.3 Effect of *Eb* WRS7 on growth of wheat crop under non-sterile condition

Surface seed sterilization, plant growth experiment, and bacterial growth conditions were the same as described above, except plants were grown in non-sterile soil. After the stress period, plants were harvested, and their growth was measured based on various parameters, such as root and shoot length and chlorophyll content.

4.2.4 Biochemical analysis

To evaluate different biochemicals in control and bacteria-treated plants, osmolyte content (proline and total soluble sugars) and lipid peroxidation assays were performed under drought stress following the standard protocols described below.

4.2.4.1 Proline content

Proline content in the leaves was determined by the standard protocol of Bates *et al.* [204]. One gram of fresh leaves was homogenized in 3 ml of 5% (w/v) sulfosalicylic acid and spun at 8500 g for 10 min to collect the supernatant. 500 µl of supernatant was diluted with sterile water to make up the volume to 1 ml, followed by adding 2 ml of 2 % ninhydrin solution. The mixture was vortexed gently and boiled for 30 min at 100 ℃. The mixture was cooled, an equal volume of toluene was added, and then the upper aqueous phase was collected to measure the absorbance at 520 nm in a spectrophotometer (Eppendorf). The proline content was calculated by plotting a standard curve using L- proline as standard (Sigma-Aldrich, USA).

4.2.4.2 Estimation of total soluble sugar (TSS)

Total Soluble Sugar (TSS) was estimated by following the standard Irigoyen *et al.* 1992 protocol using anthrone reagent [249]. Alcoholic leaf extract was prepared by homogenizing 1 g of leaves in 3 ml of 80% ethanol and adding 3 ml of freshly prepared anthrone reagent. The reaction mixture was placed in a boiling water bath for 10 min. The absorbance was then measured at 620 nm. A standard curve of glucose was prepared for quantification of soluble sugars synthesized by plants.

4.2.4.3 Estimation of lipid peroxidation

Lipid peroxidation was determined by estimating the malondialdehyde (MDA) content produced by the thiobarbituric acid reaction [250]. Alcoholic leaf extract was prepared and mixed with 1 ml of 0.5 % thiobarbituric acid containing 20 % trichloroacetic acid (TCA). The resultant mixture was boiled at 90 ℃ for 30 minutes, cooled at room temperature, and centrifuged at 5000 g for 5 minutes. The absorbance was measured at 400, 532, and 600 nm. The MDA concentration was determined by its molar extinction coefficient (155 $nm^{-1}cm^{-1}$), and the results were expressed as mmol MDA g^{-1} fresh weight (FW).

4.2.5 Effect of *Eb* WRS7 on antioxidant enzyme activities of wheat crop

Antioxidant enzymes or stress markers such as catalase (CAT) and superoxide dismutase (SOD) were determined using a standard protocol. To measure the enzyme activity, 0.5 g of leaf from bacteria-treated plants grown under drought stress and their respective control plants were homogenized with 50-mM phosphate buffer (pH 7.0) and centrifuged at 15,000 g for 20 min at 4 °C. The supernatant was used to estimate protein content and antioxidant enzyme activity. Catalase activity was measured based on the decomposition of hydrogen peroxide (HO^-) by recording the decrease in absorbance at 240 nm at 30 °C [251]. The activity of SOD was determined by the photoreduction of nitro blue tetrazolium (NBT). The reaction mixture contained phosphate buffer, NBT, riboflavin, and enzyme extract. Riboflavin was the last component to be added, and the reaction was initiated by placing the tubes in fluorescent lamps. The reaction was terminated after 10 min by removing the light source. Absorption of the reaction products was recorded at 560 nm [252].

4.2.6 Expression analysis of stress-responsive genes in wheat plant

The expression of different genes contributing to drought stress amelioration was investigated to understand the plant response to PGPR inoculation. Wheat plants were grown and treated as described above. The leaves of experimental plants were used for total RNA extraction using the CTAB method [253]. Three biological replicates were employed for each treatment. The extracted RNA was checked for its quality and quantity using the Bio-spectrometer (Eppendorf, Germany). The cDNA was synthesized using a verso cDNA synthesis kit (Thermo Fisher Scientific, USA) for gene expression profiling. Real-Time qPCR (Bio-Rad, USA) was performed on a CFX connect RT PCR System (Bio-Rad, USA), using a SsoFast EvaGreen Supermix (Bio-Rad, USA) and a gene-specific set of primers as listed in Table 4.1. One µL of cDNA was added to each PCR reaction mix (10 µL), containing 0.25 µM of each primer and 5 µL of 2X SsoFast EvaGreen Supermix (Bio-Rad, USA) under the following thermal conditions: 2 min at 50 °C; 10 min at 95 °C; 40 cycles of 15 s at 95 °C and 1 min at 60 °C. Each reaction was carried out in three technical replicates, along with a no-template control (NTC). To confirm the amplification specificity and lack of primer dimer formation, each run was performed with a melting curve analysis. Each sample was analyzed in two biological and three technical replicates at the qPCR level. Primers were designed using Sequence Manipulator Suit (https://www.bioinformatics.org/sms2/) and NCBI primer blast. Tubulin 1 (tubb1) was used as an internal control. Gene expression analysis was done using relative

quantification by the $2^{-\Delta\Delta CT}$ method [254]. The selection of stress-responsive genes for expression studies was based on available literature [243, 255].

Table 4.1. List and sequence of primers used in gene expression studies using real-time PCR (qPCR).

Primer	Primer (5' → 3') Forward Sequence	Primer (5' → 3') Reverse Sequence
CAT1	AAGTGCTCCCACCACAACAA	CTGGCCGAGAGACTTGTCAG
APX	TCAGTTTGTCCCCGTGAAGG	ACCTTTCAGGATGCGCCTTT
GPX	GTTCAGTTTGCCTGCACTCG	CAACGTGACCCTCCTTGTCA
NCED	CACTCTGTCGACTGCGCC	AAGTCGTGGATCATGGTGGG
WZE	AAGCAAACCAGATCCGAGCA	CATCGGAAGGGTGGAAACGA
SAMS	GCTGACCACTGCAAGGTACT	TGGTCACTGTCTCATCGTG
ACS1	CAGCCTCTCCAAAGACCTC	AATGCCGATCTCCTTGAGC
ACO	ATGAAGGAATTCGCGTCCGA	GGTAGCTGCTGACCTTGGTG
PC5S	TGATGGGACTCGCTTTGGTC	CACAACTCCCTTGTCACCGT
PC5R	AATGCCAAACACCCCCTCTG	TCAAGCCAGTAACCGCATCA
TPS1	TCTATGTGTTCTTCGACCCT	ACGAGTTGAGCAGGTAACGG
LEA1	CAGTACACCAAGGAGTCCGC	GCCAACACATGCGTCTAGTG
TPC1	CACTTCCGCTCGTAGCTT	CTTCTGGTAACGGTCGCCAT
Tubulin (tubb1)	CCGTCAACCTGATCCCCTTC	GTCAACCTCCTTGGTGCTCA

4.2.7 Metabolite extraction, derivatization, and GC-MS analysis

Polar and non-polar metabolites were extracted from the control and *Eb* WRS7-treated wheat plants grown under normal and drought stress. Four conditions are described as (i) control (C), i.e., plants with no stress and no PGPR inoculation, (ii) treated plants (PGPR) that included plants treated with PGPR but in the absence of drought stress, (iii) DS which were plants grown under drought stress but no PGPR inoculation, and (iv) DS + PGPR where plants were treated with PGPR and grown under drought stress. Plants were grown as described in Chapter II, section 2.2.9. To impose drought stress, plants were not watered after 15 days of germination (plants grown up to the three-leaf stage). After 15 days of stress, plants were harvested for metabolite extraction. Metabolites were extracted by crushing the plant samples to a powdered form using liquid nitrogen, followed by the addition of a 2:1 ratio of chloroform and methanol. The mixture was then homogenized and sonicated for 30 s using a probe sonicator. The homogenate was centrifuged at 15000g for 20 min at 4°C. Then, the solvent layer was collected and evaporated to dryness using a rotary vacuum concentrator. The dried supernatant was re-suspended in 1 mL methanol. 200 µl was aliquoted in a fresh microcentrifuge tube, followed

by evaporation to dryness and derivatization, as Chapter III, section 3.2.4 mentions. Later, derivatized samples were transferred to auto-sampler vials for analysis. 1 µl of the derivatized sample was loaded on Shimadzu capillary column SH-RXi-5SilMS (30 m*0.32 mm*0.25µm) through autosampler in splitless mode at 250 ℃. The constant flow rate of 1 mL/min of helium gas was maintained. Initially, the GC program was started at 80 ℃ for 3 min, followed by temperature ramping of 10 ℃/ min to 250 ℃ with a temperature hold of 2 min, followed by second ramping of 4 ℃/ min till the final temperature reached 300 ℃ and held constant for 10 minutes. Data acquisition involved a mass range of 50 to 550 m/z. Peaks were identified using NIST 14 library. The metabolomics data were obtained in .qgd file format for analysis. MetaBoAnalyst 5.0 was used for the statistical analysis.

4.2.8 Bacterial colonization assay under normal and drought stress conditions

Bacterial colonization of the plant root surface was determined following the previously described method [256] with slight modifications. To confirm bacterial root colonization, the plants were uprooted carefully and washed twice with sterile DDW to remove loosely adhered bacterial cells from the root surface. Then, 1 g of root sample was weighed and crushed, added to saline solution, and kept at 120 rpm for 2 h, serially diluted and plated on LB media (Hi-media). The colony-forming unit (CFU g^{-1}) in the root sample was determined. To ascertain that the recovered colonies were of WRS-7, some of the recovered colonies were randomly selected for DNA fingerprinting using enterobacterial repetitive intergenic consensus (ERIC) PCR as described by [17].

For further confirmation, 1–2 cm of root segment was fixed using 2.5% glutaraldehyde overnight and dehydrated with 30, 50, 70, 80, 90, and 100% gradient ethanol. The fixed roots were sputter-coated with gold, and further imaging was performed using a Field Emission Scanning Electron Microscope (FEI-APREO SEM, Thermo Fisher Scientific, USA).

4.2.9 Statistical Analysis

All the experiments were conducted in triplicates, and results were expressed as mean ± Standard Error Mean (SEM) (n = 3). Data were analysed by analysis of variance (ANOVA) and subsequently by Duncan's multiple range test at $p < 0.05$. For GC-MS analysis, three replicates of each control and test condition sample were used in the experiment. After data normalization, all significant metabolites were analysed using unsupervised principal component analysis (PCA) to observe the overall distribution trend among samples.

Differential metabolites were screened according to VIP >1 and $p < 0.05$. Univariate analysis and metabolic pathway enrichment analyses were performed using the online tool MetaboAnalyst 5.0 (https://www.metaboanalyst.ca).

4.3 Results

4.3.1 Effect of *Eb* WRS7 on growth of wheat crop under drought stress

Plant growth under non-sterile soil conditions was studied to understand how PGPR tends to interact with the rhizospheric community. *Eb* WRS7 attenuated the negative effects of drought by improving plant growth in non-sterilized soil, although not significantly different as compared to sterilized soil (Table 4.2). In *Eb* WRS7-inoculated plants, shoot length increased by 9.77% compared to sterile soil, whereas root length and chlorophyll a content decreased by 4.39% and 1.49%, respectively, in non-sterilized soil under well-watered conditions. Under drought conditions, shoot length and root length increased by 9.41% and 4.76%, respectively, whereas chlorophyll a content decreased by 6.43%.

Table 4.2. Effect of bacterial isolate *Eb* WRS7 on plant growth parameter under drought stress under non-sterile soil conditions.

Isolates	Shoot Length (cm)		Root Length (cm)		Chl. a (mg g^{-1} FW)	
	Sterile Soil	Non-Sterile Soil	Sterile Soil	Non-Sterile Soil	Sterile Soil	Non-Sterile Soil
CONTROL	22.93±1.15	25.86±0.75	21.17±0.07	22.71±0.22	11.09±0.02	11.97±0.09
STRESSED	18.98±2.08	19.16±0.48**	12.76±1.17	13.94±0.28***	8.18±1.09	7.95±0.73*
NS + WRS7	25.27±0.91*	27.74±0.99*	25.01±0.22***	23.91±0.76^{ns}	16.07±3.27***	15.83±0.67*
S + WRS7	20.92±0.11***	22.89±0.14*	23.07±0.76****	24.17±0.28^{ns}	14.77±0.91****	13.82±1.27*

[#]Value represents the mean ± SD, n=3. Symbol '*' indicates significant difference ($p < 0.05$) between uninoculated and Eb WRS7-inoculated plants under both non-stressed and stressed condition w.r.t control (well-watered non-inoculated plants).

4.3.2 Biochemical responses of plants inoculated with *Eb* WRS7 under drought stress.

Since drought imposes osmotic stress, we measured the level of osmoprotectants, namely proline content and total soluble sugar (TSS) produced in plants under drought stress (Figures. 4.1a and 4.2b). Osmoprotectants maintain osmotic potential inside the plants under water-stress conditions. As noticed in Figure 4.1, there was a significant increase in proline content under stress conditions (53.51%). In contrast, this increase was enhanced in bacteria-inoculated plants under non-stressed (199.06%) and stressed (252.86) conditions compared to uninoculated non-stressed plants. Similar results were also obtained for TSS content. The TSS content increased

by 10.98% in uninoculated plants under drought stress, whereas the inoculated plants showed an increase of 38.01% and 55.02% under non-stressed and stressed conditions, respectively. Further, the extent of lipid peroxidation was evaluated by measuring malondialdehyde (MDA), a marker for stress-induced damage [28]. No significant difference in MDA content was observed in *Eb* WRS7-treated plants under non-stressed conditions compared to uninoculated controls. However, *Eb* WRS7 inoculation significantly decreased MDA content by 29.59% in plants grown under drought stress (Figure 4.1c).

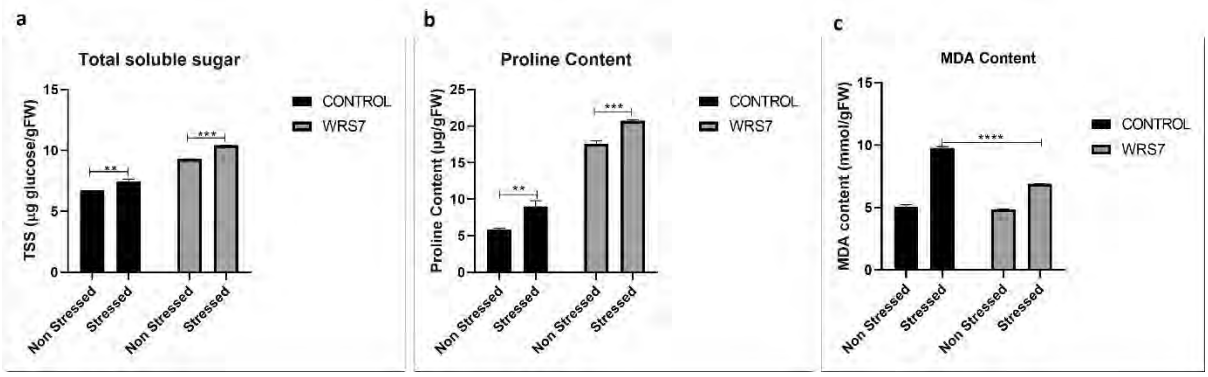

Figure 4.1. Osmolyte contents and cell membrane integrity indexes in wheat under osmotic stress. (**a)** soluble sugar content; (**b)** proline content; and (**c)** malondialdehyde (MDA) content. Values represent the mean ± SE, $n = 3$. Symbol '*' indicates significant differences among different treatments ($p < 0.05$).

The physiological changes in plants under drought stress and their amelioration by *Eb* WRS7 were also evaluated by measuring the level of different oxidative enzymes known to overcome damages induced by oxidative bursts under stress conditions. Catalase activity significantly increased in stressed conditions in both uninoculated (67.79%) and bacteria-inoculated (119.44%) plants, but no significant increase was noticed in bacteria-inoculated plants under non-stressed conditions. Similarly, SOD activity increased in plants under stress in both bacteria-uninoculated (36.84%) and bacteria-inoculated (50.15%) plants. However, a slight increase of 17.37% was also observed in bacteria-inoculated plants under non-stressed conditions (Figure. 4.2).

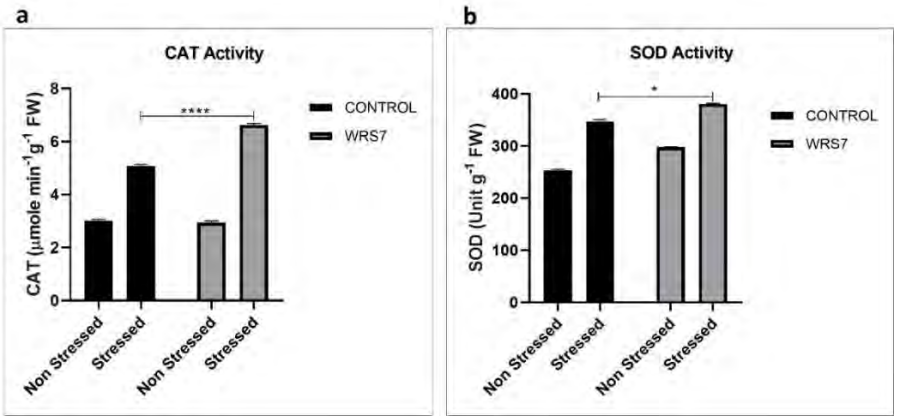

Figure 4.2. Effect of *Eb* WRS7 inoculation on (**a)** Catalase (CAT) activity and (**b)** Superoxide Dismutase (SOD) activity in wheat plants under drought stress. Values represent the mean ± SD, $n = 3$. Symbol '*' indicates significant differences among different treatments ($p < 0.05$).

4.3.3 Expression of genes encoding antioxidant enzymes

PGPR-mediated drought stress amelioration was determined through expression analysis of some of the stress-responsive genes in wheat plants (Figure 4.3). All the experiments were calibrated with the control plants and watered regularly. We analysed *Eb* WRS7-mediated gene expression of catalase (*CAT*), ascorbate peroxidase (*APX*), and glutathione peroxidase (*GPX*) in response to drought stress in the wheat plant. In the case of *CAT* gene expression, we did not observe a significant difference in bacteria-inoculated plants under non-stressed conditions (1.5-fold increase), w.r.t to control plants. However, the level of *CAT* gene expression significantly increased in uninoculated plants (threefold), and WRS7-treated plants (threefold) grown under drought stress (Figure 4.3a). For the *APX* gene, we found around a fourfold change in expression in uninoculated plants under stressed conditions. The bacterial inoculation also increased *APX* gene expression under non-stressed conditions by 4.5 folds. However, the level of APX gene expression was lower in WRS7-treated under drought stress than in plants treated with only stress or only PGPR (Figure 4.3a). The analysis of *GPX* gene expression indicated a different pattern than that of the above two genes. Its expression decreased in bacterial inoculation under non-stressed and stressed conditions, whereas in uninoculated plants under stress conditions (Figure 4.3a).

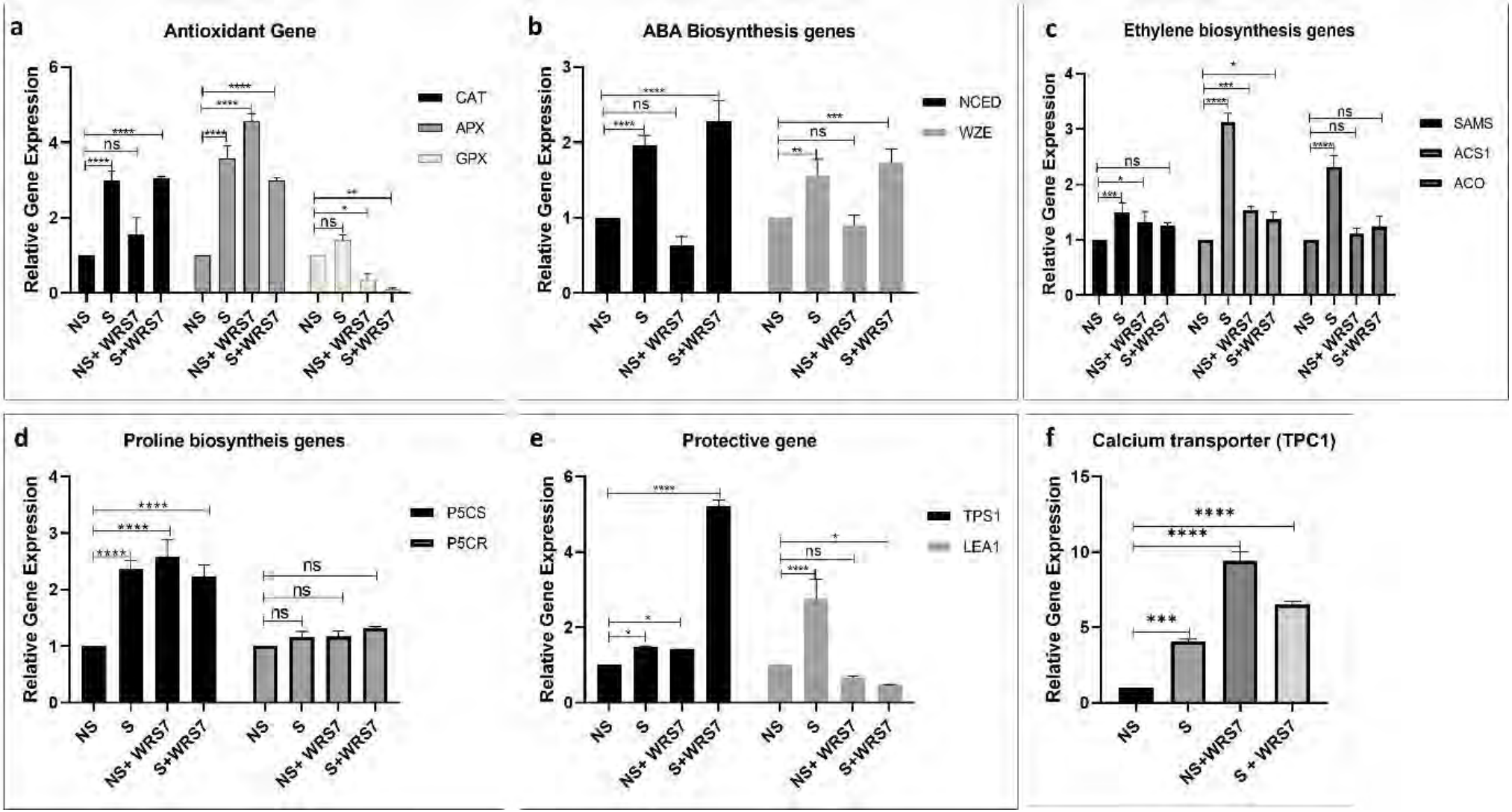
a
Antioxidant Gene
Relative Gene Expression
CAT
APX
GPX
NS
S
NS+ WRS7
S+WRS7
b
ABA Biosynthesis genes
Relative Gene Expression
NCED
WZE
c
Ethylene biosynthesis genes
Relative Gene Expression
SAMS
ACS1
ACO
d
Proline biosyntheis genes
Relative Gene Expression
P5CS
P5CR
e
Protective gene
Relative Gene Expression
TPS1
LEA1
f
Calcium transporter (TPC1)
Relative Gene Expression
NS+WRS7
S + WRS7

Figure 4.3. Effect of inoculation of *Eb* WRS7 on the expression of stress-associated genes in wheat plants. (**a)** Antioxidant Genes (CAT, PX, and GPX). (**b)** ABA Biosynthesis Gene. (**c)** Ethylene Biosynthesis Gene. (**d)** Proline Biosynthesis Gene. (**e)** Trehalose and Late Embryogenic Abundant (LEA) Gene. (**f)** Calcium Transporter *TPC1* gene under drought stress. Values represent the mean ± SD, $n = 3$. Symbol '*' indicates significant differences among different treatments ($p < 0.05$). Abbreviations: CAT = catalase; APX = Ascorbate peroxidase; GPX = Glutathione peroxidase; NCED = 9-*cis*-epoxy-carotenoid dioxygenase; WZE = wheat zeaxanthin epoxidase; SAMS = *S*-adenosyl-methionine synthetase; ACS1 = ACC synthase; ACO = ACC oxidase; P5CS = pyrroline-5-carboxylate synthetase; P5CR = pyrroline-5-carboxylate reductase; TPS1 = Trehalose Phosphate Synthase 1; TPC1 = Two-pore calcium channel protein 1.

4.3.4 Expression of genes encoding ABA and ethylene biosynthesis

ABA and ethylene are key stress hormones in plants under drought stress. We studied the expression of genes encoding the key enzymes, 9-*cis*-epoxy-carotenoid dioxygenase (*NCED*) and zeaxanthin epoxidase (*WZE*), involved in ABA biosynthesis. The basal level expression of *NCED* was observed in both control and WRS7-treated plants, where the expression was lower in inoculated plants than in the control plants. The *NCED* expression increased under drought-stress conditions. The combination of WRS7 and drought further increased its expression by 2.2-fold, but there is no significant difference between drought-stressed and bacteria-treated stressed plants, suggesting that bacteria do not affect ABA gene expression directly. Similar results were obtained for *WZE* except for the equivalent level of gene expression in both control and WRS7 (non-stressed) plants (Figure 4.3b). Since ethylene production is rapidly stimulated under abiotic stress, we looked for genes involved in its biosynthesis of *S*-adenosyl-methionine synthetase (*SAMS*), ACC synthase (*ACS 1*), and ACC oxidase (*ACO*). All three genes were highly upregulated under drought stress, showing their induction to 1.5-, 3-, and 2.3-fold induction for *SAMS*, *ACS 1*, and *ACO* genes, respectively. However, inoculation of WRS7 decreased their expression level, bringing it to the basal level observed in non-stressed control plants. (Figure 4.3c).

4.3.5 Expression of various osmolyte synthesis genes

Knowing the role of osmolytes in ameliorating drought stress, the expression of genes associated with the synthesis of osmolytes, such as proline, trehalose, and LEA protein, was analysed. Though the expression level of *P5CR* was not affected under drought stress, bacterial inoculation, or their combination (both drought stress and WRS7 inoculation) upregulated *P5CS* by 2.5- and 2.2-fold, respectively. (Figure 4.3d). For trehalose biosynthesis, the trehalose

phosphate synthase encoding gene (TPS1) expression was evaluated. There was slight induction of *TPS1* gene expression in drought- and WRS7-treated plants separately. Strangely, the combinatorial treatment of drought and WRS7 inoculation showed fivefold higher expression of *TPS1* than the other treatments (Figure 4.3e). We also examined the expression of the *LEA1* gene encoding Late Embryogenesis Abundant (LEA) proteins, which also protect plants from osmotic stress. Drought stress significantly induced the expression of *LEA1* by 2.7-fold as compared to control plants. On the other hand, WRS7-treated plants grown either in the presence or absence of drought showed a lower level of gene expression than the control plants (Figure 4.3e).

4.3.6 Expression of calcium transporter TPC1

Two-pore calcium channel protein 1 (TPC1), a voltage-gated Ca^{2+} channel in plant vacuole membranes, plays an important role in various signalling responses under abiotic stress [263, 264]. The drought stress-induced expression of TPC1 was four-fold compared to the control plants, whereas steep induction (9.4-fold) in the expression was observed in WRS7-inoculated plants. However, the level of the expression of TPC1 decreased in plants treated both with WRS7 and drought stress, yet it was higher than only drought stress-treated plants (Figure 4.3f).

4.4.7 Metabolic response of wheat in response to *Eb* WRS7 inoculation

To study PGPR-induced metabolic alterations in wheat crops under drought stress, we extracted intracellular metabolites and performed GC-MS-based untargeted metabolomics of wheat crop grown under normal and drought stress as well as with and without *Eb* WRS7 inoculation. Principal component analysis (PCA) and hierarchical cluster analysis were employed to reduce the complexity of metabolite profiling data. PCA revealed key characteristics of the data, which include both drought- and PGPR-related sample grouping. It explained the overall variance. PCA score plot showed four main clusters accounting for C, PGPR, DS, and DS + PGPR plants (Figure 4.4A). PCA analysis was also used to visualize variance between the two conditions i.e., C vs PGPR and DS vs DS + PGPR, which showed a similar clustering pattern (Figure 4.4B and C). A total variance of 90.2% (PC 1= 86.9% and PC 2= 3.3%) was observed in C vs PGPR plants (Figure 4.4B), whereas a total variance of 100% (PC 1= 100% and PC 2= 0%) was observed in DS vs DS + PGPR plants (Figure 4.4C). Following metabolite annotation, peak intensities were used to construct a hierarchical heatmap

illustrating differences in the relative concentrations in the various conditions, responding to PGPR inoculation. Heatmap showed quantitative changes in the metabolites among four samples (Figure 4.4D). Based on the hierarchical heat map, the metabolites that showed marked accumulation upon *Eb* WRS7 inoculation under drought conditions (DS + WRS7) were Indole Acetic Acid (IAA), L-proline, L-threonine, ascorbic acid, and other metabolites whereas malate was most marked accumulated metabolite under drought stress (DS).

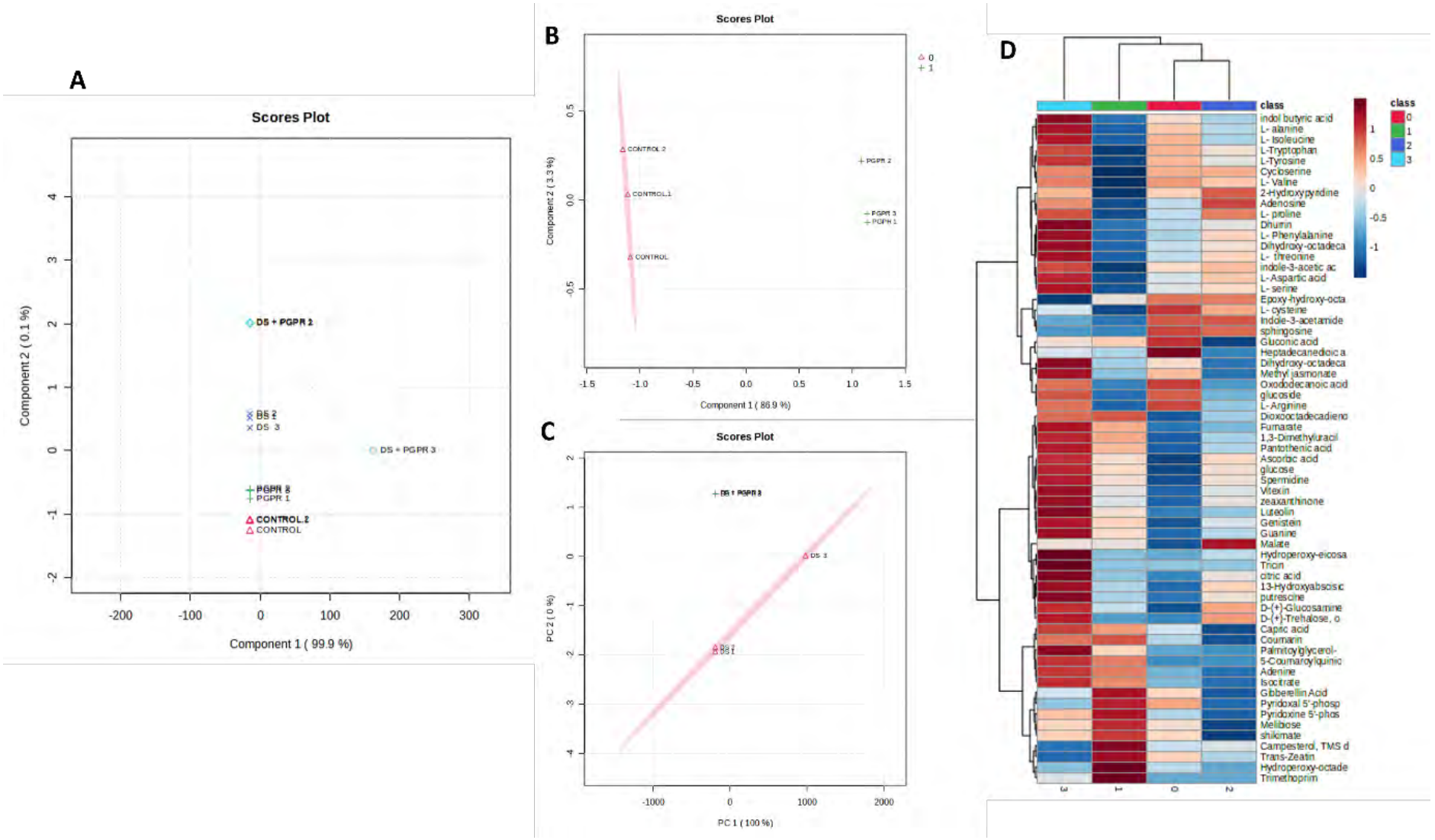
A
Scores Plot
Component 2 (0.1 %)
Component 1 (99.9 %)
DS + PGPR 2
DS 2
DS 3
DS + PGPR 3
PGPR 2
PGPR 1
CONTROL 2
CONTROL
B
Scores Plot
Component 2 (3.3 %)
Component 1 (86.9 %)
CONTROL 2
CONTROL 1
CONTROL
PGPR 2
PGPR 3
PGPR 1
C
Scores Plot
PC 2 (0 %)
PC 1 (100 %)
DS + PGPR 3
DS 3
DS 2
DS 1
D
class
indol butyric acid
L- alanine
L- Isoleucine
L-Tryptophan
L-Tyrosine
Cycloserine
L- Valine
2-Hydroxypyridine
Adenosine
L- proline
Dhurrin
L- Phenylalanine
Dihydroxy-octadeca
L- threonine
indole-3-acetic ac
L-Aspartic acid
L- serine
Epoxy-hydroxy-octa
L- cysteine
Indole-3-acetamide
sphingosine
Gluconic acid
Heptadecanedioic a
Dihydroxy-octadeca
Methyl jasmonate
Oxododecanoic acid
glucoside
L- Arginine
Dioxooctadecadieno
Fumarate
1,3-Dimethyluracil
Pantothenic acid
Ascorbic acid
glucose
Spermidine
Vitexin
zeaxanthinone
Luteolin
Genistein
Guanine
Malate
Hydroperoxy-eicosa
Trioin
citric acid
13-Hydroxyabscisic
putrescine
D-(+)-Glucosamine
D-(+)-Trehalose, o
Capric acid
Coumarin
Palmitoylglycerol-
5-Coumaroylquinic
Adenine
Isocitrate
Gibberellin Acid
Pyridoxal 5'-phosp
Pyridoxine 5'-phos
Melibiose
shikimate
Campesterol, TMS d
Trans-Zeatin
Hydroperoxy-octade
Trimethoprim

Figure 4.4. Metabolic response of wheat in response to *Eb* WRS7 inoculation. **(A)** Scores Plot (PC1 vs PC2) of partial least-squares-discriminant analysis (PLS-DA) of identified metabolites in wheat plants following drought and *Eb* WRS7 treatment. (**B**) PCA score plot separating control *vs*. PGPR-treated samples. (**C**) PCA score plot separating drought stress (DS) *vs*. PGPR-treated and stressed (DS + PGPR) samples. Each ring represents the distribution of biological replicates. **(D)** Heatmap hierarchical clustering of detected intracellular metabolite pools. Hierarchical trees were drawn based on detected metabolites in control (non-stressed), *Eb* WRS7 treated, drought stress, and PGPR-treated and drought stress treatment. Columns correspond to four different conditions, while rows represent different metabolites detected. 0, 1, 2, and 3 represent C, PGPR, DS and DS + PGPR treated plants respectively.

Pathway analysis revealed the functions and involvement of these metabolites in various metabolic pathways. Based on this observation, we conclude that the most significantly altered pathways in relation to PGPR *Eb* WRS7 application under drought stress conditions include TCA cycle metabolism, arginine and proline metabolism, Glyoxylate and dicarboxylate metabolism, glycine, serine, and threonine metabolism amongst others (Table 4.3). This indicates differences in aspects of cellular metabolism upon bacterial inoculation, resulting in altered metabolic changes under drought stress. This shows that wheat plants utilize multiple interlinked metabolic pathways as part of their interaction with *Eb* WRS7 and against drought stress. These results suggest that *Eb* WRS7 enhances drought tolerance using highly complex cellular reprogramming characterized by altered metabolism spanning several metabolic pathways.

Table 4.3. Significant metabolic pathways altered in *Eb* WRS7 inoculated- and uninoculated wheat plants responding to drought stress, generated from Metabolomics Pathway Analysis.

	Hits [#]	**Raw p**[#]	**Holm adjust**[#]	**Impact**[#]
Aminoacyl-tRNA biosynthesis	11	0.0000000156	0.0000015	0.11111
Citrate cycle (TCA cycle)	4	0.00194	0.18232	0.22337
Phenylalanine, tyrosine, and tryptophan biosynthesis	4	0.00281	0.26132	0.1016
Glyoxylate and dicarboxylate metabolism	4	0.007898	0.72663	0.18651
Glycine, serine, and threonine metabolism	4	0.012534	1	0.30168
Arginine biosynthesis	3	0.012823	1	0.08447
Arginine and proline metabolism	4	0.013916	1	0.30886
Zeatin biosynthesis	3	0.019702	1	0.00678
Glutathione metabolism	3	0.034919	1	0.00755
Vitamin B6 metabolism	2	0.036636	1	0.62179
Tryptophan metabolism	3	0.042313	1	0.32407
Sulfur metabolism	2	0.065131	1	0.06077
Tyrosine metabolism	2	0.073128	1	0.21622
Alanine, aspartate, and glutamate metabolism	2	0.12667	1	0.1295
Pyruvate metabolism	2	0.12667	1	0.15462
Cysteine and methionine metabolism	3	0.1385	1	0.04897
Isoquinoline alkaloid biosynthesis	1	0.15859	1	0.5
Stilbenoid, diarylheptanoid and gingerol biosynthesis	1	0.20578	1	0.13235
Phenylalanine metabolism	1	0.27175	1	0.47059
Phenylpropanoid biosynthesis	2	0.37723	1	0.0266
Flavonoid biosynthesis	2	0.38755	1	0.02864
Ascorbate and aldarate metabolism	1	0.40558	1	0.0033
Starch and sucrose metabolism	1	0.47093	1	0.00967
Glycolysis / Gluconeogenesis	1	0.52925	1	0.00038
Diterpenoid biosynthesis	1	0.55601	1	0.00978
Carotenoid biosynthesis	1	0.71449	1	0.00632

#The Raw *p* is the original *p-value* calculated from the enrichment analysis and the Holm *p* is the *p-value* adjusted by the Holm-Bonferroni method. Hits indicated the number of matched metabolites in the pathway from uploaded data. The Impact is the pathway impact value calculated from pathway topology analysis.

The application of *Eb* WRS7 on wheat plants under non-stress conditions induced changes in primary and secondary metabolism (Figure 4.5). Inoculation of *Eb* WRS7 decreased levels of amino acids such as alanine, aspartic acid, cysteine, serine, threonine, and proline, whereas stimulated accumulation of the TCA intermediates such as isocitrate, malate, and fumarate in host plants. Upon PGPR inoculation, alteration in ascorbic acid was also observed, which points towards growth promotion and defense priming in wheat plants. Changes in phytohormone profile in *Eb* WRS7 treated non-stressed plants were also observed. ABA and zeatin were overaccumulated, whereas IAA levels were downregulated.

Changes in metabolic profiling were also observed in wheat plants inoculated with *Eb* WRS7 under drought stress (Figure 4.5). Alteration in lipids, amino acids, phytohormones, phenolic compounds, and organic acids was observed. Pathway analysis revealed that upon PGPR application under drought stress, the most significantly altered metabolic include TCA cycle metabolism, glycolytic pathways metabolites, phenylpropanoid biosynthesis, glycine, serine and threonine metabolism, and tyrosine metabolism. The level of malic acid, a TCA cycle intermediate, was high in DS plants in comparison to DS + PGPR plants, whereas fumaric acid level was higher in DS + PGPR plants in comparison to DS plants. The amino acids phenylalanine, serine, alanine, aspartic acid, threonine, and tyrosine were elevated in PGPR-treated stressed plants compared to drought-stressed (no PGPR) plants. Similarly, differential alteration in several phytohormone levels was observed in drought stress and PGPR- inoculated drought-stressed plants. Except for trans-zeatin, other phytohormones, such as Indole-3-acetic acid, Indole butyric acid, GA, ABA, and MeJA increased in DS + PGPR plants. Higher level of polyamine (putrescine) and flavonoids were observed in PGPR- inoculated plants under drought stress.

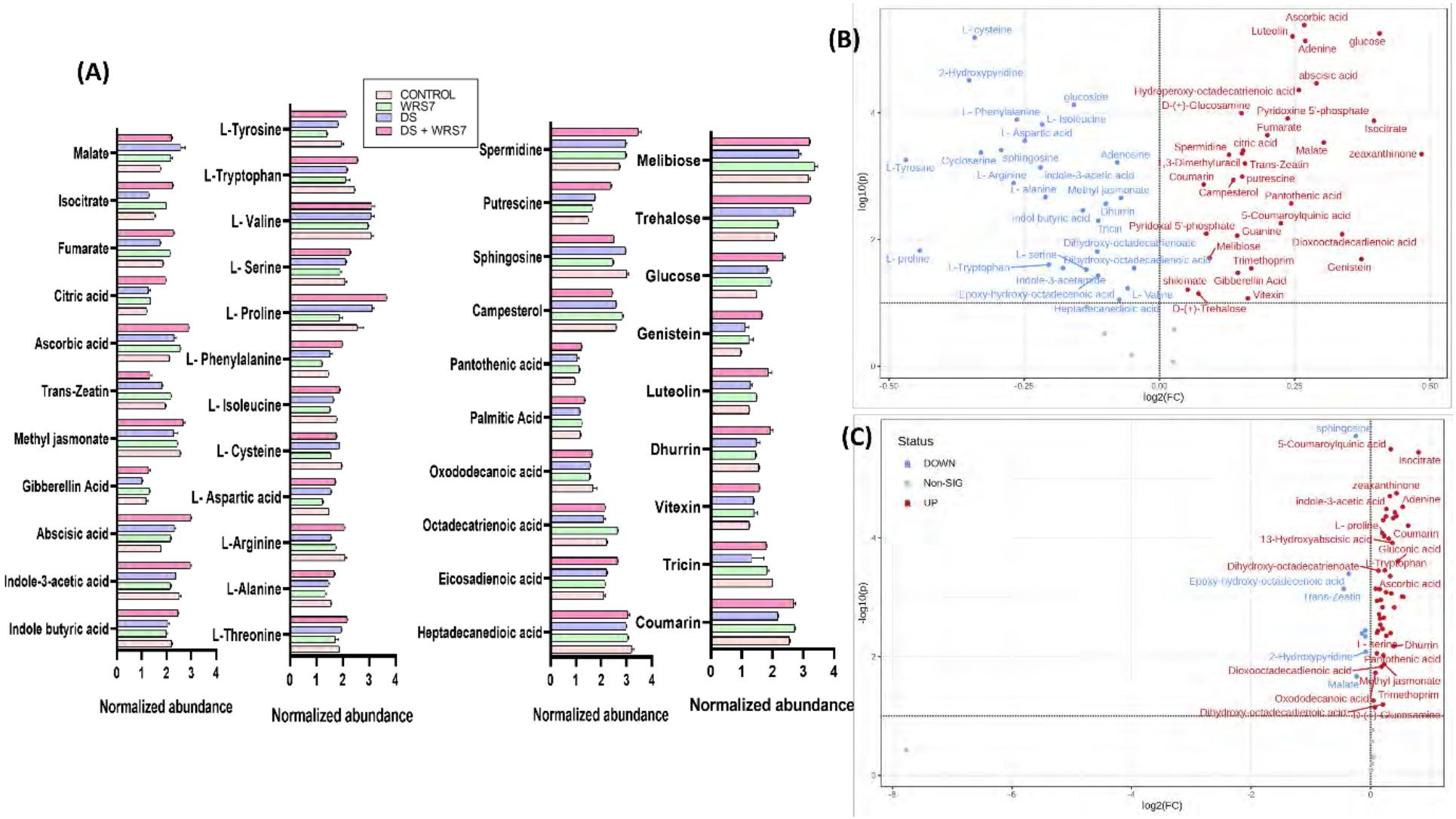
(A)
CONTROL
WRS7
DS
DS + WRS7
Malate
Isocitrate
Fumarate
Citric acid
Ascorbic acid
Trans-Zeatin
Methyl jasmonate
Gibberellin Acid
Abscisic acid
Indole-3-acetic acid
Indole butyric acid
L-Tyrosine
L-Tryptophan
L- Valine
L- Serine
L- Proline
L- Phenylalanine
L- Isoleucine
L- Cysteine
L- Aspartic acid
L-Arginine
L-Alanine
L-Threonine
Spermidine
Putrescine
Sphingosine
Campesterol
Pantothenic acid
Palmitic Acid
Oxododecanoic acid
Octadecatrienoic acid
Eicosadienoic acid
Heptadecanedioic acid
Melibiose
Trehalose
Glucose
Genistein
Luteolin
Dhurrin
Vitexin
Tricin
Coumarin
0 1 2 3 4
Normalized abundance
(B)
L-cysteine
2-Hydroxypyridine
glucoside
L- Phenylalanine
L- Isoleucine
L- Aspartic acid
L-Tyrosine
Cycloserine
Sphingosine
Adenosine
L- Arginine
Indole-3-acetic acid
L- alanine
Methyl jasmonate
Indol butyric acid
Dhurrin
Tricin
L- proline
L-Tryptophan
L- serine
Dihydroxy-octadecadienoate
Dihydroxy-octadecadienoic acid
Indole-3-acetamide
Epoxy-hydroxy-octadecenoic acid
Heptadecanedioic acid
L- Valine
Ascorbic acid
Luteolin
Adenine
glucose
abscisic acid
Hydroperoxy-octadecatrienoic acid
D-(+)-Glucosamine
Pyridoxine 5'-phosphate
Fumarate
Isocitrate
Spermidine
citric acid
Malate
zeaxanthinone
1,3-Dimethyluracil
Trans-Zeatin
Coumarin
putrescine
Campesterol
Pantothenic acid
5-Coumaroylquinic acid
Pyridoxal 5'-phosphate
Guanine
Dioxooctadecadienoic acid
Melibiose
Trimethoprim
Genistein
shikimate
Gibberellin Acid
Vitexin
D-(+)-Trehalose
log10(p)
log2(FC)
(C)
Status
DOWN
Non-SIG
UP
sphingosine
5-Coumaroylquinic acid
Isocitrate
zeaxanthinone
indole-3-acetic acid
Adenine
L- proline
Coumarin
13-Hydroxyabscisic acid
Gluconic acid
Dihydroxy-octadecatrienoate
L-Tryptophan
Epoxy-hydroxy-octadecenoic acid
Ascorbic acid
Trans-Zeatin
L- serine
Dhurrin
2-Hydroxypyridine
Pantothenic acid
Dioxooctadecadienoic acid
Methyl jasmonate
Malate
Trimethoprim
Oxododecanoic acid
Dihydroxy-octadecadienoic acid
-log10(p)
log2(FC)

Figure 4.5. Change in intracellular metabolites of the wheat plant upon treatment with *Eb* WRS7 under drought stress. **(A)** Normalized abundance of different metabolites. **(B)** Volcano map depicting contributory metabolites to the differences control (C) vs PGPR-treated, with fold change threshold (x- axis) =2 and t-tests threshold (y- axis) =0.1. **(C)** Volcano map depicting contributory metabolites to the differences in DS vs DS + PGPR, with fold change threshold (x- axis) =2 and t-tests threshold (y- axis) =0.1

4.3.8 Root Colonization of Bacteria

After the experimental period, the colonization ability of bacterial isolate WRS7 in the treated and control plants' roots was determined by CFU count, ERIC-PCR, and scanning electron microscopy. After 15 days of the drought, root-associated bacteria were detected in the range of 2.5×10^6 CFU/g of the root (Figure 4.6A). Bacterial establishment and colonization were also supported by visualization of dense adherence of bacteria on the root surface seen under a scanning electron microscope (Figure 4.7). No bacterial colonization was observed in the case of the uninoculated plant's root surface. ERIC-PCR was performed with genomic DNA of colonies obtained on LB plates and pure culture of WRS7 to confirm the identified bacteria. The banding pattern of the isolated colonies from the root surface was like that of pure culture (Figure 4.6B), confirming its colonization ability.

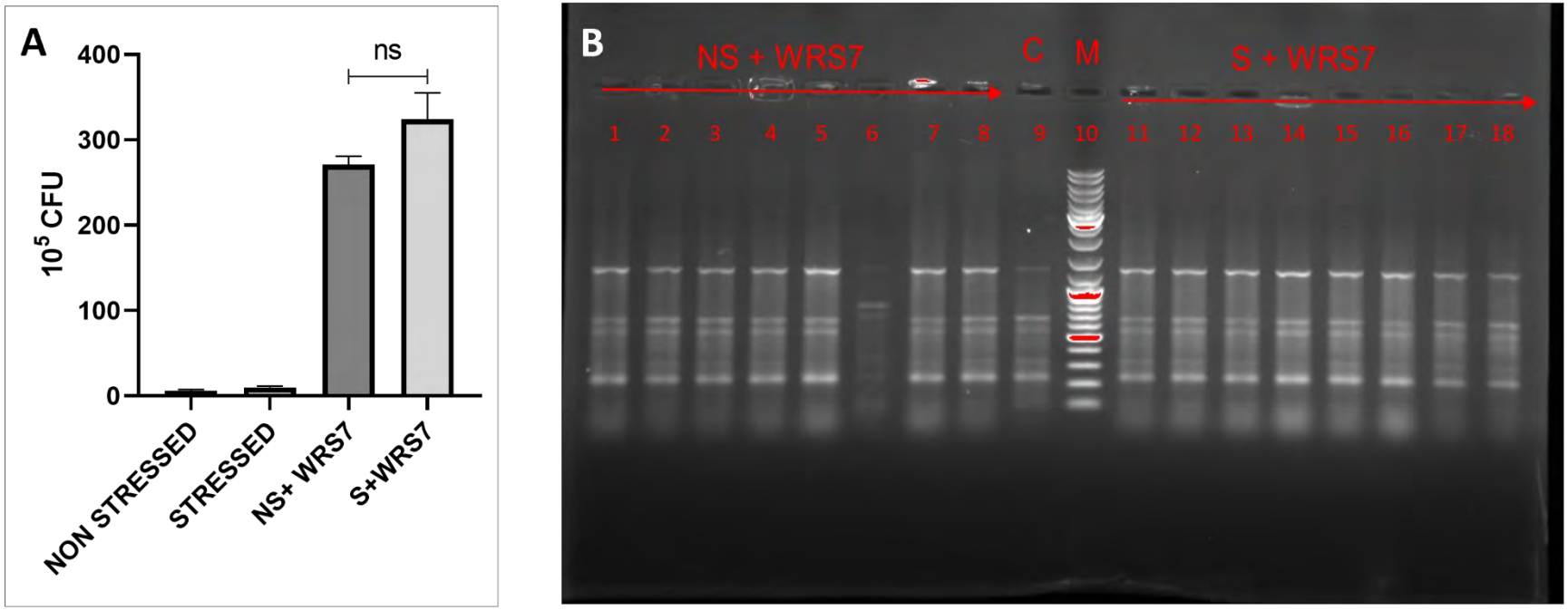

Figure 4.6. Evaluation of colonization efficiency of *Eb* WRS7 on wheat root surface. **(A)** Bacterial load in terms of CFU/ml; and **(B)** Pattern of ERIC- PCR on agarose gel electrophoresis. Lane 1-8 represents colonies isolated from WRS7 inoculated plants under non-stressed condition. Lane 11-18 represents colonies isolated from WRS7 inoculated plants under stressed conditions. C represents control WRS7 strain; M represents DNA ladder.

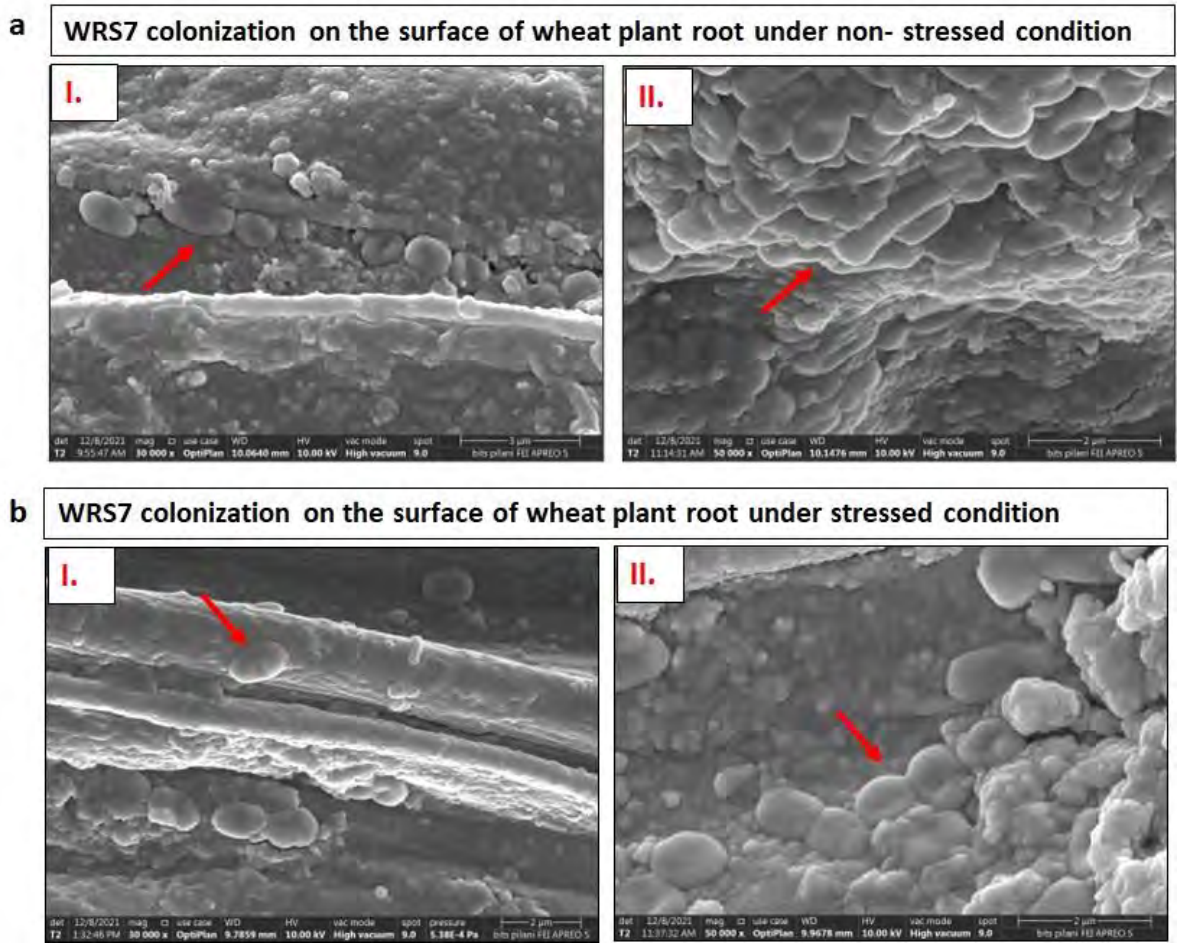

Figure 4.7. Evaluation of colonization efficiency of *Eb* WRS7 on wheat root surface employing FE-SEM. (**a)** under non-stressed conditions and (**b)** under drought stress conditions. Columns (i) and (ii) represent magnification 30,000X and 50,000X, respectively. The arrow indicates bacterial colonization on the root surface.

4.4 Discussion

Some PGPR is known to stimulate induced systemic tolerance through various mechanisms, including the production of EPS, VOCs, phytohormones, and ACC deaminase activity (Chapter I, section 1.5). These PGPR can interact with plants and modulate host functions by inducing gene expression required to alleviate the deleterious effects of abiotic stressors, including drought stress. Some studies have shown the potential of various *Enterobacter* species as PGPR and its role in ameliorating different abiotic stresses in plants [17, 223]. The present study elucidates the role of water stress-tolerant PGPR *E. bugandensis* WRS7, a wheat rhizospheric isolate, in mitigating drought stress of the wheat plant by affecting several genes, including those required for stress-related phytohormones (abscisic acid and ethylene biosynthesis), antioxidant, osmolytes, and Ca^{2+} transporter TPC. To the best of our knowledge, this is the first study highlighting the potential of *E. bugandensis* WRS7 as PGPR protecting the wheat plant from drought stress.

Although PGPR are known to ameliorate abiotic stress, once they are introduced into the soil they are not only exposed to abiotic stress (e.g., drought) but also to the native microbial communities present in the soil. They may act synergistically or antagonistically to the introduced microbial strain [257]. Therefore, native microorganisms present in the soils play a crucial role in plant-PGPR interaction under abiotic stress. Since field conditions are more complex, we first introduced the target bacteria, *Eb* WRS7, to greenhouse conditions using non-sterilized soil. With this approach, we aimed to evaluate the transferability of results from simpler to more complex conditions and determine whether soil conditions and their microbial community influence the performance of *Eb* WRS7. Our finding suggests that *Eb* WRS7 has maintained its positive effects in promoting wheat plant growth even in non-sterilized soil. However, these results might not be persistent across all soil conditions.

To establish the role of *E. bugandensis* WRS7 in drought stress amelioration through the modulation of abiotic stress-related phytohormones, we evaluated the level of genes associated with the synthesis of ABA and ethylene. ABA plays a major role in regulating water balance and drought stress tolerance in plants by inducing stomatal closure [258]. Other than stomatal closure, osmotic-responsive genes are activated due to increased ABA concentration in plants. Proteins encoded by these genes help plants maintain water balance by accumulating organic solutes, thus lowering water potential and reducing water loss under drought stress [259]. Accumulation of ABA in host plants upon PGPR inoculation under osmotic stress is a well-

established fact [260–262]. Therefore, in this study, we measured ABA accumulation by studying the expression of genes encoding ABA biosynthesis enzymes (Figure 4.3b). Zeaxanthin epoxidase (known as *WZE* in wheat) and 9-cis-epoxy-carotenoid dioxygenase (*NCED*) are the major ABA biosynthesis gene, which later catalyses the rate-limiting step. Upregulation of ABA biosynthesis genes (*NCED* and *WZE*) under drought stress in crop plants has been reported in earlier studies [243, 263], which supports our findings. We found that the expression of genes encoding ABA biosynthesis enzymes was not significant in bacteria-inoculated plants under watered and drought-stress conditions. This outcome suggests that WRS7 can assist plant growth under drought stress, independent of the ABA.

Ethylene, a gaseous hormone, is involved in regulating plant growth and development, but its concentration increases in response to various abiotic stressors, referred to as 'Stress ethylene' [264], which inhibits plants' growth and yield. There are three major enzymes involved in ethylene biosynthetic pathways, including *S*-Ado Met Synthetase (*SAMS*), ACC synthase (*ACS*), and ACC oxidase (*ACO*) [270], where *ACS* is a rate-limiting step and a major target for regulating ethylene production under stress [265]. Our results show that *Eb* WRS7 regulates the level of stress ethylene not only through ACC deaminase activity but also by regulating the expression of genes required for the biosynthesis of ethylene (Figure 4.3c). To our knowledge, this is the first study that reports the regulation of ethylene biosynthesis genes in host plants by PGPR. Future studies can be conducted to identify bacterial factors affecting the expression of the genes mentioned above.

Plants mitigate the effects of drought stress by producing osmolytes, which are triggered by a change in turgor, a key signal for the activation of osmolyte biosynthesis genes [266]. Osmolytes such as proline and TSS can be important biochemical indicators of stress tolerance in plants. Osmolytes accumulation maintains optimum turgor pressure within the cell and stabilizes the structure of various macromolecules against drought stress [267]. In the current study, WRS7-inoculated plants showed a higher accumulation of proline than the uninoculated stressed plants, as shown in the biochemical test (Figure 4.1b). However, the gene expression (*P5CS* and *P5CR*) studies did not show an equivalent increase in WRS7-treated plants (Figure 4.3d). This slight discrepancy may be attributed to a higher translation rate of corresponding proteins or high enzyme activity, leading to increased proline production [268]. Expression studies of proline biosynthesis genes were also done by various research groups under abiotic stress [269]. Ghosh *et al.* found increased expression of both *P5CS* and *P5CR* genes under

drought stress in uninoculated and bacteria-inoculated *Arabidopsis* plants [270]. We observed an increase in TSS (Figure 4.1b), another osmolyte, was also observed in bacteria-inoculated wheat plants under stressed conditions. A high amount of TSS might result from increased hydrolysis of starch, resulting in more sugar availability for osmotic adjustment to minimize the adverse effects of drought stress [271]. Accumulation of osmolytes in PGPR-inoculated plants under abiotic stress in various plant species has been reported [148, 177, 272]. The biochemical data of TSS correlated with the increased expression of the *TPS1* gene transcript, which suggests elevated trehalose biosynthesis in PGPR-primed plants under drought stress (Figure 4.3e). *TPS1* encodes the trehalose phosphate synthase (TPS) enzyme involved in trehalose biosynthesis. Trehalose is a non-reducing disaccharide involved in stress resistance and protects plants, bacteria,nd fungi [269, 273]. Fernandez and the group have observed an accumulation of *TPS1* gene transcript upon chilling in PGPR-inoculated grapevine plants [274]. Along with osmolyte production, plants also comprise osmotically active compounds, including hydrophilic proteins such as LEA proteins as a cellular response [274, 275]. ABA acts as a key signal for activating these genes, protecting cells from stress, and regulating genes involved in water transport and detoxifying enzymes [261]. LEA-type gene activation represents a damage repair pathway [276]. Our observation found increased expression of the *LEA1* gene in drought-affected plants, but decreased expression was noticed in bacteria-inoculated plants (Figure 4.3e). The decreased expression of LEA might result from other cross-talked pathways, like the antioxidant defense system for damage repair in these plants. Our observation tallied with the report of Battaglia and Covarrubias, who highlighted that inoculation of rhizobia in legume plants did not show LEA transcript in these plants [277].

Further, plants have antioxidant defense systems to protect plants and their organelles from the adverse effects of drought stress, including enzymes like catalase, superoxide dismutase, and peroxidases [35]. Increased activity of these enzymes to overcome the oxidative damage caused by environmental stressors has been demonstrated in PGPR-treated plants [271, 278]. In our study, biochemical assays showed enhanced catalase and superoxide dismutase activity in bacteria-inoculated plants under drought stress conditions (Figure 4.2a and b), suggesting defense machinery's active and improved rolen the plant for ROS detoxification [279]. We also found increased expression of *CAT* genes in uninoculated and bacteria-inoculated drought-treated plants but with no significant difference (Figure 4.3a), suggesting WRS7 might not directly regulate the catalase gene expression. However, the *APX* gene showed a significant fold increase in bacteria-inoculated plants under non-stressed conditions, whereas the GPX

gene was downregulated in bacteria-inoculated plants. Since peroxidase has many isoenzymes encoded by multigene families and their gene expression is regulated at different times and places by various abiotic stressors, the gene expression of various isoenzymes of these peroxidases can be tested in future for better understanding. Also, these enzymes have different affinities for OH^- and different functions in scavenging. Upregulation of *CAT* and *APX* genes can efficiently scavenge OH^-, preventing the accumulation of toxic reactive oxygen species. Our data suggest that a complex enzymatic system is responsible for scavenging excess ROS production due to drought stress. Bacterial isolate WRS7 modulates this response positively, protects plants from oxidative damage caused by water deficit conditions, and helps maintain the plant's structural integrity. As MDA content is one of the stress markers [2, 28], we evaluated its content in treated plant leaves. The inoculation of WRS7 caused a decrease of up to 40% in MDA content in plants as compared to its control plants grown under stress conditions (Figure 4.1c). It indicates that PGPR helps plants combat the negative effects of stress. Our results support the previous investigations stating that PGRP-inoculated plants combat oxidative damage induced by abiotic stress [28, 280].

One of the prime reactions to abiotic and biotic stress is alleviating the cytosolic Ca^{2+} concentration, and subsequent Ca^{2+} signal transduction leads to cellular responses to mitigate potential damages caused by the stress [260, 276]. Therefore, we looked for the expression of two-pore channels (TPCs) in response to PGPR and drought stress (Figure 4.3f). TPCs are voltage-gated, nicotinic acid adenine dinucleotide phosphate (NAADP)-regulated, and slow activating (SV) Ca^{2+} channels located in the vacuole membrane of plants [281]. These channels make the tonoplast and plasma membrane permeable to Ca, accumulating Ca^{2+} in the cytosol. TPC1 is involved in cation homeostasis and vacuole storage function [282]. *TaTPC1* is reportedly induced by drought, high salinity, ABA, or cold in wheat [283, 284]. By quantitative PCR analysis, we found increased expression of the *TPC1* gene under drought stress. Since the role of PGPR in modulating the level of TPC1 during drought stress has not been reported earlier, detailed characterization is required in future studies. Previously in our lab, through quantitative proteomics analysis, Singh *et al.* (2017) reported enhanced expression of Two-pore calcium channel proteins in wheat plants inoculated with *Enterobacter cloacae* under salt stress [103]. From our results, it appears that PGPR mediates Ca^{2+} signalling through TPC1 to alleviate the effect of abiotic stressors.

A metabolomics approach was used in the current study to understand the mechanisms of symbiosis of bacteria with plants and to elucidate the tolerance mechanism of wheat plants against drought stress. It helps us annotate the metabolites of wheat plants that participate in plant-microbe interaction during standard conditions and drought stress[243, 285]. A study of wheat plant metabolite reveals that Eb WRS7 induces metabolic alterations that span a wide spectrum of metabolite classes, including organic acids, sugars, phytohormones, amino acids, and lipids. The reprogramming of primary and secondary metabolites was observed upon *Eb* WRS7 inoculation under non-stressed conditions. These changes involved the accumulation of TCA cycle intermediates, decreased amino acid levels, and differential changes in phytohormones, lipids, and flavonoids. Since amino acids are catabolized upstream of TCA cycle precursors or intermediates, the differential change in amino acid levels indicates metabolite flux towards energy production and a change in the rate of protein synthesis [244, 286]. Under normal conditions, *Eb* WRS7 treatment decreased phenylalanine and tyrosine, indicating an enhanced phenylpropanoid pathway, a central hub for defense-related metabolite synthesis [287]. Furthermore, differential changes in flavonoids, such as luteolin, vitexin and tricin, were also observed in *Eb* WRS7 inoculated plants, indicating their role in plant growth and immunity [244, 288]. A differential level of ascorbic acid was noticed, which might be associated with various plant growth processes, stress perception, and downstream signalling pathways, such as the redox pathway [289, 290]. PGPR application also affected plants' hormonal networks. Increased zeatin and decreased IAA levels in *Eb* WRS7-treated non-stressed plants are correlated to growth promotion [244, 291].

Change in metabolite profile was also observed in wheat plants treated with bacteria under drought conditions (Figure 4.8). PGPR-induced amendments in amino acids, organic acids, lipids, and phytohormones levels suggest their role in ameliorating drought tolerance through complex cellular changes characterized by altered metabolism in wheat plants. Differential changes were observed in TCA cycle intermediate, such as malate and fumarate. As reported by Rzepka *et al.* (2009) and Sugiyama *et al.* (2014), malic acid and fumaric acid are associated with drought adaption due to their osmolyte properties. They also have the ability to regulate intracellular ionic content and stomatal conductance [292, 293]. Moreover, since TCA cycle intermediates function as carbon substitutes, they might help in improving the photosynthesis rate under drought stress [244]. Also, the accumulation of amino acids such as serine, threonine, proline, alanine, phenylalanine, tyrosine, cysteine, and aspartic acid help in drought tolerance by enhancing various mechanisms such as osmotic adjustments, stomatal regulation,

and oxidative stress protection [244, 294, 295]. Differential alterations were observed in the level of several phytohormones in uninoculated and PGPR-inoculated plants under drought stress. Reduced levels of ABA in PGPR-treated stressed plants indicate enhanced stomatal regulation, thus improving the photosynthetic efficiency and plant growth under drought conditions [244]. Moreover, the accumulation of polyamines and flavonoids in PGPR-treated stressed plants might improve drought adaption by regulating stomatal conductance and redox homeostasis [296–299]. Thus, this differential metabolomic study of PGPR-plant-stress interaction might help identify and understand the fundamental regulatory networks that define various metabolic changes and biochemical pathways in plants.

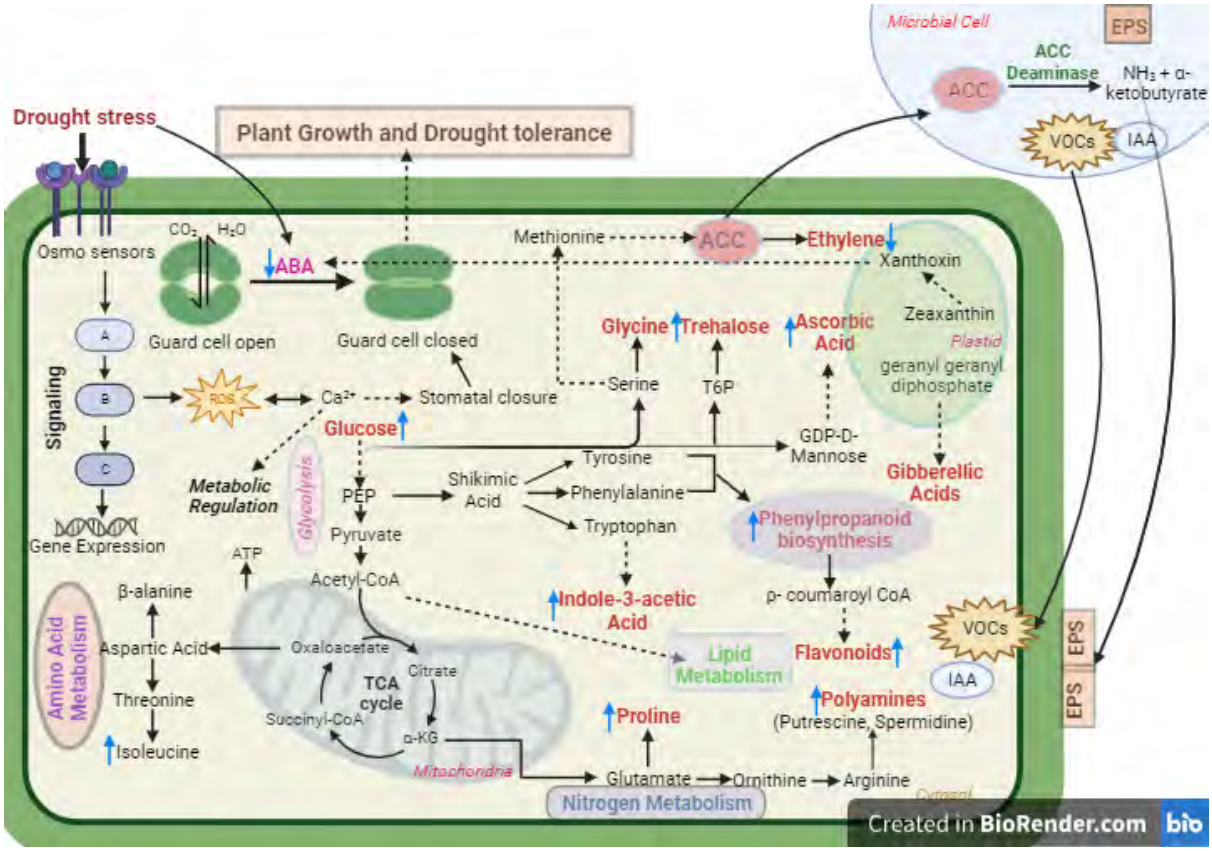

Figure 4.8. A schematic representation of metabolic response to drought stress in *Eb* WRS7 wheat plant. Drought stress triggers osmosensors and induces oxidative stress through ROS accumulation. ROS over accumulation induces gene expression and activates cell signaling cascades, including mitogen-activated-protein-kinase, Ca^{2+} ion, and hormone-mediated signaling. Drought induces activation of transcription factors and increases abscisic acid concentration, which coordinates wheat stress signaling and responses, including stomatal closure, photosynthesis, hormone production, accumulation of osmolytes and polyamines, and ROS scavenging. *Eb* WRS7 interacts with host plants and modulates their functions by inducing gene expression required to alleviate the deleterious effects of drought stress. *Eb* WRS7 treatment enhanced the phenylpropanoid pathway, a central hub for defense-related

metabolite synthesis. PGPR-induced amendments in amino acids, organic acids, lipids, and phytohormones levels suggest their role in ameliorating drought tolerance through complex cellular changes characterized by altered metabolism in wheat plants. PGPR treatment reduces the level of ABA, indicating enhanced stomatal regulation, thus improving photosynthetic efficiency and plant growth under drought conditions. The enzymatic activity of ACC deaminase, produced by *Eb* WRS7, lowers the ACC levels, reducing the level of stressed ethylene in wheat plants. Also, bacteria EPS and IAA might modulate various functions in wheat plants and improve drought adaptation in wheat plants. Abbreviations: ABA- Abscisic Acid; ACC- 1-aminocyclopropane-1-carboxylic acid; ATP- Adenosine triphosphate; EPS- exopolysaccharides; IAA- indole-3-acetic acid; α-KG- α-ketoglutarate; PEP- phosphoenolpyruvate; ROS-reactive oxygen species; VOCs- volatile organic compounds.

Finally, we investigated the colonization potential of *Eb* WRS7 as root colonization by PGPR is an important trait for plant growth stimulation and for the survival of bacteria under stress conditions [17]. All forms of motility were shown by the isolate required for chemotaxis response and root colonization [17]. Further colonization efficiency of the bacterial isolate to the root surface was determined by FESEM [300] and ERIC-PCR [301]. Earlier reports have also established DNA fingerprinting through ERIC-PCR [17, 302].

Overall, the present study demonstrates that *Enterobacter bugandensis* WRS7 is a plant growth-promoting bacteria that can ameliorate drought stress in wheat plants indicating its potential to be used as a biofertilizer for enhanced growth of host plants (Figure 4.9). *Enterobacter* sp. is primarily associated with healthcare-related infections, although not all species are known to cause infection in humans [303] (https://www.ncbi.nlm.nih.gov/books/NBK559296/). *Enterobacter bugandensis*, an emerging human pathogen, can cause nosocomial infections in neonates [304]. However, the pathogenic potential of environmental isolates has not been reported and must be investigated before their use as biofertilizer.

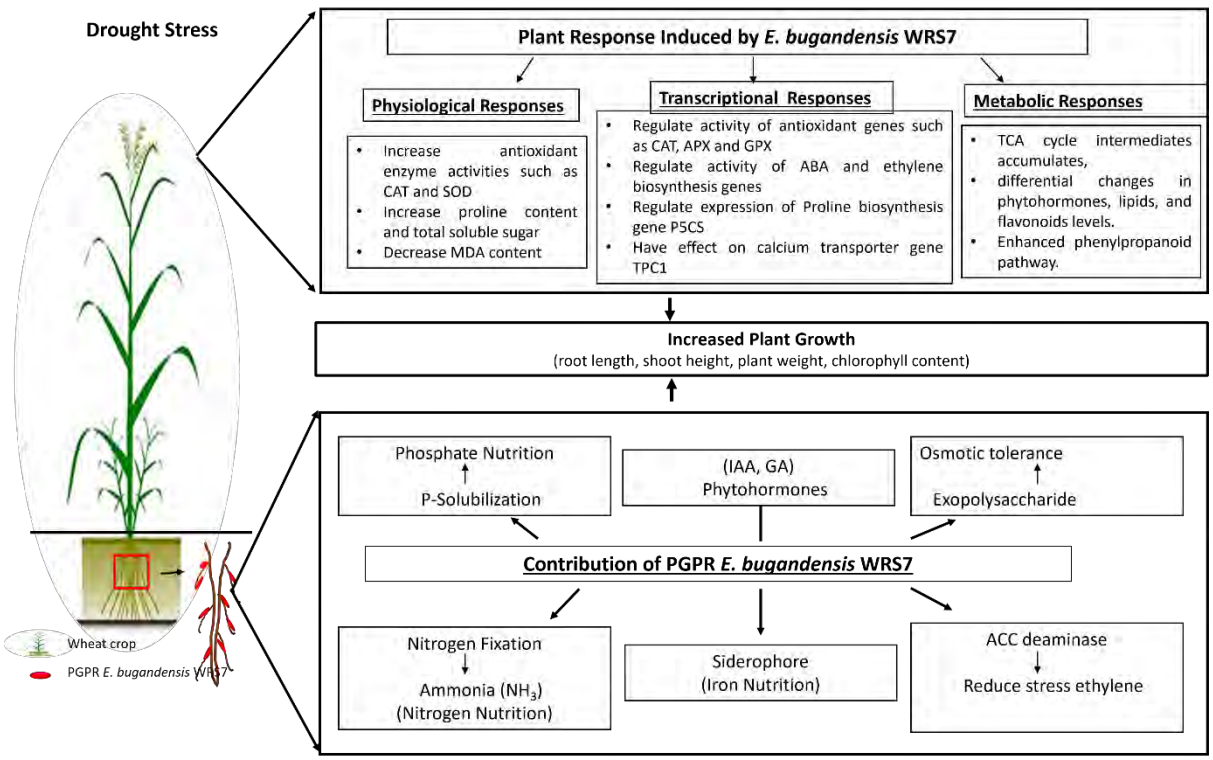

Figure 4.9. A model representing the mechanistic insights of *Eb* WRS7 to mitigate the effects of drought stress in wheat plants.

CHAPTER V

Investigating the Effect of *Enterobacter bugandensis* WRS7 on the Physiology of Host Plants Employing Proteomic Approaches.

5.1 Introduction

Drought is one of the major factors in the agriculture sector that undermines crop productivity and sustainability to a great extent. Damage caused by drought stress is controlled by modulation in the expression of numerous genes and several changes at the proteome level. Also, it has become more apparent in recent years that the translational and post-translational machinery plays a crucial role in stress adaptation [305]. Therefore, to understand the molecular mechanism of the drought stress response, a detailed identification and analysis of changes occurring at the protein level in drought-stressed plants seemed to be a rational approach. Since proteins are directly involved in influencing the novel phenotype to an altered environment by adjusting the physiological trait, the role of proteins in plant stress response, both as structural and regulatory, is important [85]. Induced protein levels will reveal information about stress-inducible signal perception and transduction and give insights about translational activity. This might build a complementary idea for future drought-responsive protein marker-assisted selection in plants [305]. Also, to find the missing information in DNA or mRNA, the proteomics approach is a better analytical method focusing on the actively translated portion of the genome. Moreover, along with molecular structure, protein function depends on cellular localization, post-translational modification, and interacting partners. Therefore, the comparative proteomics approach is a powerful and promising tool for identifying stress tolerance proteins that function in stress signalling, and cellular homeostasis [85, 306].

Uses of the PGPR have been reported to support plant growth and productivity under various abiotic stresses, including drought (Chapter I, section 1.4). In the present study, an MS-based proteomics approach was applied to decipher the proteomic profile of wheat crop inoculated with plant growth-promoting bacteria *Eb* WRS7 subjected to drought stress. This bacterium, isolated from the wheat rhizosphere (Chapter II), showed the ability to grow under drought stress and has enhanced wheat plant growth under drought stress (Chapters III and IV). To further validate the role of *Eb* WRS7, we aim to check the host plant physiology at the protein level. Robust protein profiling would help better understand the biochemical pathways of the trait behaviour of wheat plants under drought stress and microbial interaction.

Wheat (*Triticum aestivum* L.), a major staple food crop worldwide, occupies 25% of cultivated land area globally, with high nutritional value, and its grains are a rich source of glutens and other storage proteins [103, 307]. Wheat is often cultivated under water deficit conditions;

therefore, it is extremely significant to understand drought-responsive mechanisms and uncover many drought- responsive protein candidates in it [307]. Previous studies on wheat revealed molecular mechanism under abiotic stress [308, 309], including drought [266] through proteome analysis. Halder *et al.* reviewed wheat proteomics for abiotic stress tolerance and stated that proteomic analysis has significantly contributed to identifying key proteins involved in ameliorating stress tolerance in wheat crops. These proteins are primarily associated with carbon and energy metabolism, photosynthesis, redox homeostasis, defense response and signal transduction [308]. Also, proteomics studies help determine the effect of plant-microbe interaction through the identification of genes and proteins induced by soil microbes in plants, which might provide tolerance to abiotic stress [310, 311]. Moreover, proteomics studies can give insight into pathways induced during host-microbe interaction during drought stress. Previous studies have shown that plant growth-promoting bacteria can counteract the abiotic stress effects of drought in host plants by differential expression of proteins related to energy metabolism, photosynthesis, plant defence, protein degradation, and oxidative stress response [103, 115, 311, 312]. For instance, Banaei-Asl *et al.* did a gel-free proteomic analysis of canola root inoculated with bacteria *Pseudomonas fluorescens* under salt stress and found that proteins related to amino acid metabolism and tricarboxylic acid cycle were majorly affected. They concluded that bacterial inoculation increases salt tolerance in canola roots by modifying proteins related to energy metabolism and cell division [102]. Similarly, Chang *et al.* studied the combined effects of the PGPR *Pseudomonas putida* UW4 and salinity stress on the *Brassica napus* proteome using two-dimensional difference gel electrophoresis. Significantly altered protein expression levels were identified in the presence of salt and/or bacteria, where most of the identified proteins were involved in anti-oxidative processes, photosynthesis, transportation across membranes, and pathogenesis-related responses [115]. In another study, PGPR *Bacillus licheniformis* K11 could reduce drought stress by modulating the expression of stress-related proteins in *Capsicum annuum*. They found that dehydrin-like protein, vacuolar H^+-ATPase, HSPs, and pathogenesis-related protein-10 were significantly upregulated in *B. licheniformis* K11-treated drought pepper plants compared to untreated plants [116]. However, little work has focused on the combinational effect of PGPR and drought stress and the corresponding effects on plant proteomes [151, 307]. Therefore, investigation of proteome complement would give us a thorough understanding of molecular and physiological mechanisms underlying wheat stress response, including the perception of stress signal, signalling events leading to changes in gene expression, protein level as well as metabolite levels underlying plant acclimation to drought stress and acquisition of enhanced drought tolerance.

In current study, a gel-free/ label-free proteomic approach was used to identify responsive proteins in wheat inoculated with *Eb* WRS7 under drought stress to understand the drought-responsive mechanisms in wheat better. This approach is an excellent molecular technique for providing new insights into plants' molecular adaption or tolerance toward drought stress through the rigorous identification of proteins and their associated pathways. Comparative proteomic analyses were performed to determine the differentially abundant proteins involved in the wheat response to drought stress and bacterial inoculation.

5.2 Material and Methods

5.2.1 Plant growth and bacterial treatment

Drought tolerant bacterium *Eb* WRS7 was selected for the study based on its plant growth-promoting properties under drought stress (Chapters II and III). Healthy and uniform-sized seeds of wheat (*Triticum aestivum L.)* variety WH1142, obtained from the Indian Institute of Wheat and Barley Research, Karnal, were selected for the experimental study. Seeds were grown and treated with bacterium inoculum WRS7 as described previously (Chapter III Section 3.). The complete experimental setup consisted of four treatments: (i) non-stressed un-inoculated control (C), (ii) drought-stressed, uninoculated plants (DS), (iii) non-stressed inoculated (WRS7), and (iv) drought-stressed and inoculated (DS + WRS7). To impose drought stress, plants were not watered after 15 days of germination (plants grown up to the three-leaf stage). After 15 days of stress, plants were harvested and used for proteomics analysis.

5.2.2 Protein extraction and mass spectrometry analysis

Proteins were extracted using the TCA-acetone precipitation method with few modifications [103]. Samples were processed in triplicate. One gram of control and treated plants were taken in triplicated and ground in liquid nitrogen to make a fine powder using mortar and pestle. The powder was suspended in 2 ml of extraction buffer (0.9 M sucrose; 0.5 M Tris- HCl, pH 8.2; 5 mM EDTA; 5 % 2-mercaptoethanol). One mM phenylmethylsulfonyl fluoride (PMSF) was also added as a protease inhibitor. The mixture was vortexed to make a thick paste, followed by an ice-cold sonication bath for 10 min at 4 °C. Samples were then spun at 18,000 g for 20 min at 4 °C to remove cell debris. 1 ml of 100 % tricarboxylic acid (TCA) and 8 ml of 100 % ice-cold acetone were added to the supernatant, and the mixture was vortexed for 10 min and kept for 1 h for precipitation of proteins. Samples were centrifuged at 18,000 g for 20 min at 4 °C, the supernatant was discarded, and the pellet was resuspended in 1ml of ice-cold acetone.

The pellet was washed thrice with acetone to remove TCA, and finally, air dried and then dissolved in a denaturation buffer containing 7 M urea, 2 M thiourea, and 30 mM Tris, pH 8.2. Protein concentration was estimated using the Bradford method [203] with bovine serum albumin (BSA) as the standard. To remove any detergent from the samples, 100 µg of protein was enriched with chilled acetone (four times the sample volume) [312] and used for trypsin digestion (1: 100 enzyme/ protein concentration) overnight at 37 °C. All the samples were then vacuum-dried and further dissolved in 10 µl of 0.1 % formic acid in water. The supernatant was collected by centrifuging the samples at 10,000 g and then injected in the C18 Nano-LC column (75µm x 150cm x 1.7µm BEHC18 column) for separation of peptides followed by analysis of an Orbitrap Fusion Tribrid Mass Spectrometer coupled to a Thermo EASY nanoLC 1200 chromatographic system. The MS was calibrated before analysis [103]. LC-MS/MS analysis was conducted at the Proteomics Characterization Facility, C-CAMP, India.

5.2.3 Protein identification from mass spectrometry data

Mascot search engine (version 2.5.1; Matrix Science, London, UK) and Proteome Discoverer software (version 1.4.0.288; Thermo Fisher Scientific) were used for protein identification against the UniProt database of *Triticum aestivum.* The acquired raw files were processed using Proteome Discoverer software. The parameters chosen for identification included cysteine carbamidomethylation and methionine oxidation as a fixed modification and variable modification, respectively. Trypsin was specified as the proteolytic enzyme. One missed cleavage was allowed, and peptide mass tolerance was set as 10 ppm (parts per million), fragment mass tolerance was 0.8 Da, and peptide charges were set as + 2, + 3, and + 4. An automatic decoy database search was performed as part of the search for false discovery rate (FDR) identification [313]. All proteins with a confidence interval (CI) > 95% were identified successfully.

5.2.4 Bioinformatics analysis/ functional annotation

To determine the differentially expressed proteins, each treatment (DS, WRS7 and DS+WRS7) was compared to control (non-stressed, uninoculated plants). The differentially abundant proteins (DAPs) were selected based on the mean ratio with a fold-change greater than 2 or less than 0.5, and an adjusted p-value of less than 0.05. DAPs were classified using the Gene Ontology (GO) annotation tool (http://www.geneontology.org) for their molecular function, biological processes, and cellular components.

5.2.5 Statistical Analysis

The statistical significance of comparisons between multiple groups was evaluated with the one-way ANOVA test. The statistical significance of the results was evaluated by the student's t-test when two groups were compared at 95% confidence level.

5.3 Result

Proteomic analysis

A total of 887, 1038, 898, and 1069 proteins were identified in control, DS, WRS7, and DS+WRS7 plants, respectively. Out of four treatments, drought stress, either alone or in combination with PGPR inoculation, induced a higher number of different proteins (1038 and 1069, respectively). Further, Venn diagram was constructed to depict the common and unique proteins identified in each treatment, where the numbers of proteins in response to bacterial inoculation and drought stress were reported. Among the identified proteins, 845 were common to all treatments, whereas 9, 22, 7, and 16 proteins were unique in control, DS, WRS7, and DS+WRS7 plants, respectively (Figure 5.1 and Table 5.1).

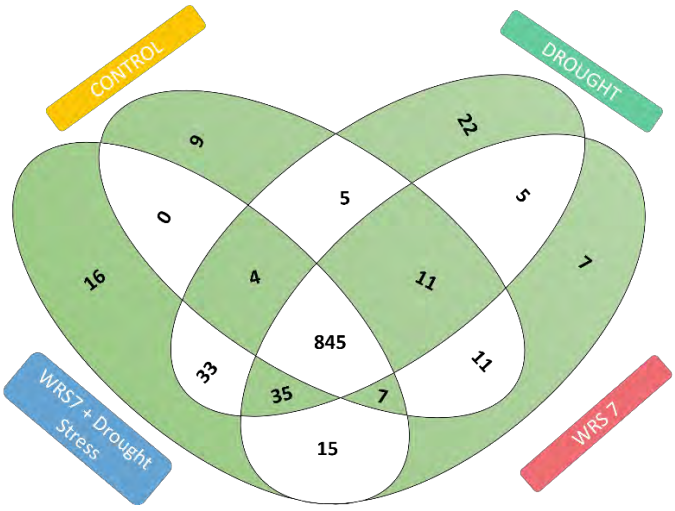

Figure 5.1. The Venn diagram represents common and unique proteins in each treatment (Control, DS, WRS7, and DS+WRS7).

Table 5.1. Uniquely expressed proteins in control, drought stress, WRS7-inoculated, and WRS7-inoculated under drought stress plants.

S. No.	UniProt ID	Control	UniProt ID	Drought Stress	UniProt ID	Bacteria inoculated	UniProt ID	Bacteria-inoculated under Drought stress
1.	P23993	Photosystem I reaction center subunit XI	Q9XEX2	Peroxiredoxin-2B	Q75M08-2	Isoform 2 of Protein disulfide isomerase-like 2-1	Q9STH1	Hsp70-Hsp90 organizing protein 3
2.	Q1ACK0	Ribulose bisphosphate carboxylase large chain	Q94KD8	Probable beta-D-xylosidase 2	P84994	Villin-like protein ABP41	Q944H0	Phosphomethylethanolamine N-methyltransferase
3.	Q9FYF4	Putative F-box protein At1g67390	P45432	COP9 signalosome complex subunit 1	P13548	V-type proton ATPase catalytic subunit A	Q2QM84	Auxin response factor 25
4.	Q9FYQ8	Transmembrane 9 superfamily member 11	F4IW10	Elongation factor G-2	Q0J6P7	Probable adenylate kinase 5	Q5N8G1	2-C-methyl-D-erythritol 4-phosphate cytidylyltransferase
5.	Q8L7U4	Co-chaperone protein p23-1	Q8RU33	Probable V-type proton ATPase subunit d	Q0J3L4	Monothiol glutaredoxin-S10	Q9LY15	Peptide methionine sulfoxide reductase A2
6.	O80934	Uncharacterized protein At2g37660	Q9LXX5	PsbP domain-containing protein 6	C6TBN2	Probable aldo-keto reductase 1	Q9LFG2	Diaminopimelate epimerase
7.	P49106	14-3-3-like protein GF14-6	P10690	Photosystem II 10 kDa polypeptide	F4JHI7	Serine/arginine-rich splicing factor SR34B	Q9S7Y7	Alpha-xylosidase 1
8.	O22788	Probable peroxygenase 3	Q7XUP6	Peptide methionine sulfoxide reductase A2-2	Q9LD13	Bifunctional pinoresinol-lariciresinol reductase 2	Q38970	Acetyl-CoA carboxylase 1
9.	P23993	Photosystem I reaction center subunit XI	Q07510	3-oxoacyl-[acyl-carrier-protein] synthase III	Q03389	Eukaryotic translation initiation factor isoform 4E-2	D3UAG2	UDP-glycosyltransferase 71K2
10.	P28260	Ribulose bisphosphate carboxylase large chain	Q9LE82	RAN GTPase-activating protein 1	Q0D673	Probable protein phosphatase 2C	Q9ZUH0	F-box/kelch-repeat protein At2g24250
11.	Q6PSU2	Conglutin-7	P49104	Ras-related protein Rab-2-B	Q1W374	Phosphomannomutase	Q84WW5	Vesicle-associated protein 1-3
12.	A2WNH1	Calmodulin-3	Q9LZI2	UDP-glucuronic acid decarboxylase 2	Q944B6	Arogenate dehydrogenase 1	Q6BEH3	Chalcone--flavanone isomerase

13.			Q38885	Preprotein translocase subunit SCY1	B6TRH4	Riboflavin biosynthesis protein PYRD	Q647G3	Oleosin Ara h 15.0101
14.			P55747	Serine carboxypeptidase II-1	P49133	Triose phosphate/phosphate translocator	Q5JNA1	B3 domain-containing protein Os03g0120900
15.			P24525	Peptidyl-prolyl cis-trans isomerase	P49043	Vacuolar-processing enzyme	P93262	Phosphoglucomutase
16.			B0YPQ0	Plastid 30S ribosomal protein S18			Q9AT34	40S ribosomal protein S15a
17.			P26518	Glyceraldehyde-3-phosphate dehydrogenase				
18.			Q85V57	ATP synthase subunit beta				
19.			P53504	Actin-1				
20.			P09439	Seed linoleate 9S-lipoxygenase-2				
21.			Q9SV20	Coatomer subunit beta-2				
22.			Q7XXD4	Probable inactive methyltransferase				

Further, we compared differentially expressed proteins between different treatments named as T1 to T5: T1 (control vs drought-stressed plants), T2 (control vs *Eb* WRS7-inoculated plants), T3 (control vs *Eb* WRS7-inoculated plants under drought stress), T4 (*Eb* WRS7-inoculated plants vs drought-stressed plants), and T5 (*Eb* WRS7-inoculated plants vs *Eb* WRS7-inoculated plants under drought stress). Differentially accumulated proteins were classified into three functional groups: 'Molecular function', 'biological process', and 'cellular component' using gene ontology (GO) annotation software (Figure 5.2). Biological process refers to a biological objective to which the gene or gene product contributes. In contrast, molecular function is defined as a gene product's biochemical activity (including specific binding to ligands or structures). Cellular component refers to the place in the cell where a gene product is active [314].

A total of 440 DAPs were identified in T-1. Among these proteins, 264 were upregulated, whereas 176 were downregulated. In T-2, a total of 339 DAPs were identified. Among these proteins, the expression of 197 proteins was upregulated and 142 proteins was downregulated. In T-3, a total of 422 DAPs were identified. Among these proteins, 302 were upregulated, whereas 120 were downregulated. In T-4, a total of 485 DAPs were identified. Among these proteins, 130 were upregulated whereas 335 were downregulated. In T-5, a total of 458 DAPs were identified. Among these proteins, 158 were upregulated, whereas 300 were downregulated.

Most of the annotated molecular function was found associated with binding (30%) and catalytic (19%) activity, while protein folding (5%), stress response (8%), response to stimulus (2%), regulation (15%) and signaling (3%) processes were the most annotated biological function, and cell organelles (25%) and cytoplasm (31%) were major cellular component involved in T-1 (Figure 5.2A). For the T-2 treatment, 28% of DAPs were categorized as binding activity, 13% as transporter, and 17% as catalytic activity (Figure 5.2B). Bacterial inoculation slightly increased expression of regulatory proteins (16%), protein folding (6%), stress response (7%), response to stimulus (3%), and signaling (3%) as compared to its control counterpart. For the T-3 treatment, 24% protein was recognized for binding activity, 16% for transporter activity, and 15% for catalytic activity. An increase in stress-responsive proteins (9%) was also seen in the T-3 treatment plants (Figure 5.2C). For the T-4 treatment, 27% of protein were recognized for binding activity, 12% for transporter activity, and 21% for catalytic activity (Figure 5.2D), while protein folding (6%), stress response (3%), response to stimulus

(3%), regulation (18%) and signaling (4%) processes were the major annotated biological function. For the T-5 treatment, 24% of protein were recognized for binding activity, 13% for transporter activity, and 20% for catalytic activity (Figure 5.2E), while protein folding (7%), stress response (4%), response to stimulus (4%), regulation (19%) and signaling (6%) processes were the major annotated biological function.

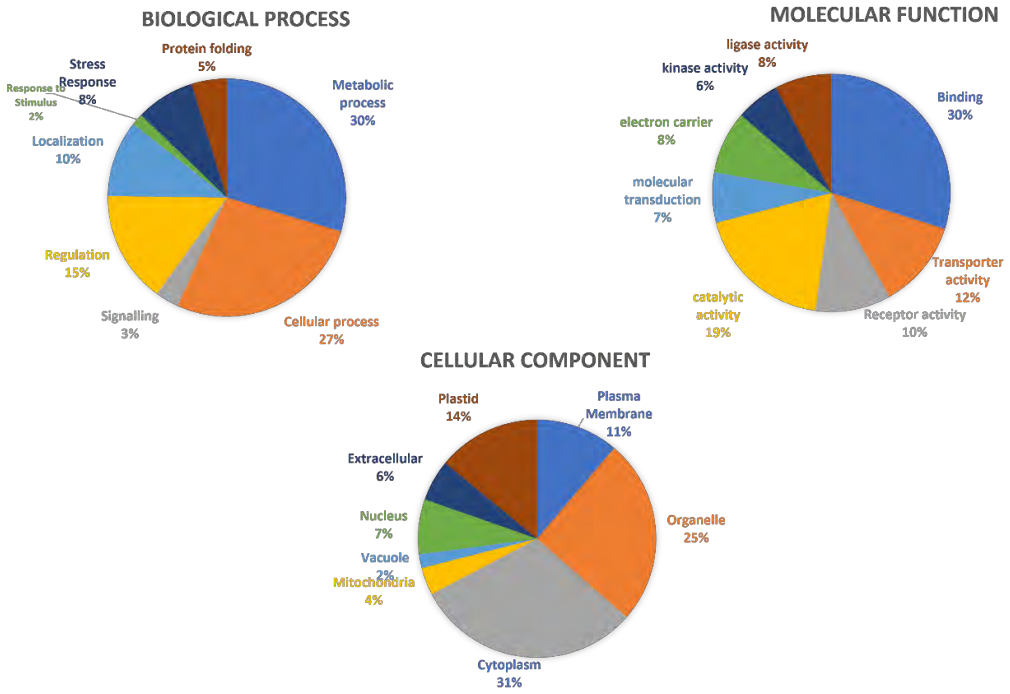

Figure 5.2 A. Pie charts showing the distribution of differentially abundant proteins based on their predicted biological process (A), molecular functions (B), and cellular process (C) in Treatment T-1.

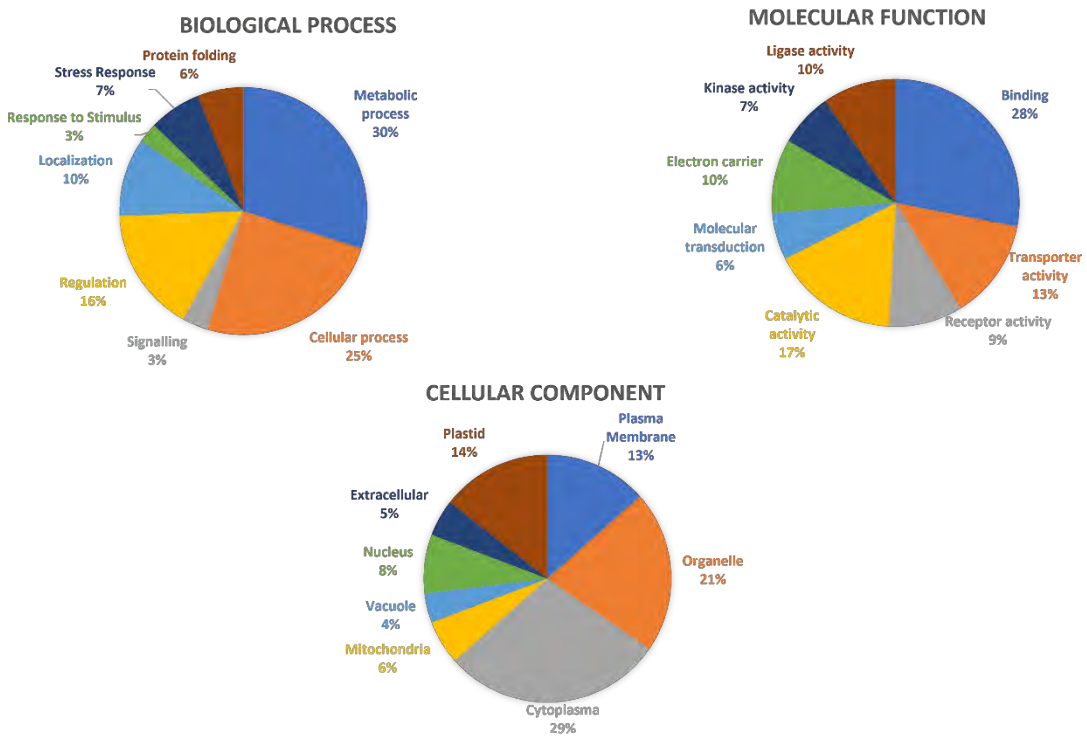

Figure 5.2 B. Pie charts showing the distribution of differentially abundant proteins based on their predicted biological process (A), molecular functions (B), and cellular process (C) in Treatment T-2.

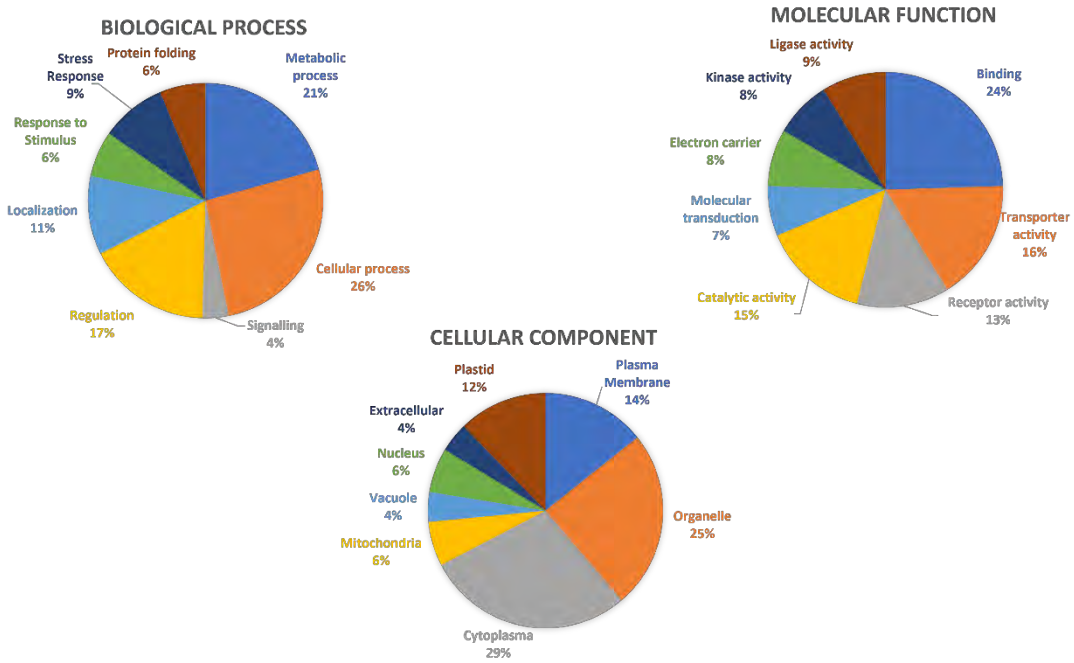

Figure 5.2 C. Pie charts showing the distribution of differentially abundant proteins based on their predicted biological process (A), molecular functions (B), and cellular process (C) in Treatment T-3.

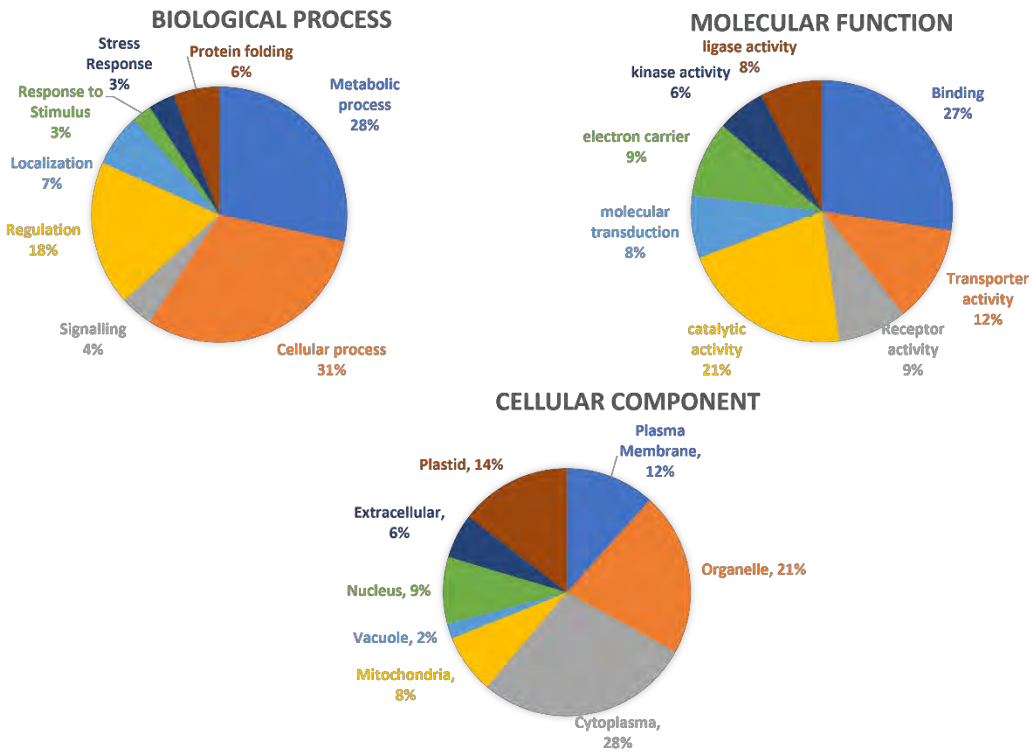

Figure 5.2 D. Pie charts showing the distribution of differentially abundant proteins based on their predicted biological process (A), molecular functions (B), and cellular process (C) in Treatment T-4.

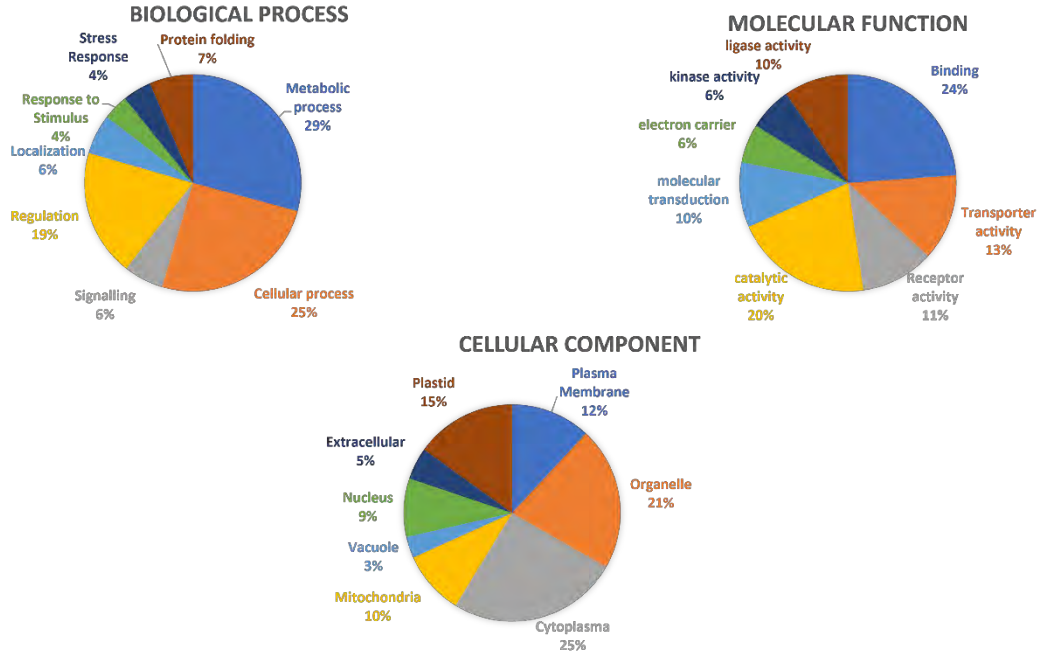

Figure 5.2 E. Pie charts showing the distribution of differentially abundant proteins based on their predicted biological process (A), molecular functions (B), and cellular process (C) in Treatment T-5.

Functional annotation and classification of identified proteins.

To assign biological information to the identified proteins, they were classified based on their function. Knowing the functions of the proteins will help in understanding the nature of the identified protein. The fifteen functional groups included the proteins involved in the cell wall synthesis and cytoskeleton, chromatin-associated protein, defence protein, ion/electron transport, lipid metabolism, metabolic pathway, photosynthesis, protein biosynthesis, protein degradation, protease inhibitor, seed storage, secondary metabolite synthesis, stress-related, transcription control, and some others with known biological functions. Most identified proteins were related to metabolic pathways, photosynthesis, and stress mechanisms. The differential expression of proteins belonging to different categories was expressed as upregulated and downregulated based on significant changes of $\geq$ 2-fold or $\leq$ 0.5 in the level of proteins, respectively, were differentiated. Among 126 proteins belonging to the classes mentioned above that showed predominant changes under drought stress (T-1); 53 were upregulated, and 73 were down-regulated (Figure 5.3 A and Table 5.2). The maximum change was observed in metabolic proteins, including glyceraldehyde-3-phosphate dehydrogenase GAPB and enolase 1. The higher increase (upregulated proteins) in protein number was observed for secondary metabolites (80%) such as polyamines and flavonoids, followed by defence and protein degradation (67% respectively) and lipid metabolism (58%). In response to bacterial inoculation (T-2), the expression level of 107 proteins showed significant changes, of which 53 were upregulated, and 54 were downregulated (Figure 5.3 B and Table 5.2). Chromatin-associated and secondary metabolites proteins were upregulated; other categories showed both upregulation and downregulation. The expression level of 131 proteins showed significant changes in treatment T-3, of which 41 were upregulated, and 90 were downregulated (Figure 5.3 C and Table 5.2). The proteins related to metabolic and stress-related proteins were predominantly differentially regulated as compared to others. In the comparison of drought stress and bacteria-treated plants (T-4), 119 proteins showed significant changes, of which 62 were upregulated whereas 57 were downregulated (Figure 5.3 D and Table 5.2). Among 106 proteins that showed predominant changes in treatment T-1, 51 were upregulated, and 55 were downregulated (Figure 5.3 E and Table 5.2).

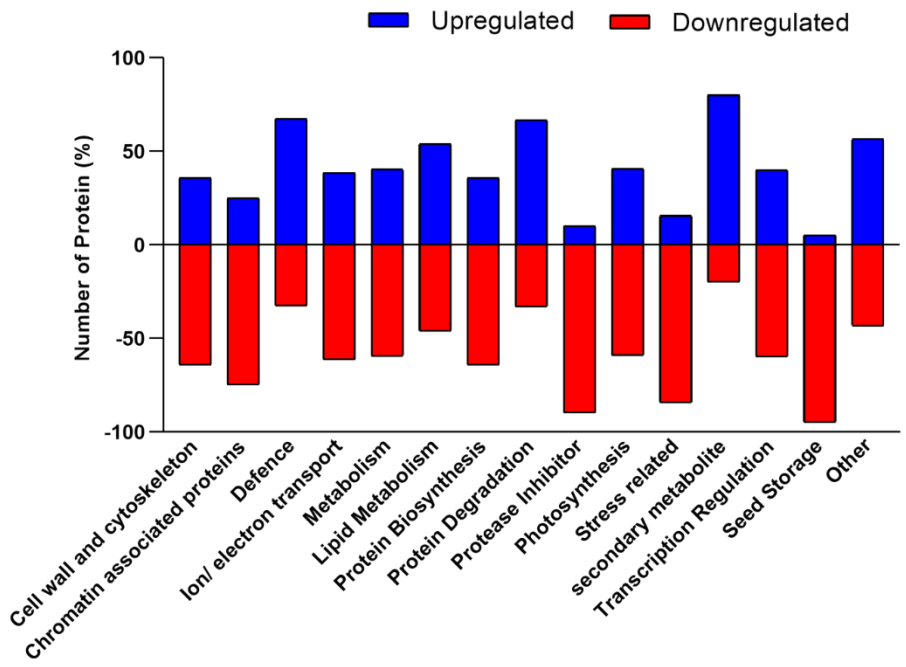

Figure 5.3 A. Number of proteins upregulated/downregulated in each functional category in treatment T-1.

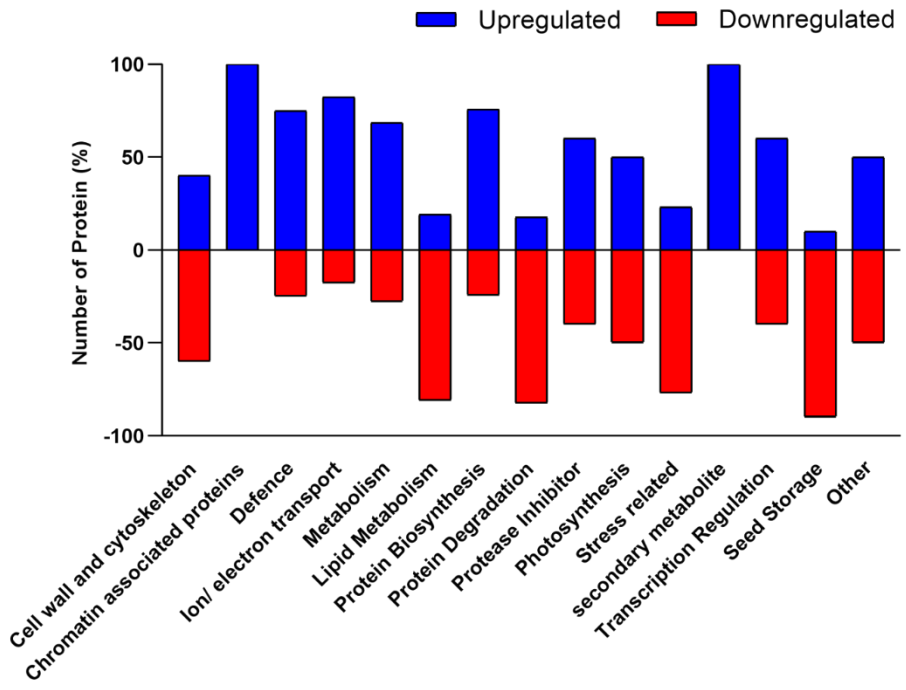

Figure 5.3 B. Number of proteins upregulated/downregulated in each functional category in treatment T-2.

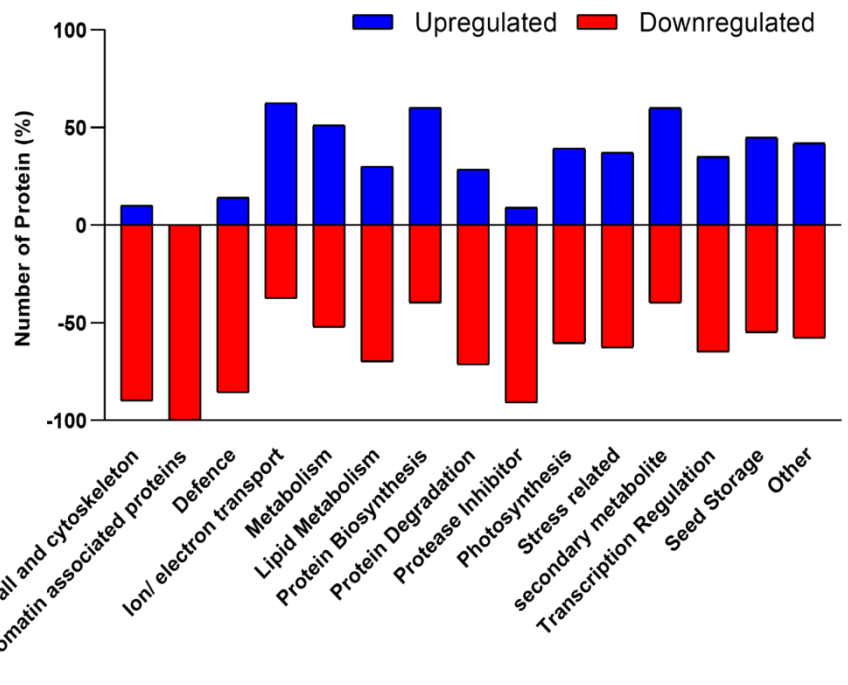

Figure 5.3 C. Number of proteins upregulated/downregulated in each functional category in treatment T-3.

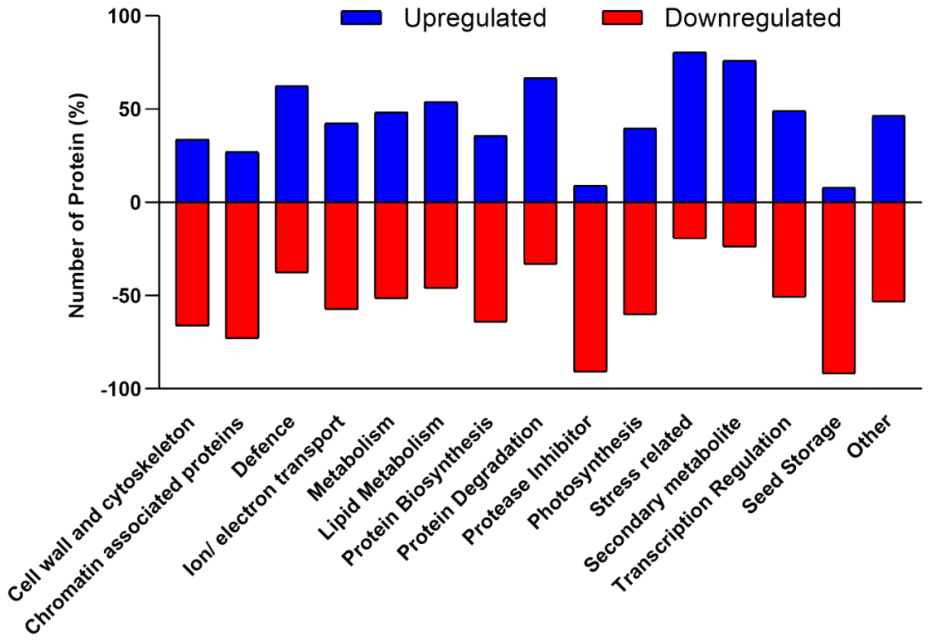

Figure 5.3 D. Number of proteins upregulated/downregulated in each functional category in treatment T-4.

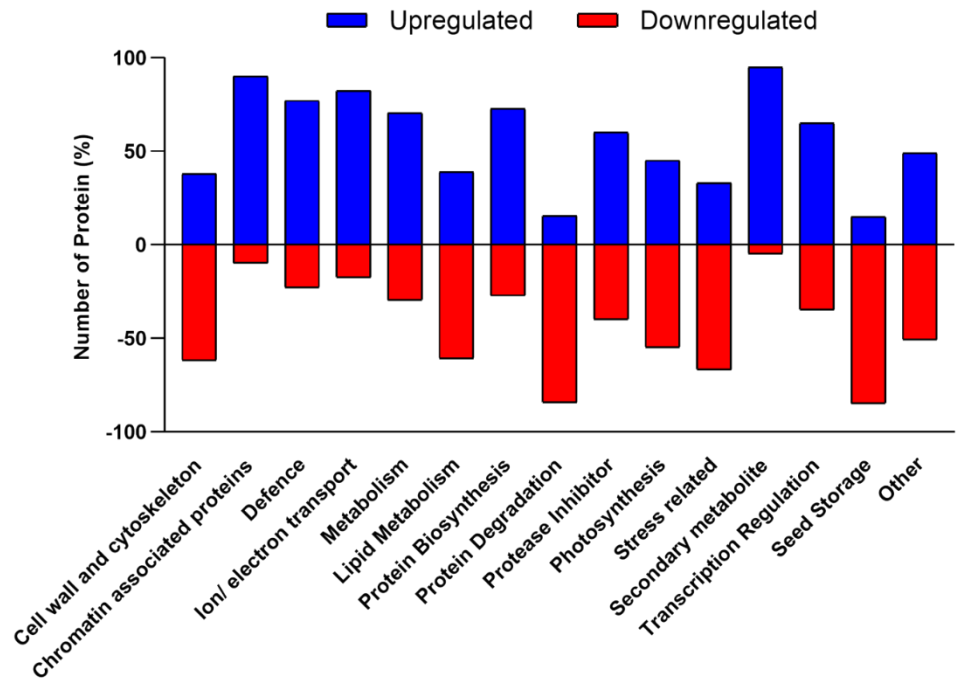

Figure 5.3 E. Number of proteins upregulated/downregulated in each functional category in treatment T-5.

Hierarchical Cluster analysis of differentially expressed proteins.

Hierarchical Cluster analysis of the 95 DAPs common to all treatments (T-1, T-2, T-3, T-4, T-5) was performed with their UniProt-ID (Table 5.1, Figure 5.4). These proteins were chosen based on their role in plant growth and development, defence, and abiotic stress. In the T-1 treatment (under drought stress), proteins that were majorly upregulated are Ribulose bisphosphate carboxylase large and small chain (UniProt ID- O62964 and P26667 respectively), Chlorophyll a-b binding protein CP24 10B (UniProt ID- P27525), 60S ribosomal protein L11 (UniProt ID -A2YDY2) and Heat shock 70 kDa protein (UniProt ID -P11143). The downregulated proteins belonged to Probable V-type proton ATPase subunit H (UniProt ID- Q84ZC0), 2-Cys peroxiredoxin BAS1-like (UniProt ID -Q9C5R8), 60S ribosomal protein L9 (UniProt ID- P49210) and 40S ribosomal protein S2-3 (UniProt ID- P49688). Bacterial inoculation (T-2) enhanced the expression of the proteins such as Photosystem I reaction center subunit IV B (UniProt ID- Q41229), Indole-3-acetaldehyde oxidase (UniProt ID- O23888) and 4-hydroxy-tetrahydrodipicolinate synthase 1 (UniProt ID- P24846). Under the drought stress, bacterial inoculation (T-3) enhanced the expression of Pyridoxal 5'-phosphate synthase subunit PDX1.1 (UniProt ID- O80448), 9-cis-epoxy carotenoid dioxygenase NCED1 (UniProt ID- Q6YVJ0), ABC transporter G family member 40 (UniProt ID- Q9M9E1), and Chalcone synthase 3 (UniProt ID- P48392). The downregulated proteins were belonging to S-

adenosylmethionine synthase 2 (UniProt ID- P43281), and Serine/threonine-protein kinase SAPK5 (UniProt ID- Q7XKA8). In T-4, ABC transporter C family member 7 (UniProt ID- Q9LK62), Abscisic acid receptor PYL10 (UniProt ID- Q7XBY6), Dehydrin COR410 (UniProt ID- P46524) proteins were significantly upregulated. L-ascorbate peroxidase 2, cytosolic (UniProt ID- Q9FE01) and Dehydrin COR410 (UniProt ID- P46524) were upregulated in T-5 plants.

Table 5.2. The identified proteins with their UniProt -ID used for hierarchical cluster analysis.

UniPort ID	Protein Name	T-1	T-2	T-3	T-4	T-5
P12810	16.9 kDa class I heat shock protein 1	1.59	1.26	2.10	1.02	1.26
Q9SIV2	26S proteasome non-ATPase regulatory subunit 2 homolog A.	0.75	0.56	2.19	1.35	1.93
Q9C5R8	2-Cys peroxiredoxin BAS1-like, chloroplastic	0.17	0.18	0.09	0.99	0.52
A1E9H0	30S ribosomal protein S19, chloroplastic	0.53	1.56	0.39	0.34	0.25
A2ZB00	40S ribosomal protein S16	1.99	2.18	2.54	0.16	0.29
P49688	40S ribosomal protein S2-3	1.31	0.75	1.57	0.41	0.76
P24846	4-hydroxy-tetrahydrodipicolinate synthase 1, chloroplastic	1.93	2.48	3.55	1.99	1.43
O22386	50S ribosomal protein L12, chloroplastic	0.76	2.23	2.47	0.34	1.11
Q8L803	50S ribosomal protein L9, chloroplastic	0.53	1.95	2.89	0.51	0.58
A2YDY2	60S ribosomal protein L11	17.19	2.11	2.11	0.23	0.41
P49210	60S ribosomal protein L9	0.26	1.53	0.77	0.17	0.51
Q6YVJ0	9-cis-epoxycarotenoid dioxygenase NCED1, chloroplastic	2.66	0.82	3.05	1.84	1.04
Q7GB25	ABC transporter C family member 5	0.43	0.90	0.35	0.48	0.39
Q9LK62	ABC transporter C family member 7	1.24	0.20	0.70	6.09	3.44
Q9M9E1	ABC transporter G family member 40	0.87	2.03	2.27	0.33	1.12
Q7XBY6	Abscisic acid receptor PYL10	2.96	1.05	2.91	2.01	0.74
A2XID3	Allene oxide cyclase, chloroplastic	1.97	1.32	2.29	1.50	1.74
C6KEM4	Aminoaldehyde dehydrogenase 2	0.67	1.08	1.45	0.62	1.34

Q6EU94	Aquaporin PIP1-1	2.29	0.81	2.55	0.64	0.47
B3VMC0	Betaine aldehyde dehydrogenase 2	2.05	1.62	2.66	1.27	1.03
O81852	Bifunctional aspartokinase/homoserine dehydrogenase 2, chloroplastic	2.07	1.18	3.07	1.55	1.83
Q2QY10	Calcium-binding protein CBP	0.46	0.61	0.66	0.13	0.18
Q6I587	Calcium-dependent protein kinase 15	0.96	0.95	1.76	1.01	1.85
P27164	Calmodulin-related protein	1.24	0.90	1.25	0.27	0.28
Q43206	Catalase-1	1.70	1.67	1.79	1.02	1.07
Q9C5D0	CBS domain-containing protein CBSX2, chloroplastic	2.22	1.23	2.03	1.79	1.65
P48392	Chalcone synthase 3	2.21	1.13	3.06	0.53	0.19
P27525	Chlorophyll a-b binding protein CP24 10B, chloroplastic	20.09	2.13	2.01	0.76	0.64
P12332	Chlorophyll a-b binding protein, chloroplastic (Fragment)	2.17	1.86	2.29	1.23	2.26
Q9STS7	Chloroplastic lipocalin	0.97	1.59	2.46	0.79	1.55
O80433	Citrate synthase, mitochondrial	2.17	1.07	3.66	0.16	0.62
P46524	Dehydrin COR410	2.24	0.78	2.56	2.88	2.29
P32296	Delta-1-pyrroline-5-carboxylate synthase	2.19	1.73	2.14	1.79	1.24
Q9ZRI8	Formate dehydrogenase, mitochondrial	2.29	1.55	2.28	1.49	0.76
A2YQL4	Fructokinase-2	0.69	2.02	1.28	0.34	0.63
Q6ZBZ2	Germin-like protein 8-14	2.10	1.63	2.51	1.29	1.53
P93000	Germin-like protein subfamily 2-member 3	2.09	2.17	2.05	0.85	0.36
Q02438	Glucan endo-1,3-beta-glucosidase GV	1.22	2.16	2.12	2.43	2.56
P18492	Glutamate-1-semialdehyde 2,1-aminomutase, chloroplastic	0.39	1.78	1.45	1.90	1.38

P13564	Glutamine synthetase leaf isozyme, chloroplastic	2.41	1.03	2.09	2.02	2.34
Q8LE52	Glutathione S-transferase DHAR3, chloroplastic	1.08	1.10	2.17	0.98	2.88
A2Z9B8	Glycine cleavage system H protein, mitochondrial	2.25	0.84	2.54	2.66	3.00
Q43472	Glycine-rich RNA-binding protein blt801	1.71	1.02	2.39	0.69	2.34
Q9LSV0	Glyoxylate/succinic semialdehyde reductase 1	1.71	0.76	1.19	0.93	0.26
O49809	Glyoxysomal fatty acid beta-oxidation multifunctional protein MFP-a	0.73	2.06	0.87	0.32	0.38
Q9LDZ0	Heat shock 70 kDa protein 10, mitochondrial	2.60	1.51	2.49	1.03	0.99
P11143	Heat shock 70 kDa protein	2.99	1.15	2.24	0.51	1.33
P37900	Heat shock 70 kDa protein, mitochondrial	2.88	1.41	2.29	0.75	0.56
Q0J4P2	Heat shock protein 81-1	2.09	1.20	2.08	0.57	0.99
Q84XG9	IAA-amino acid hydrolase ILR1-like 1	1.69	1.76	2.07	0.95	1.17
O23888	Indole-3-acetaldehyde oxidase	1.26	1.88	2.25	2.07	0.29
Q9ZTZ7	K (+) efflux antiporter 1, chloroplastic	2.16	1.67	2.62	0.34	0.37
Q948T6	Lactoylglutathione lyase	1.47	1.04	2.31	0.59	0.84
Q9FE01	L-ascorbate peroxidase 2, cytosolic	1.60	0.86	2.55	0.70	2.98
Q84UI5	Mitogen-activated protein kinase 1	1.54	1.12	2.28	0.49	0.25
Q336X9	Mitogen-activated protein kinase 6	2.10	1.19	2.07	1.77	0.90
Q6ZJ08	Monodehydroascorbate reductase 4, cytosolic	2.09	0.49	2.05	2.28	0.56
Q93XI4	N-carbamoylputrescine amidase	1.62	1.01	1.62	0.99	0.62
Q10G56	Ornithine aminotransferase, mitochondrial	2.07	1.29	2.31	0.71	2.03
P45851	Oxalate oxidase 2	2.18	1.53	2.49	0.86	0.98

Q6AUK5	Peptide methionine sulfoxide reductase B3, chloroplastic	2.64	1.11	2.62	2.28	2.27
A5H8G4	Peroxidase 1	2.78	1.37	3.34	0.83	0.98
O23237	Peroxidase 49	2.13	0.97	2.39	2.18	2.03
Q05855	Peroxidase	1.87	0.98	1.40	1.89	1.42
Q5S1S6	Peroxiredoxin Q, chloroplastic	1.43	1.56	1.38	0.28	0.88
Q8S8X4	Photosystem I P700 chlorophyll a apoprotein A1	0.42	0.16	0.12	2.63	0.77
Q41229	Photosystem I reaction center subunit IV B, chloroplastic	0.66	3.09	3.62	0.21	1.17
P82339	Photosystem I reaction center subunit N (Fragment)	0.68	1.84	0.39	0.37	0.21
P83970	Plasma membrane ATPase	1.84	1.88	1.86	0.98	0.99
Q65XA0	Probable glutathione S-transferase DHAR1, cytosolic	2.61	1.14	2.98	0.89	0.96
Q67UK9	Probable glutathione S-transferase DHAR2, chloroplastic	2.16	0.64	2.32	0.25	2.62
Q6ZJJ1	Probable L-ascorbate peroxidase 4, peroxisomal	1.45	1.45	2.02	0.99	1.39
P0C0L0	Probable L-ascorbate peroxidase 5, chloroplastic	2.54	1.25	2.19	2.63	1.33
Q69SV0	Probable L-ascorbate peroxidase 8, chloroplastic	2.10	1.04	2.13	0.49	2.19
O22788	Probable peroxygenase 3	1.76	0.01	25.36	0.45	0.52
Q40648	Probable voltage-gated potassium channel subunit beta	2.86	1.40	2.15	0.53	0.98
Q84ZC0	Probable V-type proton ATPase subunit H	0.13	1.51	0.61	0.87	0.41
P52184	Profilin-1	2.09	1.00	2.66	2.07	2.65
P49232	Profilin-1	2.57	1.21	2.20	2.12	1.81
O80448	Pyridoxal 5'-phosphate synthase subunit PDX1.1	1.76	1.46	2.86	1.62	0.82
Q9MTQ6	Red chlorophyll catabolite reductase (Fragment)	2.39	1.41	1.79	1.71	1.28

O62964	Ribulose bisphosphate carboxylase large chain	71.15	0.48	25.39	2.39	25.34
P26667	Ribulose bisphosphate carboxylase small subunit, chloroplastic 2	22.21	1.42	82.76	1.29	0.82
P08474	Ribulose bisphosphate carboxylase small subunit, chloroplastic	2.52	2.29	3.16	1.09	1.38
A6XMY9	S-adenosylmethionine synthase 1	1.94	1.27	1.01	0.82	1.26
P43281	S-adenosylmethionine synthase 2	2.14	0.70	1.26	2.38	0.94
A9P2P4	S-adenosylmethionine synthase 3	2.57	1.60	1.71	0.96	1.06
Q7XKA8	Serine/threonine-protein kinase SAPK5	2.47	0.41	1.42	1.13	3.45
Q9SMB1	Spermidine synthase 1	1.78	1.36	2.11	1.12	0.86
B9F3B6	Succinate-semialdehyde dehydrogenase, mitochondrial	2.06	1.05	2.58	0.87	0.74
P11964	Superoxide dismutase [Cu-Zn], chloroplastic	2.11	0.96	2.49	2.16	5.89
O65175	Superoxide dismutase [Cu-Zn], chloroplastic	2.10	1.56	2.33	0.90	0.67
Q0JCU7	Zeaxanthin epoxidase, chloroplastic	2.56	0.75	2.77	2.22	0.69

[#]Proteins having ratio >2.0 was considered as upregulated, whereas values <0.50 were kept as downregulated.

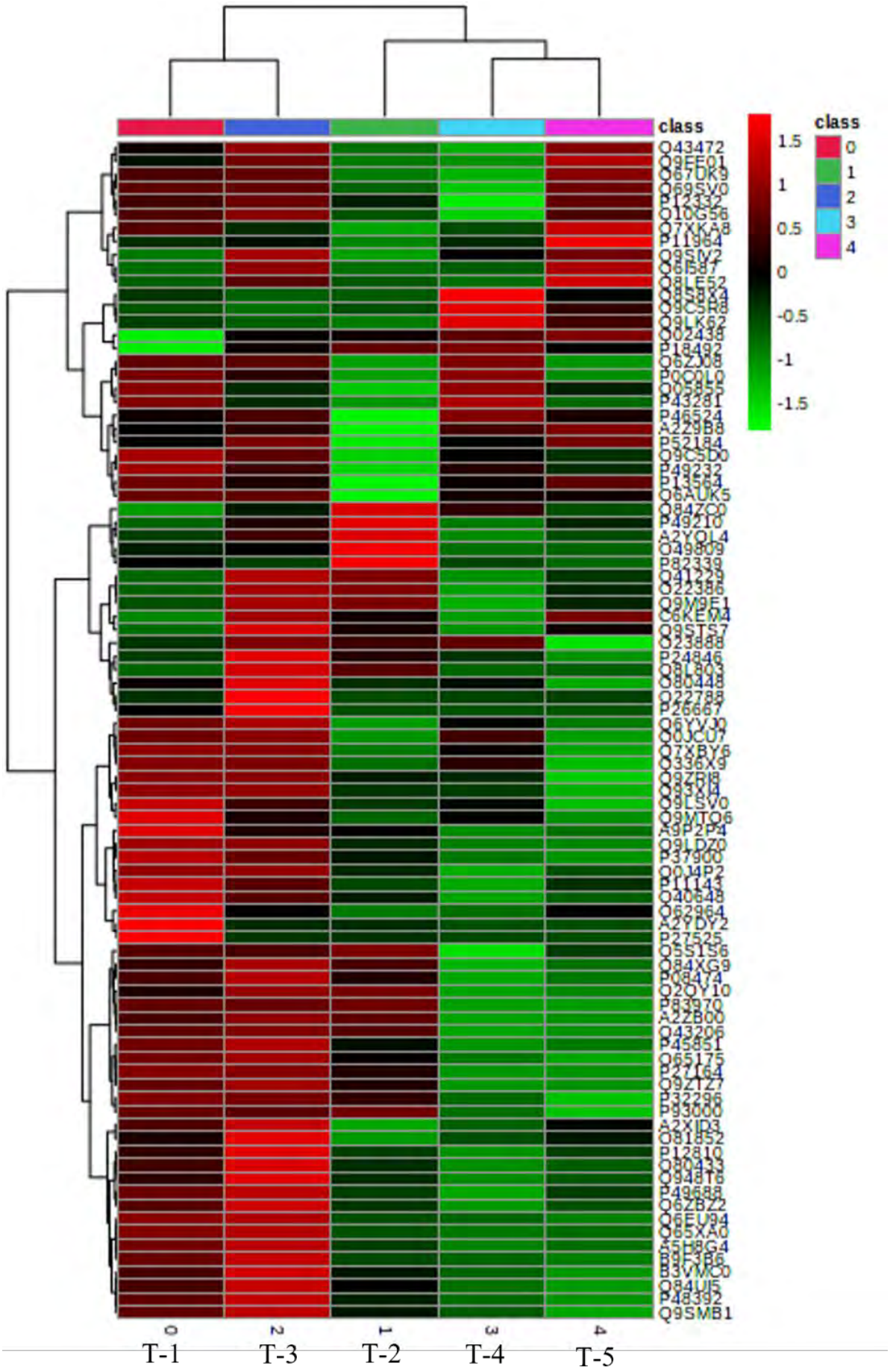
class
class
0
1
2
3
4
1.5
1
0.5
0
-0.5
-1
-1.5
T-1
T-3
T-2
T-4
T-5

Figure 5.4. Hierarchical clustering of the 95 DAPs involved in the treatments T-1, T-2, T-3, T-4, and T-5. The data were normalized using Z-score transformation, and cluster analysis was performed using the Java Treeview software (https://jtreeview.sourceforge.net/) using Euclidean distances and Ward's minimum criteria as algorithms for clusterogram construction. Red and green indicate the higher and lower expression levels, respectively.

Differential abundant proteins in *Eb* WRS7-treated wheat plant under drought stress.

The application of *Eb* WRS7 on wheat plants under drought conditions induced changes in the expression of some important proteins (Table 5.2 and Figure 5.5). Indicators of drought conditions such as glutamine synthetase and ferredoxin were upregulated in uninoculated, and *Eb* WRS7 inoculated wheat plants under drought stress. Proteins involved in cell redox homeostases, such as catalase, peroxidase, superoxide dismutase, and peroxiredoxin, were also upregulated. S-adenosylmethionine synthase 1, an enzyme involved in ethylene biosynthesis, was downregulated upon bacterial inoculation under drought stress. Allene oxide synthase 1, an enzyme involved in the biosynthesis of jasmonic acid, was upregulated upon bacterial inoculation (T-2 and T-3). Since MAPK may regulate the expression of various genes involved in biotic and abiotic stress response, their expression was up regulated in treatments 2 and 3. Expression of Serine/threonine-protein kinase SAPK5 and DEAD-box ATP-dependent RNA helicase 38 was upregulated in T-1 and T-3, which highlights their role in signal transduction of hyperosmotic response.

Table 5.3. Differentially Abundant Proteins in *Eb* WRS7-treated wheat plant under drought-stress.

UniPort ID	Protein Name	T1[#]	T2[#]	T3[#]	T4[#]	T5[#]
A. Stress and defense response						
Q43470	14-3-3-like protein B	3.19	6.79	5.62	0.47	0.83
P29305	14-3-3-like protein A	0.87	1.71	1.46	0.51	0.85
P49106	14-3-3-like protein GF14-6	0.14	0.69	0	0.20	0
Q0JNR2	Cysteine proteinase inhibitor 12	2.12	1.44	2.14	1.47	2.94
Q38950	Serine/threonine-protein phosphatase 2A 65 kDa regulatory subunit A beta isoform	1.46	6.15	4.08	0.24	0.66
Q2QM47	Serine/threonine-protein phosphatase BSL2 homolog	1.53	0	5.19	0	0
Q0E2S4	Serine/threonine-protein phosphatase PP2A-3 catalytic subunit	2.04	0.54	3.31	3.78	3.13
Q10RI7	DEAD-box ATP-dependent RNA helicase 38	3.32	2.93	4.22	0.26	0.33
Q9LFN6	DEAD-box ATP-dependent RNA helicase 56	0.89	1.88	1.23	0.47	0.65
Q9SJN2	Pentatricopeptide repeat-containing protein At2g36240	1.45	1.71	2.92	2.05	2.11
Q9LZ19	Pentatricopeptide repeat-containing protein At5g04780	1.82	1.52	2.49	1.19	1.64
Q6ZBZ2	Germin-like protein 8-14	2.10	1.63	2.51	1.29	1.53
P93000	Germin-like protein subfamily 2-member 3	2.09	2.17	2.05	0.85	0.36
P52409	Glucan endo-1,3-beta-glucosidase	0.89	2.29	2.88	1.37	1.76
Q84UI5	Mitogen-activated protein kinase 1	1.54	1.12	2.28	0.49	0.25
Q336X9	Mitogen-activated protein kinase 6	2.11	1.19	2.07	1.77	0.90
Q7XKA8	Serine/threonine-protein kinase SAPK5	2.47	0.41	1.42	1.13	2.44
B. Antioxidant Proteins						
P11964	Superoxide dismutase [Cu-Zn], chloroplastic	2.11	0.96	2.49	2.16	5.89

O65175	Superoxide dismutase [Cu-Zn], chloroplastic	2.10	1.56	2.33	0.90	0.67
A5H8G4	Peroxidase 1	2.78	1.37	3.34	0.83	0.99
O23237	Peroxidase 49	2.13	0.98	2.39	2.18	2.03
Q05855	Peroxidase	1.86	0.98	1.40	1.89	1.42
Q5S1S6	Peroxiredoxin Q, chloroplastic	1.43	1.55	1.37	0.28	0.88
Q43206	Catalase-1	2.10	1.67	2.17	1.02	1.07
Q9C5R8	2-Cys peroxiredoxin BAS1-like, chloroplastic	0.17	0.17	0.09	0.99	0.52
Q9FE01	L-ascorbate peroxidase 2, cytosolic	1.60	0.86	2.55	0.70	2.98
Q8LE52	Glutathione S-transferase DHAR3, chloroplastic	1.08	1.10	2.17	0.98	2.88
Q65XA0	Probable glutathione S-transferase DHAR1, cytosolic	2.61	1.14	2.98	0.89	0.97
Q67UK9	Probable glutathione S-transferase DHAR2, chloroplastic	2.15	0.64	2.32	0.24	2.64
O80448	Pyridoxal 5'-phosphate synthase subunit PDX1.1	1.76	1.45	2.86	1.62	0.82
Q9STS7	Chloroplastic lipocalin	0.97	1.59	2.46	0.79	1.55
Q6ZJJ1	Probable L-ascorbate peroxidase 4, peroxisomal	1.45	1.45	2.02	0.99	1.39
P0C0L0	Probable L-ascorbate peroxidase 5, chloroplastic	2.54	1.25	2.19	2.63	1.34
Q69SV0	Probable L-ascorbate peroxidase 8, chloroplastic	2.10	1.04	2.13	0.49	2.19
Q9FNE2	Glutaredoxin-C2	1.17	1.28	2.07	0.12	1.26
P55142	Glutaredoxin-C6	1.75	0.97	1.98	1.61	1.33
Q9ZP21	Thioredoxin M-type, chloroplastic	1.51	1.14	2.26	0.66	0.51
Q9SGS4	Thioredoxin-like protein CDSP32, chloroplastic	0.76	1.30	1.44	0.59	1.11
O64394	Thioredoxin H-type	0.76	1.55	0.83	0.49	0.53
P09856	Thioredoxin F-type, chloroplastic	2.67	1.72	4.13	1.55	2.39
Q7X8R5	Thioredoxin M2, chloroplastic	1.79	2.57	2.54	0.69	0.99

C. Osmoprotectant						
Q03968	Late embryogenesis abundant protein, group 3	1.27	0	1.95	-	-
P32296	Delta-1-pyrroline-5-carboxylate synthase	2.18	1.72	2.14	0.79	0.24
P46524	Dehydrin COR410	2.23	0.77	2.55	2.88	2.29
B3VMC0	Betaine aldehyde dehydrogenase 2	2.05	1.62	2.66	1.26	1.03
D. Photosynthesis						
P08221	Chlorophyll a-b binding protein (LHCII), I, chloroplastic	2.14	2.36	3.27	2.01	1.87
P27523	Chlorophyll a-b binding protein (LHCII), III, chloroplastic	1.63	1.48	2.79	0.63	2.11
Q9XF89	Chlorophyll a-b binding protein CP26, chloroplastic	2.09	2.13	2.01	0.45	0.41
P26320	Oxygen-evolving enhancer protein (OEE) 1, chloroplastic	0.53	1.28	1.06	0.70	0.87
Q00434	Oxygen-evolving enhancer protein (OEE) 2, chloroplastic	0.87	2.09	1.1	0.42	0.86
Q9AYU0	Quinone-oxidoreductase QR2	1.92	1.27	2.33	2.61	0.65
Q7X9A6	Cytochrome b6	1.06	1.09	2.13	0.97	1.96
P36213	Photosystem I reaction center subunit II, chloroplastic	0.29	1.94	3.02	0.83	0.76
P13192	Photosystem I reaction center subunit III, chloroplastic	0.72	0.96	1.04	0.74	1.09
P13194	Photosystem I reaction center subunit IV, chloroplastic	0.65	0.97	3.62	1.01	1.25
Q00327	Photosystem I reaction center subunit V, chloroplastic	0.53	1.52	1.29	0.35	0.85
P12112	ATP synthase subunit alpha, chloroplastic	0.18	1.56	2.11	0.12	0.56
P20858	ATP synthase subunit beta, chloroplastic	0.65	1.93	2.11	0.75	1.09
P0C1M0	ATP synthase subunit gamma, chloroplastic	1.32	1.58	1.45	0.51	0.56
O62964	Ribulose bisphosphate carboxylase large chain	71.15	0.48	25.39	2.39	25.34
P26667	Ribulose bisphosphate carboxylase small subunit, chloroplastic	22.21	1.42	82.76	1.29	0.82
P08474	Ribulose bisphosphate carboxylase small subunit, chloroplastic	2.52	2.30	3.17	1.09	1.38

P12628	NADP-dependent malic enzyme	1.5	0.98	1.39	0.95	0.75
P40880	Carbonic anhydrase, chloroplastic	1.91	1.10	1.44	0.87	0.62
P00228	Ferredoxin, chloroplastic	2.06	0.61	1.99	0.92	0.20
P00455	Ferredoxin--NADP reductase, chloroplastic	0.69	1.36	1.08	0.50	0.79
P41343	Ferredoxin--NADP reductase, chloroplastic	0.42	2.14	1.80	0.19	0.31
E. Carbon metabolism						
P26517	Glyceraldehyde-3-phosphate dehydrogenase 1, cytosolic	1.68	2.06	2.44	0.55	0.76
P08477	Glyceraldehyde-3-phosphate dehydrogenase 2, cytosolic (Fragment)	1.27	1.12	1.40	0.24	0.36
P25857	Glyceraldehyde-3-phosphate dehydrogenase GAPB, chloroplastic	3.64	1.60	1.06	2.27	0.66
Q9SAJ6	Glyceraldehyde-3-phosphate dehydrogenase GAPCP1, chloroplastic	1.04	1.24	1.20	0.16	0.79
Q0JGZ6	Fructokinase-1	1.61	2.34	1.67	0.48	0.50
A2YQL4	Fructokinase-2	1.68	2.02	1.28	0.34	0.63
P09195	Fructose-1,6-bisphosphatase, chloroplastic	2.07	1.48	2.05	0.66	0.37
P46267	Fructose-1,6-bisphosphatase, cytosolic	1.85	0.93	2.07	0.69	0.35
Q944G9	Fructose-bisphosphate aldolase 2, chloroplastic	2.17	1.27	2.18	0.66	0.66
Q10A30	Fructose-bisphosphate aldolase 2, cytoplasmic	2.11	1.15	2.28	0.49	0.51
P26301	Enolase 1	2.78	1.61	2.29	2.39	1.32
Q9LKA3	Malate dehydrogenase 2, mitochondrial	0.30	1.26	0.70	0.19	0.69
Q42972	Malate dehydrogenase, glyoxysomal	0.39	1.33	0.63	0.63	2.10
P12782	Phosphoglycerate kinase, chloroplastic	1.17	1.01	1.21	1.15	1.19
Q9SAJ4	Phosphoglycerate kinase 3, cytosolic	1.91	0.78	2.64	2.38	3.38
Q1ACL0	Pyruvate dehydrogenase E1 component subunit beta	1.15	0.96	0.98	1.19	1.02
Q0J0H4	Pyruvate dehydrogenase E1 component subunit beta-2	1.31	1.19	1.23	1.09	1.03

Q2QNG7	ATP-citrate synthase alpha chain protein 3	1.26	3.33	1.33	1.08	1.09
Q93VT8	ATP-citrate synthase beta chain protein 1	0.25	0.79	0.77	0.31	0.97
P30523	Glucose-1-phosphate adenylyl transferase small subunit	0.74	2.09	1.09	0.35	0.53
P30524	Glucose-1-phosphate adenylyl transferase large subunit 1	1.02	2.49	2.62	0.23	0.58
F. ATP synthesis						
P12112	ATP synthase subunit alpha, chloroplastic	0.18	1.56	1.21	0.12	0.56
P20858	ATP synthase subunit beta, chloroplastic	0.64	1.93	2.12	0.75	1.09
P19023	ATP synthase subunit beta, mitochondrial	1.25	0.55	1.1	0.46	1.37
Q41629	ADP, ATP carrier protein 1, mitochondrial	0.65	0.77	0.63	0.85	0.83
B4FK49	Nucleoside diphosphate kinase 1	0.90	2.18	4.05	0.75	0.44
A6N0M9	Nucleoside diphosphate kinase 1	1.41	2.06	4.49	0.89	0.74
P00412	Cytochrome c oxidase subunit 2	0.41	0.64	0.78	0.64	1.22
P37841	Cytochrome b-c1 complex subunit Rieske, mitochondrial	0.54	0.87	1.33	0.40	0.66
G. Protein biosynthesis, folding and degradation						
A1E9H0	30S ribosomal protein S19, chloroplastic	0.52	1.55	1.39	0.34	0.25
A2ZB00	40S ribosomal protein S16	1.99	2.17	2.54	0.16	0.29
P34788	40S ribosomal protein S18	1.57	1.05	1.21	0.55	0.68
P49688	40S ribosomal protein S2-3	1.30	0.75	1.57	0.41	0.76
O22386	50S ribosomal protein L12, chloroplastic	0.76	2.23	2.46	0.34	1.11
Q6L378	50S ribosomal protein L20, chloroplastic	0.90	0.29	10.41	3.08	1.39
Q8L803	50S ribosomal protein L9, chloroplastic	0.53	1.94	2.88	0.51	0.58
A2YDY2	60S ribosomal protein L11	17.19	2.11	2.11	0.23	0.41
Q943F3	60S ribosomal protein L18a	0.29	2.07	1.23	1.09	0.39

P49210	60S ribosomal protein L9	0.26	1.53	0.77	0.17	0.51
P46252	60S acidic ribosomal protein P2A	0.98	1.50	3.02	0.65	2.01
P41095	60S acidic ribosomal protein P0	2.05	2.87	3.54	1.71	2.07
P50346	60S acidic ribosomal protein P0	3.66	0.91	2.14	4.42	1.12
O24310	Elongation factor Tu, chloroplastic	0.95	0.69	2.15	1.36	3.07
Q9ASR1	Elongation factor 2	1.06	2.03	2.17	1.03	1.07
Q43467	Elongation factor Tu, chloroplastic	1.15	1.01	0.54	0.48	1.68
P29546	Elongation factor 1-beta	2.08	3.04	2.60	0.56	0.52
Q03033	Elongation factor 1-alpha 1	0.68	1.33	0.68	0.51	0.51
P28996	Elongation factor 2	1.22	2.07	0.74	0.39	1.24
Q40680	Elongation factor 1-delta 1	1.05	2.34	1.19	0.45	0.51
O23627	Glycine--tRNA ligase, mitochondrial 1	0.93	0.54	1.30	1.35	2.41
Q43207	70 kDa peptidyl-prolyl isomerase	0.85	1.25	2.07	0.59	1.65
O49939	Peptidyl-prolyl cis-trans isomerase, chloroplastic	0.76	1.05	0.85	0.73	0.81
Q9SSA5	Peptidyl-prolyl cis-trans isomerase CYP38, chloroplastic	1.89	2.25	1.54	0.84	0.68
Q9SR70	Peptidyl-prolyl cis-trans isomerase FKBP16-4, chloroplastic	1.49	1.43	2.06	1.04	1.44
P21569	Peptidyl-prolyl cis-trans isomerase	1.18	0.77	2.25	1.76	2.34
P12810	16.9 kDa class I heat shock protein 1	1.59	1.26	2.10	0.97	1.26
Q9LDZ0	Heat shock 70 kDa protein 10, mitochondrial	2.60	1.51	2.49	1.03	0.99
P11143	Heat shock 70 kDa protein	2.99	1.15	2.24	0.51	1.33
P37900	Heat shock 70 kDa protein, mitochondrial	2.88	1.41	2.29	0.75	0.56
Q0J4P2	Heat shock protein 81-1	2.09	1.20	2.08	0.57	0.99
P13853	17.6 kDa class I heat shock protein 3	1.18	2.06	3.28	0.57	2.56

P52711	Serine carboxypeptidase II-3	2.76	1.82	2.01	1.51	1.11
P21529	Serine carboxypeptidase 3	2.93	3.22	2.19	1.11	1.35
P52712	Serine carboxypeptidase-like	0.40	0.45	0.57	0.90	1.29
P55748	Serine carboxypeptidase II-2 (Fragment)	1.28	1.95	1.33	0.66	0.68
P08818	Serine carboxypeptidase 2	1.49	2.28	1.64	0.45	0.49
Q0JNR2	Cysteine proteinase inhibitor 12	2.12	1.44	2.14	1.47	2.34
P0DKJ9	26S proteasome regulatory subunit 7A	0.24	0.71	0.98	0.35	1.35
P46466	26S proteasome regulatory subunit 4 homolog	0.43	0.32	0.89	1.33	2.28
Q9SIV2	26S proteasome non-ATPase regulatory subunit 2 homolog A	0.75	0.56	2.19	1.35	2.23
Q75GT3	Chaperone protein ClpB2, chloroplastic	2.06	1.18	2.36	0.95	1.99
P29185	Chaperonin CPN60-1, mitochondrial	3.21	1.43	2.24	0.94	0.65
H. Metabolism related proteins						
Q93XI4	N-carbamoylputrescine amidase	1.62	1.01	1.62	0.99	0.62
Q9SMB1	Spermidine synthase 1	1.78	1.36	2.11	1.12	0.86
Q66GP9	NO-associated protein 1, chloroplastic/mitochondrial	0.37	0.32	0.21	1.14	0.64
P45851	Oxalate oxidase 2	2.19	1.53	2.49	0.86	0.99
Q6AUK5	Peptide methionine sulfoxide reductase B3, chloroplastic	2.64	1.11	2.62	2.28	2.27
Q10G56	Ornithine aminotransferase, mitochondrial	2.07	1.29	2.31	0.71	2.03
Q9FI78	Shikimate O-hydroxycinnamoyltransferase	1.60	1.28	1.78	1.25	0.57
Q38J50	caffeic acid 3-O-methyltransferase	1.58	1.12	1.69	1.28	1.44
Q6ETN3	4-coumarate--CoA ligase 3	1.68	1.42	1.56	1.19	1.39
Q9S9N9	Cinnamoyl-CoA reductase 1	1.28	1.17	1.85	1.19	1.21
P38076	Cysteine synthase	1.54	1.01	1.70	1.68	1.51

Q8GYB8	12-oxophytodienoate reductase 2	2.24	2.12	1.46	1.52	0.69
Q6Z965	12-oxophytodienoate reductase 7	2.36	2.16	1.59	1.06	0.50
P24846	4-hydroxy-tetrahydrodipicolinate synthase 1, chloroplastic	1.93	2.47	3.55	1.99	1.43
P29114	Linoleate 9S-lipoxygenase 1	1.06	1.55	1.67	0.38	0.18
I. Cell organization-related proteins						
Q6YDN9	Xyloglucan endotransglucosylase/hydrolase	0.87	1.17	1.69	1.09	0.97
P52184	Profilin-1	2.09	1.01	2.67	2.07	2.65
P49232	Profilin-1	2.57	1.21	2.20	2.12	1.81
B9DHQ0	Tubulin alpha-5 chain	1.30	0.79	2.01	0.38	2.32
O49068	Tubulin gamma-2 chain	1.91	0.76	1.98	0.66	1.99
Q9ZRA9	Tubulin beta-4 chain	1.87	0.89	2.11	0.17	0.35

[#] values represent the fold change.

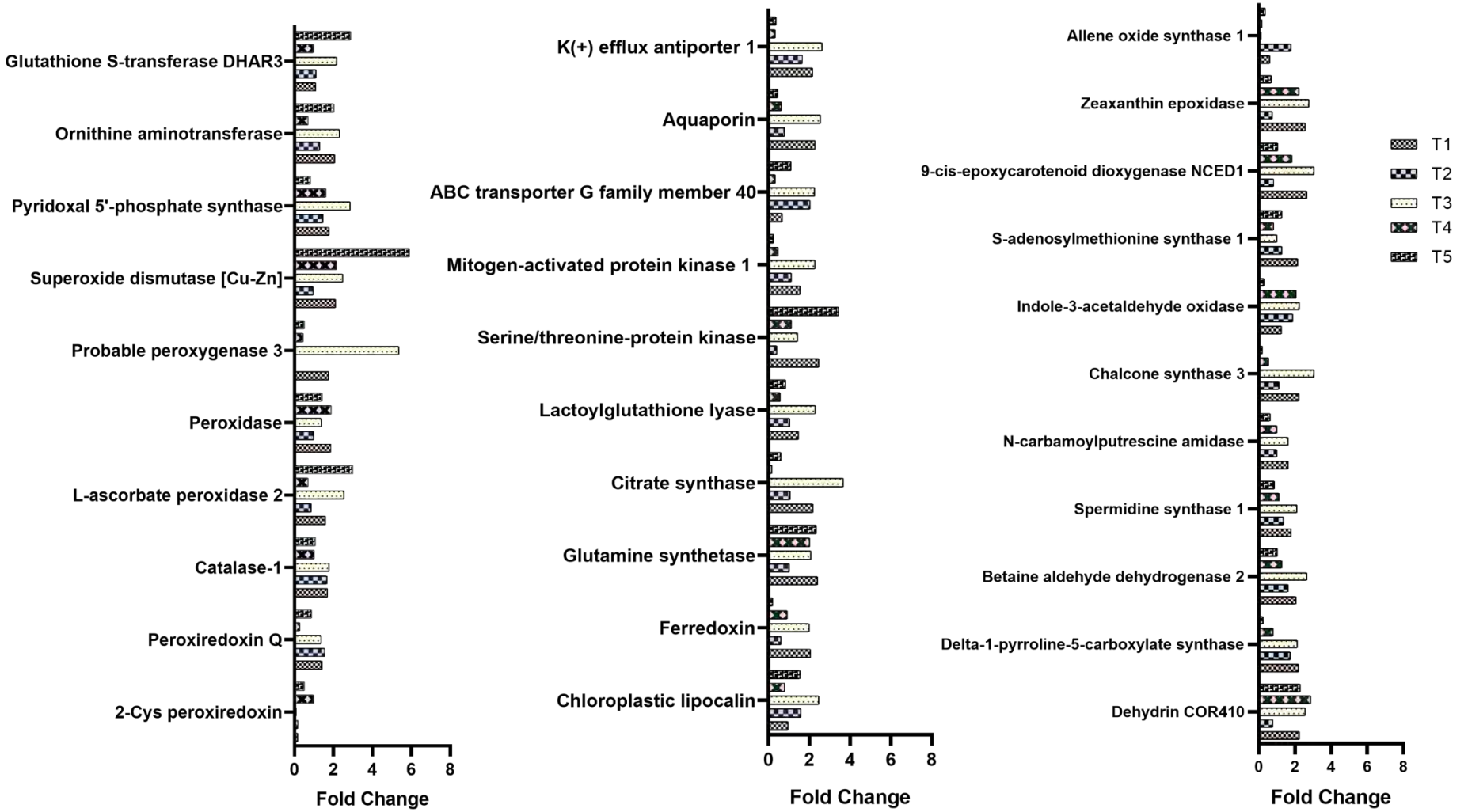

Figure 5.5. Differentially abundant proteins involved in drought stress in T-1, T-2, T-3, T-4, and T-5.

5.4 Discussion

Plant tolerance to drought is a complex attribute that requires a global view to understand its underlying mechanism. Previous studies demonstrated that bacterial inoculation of PGPR can differentially regulate the expression of the proteins in response to drought and other stresses [103, 114, 246]. In the present study, MS-based proteomic analysis was applied to decipher the alteration in proteomic profiling of the wheat plant subjected to drought stress inoculated with PGPR *Eb* WRS7. This study gave insight that the PGPR influences protein expression in the host and modulates protein dynamics in plant drought adaptation. PGPR-plant interaction enhances our understanding of how these regulatory mechanisms help host plants mitigate the deleterious effects of drought and hence offers a holistic view of the molecular foundation underlying a plant's ability to endure drought stress. The knowledge gained from this study holds the potential to reshape agricultural practices and improve drought tolerance in plants.

The present study found more proteins under drought stress in uninoculated, and PGPR inoculated plants. These proteins include antioxidants (Glutaredoxin, Superoxide Dismutase, L-ascorbate peroxidase), stress-related proteins (LEA proteins), and Heat shock proteins (16.9 kDa HSPs and Heat-shock 70kDa protein). Moreover, vesicle-associated proteins were also found. Abundances of these proteins under stress have been reported by earlier studies [246, 304, 314]

The high throughput proteomics identified multiple classes of proteins that respond to and alleviate drought stress in the presence and absence of PGPR *Eb* WRS7. These proteins include antioxidant enzymes, phytohormone-related proteins, metabolism- and photosynthesis-related proteins, transporters proteins, osmotic homeostasis-related proteins, and secondary metabolism-related proteins (Table 5.2), details of which are described below in the context of the present study. Among the DAPs, a large portion of these proteins were encoded either by the chloroplasts or mitochondria, suggesting that drought stress strongly affects the function of these organelles.

Photosynthesis-related proteins

Photosynthesis is one of the most important metabolic processes sensitive to environmental stresses, including drought stress. Drought stress primarily reduces the stomatal aperture in leaves, which reduces CO_2 availability and thus minimizes the energy for plant growth.

Drought negatively affected photosynthesis-related protein abundances, such as Ribulose-1,5-bisphosphate carboxylase/oxygenase (Rubisco), oxygen-evolving enhancer proteins, and others [315]. The observed decline in energy- and photosynthesis-related proteins during drought stress clearly indicates reduced growth and yield of wheat plants due to drought stress.

Rubisco, localized in the stroma of chloroplast, is the key photosynthetic enzyme in CO_2 fixation and oxygenation in the Calvin cycle. Rubisco inactivation impacts the photosynthesis under drought stress [316]. In our study, small and large subunits of Rubisco were upregulated by drought stress upon bacterial treatment, suggesting that *Eb* WRS7 could safeguard the photosynthesis process in stressed plants to support energy and organic compounds. Abd El-Daim *et al.* (2019) also found that *Bacillus velezensis* 5113-treated plants have high levels of photosynthesis proteins under abiotic stress in wheat plants [114]. Kandasamy *et al.* (2009) reported that PGPR *P. fluorescens* protects photosynthesis in rice plants under drought conditions by increasing the levels of chaperones that support the assembly of Rubisco, which further increased the photosynthetic efficiency and helped both growth and stress tolerance in rice plants [317].

Oxygen-evolving enhancer proteins 1 and 2 (OEE1 and OEE2) are very important members of the oxygen-evolving complex, which is involved in the photo-oxidation of water during the light reactions of photosynthesis. These proteins are susceptible to stress and can easily be inhibited by stress conditions [318]. OEE1 is involved in the light reaction of PSII and the stability of the oxygen-evolving complex, while OEE2 catalyse water splitting. A few reports have shown a decreased abundance of OEE proteins during drought stress [314, 315, 319]. This is in accordance with our study, where OEE1 decreased upon drought stress (0.53-fold), whereas a decrease in OEE2 expression was not significant (0.88-fold). However, bacterial inoculation had no change in OEE1 and OEE2 expression (1.06-fold and 1.1-fold respectively). In contrast, PSI light-harvesting chlorophyll a/b-binding proteins were upregulated in uninoculated and inoculated plants. Chlorophyll a/b-binding proteins are involved in the electron transport process in the light-harvesting complex and are responsible for the oxidation of water and the production of O_2 [315]. They are also known to regulate plant response to abiotic stress, and their expression increases under drought, salt, heat, and cold stress [320]. In the current study, the abundance of these proteins increased in uninoculated and PGPR-inoculated plants. The downregulation of OEE proteins and upregulation of chlorophyll a/b-binding protein suggested that these proteins contribute to the photosynthetic process during

drought stress and might be involved in drought stress response in wheat. This further indicates that PGPR promote drought tolerance by protecting the photosynthetic system and maintaining plant photosynthetic efficiency.

Ferredoxin–NADP reductase, a redox flavoenzyme, transfers electrons from reduced ferredoxin to NADPH for the final step in linear electron flow in photosynthesis [315]. In our study, ferredoxin protein upregulated under drought conditions, whereas Ferredoxin–NADP reductase enzyme downregulated (0.42-fold) in uninoculated plants but was non-significantly upregulated (1.8-fold) in bacterial inoculated plants. This is supported by drought stress-induced upregulation of components involved in ferredoxin-dependent cyclic electron transfer [321].

PSI is a multi-subunit complex that catalyzes the oxidation of plastocyanin and the reduction of ferredoxin by absorbed light energy [315]. In our study, photosystem I reaction center subunits II (PSI subunit II), III (PSI subunit III), IV (PSI subunit IV), and V (PSI subunit V) were identified. However, only PSI subunits II and IV showed significant differential expression. Their expression decreased under drought stress by 0.29- and 0.65-fold, respectively, whereas it increased by 3.02- and 3.62-fold in *Eb* WRS7-inoculated plants under drought stress. PSI subunit II helps assemble other subunits of the PSI reaction center, and its decreased expression suggests reduced binding stability for other subunits of PSI during drought stress. Additionally, PSI subunits II and IV also interact with ferredoxin [322], indicating that the electron transport mechanism was inhibited by drought stress.

ATP synthase transfers protons through the thylakoid membrane. Several subunits of the ATP synthase complex, such as ATP synthase alpha, beta, gamma, and delta subunits, were identified in the current study. ATP synthase subunits alpha and beta were down-regulated (0.18- and 0.65-fold, respectively) under drought stress. However, bacterial inoculation upregulated the ATP synthase subunit alpha (2.11-fold) expression. Decreased ATP synthase abundance under drought leads to decreased ATP production, resulting in reduced photosynthetic processes and a decreased consumption of ATP [323]. Differential expression of the ATP synthase subunit indicates that the whole machinery for ATP synthesis might be regulated under drought stress. Zadražnik *et al.* (2019) also reported a similar pattern of ATP synthase subunits under drought stress in common beans [315].

Carbohydrate and energy metabolism-related proteins

In the current study, proteins involved in carbohydrate and energy metabolism (e.g., glycolysis, tricarboxylic acid (TCA) cycle, electron transport chain, and ATP synthesis) were differentially abundant in wheat under drought stress. The glycolytic pathway responds under drought [324–326]. In our results, the abundance of fructokinase was upregulated, although non-significantly, in uninoculated (1.61-fold) and *Eb* WRS7 (1.67-fold) inoculated wheat plants under stress. Also, the amounts of other enzymes such as glyceraldehyde 3-phosphate dehydrogenase (GAPDH), fructose-bisphosphate aldolase (FBA), Phosphoglycerate kinase (Table 5.2) also increased, which indicates a possible increased flux of carbohydrates to the TCA cycle [327]. This is further supported by the increase in pyruvate dehydrogenase E1 and E2 subunit and citrate synthase, which link the glycolysis pathway to the TCA cycle. These results indicate an increase in carbon metabolism, which would provide more energy for stress tolerance and suggest that bacterial inoculation improves stress tolerance by improving energy metabolism in plants [325, 327]. The increased energy production might have caused decreased carbohydrate synthesis, which reduces plant biomass under drought stress.

Protein synthesis/degradation-related proteins

The abundance of proteins involved in their synthesis and modification, such as molecular chaperones, ribosomal proteins, and heat shock proteins (HSPs), were altered significantly, which could benefit stress adaptation. In the present study, most ribosomal proteins increased significantly under drought. Accumulation of these proteins has also been reported in wheat, cucumber, and maize under stress [103, 328]. The role of HSPs in protein folding and maintaining protein homeostasis under drought stress has been widely discussed [329–331]. Besides, protein degradation-related proteins such as proteasomes, proteases, ubiquitin enzymes, and peptidases also increased in response to drought stress since these are important for removing abnormal and damaged proteins during stress [324]. The proteases, which help in protein modification and corrections under drought, were also accumulated in the current study. Hence, it can be assumed that regulation of the translational machinery is an important component of drought stress response in plants. These differential proteins and response mechanisms under stress are consistent with previous studies [103, 332–334].

Antioxidant-related proteins/ cell redox homeostasis

In plants, ROS overproduction during abiotic stress is responsible for oxidative stress-induced damage to macromolecules and plants' cellular structures [326]. Peroxidase (POD), along with superoxide dismutase (SOD), catalase (CAT), and glutathione peroxidase eliminate harmful free radicals under adverse conditions in a variety of crops. In our study, it was found that peroxidase and other antioxidant expressions were significantly increased in *Eb* WRS7-inoculated drought-stressed wheat plants. These results were also validated by biochemical and gene expression analysis described in Chapter 4. This demonstrated that bacteria-inoculated wheat plants accumulate more antioxidants that respond to drought stress more effectively to eliminate ROS.

Glutathione S-transferase (GST) is an essential component of the plant defense system in response to various abiotic stresses, protecting plants from oxidative damage [246, 317]. In this study, Glutathione S-transferase DHAR3 was upregulated in *Eb* WRS7 inoculated plants under drought stress but had no change in uninoculated plants. Priming of *P. fluorescens* also upregulated the GST expression in rice plants [317]. Similarly, upregulated GST was observed in wheat plants upon inoculation with *Enterobacter cloacae* SBP-8 under salt stress [103].

2-Cys peroxiredoxin, an antioxidant enzyme primarily crucial in the photosynthesizing leaf and developing shoot [103], was downregulated under drought stress. Lipocalin which prevents lipids peroxidation of thylakoidal membrane and confers protection against oxidative stress [335], was upregulated in *Eb* WRS7 inoculated plants. Therefore, we speculated that the combination of various antioxidants protects wheat plants from drought conditions and increases their tolerance.

Pyridoxal 5'-phosphate synthase was upregulated in uninoculated (1.76-fold) plants and bacteria inoculated (2.86-fold) under drought stress. Pyridoxal 5′-phosphate (PLP) is a quencher of singlet oxygen in plants that might protect cellular membranes from lipid peroxidation.

Osmotic homeostasis-related proteins

Osmotic regulation is crucial for drought tolerance in plants. Some important osmotic homeostasis-related proteins, such as dehydrin (DHN), late embryogenesis abundant (LEA) protein, delta-1-pyrroline-5-carboxylate synthase (P5CS), and betaine aldehyde dehydrogenase

(BADH), accumulated in wheat plant under drought stress. These proteins stabilize cellular components in response to water deficit conditions [116, 324]. In the present study, Late embryogenesis abundant protein, group 3 (UniPorT ID Q03968) was found in uninoculated and *Eb* WRS7-inoculated plants under drought stress only and was increased up to 1.95-fold in bacteria-inoculated plants. An increase in LEA protein under stress validates gene expression analysis of the gene encoding LEA protein described in our study (Chapter 4). Dehydrin COR410 and Betaine aldehyde dehydrogenase were also upregulated in both uninoculated (2.2-fold and 2.05-fold, respectively) and bacteria inoculated (2.6-fold and 2.66-fold, respectively) plants under drought stress. *B. licheniformis* K11-treated drought pepper also showed increased expression of dehydrin proteins [116]. BADH accumulation was observed in barley leaves under drought conditions [336, 337]. BADH mediates osmotic homeostasis by converting betaine aldehyde to glycine betaine, positively affecting plant adaptation to drought stress [324]. Delta-1-pyrroline-5-carboxylate synthase (P5CS) plays a key role in proline biosynthesis, leading to osmoregulation in plants. In the present study, P5CS protein was accumulated under drought-stressed plants, thereby enhancing the drought tolerance. Proline expression was also increased under drought stress in biochemical assays and gene expression studies (Chapter 4).

Cell wall and cytoskeleton-related proteins

Lignin is the major constituent of the cell wall, which not only participates in plant defense against fungi but also enhances the resistance to drought stress. Increased lignin content during drought stress helps maintain the normal osmotic pressure of the cells, thereby enhancing the drought tolerance of plants [326]. In the present study, proteins related to lignin biosynthesis, such as shikimate O-hydroxycinnamoyl transferase, 4-coumarate--CoA ligase, caffeic acid 3-O-methyltransferase and cinnamoyl-CoA reductase were found to be increased under drought in both uninoculated (1.58-fold) and *Eb* WRS7 inoculated (1.78-fold) wheat plants.

Another key enzyme, xyloglucan endotransglucosylase/hydrolase, strengthens the cell wall and maintains its integrity [326]. It was upregulated upon bacterial inoculation under stress, although non-significant (1.69-fold) and down-regulated under drought conditions (0.87-fold). This suggests that bacterial inoculation increases the ability of wheat plants to maintain better cell wall integrity under drought stress, thus maintaining a stable cellular environment. Also, it plays a major role in root elongation [326], suggesting a better root system in *Eb* WRS7 inoculated plants. It has been reported that overexpression of xyloglucan

endotransglucosylase/hydrolase increases drought tolerance in transgenic *A. thaliana* plants [338]. These results indicate that the cell wall synthesis is enhanced in *Eb* WRS7 inoculated wheat plants under drought stress, which may be associated with drought adaptation. In addition to proteins involved in cell wall strengthening, alteration in cytoskeletal protein was also observed. Profilin, a cytoskeleton protein, was also found to be increased upon drought stress in uninoculated and bacteria-inoculated plants. This protein binds to actin and affects the cytoskeleton structure, thereby protecting cellular integrity under salt stress [103]. Another cytoskeletal protein required for maintaining cell integrity- Tubulin- was also upregulated under stressed conditions. Increase in cytoskeleton proteins were also reported in earlier studies [103]

Transporters proteins

Plant membrane transport system plays an important role in drought stress adaptation [339]. ABC-G subfamily is an important transporter family among various ABC transporters during drought stress. It has a high affinity for the stress hormone abscisic acid (ABA). It exports ABA from the root xylem to leaf stomatal cells to reduce transpiration, thereby conferring drought tolerance [340, 341]. Interestingly, in our finding, uninoculated wheat plants under drought stress (0.87-fold) have no significant effect on ABCG transporter protein, but their abundance increases upon bacterial inoculation under normal and drought conditions (2.03- and 2.37-fold, respectively). This indicates the role of ABA in both biotic and abiotic stress. Besides its prominent role in plant response to abiotic stress, ABA is a crucial regulator in plant biotic defense responses [342]. Another member protein important to drought stress is aquaporin (AQP), which facilitates water movement across the cells. Among the known AQP subfamilies, members of tonoplast intrinsic protein (TIP) and plasma membrane intrinsic protein (PIP) showed the most significant expression under drought conditions [343]. In the current study, drought stress upregulated the expression of aquaporin PIP1-1 in uninoculated and bacteria-inoculated plants (2.29- and 2.55-fold, respectively). Upregulation of aquaporin under drought has been reported by many researchers across the plant kingdom [344, 345].

K^+ is an important element in plant growth and in water stress responses. K^+ uptake and efflux control cell water potential and turgor in osmotic regulation [346, 347]. Under the control of abscisic acid, K^+ transporter acts as an important element in osmotic adjustment by balancing potassium homeostasis in cell growth and drought stress responses [348]. Sheng *et al.* (2014) have reported that K^+ efflux antiporter (KEA) plays an important role in chloroplast

development and drought tolerance in rice [348]. K (+) efflux antiporter one was also found in the current study, and its abundance was increased in uninoculated and *Eb* WRS7 inoculated (2.15- and 2.65-fold, respectively) wheat plants under drought stress. The abundance of changes in these transport-related proteins under drought stress indicates that the ion/metabolite exchange is crucial for plants to survive in water-deficit conditions.

Phytohormone-related proteins

Abscisic acid (ABA) serves as an important signaling molecule for plants' adaptive response to drought stress [347, 348]. After drought stress, ABA enables plants to recover from water-deficit conditions by mediating stomatal closure, increasing hydraulic conductivity, and stimulating root cell elongation [349]. Changes in protein abundance support the elevated ABA biosynthesis in wheat under drought stress. Enzymes, zeaxanthin epoxidase (ZEP) and 9-cis-epoxy carotenoid dioxygenase (NCED), involved in ABA biosynthesis were found to be upregulated under drought stress in the current study as well as has been demonstrated in earlier studies also [350–353], which suggested that these enzymes act as important factors in core ABA biosynthesis. A high abundance of ABA biosynthesis enzymes also correlated with our gene expression studies, where the genes encoding enzymes involved in ABA synthesis were upregulated (Chapter 4).

Ethylene is an important signaling molecule critical in mediating plants' abiotic stress responses. In this research, the key enzyme 1-aminocyclopropane-1-carboxylate oxidase (ACO), which catalyzes the final step of ethylene biosynthesis, was increased in abundance in uninoculated plants (1.89-fold) but showed no significant change in abundance upon bacterial inoculation (1.09-fold) under drought. Another enzyme, S-adenosylmethionine synthetase (SAMS), involved in ethylene biosynthesis in plants [354], was upregulated under drought stress (2.14-fold), but *Eb* WRS7 inoculation had no impact on its abundances (1.02- fold). Usually, PGPR are known to decrease by degrading the precursor of ethylene, ACC, through their ACC deaminase activity. Interestingly, our study found a decrease in the expression of enzymes required for ethylene biosynthesis (chapter 4) supported by a decreased level of enzymes required for ethylene biosynthesis at the protein level. To the best of our knowledge, this is the first study that suggests that PGPR regulate ethylene biosynthesis in plants. However, the bacterial factor responsible for this regulation needs to be investigated. Also, the upregulation of SAMS under drought stress helps the plant to tolerate the drought stress as it is involved in the methylation of lignin monomer [85]. The upregulation of ethylene

biosynthesis-related proteins was also reported by Yan and the group in wheat under drought [355]. These findings suggest that *Eb* WRS7 inoculation might help the wheat plant to overcome the negative effect of drought by lowering the ethylene synthesis in the wheat plant.

Jasmonic acid (JA) has been associated with plant defense to biotic and abiotic stresses. Thus, several studies showed that JAs levels increased upon exposure to drought and salt stresses [352, 356]. Dong *et al.* (2007) reported that the application of methyl jasmonate (MeJA) to rice seedlings can moderately reduce the damage caused by drought stress [357]. In another study, Xu *et al.* (2019) reported that JA immediately accumulates under drought stress in foxtail millet seedlings, and the cell turgor pressure decreases quickly [64]. However, in this research, the key enzyme of JA biosynthesis, allene oxide synthase (AOS), was reduced under drought stress significantly in uninoculated (0.59-fold) but was upregulated upon *Eb* WRS7 inoculation under normal and drought stress (1.78- and 1.54- fold respectively). Enzyme Allene oxide cyclase, involved in the production of JA precursor-12-oxo-phytodienoic acid (OPDA)- was upregulated upon bacterial inoculation. This finding suggests that JA might participate in the mechanisms of plant defence against biotic stress (bacterial inoculation) but not water stress in wheat plants as it was not possible to determine transient accumulation of JA under drought, so further experiments are required to validate it. These results demonstrated that the phytohormone metabolic pathway contributes to stress-responsive processes.

Other proteins

In addition to the above-mentioned stress-related proteins and enzymes, some other important proteins also play a critical role in ameliorating drought stress. One such protein is glutamine synthetase (GS), which is considered a good indicator of drought stress [358, 359]. GS helps eliminate ammonia produced under unfavourable conditions. We observed enhanced accumulation (2.4-fold) of GS in the presence of drought stress. However, PGPR *Eb* WRS7 inoculation led to decreased abundance, which suggests that PGPR helps the wheat plant overcome drought's negative effects. Similarly, an abundance of proteins belonging to different metabolic pathways, including amino acid metabolism, polyamine metabolism, fatty acid metabolism, and nucleotide metabolism (Table 5.2), were also affected by drought. The changes in fatty acid/lipid composition may help maintain membrane integrity and prevent cellular compartments from damage under drought stress [343]. In addition, flavonoid biosynthesis related protein (chalcone synthase) involved in secondary metabolism was also upregulated in response to drought in uninoculated and *Eb* WRS7 inoculated plants. It has been

proposed that flavonoids have antioxidant capacity to protect plants against abiotic stress [343,360]. Our proteomic data correlates with the metabolomic analysis, which showed abundance of polyamines and flavonoids under stress (Chapter 4). DEAD-box ATP-dependent RNA helicase 38 was also found to be highly abundant under stress in uninoculated, and *Eb* WRS7 inoculated plants. They are critical for regulatingABA signalling and the drought stress response via inhibition of PP2CA activity [361].

To summarize, proteomic analysis revealed important proteins in adaptive mechanisms conferred by plant growth-promoting rhizobacteria *Eb* WRS7 in wheat to overcome drought stress. However, the precise functions of identified proteins and identification of key plant pathways under stress remain to be further elucidated. Besides, the role of differentially abundant proteins specific to bacterial inoculation must be investigated. Further work should also explore changes in post-translational modifications, such as phosphorylation, methylation, and acetylation, which significantly regulate cell signaling. Therefore, the future detection of protein modifications will provide new insights into the drought-tolerance mechanisms of wheat upon bacterial inoculation.

Summary

Although chemical fertilizers have greatly contributed to agriculture management under abiotic stress conditions, alternative fertilizers are needed for sustainable and eco-friendly agriculture. Plant Growth Promoting Rhizobacteria (PGPR) are promising plant growth promoters that are actively involved in plant growth and improvement through various mechanisms. These rhizobacteria colonize the plant roots and can benefit the host plant through nutrition acquisition, phytohormone production, biocontrol, and induced systemic tolerance (IST). IST refers to PGPR-induced interaction that leads to various physiological and biochemical changes that protect host plants from the deleterious effects of abiotic stresses. The PGPR-induced abiotic stress tolerance in plants is critically important in mitigating the negative impact of climate change, including drought, on crop production. Therefore, a better understanding of molecular crosstalk between these beneficial microorganisms and plants can be exploited to alter plant metabolism and provide resistance to abiotic stresses. Therefore, the present study aimed to characterize the efficient drought-tolerant bacteria from the rhizosphere of wheat plants growing in Rajasthan, India, and characterize their effect on plant growth under drought stress through functional studies following transcriptomic, proteomic, and metabolomic analysis. Throughout the study, the major achievements are as follows:

1. A total of nine drought-tolerant bacteria were isolated from wheat plants growing in the Shekhawati region of Rajasthan. Most of the bacterial isolates recovered in the present study exhibited ACC deaminase activity, production of indole acetic acid (IAA) and siderophore, solubilization of inorganic phosphate, fixation of atmospheric nitrogen, and HCN production based on qualitative and quantitative screening. These isolates were identified as a members of different bacterial genera, namely *Enterobacter, Pseudomonas, Kosakonia, Siccibacter, Acinetobacter,* and *Stenotrophomonas* based on partial sequence analysis of the 16S rRNA gene. The bacterial isolates were also subjected to biochemical assessment and substrate utilization tests. Their growth pattern under osmotic stress was also studied to test their osmotic tolerance. Further, to test the efficacy of bacterial isolates as biofertilizers, plant growth studies under drought stress conditions under laboratory conditions were conducted. Also, based on their PGP activities, different consortia were also formulated and tested to promote wheat plant growth under drought stress. Among the tested isolates and consortia, *Enterobacter bugandensis* WRS7 was found to be most effective for increasing the wheat plant's growth parameters and protecting the wheat plants from the deleterious effects of drought stress.

2. The stress tolerance mechanism of *Eb* WRS7 to mitigate osmotic stress was investigated by employing morphological, biochemical, and metabolic approaches. *Eb* WRS7 showed better growth and survival under osmotic stress conditions. Electron microscopy did not show significant morphological changes but showed vesicle-like structures in response to osmotic stress. In response to osmotic stress-induced oxidative stress, the bacteria modulate their membrane fatty acid composition, leading to changed membrane fluidity for their survival under osmotic stress. As an osmoadaptation mechanism, the accumulation of inorganic ions and organic osmolytes was observed. Higher concentrations of Na^+ and Ca^{2+} over K^+ under stress suggest the role of these ions in maintaining osmotic balance and activation of Ca^{2+} dependent osmotic stress signalling pathway in *Eb* WRS7. Activation of signaling cascade under stress conditions suggests its role in osmoadaptation through physiological and metabolic modulations. Metabolomics profiling showed metabolic capabilities such as the production of osmolytes, polyamines, 2, 3-butanediol, quaternary ammonium compounds, sugars, and higher accumulation of the glycolytic pathway, and TCA cycle metabolites, used for survival under drought/osmotic stress. Overall, metabolite fingerprint reveals the mechanisms adapted by PGPR and highlights the importance of stress-responsive metabolites and their metabolic pathways, which in the future may be targeted for the metabolic engineering of this PGPR for rhizosphere engineering.

3. Based on the experimental observations, *Eb* WRS7 was selected for biochemical and molecular studies to understand PGPR-assisted physiological changes and adaption mechanism in the host plant (wheat) under drought stress. *Eb* WRS7 protects plants from the adverse effects of drought stress by modulating host physiology and expression of stress-related genes and improves plant growth. The inoculation of *Eb* WRS7 stimulates the accumulation of osmolytes and enhances the level of antioxidative enzymes as compared to uninoculated plants. Further, the gene expression analysis suggests that *Eb* WRS7 differentially regulates the expression of stress-associated genes, including those required for the synthesis of trehalose and prolines (osmolytes), antioxidative enzymes, phytohormone biosynthesis, and Calcium transporter TPC1. To our knowledge, PGPR-mediated inhibition of ethylene biosynthesis by regulating the expression of *SAMS*, *ACS1*, and *ACO*, as well as modulation of the TPC1 transporter, is being reported for the first time in the present study. Moreover, the current study used a metabolomics approach to elucidate the tolerance mechanism of Eb WRS7-treated wheat plants against drought stress. Wheat plant metabolite study reveals that *Eb* WRS7 induces metabolic alterations that span a wide spectrum of metabolite classes, including organic acids, sugars, phytohormones, amino acids, and lipids. Finally, the colonization potential of *Eb* WRS7 was investigated. CFU

counting of bacteria recovered from bacteria-treated plants and identical ERIC profile of isolated bacteria to that of a pure culture of *Eb* WRS7 confirmed colonization of the bacteria in plant roots.

4. Differentially abundant proteins were analysed by a gel-free/ label-free proteomic analysis in wheat plant inoculated with Eb WRS7 to understand bacteria-mediated stress protection. Proteomic analysis reveals that drought stress affects the physiology of wheat plants as photosynthesis-related protein abundances decreased in heat plants under drought stress. In contrast, the abundance of stress- and defence-related proteins, osmoprotectant, and antioxidant proteins were increased. *Eb* WRS7 inoculation resulted in a significant metabolic modulation and affected the abundance of several proteins in wheat plants. *Eb* WRS7 also enhanced the tolerance of wheat exposed to drought stress by utilizing similar metabolic and molecular regulatory strategies. The success of *Eb* WRS7 in improving abiotic stress tolerance seems to be related to its ability to tune the expression of several proteins related to stress défense, photosynthesis as well as energy supply. *Eb* WRS7 also modulates several metabolic pathways of amino acids, increasing the accumulation of osmoprotectant like proline, dehydrin, hence governing osmotic homeostasis and strengthening of cell walls in bacteria-treated wheat plants. Therefore, using the proteomic approaches, the observed evidence supports that applying a beneficial PGPR to wheat plants could be used as an effective tool to overcome drought stress. This investigation confirmed that drought-tolerant PGPR *Eb* WRS7 can be exploited as a promising biofertilizer with multifarious properties.

The results of the present study indicate that bacteria that can tolerate osmotic stress and other PGP properties were successful in protecting the wheat plant by several approaches under abiotic stress, such as drought. The plant-protecting effect of bacterial strain was characterized by a physiological, biochemical, and molecular method of proteomic analysis. *Eb* WRS7 can be used as a biofertilizer candidate to promote plant growth in drought-stress conditions. These findings contribute to our understanding of PGPR-mediated drought tolerance in wheat plants and provide information to better understand the plant-microbe interaction under environmental stress.

Future Scope of work

Plant growth-promoting rhizobacteria (PGPR) enhance plant growth and productivity and stimulate abiotic stress tolerance in plants, therefore serving as promising biofertilizers for stress agriculture. In the present study, the ability of drought-tolerant bacteria to have various PGP characteristics, including ACC deaminase activity, has been tested under drought stress conditions on wheat plants. Therefore, few selected strains serve as effective and potential biofertilizers. These bacterial bioinoculants can be used as an alternative to chemical fertilizers and pesticides as agricultural supplements to mitigate the biotic and abiotic stress responses. The present work can be extended in future studies in the following aspects:

(i) Since the isolate used in the present study belongs to the genus *Enterobacter*, which encompasses several human pathogens, its biosafety and environmental considerations before mass application needs to be evaluated and scientifically validated.

(ii) Since vesicle-like structures in response to osmotic stress were observed in *Eb* WRS7 cells. Factors stimulating these vesicle generation and their specialized functions in PGPR and plant-microbe interaction have not been well studied. Therefore, specific experiments are required to know the exact function of these vesicle-like structures in future studies.

(iii) The role of VOCs can be explored regarding their direct role in the bacteria defense system and ameliorating abiotic stress in plants.

(iv) In the current study, ethylene biosynthesis genes in host plants that were regulated by PGPR were reported. Future studies can be conducted to identify bacterial factors affecting the expression of ethylene biosynthesis genes.

References

1. Clarke D, Hess TM, Haro-Monteagudo D, Semenov MA, Knox JW. Assessing future drought risks and wheat yield losses in England. *Agric For Meteorol*. 2021; 297:108248.

2. Hossain A, Skalicky M, Brestic M, Maitra S, Ashraful Alam M, Syed MA, *et al.* Consequences and mitigation strategies of abiotic stresses in wheat (*Triticum aestivum* L.) under the changing climate. *Agronomy*. 2021;11.

3. Ramadas S, Kumar TMK, Singh GP. Wheat Production in India: Trends and Prospects. In: Shah F, Khan Z, Iqbal A, Turan M, Olgun M, editors. Recent Advances in Grain Crops Research. *Rijeka: IntechOpen*; 2019.

4. Sharma, I., Tyagi, B. S., Singh, G., Venkatesh, K., & Gupta, O. P. Enhancing wheat production-A global perspective. *Indian J. Agric. Sci*, 2015; 85(1), 3-13.

5. Daloz AS, Rydsaa JH, Hodnebrog, Sillmann J, van Oort B, Mohr CW, *et al.* Direct and indirect impacts of climate change on wheat yield in the Indo-Gangetic plain in India. *J Agric Food Res*. 2021;4.

6. Khalid MF, Hussain S, Ahmad S, Ejaz S, Zakir I, Ali MA, *et al.* Impacts of abiotic stresses on growth and development of plants. *In: Plant tolerance to environmental stress. CRC Press*; 2019. p. 1–8.

7. Arora S, Jha PN. Impact of plant-associated microbial communities on host plants under abiotic stresses. *Microbial Interventions in Agriculture and Environment: Volume 2: Rhizosphere, Microbiome and Agro-ecology*, 2019; 303-340.

8. Sareen S, Budhlakoti N, Mishra KK, Bharad S, Potdukhe NR, Tyagi BS, *et al.* Resilience to terminal drought, heat, and their combination stress in wheat genotypes. *Agronomy*. 2023; 13:891.

9. Hashem A, Abd_Allah EF, Alqarawi AA, Al-Huqail AA, Wirth S, Egamberdieva D. The Interaction between arbuscular mycorrhizal fungi and endophytic bacteria enhances plant growth of *Acacia gerrardii* under salt stress. *Front Microbiol*. 2016;7.

10. Caverzan A, Casassola A, Brammer SP. Antioxidant responses of wheat plants under stress. *Genet Mol Biol*. 2016; 39:1–6.

11. de Vries FT, Griffiths RI, Knight CG, Nicolitch O, Williams A. Harnessing rhizosphere microbiomes for drought-resilient crop production. *Science*. 2020; 368:270–4.

12. Carlson R, Tugizimana F, Steenkamp PA, Dubery IA, Hassen AI, Labuschagne N. Rhizobacteria-induced systemic tolerance against drought stress in *Sorghum bicolor* (L.) Moench. *Microbiol Res*. 2020; 232:126388.

13. Rampino P, Pataleo S, Gerardi C, Mita G, Perrotta C. Drought stress response in wheat: Physiological and molecular analysis of resistant and sensitive genotypes. *Plant Cell Environ*. 2006; 29:2143–52.

14. Babele PK, Kudapa H, Singh Y, Varshney RK, Kumar A. Mainstreaming orphan millets for advancing climate smart agriculture to secure nutrition and health. *Front Plant Sci*. 2022;13.

15. Aslam MM, Farhat F, Siddiqui MA, Yasmeen S, Khan MT, Sial MA, *et al.* Exploration of physiological and biochemical processes of canola with exogenously applied fertilizers and plant growth regulators under drought stress. *PLoS One*. 2021;16: e0260960.

16. Basu A, Prasad P, Das SN, Kalam S, Sayyed RZ, Reddy MS, *et al.* Plant Growth Promoting Rhizobacteria (PGPR) as Green Bioinoculants: Recent Developments, Constraints, and Prospects. *Sustainability*. 2021;13.

17. Singh RP, Jha P, Jha PN. The plant-growth-promoting bacterium *Klebsiella* sp. SBP-8 confers induced systemic tolerance in wheat (*Triticum aestivum*) under salt stress. *J Plant Physiol*. 2015; 184:57–67.

18. Nezhadahmadi A, Prodhan ZH, Faruq G. Drought Tolerance in Wheat. *The Scientific World Journal*. 2013; 2013:610721.

19. Ahemad M, Kibret M. Mechanisms and applications of plant growth promoting rhizobacteria: Current perspective. *J King Saud Univ Sci*. 2014; 26:1–20.

20. Singh RP, Shelke GM, Kumar A, Jha PN. Biochemistry and genetics of ACC deaminase: a weapon to "stress ethylene" produced in plants. *Front Microbiol*. 2015; 6:937.

21. Ankati S, Podie AR. Understanding plant-beneficial microbe interactions for sustainable agriculture. *Journal of Spices and Aromatic Crops*. 2018; 27:93–105.

22. Bhattacharyya PN, Jha DK. Plant growth-promoting rhizobacteria (PGPR): emergence in agriculture. *World J Microbiol Biotechnol*. 2012; 28:1327–50.

23. Goswami D, Thakker JN, Dhandhukia PC. Portraying mechanics of plant growth promoting rhizobacteria (PGPR): A review. *Cogent Food Agric*. 2016; 2:1127500.

24. Vardharajula S, Zulfikar Ali S, Grover M, Reddy G, Bandi V. Drought-tolerant plant growth promoting *Bacillus sp*.: effect on growth, osmolytes, and antioxidant status of maize under drought stress. *J Plant Interact*. 2011; 6:1–14.

25. Wang C-J, Yang W, Wang C, Gu C, Niu D-D, Liu H-X, *et al.* Induction of drought tolerance in cucumber plants by a consortium of three plant growth-promoting rhizobacterium strains. *PLoS One*. 2012;7: e52565.

26. Sarma RK, Saikia R. Alleviation of drought stress in mung bean by strain *Pseudomonas aeruginosa* GGRJ21. *Plant Soil*. 2014; 377:111–26.

27. Rashid U, Yasmin H, Hassan MN, Naz R, Nosheen A, Sajjad M, *et al.* Drought-tolerant *Bacillus megaterium* isolated from semi-arid conditions induces systemic tolerance of wheat under drought conditions. *Plant Cell Rep*. 2021;1–21.

28. Gontia-Mishra I, Sapre S, Sharma A, Tiwari S. Amelioration of drought tolerance in wheat by the interaction of plant growth-promoting rhizobacteria. *Plant Biol*. 2016; 18:992–1000.

29. Khan N, Bano A. Exopolysaccharide producing rhizobacteria and their impact on growth and drought tolerance of wheat grown under rainfed conditions. *PLoS One*. 2019;14: e0222302.

30. Kaushal M, Wani SP. Plant-growth-promoting rhizobacteria: drought stress alleviators to ameliorate crop production in drylands. *Ann Microbiol*. 2016; 66:35–42.

31. Niu X, Song L, Xiao Y, Ge W. Drought-tolerant plant growth-promoting rhizobacteria associated with foxtail millet in a semi-arid agroecosystem and their potential in alleviating drought stress. *Front Microbiol*. 2018; 8:2580.

32. Pereira SIA, Abreu D, Moreira H, Vega A, Castro PML. Plant growth-promoting rhizobacteria (PGPR) improve the growth and nutrient use efficiency in maize (*Zea mays* L.) under water deficit conditions. *Heliyon.* 2020;6.

33. Li X, Sun P, Zhang Y, Jin C, Guan C. A novel PGPR strain *Kocuria rhizophila* Y1 enhances salt stress tolerance in maize by regulating phytohormone levels, nutrient acquisition, redox potential, ion homeostasis, photosynthetic capacity, and stress-responsive genes expression. *Environ Exp Bot*. 2020; 174:104023.

34. Jochum MD, McWilliams KL, Borrego EJ, Kolomiets M V, Niu G, Pierson EA, *et al.* Bioprospecting plant growth-promoting rhizobacteria that mitigate drought stress in grasses. *Front Microbiol*. 2019; 10:2106.

35. Gowtham HG, Singh B, Murali M, Shilpa N, Prasad M, Aiyaz M, *et al.* Induction of drought tolerance in tomato upon the application of ACC deaminase producing plant growth promoting rhizobacterium *Bacillus subtilis* Rhizo SF 48. *Microbiol Res*. 2020; 234:126422.

36. Chen L, Liu Y, Wu G, Veronican Njeri K, Shen Q, Zhang N, *et al.* Induced maize salt tolerance by rhizosphere inoculation of *Bacillus amyloliquefaciens* SQR9. *Physiol Plant*. 2016; 158:34–44.

37. Timmusk S, Abd El-Daim IA, Copolovici L, Tanilas T, Kännaste A, Behers L, *et al.* Drought-tolerance of wheat improved by rhizosphere bacteria from harsh environments: enhanced biomass production and reduced emissions of stress volatiles. *PLoS One*. 2014;9: e96086.

38. Naseem H, Bano A. Role of plant growth-promoting rhizobacteria and their exopolysaccharide in drought tolerance of maize. *J Plant Interact*. 2014; 9:689–701.

39. Ashraf M, Hasnain S, Berge O, Mahmood T. Inoculating wheat seedlings with exopolysaccharide-producing bacteria restricts sodium uptake and stimulates plant growth under salt stress. *Biol Fertil Soils*. 2004; 40:157–62.

40. Zhang H, Kim M-S, Sun Y, Dowd SE, Shi H, Paré PW. Soil bacteria confer plant salt tolerance by tissue-specific regulation of the sodium transporter HKT1. *Molecular Plant-Microbe Interactions*. 2008; 21:737–44.

41. Jha Y, Subramanian RB, Patel S. Combination of endophytic and rhizospheric plant growth promoting rhizobacteria in *Oryza sativa* shows higher accumulation of osmoprotectant against saline stress. *Acta Physiol Plant*. 2011; 33:797–802.

42. Nadeem SM, Zahir ZA, Naveed M, Nawaz S. Mitigation of salinity-induced negative impact on the growth and yield of wheat by plant growth-promoting rhizobacteria in naturally saline conditions. *Ann Microbiol*. 2013; 63:225–32.

43. Kim K, Jang Y-J, Lee S-M, Oh B-T, Chae J-C, Lee K-J. Alleviation of salt stress by *Enterobacter* sp. EJ01 in tomato and *Arabidopsis* is accompanied by up-regulation of conserved salinity responsive factors in plants. *Mol Cells*. 2014; 37:109.

44. Ali S, Charles TC, Glick BR. Amelioration of high salinity stress damage by plant growth-promoting bacterial endophytes that contain ACC deaminase. *Plant Physiology and Biochemistry*. 2014; 80:160–7.

45. Vaishnav A, Kumari S, Jain S, Varma A, Tuteja N, Choudhary DK. PGPR-mediated expression of salt tolerance gene in soybean through volatiles under sodium nitroprusside. *J Basic Microbiol*. 2016; 56:1274–88.

46. Abd El-Daim IA, Bejai S, Meijer J. Improved heat stress tolerance of wheat seedlings by bacterial seed treatment. *Plant Soil*. 2014; 379:337–50.

47. Chandra D, Sharma AK. Isolation and characterization of plant growth promoting bacteria containing ACC deaminase from soil collected from central Himalayan region of Uttarakhand, India. *Int J Curr Microbiol Appl Sci*. 2016; 5:436–45.

48. Glick BR, Todorovic B, Czarny J, Cheng Z, Duan J, McConkey B. Promotion of plant growth by bacterial ACC deaminase. *CRC Crit Rev Plant Sci*. 2007; 26:227–42.

49. Chatterjee P, Samaddar S, Anandham R, Kang Y, Kim K, Selvakumar G, *et al.* Beneficial soil bacterium *Pseudomonas frederiksbergensis* OS261 augments salt tolerance and promotes red pepper plant growth. *Front Plant Sci*. 2017; 8:705.

50. Choudhury AR, Choi J, Walitang DI, Trivedi P, Lee Y, Sa T. ACC deaminase, and indole acetic acid producing endophytic bacterial co-inoculation improves physiological traits of red pepper (*Capsicum annum* L.) under salt stress. *J Plant Physiol*. 2021; 267:153544.

51. Maxton A, Singh P, Masih SA. ACC deaminase-producing bacteria mediated drought and salt tolerance in *Capsicum annuum*. *J Plant Nutr*. 2018; 41:574–83.

52. Murali M, Singh SB, Gowtham HG, Shilpa N, Prasad M, Aiyaz M, *et al.* Induction of drought tolerance in *Pennisetum glaucum* by ACC deaminase producing PGPR-*Bacillus amyloliquefaciens* through Antioxidant defense system. *Microbiol Res*. 2021; 253:126891.

53. Ojuederie OB, Babalola OO. Growth enhancement and extenuation of drought stress in maize inoculated with multifaceted ACC deaminase producing rhizobacteria. *Front Sustain Food Syst*. 2023; 6:1076844.

54. Bhagat N, Raghav M, Dubey S, Bedi N. Bacterial exopolysaccharides: Insight into their role in plant abiotic stress tolerance. *J. Microbiol. Biotechnol*. 2021; 31(8): 1045-1059.

55. Sunita K, Mishra I, Mishra J, Prakash J, Arora NK. Secondary Metabolites from Halotolerant Plant Growth Promoting Rhizobacteria for Ameliorating Salinity Stress in Plants. *Front Microbiol*. 2020;11.

56. Kaushal M, Wani SP. Rhizobacterial-plant interactions: strategies ensuring plant growth promotion under drought and salinity stress. *Agric Ecosyst Environ*. 2016; 231:68–78.

57. Bashan Y, Holguin G, De-Bashan LE. Azospirillum-plant relationships: physiological, molecular, agricultural, and environmental advances (1997-2003). *Can J Microbiol*. 2004; 50:521–77.

58. Kaci Y, Heyraud A, Barakat M, Heulin T. Isolation, and identification of an EPS-producing Rhizobium strain from arid soil (Algeria): characterization of its EPS and the effect of inoculation on wheat rhizosphere soil structure. *Res Microbiol*. 2005; 156:522–31.

59. Ghosh D, Gupta A, Mohapatra S. A comparative analysis of exopolysaccharide and phytohormone secretions by four drought-tolerant rhizobacterial strains and their impact on osmotic-stress mitigation in *Arabidopsis thaliana*. *World J Microbiol Biotechnol*. 2019; 35:1–15.

60. Ryu C-M, Farag MA, Hu C-H, Reddy MS, Wei H-X, Paré PW, *et al.* Bacterial volatiles promote growth in *Arabidopsis*. *Proceedings of the National Academy of Sciences*. 2003; 100:4927–32.

61. Zhang H, Murzello C, Sun Y, Kim M-S, Xie X, Jeter RM, *et al.* Choline and osmotic-stress tolerance induced in *Arabidopsis* by the soil microbe *Bacillus subtilis* (GB03). *Molecular plant-microbe interactions*. 2010; 23:1097–104.

62. Cho SM, Kang BR, Han SH, Anderson AJ, Park J-Y, Lee Y-H, *et al.* 2R, 3R-butanediol, a bacterial volatile produced by *Pseudomonas chlororaphis* O6, is involved in induction of systemic tolerance to drought in *Arabidopsis thaliana*. *Molecular plant-microbe interactions*. 2008; 21:1067–75.

63. Cheng S, Jiang J-W, Tan L-T, Deng J-X, Liang P-Y, Su H, *et al.* Plant Growth-Promoting ability of mycorrhizal *Fusarium* Strain KB-3 enhanced by its IAA producing endohyphal bacterium, *Klebsiella aerogenes*. *Front Microbiol*. 2022; 13:855399.

64. Liu Y, Shi Z, Yao L, Yue H, Li H, Li C. Effect of IAA produced by *Klebsiella oxytoca* Rs-5 on cotton growth under salt stress. *J Gen Appl Microbiol*. 2013; 59:59–65.

65. Meliani A, Bensoltane A, Benidire L, Oufdou K. Plant growth-promotion and IAA secretion with *Pseudomonas fluorescens* and *Pseudomonas putida*. *Research & Reviews: Journal of Botanical Sciences*. 2017; 6:16–24.

66. Panigrahi S, Mohanty S, Rath CC. Characterization of endophytic bacteria *Enterobacter cloacae* MG00145 isolated from *Ocimum sanctum* with Indole Acetic Acid (IAA) production and plant growth promoting capabilities against selected crops. *South African Journal of Botany*. 2020; 134:17–26.

67. Sachdev DP, Chaudhari HG, Kasture VM, Dhavale DD, Chopade BA. Isolation and characterization of indole acetic acid (IAA) producing *Klebsiella pneumoniae* strains from rhizosphere of wheat (*Triticum aestivum*) and their effect on plant growth. *Indian journal of experimental biology*. 2009; 47: 993-1000.

68. Marulanda A, Barea J-M, Azcón R. Stimulation of plant growth and drought tolerance by native microorganisms (AM fungi and bacteria) from dry environments: mechanisms related to bacterial effectiveness. *J Plant Growth Regul*. 2009; 28:115–24.

69. Arzanesh MH, Alikhani HA, Khavazi K, Rahimian HA, Miransari M. Wheat (*Triticum aestivum* L.) growth enhancement by *Azospirillum* sp. under drought stress. *World J Microbiol Biotechnol*. 2011; 27:197–205.

70. Meena KK, Sorty AM, Bitla UM, Choudhary K, Gupta P, Pareek A, *et al.* Abiotic stress responses and microbe-mediated mitigation in plants: The omics strategies. *Frontiers in Plant Science*. 2017;8.

71. Sharma M, Sudheer S, Usmani Z, Rani R, Gupta P. Deciphering the Omics of Plant-Microbe Interaction: Perspectives and New Insights. *Curr Genomics*. 2020; 21:343–62.

72. Gamalero E, Bona E, Glick BR. Current Techniques to Study Beneficial Plant-Microbe Interactions. *Microorganisms*. 2022;10.

73. Zhang C, Li X, Yin L, Liu C, Zou H, Wu Z, *et al.* Analysis of the complete genome sequence of *Brevibacterium frigoritolerans* ZB201705 isolated from drought- and salt-stressed rhizosphere soil of maize. *Ann Microbiol*. 2019; 69:1489–96.

74. Singh RP, Nalwaya S, Jha PN. The draft genome sequence of the plant growth promoting rhizospheric bacterium *Enterobacter cloacae* SBP-8. *Genom Data*. 2017; 12:81–3.

75. Gupta A, Gopal M, Thomas G V, Manikandan V, Gajewski J, Thomas G, *et al.* Whole genome sequencing and analysis of plant growth promoting bacteria isolated from the rhizosphere of plantation crops coconut, cocoa and arecanut. *PLoS One*. 2014;9: e104259.

76. Aloo BN, Mbega ER, Makumba BA, Friedrich I, Hertel R, Daniel R. Whole-genome sequences of three plant growth-promoting rhizobacteria isolated from *solanum tuberosum* l. rhizosphere in Tanzania. *Microbiol Resour Announc*. 2020; 9:10–1128.

77. Noori F, Etesami H, Noori S, Forouzan E, Salehi Jouzani G, Malboobi MA. Whole genome sequence of *Pantoea agglomerans* ANP8, a salinity and drought stress–resistant bacterium isolated from alfalfa (*Medicago sativa* L.) root nodules. *Biotechnology Reports*. 2021;29: e00600.

78. Alavi P, Starcher MR, Zachow C, Müller H, Berg G. Root-microbe systems: The effect and mode of interaction of stress protecting agent (SPA) *Stenotrophomonas rhizophila* DSM14405T. *Front Plant Sci*. 2013; 141.

79. Mellidou I, Ainalidou A, Papadopoulou A, Leontidou K, Genitsaris S, Karagiannis E, *et al.* Comparative transcriptomics, and metabolomics reveal an intricate priming mechanism involved in PGPR-mediated salt tolerance in tomato. *Front Plant Sci*. 2021; 12:713984.

80. Morcillo RJL, Vílchez JI, Zhang S, Kaushal R, He D, Zi H, *et al.* Plant Transcriptome Reprograming and Bacterial Extracellular Metabolites Underlying Tomato Drought Resistance Triggered by a Beneficial Soil Bacteria. *Metabolites*. 2021;11.

81. Akbar A, Han B, Khan AH, Feng C, Ullah A, Khan AS, *et al.* A transcriptomic study reveals salt stress alleviation in cotton plants upon salt tolerant PGPR inoculation. *Environ Exp Bot*. 2022; 200:104928.

82. Barnawal D, Bharti N, Pandey SS, Pandey A, Chanotiya CS, Kalra A. Plant growth-promoting rhizobacteria enhance wheat salt and drought stress tolerance by altering endogenous phytohormone levels and *TaCTR1/TaDREB2* expression. *Physiol Plant*. 2017; 161:502–14.

83. SkZ A, Vardharajula S, Vurukonda SSKP. Transcriptomic profiling of maize (*Zea mays* L.) seedlings in response to *Pseudomonas putida* stain FBKV2 inoculation under drought stress. *Ann Microbiol*. 2018; 68:331–49.

84. Kosová K, Vítámvás P, Prášil IT, Renaut J. Plant proteome changes under abiotic stress - Contribution of proteomics studies to understanding plant stress response. *Journal of Proteomics*. 2011; 74:1301–22.

85. Kosová K, Vítámvás P, Urban MO, Prášil IT, Renaut J. Plant abiotic stress proteomics: The major factors determining alterations in cellular proteome. *Frontiers in Plant Science*. 2018;9.

86. Kosová K, Vítámvás P, Skuhrovec J, Vítámvás J, Planchon S, Renaut J, *et al.* Proteomic responses of two spring wheat cultivars to the combined water deficit and aphid (*Metopolophium dirhodum*) treatments. *Front Plant Sci*. 2022;13.

87. Ahmad P, Abdel Latef AAH, Rasool S, Akram NA, Ashraf M, Gucel S. Role of proteomics in crop stress tolerance. *Frontiers in Plant Science*. 2016; 1336.

88. Komatsu S, Kamal AHM, Hossain Z. Wheat proteomics: Proteome modulation and abiotic stress acclimation. *Frontiers in Plant Science*. 2014; 5:684.

89. Imam J, Shukla P, Mandal NP, Variar M. Microbial Interactions in Plants: Perspectives and Applications of Proteomics. *Curr Protein Pept Sci*. 2017;18.

90. Jayaraman D, Forshey KL, Grimsrud PA, Ané JM. Leveraging proteomics to understand plant-microbe interactions. *Frontiers in Plant Science*. 2012; 3:44.

91. Ángeles Castillejo M, Maldonado AM, Ogueta S, Jorrín J V. Proteomic analysis of responses to drought stress in sunflower (*Helianthus annuus*) leaves by 2DE gel electrophoresis and mass spectrometry. *The Open Proteomics Journal*. 2008;1(1). 2008.

92. Cramer GR, Van Sluyter SC, Hopper DW, Pascovici D, Keighley T, Haynes PA. Proteomic analysis indicates massive changes in metabolism prior to the inhibition of growth and photosynthesis of grapevine (*Vitis vinifera* L.) in response to water deficit. *BMC Plant Biol*. 2013; 13:49.

93. Mirzaei M, Soltani N, Sarhadi E, Pascovici D, Keighley T, Salekdeh GH, *et al.* Shotgun proteomic analysis of long-distance drought signaling in rice roots. *J Proteome Res*. 2012; 11:348–58.

94. Mohammadi PP, Moieni A, Komatsu S. Comparative proteome analysis of drought-sensitive and drought-tolerant rapeseed roots and their hybrid F1 line under drought stress. *Amino Acids*. 2012; 43:2137–52.

95. Alvarez S, Roy Choudhury S, Pandey S. Comparative quantitative proteomics analysis of the ABA response of roots of drought-sensitive and drought-tolerant wheat varieties identifies proteomic signatures of drought adaptability. *J Proteome Res*. 2014; 13:1688–701.

96. Budak H, Akpinar BA, Unver T, Turktas M. Proteome changes in wild and modern wheat leaves upon drought stress by two-dimensional electrophoresis and nanoLC-ESI–MS/MS. *Plant Mol Biol*. 2013;83:89–103.

97. Caruso G, Cavaliere C, Foglia P, Gubbiotti R, Samperi R, Laganà A. Analysis of drought responsive proteins in wheat (*Triticum durum*) by 2D-PAGE and MALDI-TOF mass spectrometry. *Plant Science*. 2009; 177:570–6.

98. Jiang S-S, Liang X-N, Li X, Wang S-L, Lv D-W, Ma C-Y, *et al.* Wheat drought-responsive grain proteome analysis by linear and nonlinear 2-DE and MALDI-TOF mass spectrometry. *Int J Mol Sci*. 2012; 13:16065–83.

99. Kamal AHM, Cho K, Choi J-S, Jin Y, Park C-S, Lee JS, *et al.* Patterns of protein expression in water-stressed wheat chloroplasts. *Biol Plant*. 2013; 57:305–12.

100. Vaseva II, Grigorova BS, Simova-Stoilova LP, Demirevska KN, Feller U. Abscisic acid and late embryogenesis abundant protein profile changes in winter wheat under progressive drought stress. *Plant Biol*. 2010; 12:698–707.

101. Qin Y, Druzhinina IS, Pan X, Yuan Z. Microbially mediated plant salt tolerance and microbiome-based solutions for saline agriculture. *Biotechnol Adv*. 2016; 34:1245–59.

102. Banaei-Asl F, Bandehagh A, Uliaei ED, Farajzadeh D, Sakata K, Mustafa G, *et al.* Proteomic analysis of canola root inoculated with bacteria under salt stress. *J Proteomics*. 2015; 124:88–111.

103. Singh RP, Runthala A, Khan S, Jha PN. Quantitative proteomics analysis reveals the tolerance of wheat to salt stress in response to *Enterobacter cloacae* SBP-8. *PLoS One*. 2017;12.

104. Yadav R, Chakraborty S, Ramakrishna W. Wheat grain proteomic and protein–metabolite interactions analyses provide insights into plant growth promoting bacteria–arbuscular mycorrhizal fungi–wheat interactions. *Plant Cell Rep*. 2022; 41:1417–37.

105. Lade SB, Román C, Cueto-Ginzo AI, Serrano L, Sin E, Achón MA, *et al.* Host-specific proteomic and growth analysis of maize and tomato seedlings inoculated with *Azospirillum brasilense* Sp7. *Plant Physiology and Biochemistry*. 2018; 129:381–93.

106. Naher UA, Panhwar QA, Othman R, Shamshuddin J, Ismail MR, Zhou E. Proteomic study on growth promotion of PGPR inoculated aerobic rice (*Oryza sativa* L.) cultivar MR219-9. *Pak J Bot*. 2018; 50:1843–52.

107. Leandro MR, Rangel PL, dos Santos TC, Andrade LF, de Souza Vespoli L, Rangel ALS, *et al.* Colonization of *Arabidopsis thaliana* by *Herbaspirillum seropedicae* promotes its growth and changes its proteomic profile. *Plant Soil*. 2019; 443:429–47.

108. Witzel K, Üstün S, Schreiner M, Grosch R, Börnke F, Ruppel S. A proteomic approach suggests unbalanced proteasome functioning induced by the growth-promoting bacterium *Kosakonia radicincitans* in *Arabidopsis*. *Front Plant Sci*. 2017; 8:661.

109. Bandyopadhyay P, Yadav BG, Kumar SG, Kumar R, Kogel K-H, Kumar S. *Piriformospora indica* and *Azotobacter chroococcum* consortium facilitates higher acquisition of N, P with improved carbon allocation and enhanced plant growth in *Oryza sativa*. *Journal of Fungi*. 2022; 8:453.

110. Nunes R de O, Domiciano Abrahao G, de Sousa Alves W, Aparecida de Oliveira J, Cesar Sousa Nogueira F, Pasqualoto Canellas L, *et al.* Quantitative proteomic analysis reveals altered enzyme expression profile in *Zea mays* roots during the early stages of colonization by *Herbaspirillum seropedicae. Proteomics*. 2021; 21:2000129.

111. Nguyen THN, Brechenmacher L, Aldrich JT, Clauss TR, Gritsenko MA, Hixson KK, *et al.* Quantitative phosphoproteomic analysis of soybean root hairs inoculated with *Bradyrhizobium japonicum. Molecular & cellular proteomics*. 2012; 11:1140–55.

112. Kim JS, Lee JE, Nie H, Lee YJ, Kim ST, Kim S-H. Physiological and proteomic analysis of plant growth enhancement by the rhizobacteria *Bacillus* sp. JS. *Genes Genomics*. 2018; 40:129–36.

113. Dhawi F. Plant growth promoting Rhizobacteria (PGPR) regulated Phyto and microbial beneficial protein interactions. *Open Life Sci*. 2020; 15:68–78.

114. Abd El-Daim IA, Bejai S, Meijer J. *Bacillus velezensis* 5113 induced metabolic and molecular reprogramming during abiotic stress tolerance in wheat. *Sci Rep*. 2019; 9:16282.

115. Cheng Z, Woody OZ, McConkey BJ, Glick BR. Combined effects of the plant growth-promoting bacterium *Pseudomonas putida* UW4 and salinity stress on the *Brassica napus* proteome. *Applied Soil Ecology*. 2012; 61:255–63.

116. Lim J-H, Kim S-D. Induction of drought stress resistance by multi-functional PGPR *Bacillus licheniformis* K11 in pepper. *Plant Pathol J*. 2013; 29:201.

117. Wang X-H, Wang Q, Nie Z-W, He L-Y, Sheng X-F. *Ralstonia eutropha* Q2-8 reduces wheat plant above-ground tissue cadmium and arsenic uptake and increases the expression of the plant root cell wall organization and biosynthesis-related proteins. *Environmental Pollution*. 2018; 242:1488–99.

118. Kalozoumis P, Savvas D, Aliferis K, Ntatsi G, Marakis G, Simou E, *et al.* Impact of plant growth-promoting rhizobacteria inoculation and grafting on tolerance of tomato to combined water and nutrient stress assessed via metabolomics analysis. *Front Plant Sci*. 2021; 12:670236.

119. Yadav AN. Agriculturally important microbiomes: biodiversity and multifarious PGP attributes for amelioration of diverse abiotic stresses in crops for sustainable agriculture. *Biomed J Sci Tech Res*. 2017; 1:861–4.

120. Bhargava P, Khan M, Verma A, Singh A, Singh S, Vats S, *et al.* Metagenomics as a tool to explore new insights from plant-microbe interface. *Plant microbe interface*. 2019;271–89.

121. Xu L, Dong Z, Chiniquy D, Pierroz G, Deng S, Gao C, *et al.* Genome-resolved metagenomics reveals role of iron metabolism in drought-induced rhizosphere microbiome dynamics. *Nat Commun*. 2021; 12:3209.

122. No JH, Nishu S Das, Hong J-K, Lyou ES, Kim MS, Wee GN, *et al.* Raman-deuterium isotope probing, and metagenomics reveal the drought tolerance of the soil microbiome and its promotion of plant growth. *mSystems*. 2022;7: e01249-21.

123. Methe BA, Li K, Talley SP, Gupta N, Frank B, Xu W, *et al.* Functional genes that distinguish Maize phyllosphere metagenomes in drought and well-watered conditions. *BioRxiv.* 2017;104331.

124. Abdul Rahman NSN, Abdul Hamid NW, Nadarajah K. Effects of Abiotic Stress on Soil Microbiome. *Int J Mol Sci*. 2021;22.

125. Bray EA. Responses to abiotic stresses. *Biochemistry and molecular biology of plants*. 2000;1158–203.

126. Zhang X, Obringer R, Wei C, Chen N, Niyogi D. Droughts in India from 1981 to 2013 and implications to wheat production. *Sci Rep*. 2017; 7:44552.

127. Marček T, Hamow KA, Végh B, Janda T, Darko E. Metabolic response to drought in six winter wheat genotypes. *PLoS One*. 2019;14: e212411.

128. Ghosh D, Gupta A, Mohapatra S. A comparative analysis of exopolysaccharide and phytohormone secretions by four drought-tolerant rhizobacterial strains and their impact on osmotic-stress mitigation in *Arabidopsis thaliana*. *World J Microbiol Biotechnol*. 2019; 35:90.

129. Busse MD, Bottomley PJ. Growth and nodulation responses of *Rhizobium meliloti* to water stress induced by permeating and nonpermeating solutes. *Appl Environ Microbiol*. 1989; 55:2431–6.

130. K ZD, Pat L, Beth HN, Zhengyu F, Daniel K, Phyllis H, *et al.* Isolation and Characterization of Endophytic Colonizing Bacteria from Agronomic Crops and Prairie Plants. *Appl Environ Microbiol*. 2002; 68:2198–208.

131. Tamura K, Stecher G, Peterson D, Filipski A, Kumar S. MEGA6: molecular evolutionary genetics analysis version 6.0. *Mol Biol Evol*. 2013; 30:2725–9.

132. Harley JP, Prescott LM. Laboratory Exercises in Microbiology 5th Edition the McGraw-Hill Companies. 2002.

133. Kasana RC, Salwan R, Dhar H, Dutt S, Gulati A. A rapid and easy method for the detection of microbial cellulases on agar plates using Gram's iodine. *Curr Microbiol*. 2008; 57:503–7.

134. Reinhold-Hurek B, Hurek T, Gillis M, Hoste B, Vancanneyt M, Kersters K, *et al. Azoarcus* gen. nov., nitrogen-fixing proteobacteria associated with roots of Kallar grass (*Leptochloa fusca* (L.) Kunth), and

description of two species, *Azoarcus indigens* sp. nov. and *Azoarcus communis* sp. nov. *Int J Syst Evol Microbiol*. 1993; 43:574–84.

135. Mehta S, Nautiyal CS. An efficient method for qualitative screening of phosphate-solubilizing bacteria. *Curr Microbiol*. 2001; 43:51–6.

136. Ames BN. [10] Assay of inorganic phosphate, total phosphate and phosphatases. In: Methods in enzymology. Elsevier; 1966. p. 115–8.

137. Gordon SA, Weber RP. Colorimetric estimation of indoleacetic acid. *Plant Physiol*. 1951; 26:192.

138. Gang S, Sharma S, Saraf M, Buck M, Schumacher J. Analysis of indole-3-acetic acid (IAA) production in *Klebsiella* by LC-MS/MS and the Salkowski method. *Bio Protoc*. 2019;9: e3230–e3230.

139. Louden BC, Haarmann D, Lynne AM. Use of blue agar CAS assay for siderophore detection. *J Microbiol Biol Educ*. 2011; 12:51–3.

140. Schwyn B, Neilands JB. Universal chemical assay for the detection and determination of siderophores. *Anal Biochem*. 1987; 160:47–56.

141. Penrose DM, Glick BR. Methods for isolating and characterizing ACC deaminase-containing plant growth-promoting rhizobacteria. *Physiol Plant*. 2003; 118:10–5.

142. Tapia-Hernández A, Bustillos-Cristales MR, Jiménez-Salgado T, Caballero-Mellado J, Fuentes-Ramirez LE. Natural endophytic occurrence of *Acetobacter diazotrophicus* in pineapple plants. *Microb Ecol*. 2000; 39:49–55.

143. Rokhbakhsh-Zamin F, Sachdev D, Kazemi-Pour N, Engineer A, Pardesi KR, Zinjarde S, *et al.* Characterization of plant-growth-promoting traits of *Acinetobacter* species isolated from rhizosphere of *Pennisetum glaucum*. *J Microbiol Biotechnol*. 2011; 21:556–66.

144. Dye DW. The inadequacy of the usual determinative tests for the identification of *Xanthomonas sp. N.Z. Jl Sci.* 1962;5.

145. Abd El-Rahman AF, Shaheen HA. Biological control of the brown rot of potato, *Ralstonia solanacearum* and effect of bacterization with antagonists on promotion of potato growth. *Egyptian J Biol Pest Control*. 2016; 26:733–9.

146. Bindel Connelly M, Young GM, Sloma A. Extracellular proteolytic activity plays a central role in swarming motility in *Bacillus subtilis*. *J Bacteriol*. 2004; 186:4159–67.

147. Duxbury AC, Yentsch CS. Plankton pigment nomographs. *J Mar Res.* 1956; 15(1).

148. Vaishnav A, Choudhary DK. Regulation of drought-responsive gene expression in *Glycine max* l. Merrill is mediated through *Pseudomonas simiae* strain AU. *J Plant Growth Regul*. 2019; 38:333–42.

149. Lugojan C, Ciulca S. Evaluation of relative water content in winter wheat. *J. hortic. for.* 2011; 15:173–7.

150. Egamberdieva D, Wirth S, Bellingrath-Kimura SD, Mishra J, Arora NK. Salt-tolerant plant growth promoting rhizobacteria for enhancing crop productivity of saline soils. *Front Microbiol*. 2019; 10:2791.

151. Chandra P, Wunnava A, Verma P, Chandra A, Sharma R K. Strategies to mitigate the adverse effect of drought stress on crop plants—influences of soil bacteria: A review. *Pedosphere*. 2021; 31:496–509.

152. Sayahi N, Djemal R, Ben Merdes K, Saidii MN, Yengui M, Gdoura R, *et al.* Characterization of *Siccibacter* sp. Strain C2 a novel rhizobacterium that enhances tolerance of barley to salt stress. *Curr Microbiol*. 2022; 79:239.

153. González Espinosa J, Hernández Gómez YF, Javier Martínez Y, Flores Gallardo FJ, Pacheco Aguilar JR, Ramos López MÁ, *et al. Kosakonia cowanii* Ch1 isolated from Mexican chili powder reveals growth inhibition of phytopathogenic fungi. *Microorganisms*. 2023; 11:1758.

154. Gontia-Mishra I, Sapre S, Kachare S, Tiwari S. Molecular diversity of 1-aminocyclopropane-1-carboxylate (ACC) deaminase producing PGPR from wheat (*Triticum aestivum* L.) rhizosphere. *Plant Soil*. 2017; 414:213–27.

155. Singh RP, Jha PN. The PGPR *Stenotrophomonas maltophilia* SBP-9 augments resistance against biotic and abiotic stress in wheat plants. *Front Microbiol*. 2017; 8:1945.

156. Ojuederie OB, Babalola OO. Growth enhancement and extenuation of drought stress in maize inoculated with multifaceted ACC deaminase producing rhizobacteria. *Front Sustain Food Syst*. 2023; 6:1076844.

157. Wang T, Wang S, Tang X, Fan X, Yang S, Yao L, *et al.* Isolation of urease-producing bacteria and their effects on reducing Cd and Pb accumulation in lettuce (*Lactuca sativa* L.). *Environ. Sci. Pollut. Res*. 2020; 27:8707–18.

158. Narayanan M, Pugazhendhi A, David S, Chi NTL, Nasif O, Alharbi SA, *et al.* Influence of *Kosakonia* sp. on the growth of *Arachis hypogaea* L. on arid soil. *Agronomy*. 2022; 12:1801.

159. Reetha S, Bhuvaneswari G, Thamizhiniyan P, Mycin TR. Isolation of indole acetic acid (IAA) producing rhizobacteria of *Pseudomonas fluorescens* and *Bacillus subtilis* and enhance growth of onion (*Allim cepa* L.). *Int J Curr Microbiol Appl Sci*. 2014; 3:568–74.

160. Shahzad SM, Arif MS, Riaz M, Iqbal Z, Ashraf M. PGPR with varied ACC-deaminase activity induced different growth and yield response in maize (*Zea mays* L.) under fertilized conditions. *Eur J Soil Biol*. 2013; 57:27–34.

161. Panigrahi S, Rath CC. Condition optimization for phosphate solubilization by *Kosakonia cowanii* MK834804, an endophytic bacterium isolated from *Aegle marmelos*. *Int J Curr Microbiol App Sci*. 2019; 8:2823–35.

162. Kiprotich K, Muoma J, Omayio DO, Ndombi TS, Wekesa C. Molecular characterization and mineralizing potential of phosphorus solubilizing bacteria colonizing common bean (*Phaseolus vulgaris* L.) rhizosphere in western Kenya. *Int J Microbiol*. 2023;2023.

163. Martin F, Winspear MJ, MacFarlane JD, Oaks A. Effect of methionine sulfoximine on the accumulation of ammonia in C3 and C4 leaves: the relationship between NH3 accumulation and photorespiratory activity. *Plant Physiol*. 1983; 71:177–81.

164. Lugtenberg B, Kamilova F. Plant-growth-promoting rhizobacteria. *Annu Rev Microbiol*. 2009; 63:541–56.

165. Sinha AK, Parli B V. Siderophore production by bacteria isolated from mangrove sediments: a microcosm study. *J Exp Mar Biol Ecol*. 2020; 524:151290.

166. Sivasakthi S, Usharani G, Saranraj Pjaj. Biocontrol potentiality of plant growth promoting bacteria (PGPR)-*Pseudomonas fluorescens* and *Bacillus subtilis*: A review. *Afr J Agric Res*. 2014; 9:1265–77.

167. Dorjey S, Dolkar D, Sharma R. Plant growth promoting rhizobacteria *Pseudomonas*: a review. *Int J Curr Microbiol App Sci*. 2017; 6:1335–44.

168. Karthikeyan B, Joe MM, Islam MR, Sa T. ACC deaminase containing diazotrophic endophytic bacteria ameliorate salt stress in *Catharanthus roseus* through reduced ethylene levels and induction of antioxidative defense systems. *Symbiosis*. 2012; 56:77–86.

169. Jha CK, Annapurna K, Saraf M. Isolation of rhizobacteria from *Jatropha curcas* and characterization of produced ACC deaminase. *J Basic Microbiol*. 2012; 52:285–95.

170. Ordentlich A, Elad Y, Chet I. The role of chitinase of *Serratia marcescens* in biocontrol of *Sclerotium rolfsii*. *Phytopathology*. 1988; 78:84–8.

171. Singh RK, Singh P, Guo D-J, Sharma A, Li D-P, Li X, *et al.* Root-derived endophytic diazotrophic bacteria *Pantoea cypripedii* AF1 and *Kosakonia arachidis* EF1 promote nitrogen assimilation and growth in sugarcane. *Front Microbiol*. 2021; 12:774707.

172. Saxena P, Chakdar H, Singh A, Shirodkar S, Srivastava AK. Microbial diversity of *Azadirachta indica* (Neem) gum: An unexplored niche. *J Appl Biol Biotechnol*. 2023; 11:209–19.

173. Lugtenberg BJJ, Dekkers L, Bloemberg G V. Molecular determinants of rhizosphere colonization by *Pseudomonas*. *Annu Rev Phytopathol*. 2001; 39:461–90.

174. Burrows LL. *Pseudomonas aeruginosa* twitching motility: type IV pili in action. *Annu Rev Microbiol*. 2012; 66:493–520.

175. O'Toole GA, Kolter R. Initiation of biofilm formation in *Pseudomonas fluorescens* WCS365 proceeds via multiple, convergent signalling pathways: a genetic analysis. *Mol Microbiol*. 1998; 28:449–61.

176. Noman A, Ali Q, Maqsood J, Iqbal N, Javed MT, Rasool N, *et al.* Deciphering physio-biochemical, yield, and nutritional quality attributes of water-stressed radish (*Raphanus sativus* L.) plants grown from Zn-Lys primed seeds. *Chemosphere*. 2018; 195:175–89.

177. Ansari FA, Jabeen M, Ahmad I. *Pseudomonas azotoformans* FAP5, a novel biofilm-forming PGPR strain, alleviates drought stress in wheat plant. *Int J Environ Sci Technol*. 2021; 18:3855–70.

178. Martins SJ, Rocha GA, de Melo HC, de Castro Georg R, Ulhôa CJ, de Campos Dianese É, *et al.* Plant-associated bacteria mitigate drought stress in soybean. *Environ. Sci. Pollut. Res*. 2018; 25:13676–86.

179. Murali M, Singh SB, Gowtham HG, Shilpa N, Prasad M, Aiyaz M, *et al.* Induction of drought tolerance in *Pennisetum glaucum* by ACC deaminase producing PGPR-*Bacillus amyloliquefaciens* through Antioxidant defense system. *Microbiol Res*. 2021; 253:126891.

180. Abbasi S, Kafi SA, Karimi E, Sadeghi A. *Streptomyces* consortium improved quality attributes of bell pepper fruits, induced plant defense priming, and changed microbial communities of rhizosphere under commercial greenhouse conditions. *Rhizosphere*. 2022; 23:100570.

181. Samain E, Ernenwein C, Aussenac T, Selim S. Effective and durable systemic wheat-induced resistance by a plant-growth-promoting rhizobacteria consortium of *Paenibacillus* sp. strain B2 and *Arthrobacter* sp. strain AA against *Zymoseptoria tritici* and drought stress. *Physiol Mol Plant Pathol*. 2022; 119:101830.

182. Babele PK, Kudapa H, Singh Y, Varshney RK, Kumar A. Mainstreaming orphan millets for advancing climate smart agriculture to secure nutrition and health. *Front Plant Sci*. 2022; 0:2806.

183. Gupta A, Rico-Medina A, Caño-Delgado AI. The physiology of plant responses to drought. *Science*. 2020; 368:266–9.

184. De Vries FT, Griffiths RI, Knight CG, Nicolitch O, Williams A. Harnessing rhizosphere microbiomes for drought-resilient crop production. *Science*. 2020; 368:270–4.

185. Hartman K, Tringe SG. Interactions between plants and soil shaping the root microbiome under abiotic stress. *Biochemical Journal*. 2019; 476:2705–24.

186. Williams A, de Vries FT. Plant root exudation under drought: implications for ecosystem functioning. *New Phytologist*. 2019; C.

187. Chai YN, Schachtman DP. Root exudates impact plant performance under abiotic stress. *Trends Plant Sci.* 2022; 27:80–91.

188. Korenblum E, Dong Y, Szymanski J, Panda S, Jozwiak A, Massalha H, *et al.* Rhizosphere microbiome mediates systemic root metabolite exudation by root-to-root signaling. *Proc Natl Acad Sci U S A*. 2020; 117:3874–83.

189. Ngumbi E, Kloepper J. Bacterial-mediated drought tolerance: current and future prospects. *Applied Soil Ecology*. 2016 Sep 1; 105:109-25.

190. Jeon JS, Rybka D, Carreno-Quintero N, De Vos R, Raaijmakers JM, Etalo DW. Metabolic signatures of rhizobacteria-induced plant growth promotion. *Plant, Cell & Environment*. 2022 Oct;45(10):3086-99.

191. Ahkami AH, Allen White R, Handakumbura PP, Jansson C. Rhizosphere engineering: Enhancing sustainable plant ecosystem productivity. *Rhizosphere*. 2017; 3:233–43.

192. Ke J, Wang B, Yoshikuni Y. Microbiome Engineering: Synthetic Biology of Plant-Associated Microbiomes in Sustainable Agriculture. *Trends Biotechnol*. 2021; 39:244–61.

193. Paul D. Osmotic stress adaptations in rhizobacteria. *J Basic Microbiol*. 2013; 53:101–10.

194. Yoon Y, Lee H, Lee S, Kim S, Choi KH. Membrane fluidity-related adaptive response mechanisms of foodborne bacterial pathogens under environmental stresses. *Food Research International*. 2015; 72:25–36.

195. Zhang H, Sun X, Dai M. Improving crop drought resistance with plant growth regulators and rhizobacteria: Mechanisms, applications, and perspectives. *Plant Commun*. 2022;3.

196. Fernie AR, Schauer N. Metabolomics-assisted breeding: a viable option for crop improvement? *Trends in genetics*. 2009; 25:39–48.

197. Bueno PCP, Lopes NP. Metabolomics to characterize adaptive and signaling responses in legume crops under abiotic stresses. *ACS Omega*. 2020; 5:1752–63.

198. Magerand R, Rey P, Blanchard L, de Groot A. Redox signaling through zinc activates the radiation response in *Deinococcus* bacteria. *Sci Rep*. 2021; 11:4528.

199. Tu J, Zhao Q, Wei L, Yang Q. Heavy metal concentration and speciation of seven representative municipal sludges from wastewater treatment plants in Northeast China. *Environ Monit Assess*. 2012; 184:1645–55.

200. Górka B, Wieczorek PP. Simultaneous determination of nine phytohormones in seaweed and algae extracts by HPLC-PDA. *Journal of Chromatography B*. 2017; 1057:32–9.

201. Sandhya V, Ali SkZ, Venkateswarlu B, Reddy G, Grover M. Effect of osmotic stress on plant growth promoting *Pseudomonas* sp. *Arch Microbiol*. 2010;192:867–76.

202. DuBois Michel, Gilles KA, Hamilton JK, Rebers PA, Smith Fred. Colorimetric Method for Determination of Sugars and Related Substances. *Anal Chem*. 1956; 28:350–6.

203. Bradford MM. A rapid and sensitive method for the quantitation of microgram quantities of protein utilizing the principle of protein-dye binding. *Anal Biochem*. 1976; 72:248–54.

204. Bates LS, Waldren RP, Teare ID. Rapid determination of free proline for water-stress studies. *Plant Soil*. 1973; 39:205–7.

205. Singh RP, Jha PN. Analysis of fatty acid composition of PGPR *Klebsiella* sp. SBP-8 and its role in ameliorating salt stress in wheat. *Symbiosis*. 2017; 73:213–22.

206. Kumar M, Mishra S, Dixit V, Kumar M, Agarwal L, Chauhan PS, *et al.* Synergistic effect of *Pseudomonas putida* and *Bacillus amyloliquefaciens* ameliorates drought stress in chickpea (*Cicer arietinum* L.). *Plant Signal Behav*. 2016;11: e1071004.

207. Caruana JC, Walper SA. Bacterial Membrane Vesicles as Mediators of Microbe – Microbe and Microbe – Host Community Interactions. *Front Microbiol*. 2020;11.

208. Potter M, Hanson C, Anderson AJ, Vargis E, Britt DW. Abiotic stressors impact outer membrane vesicle composition in a beneficial rhizobacterium: Raman spectroscopy characterization. *Sci Rep*. 2020; 10:21289.

209. McMillan HM, Zebell SG, Ristaino JB, Dong X, Kuehn MJ. Protective plant immune responses are elicited by bacterial outer membrane vesicles. *Cell Rep*. 2021;34.

210. Schwechheimer C, Kuehn MJ. Outer-membrane vesicles from Gram-negative bacteria: biogenesis and functions. *Nature Reviews Microbiology*. 2015; 13:605–19.

211. Pagnout C, Razafitianamaharavo A, Sohm B, Caillet C, Beaussart A, Delatour E, *et al.* Osmotic stress and vesiculation as key mechanisms controlling bacterial sensitivity and resistance to TiO2 nanoparticles. *Communications Biology*. 2021; 4:1–15.

212. Babele PK, Singh G, Singh A, Kumar A, Tyagi MB, Sinha RP. UV-B radiation and temperature stress-induced alterations in metabolic events and defense mechanisms in a bloom-forming cyanobacterium *Microcystis aeruginosa*. Acta Physiol Plant. 2017;39.

213. Hong R, Kang TY, Michels CA, Gadura N. Membrane lipid peroxidation in copper alloy-mediated contact killing of *Escherichia coli. Appl Environ Microbiol*. 2012; 78:1776–84.

214. Babele PK, Kumar J, Chaturvedi V. Proteomic De-regulation in cyanobacteria in response to abiotic stresses. *Front Microbiol*. 2019;10 JUN.

215. Sleator RD, Hill C. Bacterial osmoadaptation: the role of osmolytes in bacterial stress and virulence. *FEMS Microbiol Rev*. 2002; 26:49–71.

216. Wood JM. Bacterial responses to osmotic challenges. *Journal of General Physiology*. 2015; 145:381–8.

217. Shabala S, Shabala L. Ion transport and osmotic adjustment in plants and bacteria. *Biomol Concepts.* 2011; 2:407–19.

218. Szatmári D, Sárkány P, Kocsis B, Nagy T, Miseta A, Barkó S, *et al.* Intracellular ion concentrations and cation-dependent remodelling of bacterial MreB assemblies. *Scientific Reports* 2020 10:1. 2020;10:1–13.

219. Stephan AB, Kunz HH, Yang E, Schroeder JI. Rapid hyperosmotic-induced Ca^{2+} responses in *Arabidopsis thaliana* exhibit sensory potentiation and involvement of plastidial KEA transporters. *Proc Natl Acad Sci U S A.* 2016;113: E5242–9.

220. Dominguez DC. Calcium signalling in bacteria. *Mol Microbiol*. 2004; 54:291–7.

221. Gupta S, Seth R, Sharma A. Plant growth-promoting rhizobacteria play a role as phytostimulators for sustainable agriculture. *Plant-microbe interaction: an approach to sustainable agriculture*. 2016;475–93.

222. Bottini R, Cassán F, Piccoli P. Gibberellin production by bacteria and its involvement in plant growth promotion and yield increase. *Appl Microbiol Biotechnol*. 2004; 65:497–503.

223. Bhatt RM, Selvakumar G, Upreti KK, Boregowda PC. Effect of biopriming with *Enterobacter* strains on seed germination and seedling growth of tomato (*Solanum lycopersicum* L.) under osmotic stress. *Proceedings of the National Academy of Sciences, India Section B: Biological Sciences.* 2015; 85:63–9.

224. Rahman NSNA, Hamid NWA, Nadarajah K. Effects of abiotic stress on soil microbiome. *International Journal of Molecular Sciences*. 2021; 22: 9036.

225. Sunita K, Mishra I, Mishra J, Prakash J, Arora NK. Secondary metabolites from halotolerant plant growth promoting rhizobacteria for ameliorating salinity stress in plants. *Front Microbiol*. 2020; 11:2619.

226. Chwastek G, Surma MA, Rizk S, Grosser D, Lavrynenko O, Rucińska M, *et al.* Principles of membrane adaptation revealed through environmentally induced bacterial lipidome remodelling. *Cell Rep*. 2020; 32:108165.

227. Willdigg JR, Helmann JD. Mini Review: Bacterial membrane composition and its modulation in response to stress. *Front Mol Biosci*. 2021;8.

228. Gong X, Yu H, Chen J, Han B. Cell surface properties of *Lactobacillus salivarius* under osmotic stress. *European Food Research and Technology*. 2012; 4:671–8.

229. Shabala L, Ross T. Cyclopropane fatty acids improve *Escherichia coli* survival in acidified minimal media by reducing membrane permeability to H^+ and enhanced ability to extrude H^+. *Res Microbiol.* 2008; 159:458–61.

230. Karlinsey JE, Fung AM, Johnston N, Goldfine H, Libby SJ, Fang FC. Cyclopropane fatty acids are important for *Salmonella enterica* serovar typhimurium virulence. *Infect Immun*. 2022,90.

231. Guillot A, Obis D, Mistou MY. Fatty acid membrane composition and activation of glycine-betaine transport in Lactococcus lactis subjected to osmotic stress. *Int J Food Microbiol*. 2000; 55:47–51.

232. Rajaeian S, Ehsanpour AA, Javadi M, Shojaee B. Ethanolamine induced modification in glycine betaine and proline metabolism in *Nicotiana rustica* under salt stress. *Biol Plant*. 2017; 61:797–800.

233. Akhova A V., Tkachenko AG. Multifaceted role of polyamines in bacterial adaptation to antibiotic-mediated oxidative stress. *The Microbiological Society of Korea*. 2020; 56:103–10.

234. Yi HS, Ahn YR, Song GC, Ghim SY, Lee S, Lee G, *et al.* Impact of a Bacterial Volatile 2,3-Butanediol on *Bacillus subtilis* Rhizosphere Robustness. *Front Microbiol*. 2016;7 JUN.

235. Kong HG, Shin TS, Kim TH, Ryu CM. Stereoisomers of the bacterial volatile compound 2,3-butanediol differently elicit systemic defense responses of pepper against multiple viruses in the field. *Front Plant Sci*. 2018; 9:90.

236. Ghosh D, Gupta A, Mohapatra S. A comparative analysis of exopolysaccharide and phytohormone secretions by four drought-tolerant rhizobacterial strains and their impact on osmotic-stress mitigation in *Arabidopsis thaliana*. *World J Microbiol Biotechnol*. 2019; 35:1–15.

237. Morcillo RJL, Vílchez JI, Zhang S, Kaushal R, He D, Zi H, *et al.* Plant transcriptome reprograming and bacterial extracellular metabolites underlying tomato drought resistance triggered by a beneficial soil bacteria. *Metabolites*. 2021; 11:369.

238. Zhang Y, Mao B, Tang X, Liu X, Zhao J, Zhang H, *et al.* Integrative genome and metabolome analysis reveal the potential mechanism of osmotic stress tolerance in *Bifidobacterium bifidum*. *LWT.* 2022; 159:113199.

239. Joghee NN, Jayaraman G. Metabolomic characterization of halophilic bacterial isolates reveals strains synthesizing rare diaminoacids under salt stress. *Biochimie*. 2014; 102:102–11.

240. Wang M, Zhao S, Wang L, Chen S, Li S, Lei X, *et al.* Salt stress-induced changes in microbial community structures and metabolic processes result in increased soil cadmium availability. *Science of The Total Environment.* 2021; 782:147125.

241. Feehily C, Karatzas KAG. Role of glutamate metabolism in bacterial responses towards acid and other stresses. *J Appl Microbiol*. 2013; 114:11–24.

242. Wang X, Li Q, Xie J, Huang M, Cai J, Zhou Q, *et al.* Abscisic acid and jasmonic acid are involved in drought priming-induced tolerance to drought in wheat. *Crop J*. 2021; 9:120–32.

243. Ahmad P, Jamsheed S, Hameed A, Rasool S, Sharma I, Azooz MM, *et al.* Drought stress induced oxidative damage and antioxidants in plants. *In: Oxidative damage to plants. Elsevier*; 2014. p. 345–67.

244. Lephatsi MM, Meyer V, Piater LA, Dubery IA, Tugizimana F. Plant responses to abiotic stresses and rhizobacterial biostimulants: Metabolomics and epigenetics perspectives. *Metabolites.* 2021; 11:457.

245. Nephali L, Moodley V, Piater L, Steenkamp P, Buthelezi N, Dubery I, *et al.* A metabolomic landscape of maize plants treated with a microbial biostimulant under well-watered and drought conditions. *Front Plant Sci*. 2021; 12:676632.

246. Lucini L, Colla G, Moreno MBM, Bernardo L, Cardarelli M, Terzi V, *et al.* Inoculation of *Rhizoglomus irregulare* or *Trichoderma atroviride* differentially modulates metabolite profiling of wheat root exudates. *Phytochemistry*. 2019; 157:158–67.

247. Zhao Y, Zhang F, Mickan B, Wang D, Wang W. Physiological, proteomic, and metabolomic analysis provide insights into Bacillus sp.-mediated salt tolerance in wheat. *Plant Cell Rep*. 2022;1–24.

248. Vílchez JI, Niehaus K, Dowling DN, González-López J, Manzanera M. Protection of pepper plants from drought by *Microbacterium* sp. 3J1 by modulation of the plant's glutamine and α-ketoglutarate content: A comparative metabolomics approach. *Front Microbiol*. 2018;9 FEB.

249. Irigoyen JJ, Einerich DW, Sánchez-Díaz M. Water stress induced changes in concentrations of proline and total soluble sugars in nodulated alfalfa (*Medicago sativa*) plants. *Physiol Plant*. 1992; 84:55–60.

250. Hodges DM, DeLong JM, Forney CF, Prange RK. Improving the thiobarbituric acid-reactive-substances assay for estimating lipid peroxidation in plant tissues containing anthocyanin and other interfering compounds. *Planta*. 1999; 207:604–11.

251. Aebi H. [13] Catalase in vitro. *In: Methods in enzymology. Elsevier*; 1984. p. 121–6.

252. Giannopolitis CN, Ries SK. Superoxide dismutases: II. Purification and quantitative relationship with water-soluble protein in seedlings. *Plant Physiol*. 1977; 59:315–8.

253. White EJ, Venter M, Hiten NF, Burger JT. Modified cetyltrimethylammonium bromide method improves robustness and versatility: the benchmark for plant RNA extraction. *Wiley Online Li*brary; 2008.

254. Livak KJ, Schmittgen TD. Analysis of relative gene expression data using real-time quantitative PCR and the $2^{-\Delta\Delta CT}$ method. *Methods*. 2001; 25:402–8.

255. Dudziak K, Zapalska M, Börner A, Szczerba H, Kowalczyk K, Nowak M. Analysis of wheat gene expression related to the oxidative stress response and signal transduction under short-term osmotic stress. *Sci Rep*. 2019; 9:2743.

256. Simons M, Van Der Bij AJ, Brand I, De Weger LA, Wijffelman CA, Lugtenberg BJ. Gnotobiotic system for studying rhizosphere colonization by plant growth-promoting *Pseudomonas* bacteria. *Mol Plant Microbe Interact.* 1996; 9:600–7.

257. Choi W-G, Toyota M, Kim S-H, Hilleary R, Gilroy S. Salt stress-induced Ca^{2+} waves are associated with rapid, long-distance root-to-shoot signaling in plants. *Proceedings of the National Academy of Sciences*. 2014; 111:6497–502.

258. Larisch N, Kirsch SA, Schambony A, Studtrucker T, Böckmann RA, Dietrich P. The function of the two-pore channel TPC1 depends on dimerization of its carboxy-terminal helix. *Cellular and Molecular Life Sciences*. 2016; 73:2565–81.

259. Moreira H, Pereira SIA, Marques APGC, Rangel AOSS, Castro PML. Effects of soil sterilization and metal spiking in plant growth promoting rhizobacteria selection for phytotechnology purposes. *Geoderma*. 2019; 334:72–81.

260. Zhu J-K. Salt and drought stress signal transduction in plants. *Annu Rev Plant Biol*. 2002; 53:247–73.

261. Estrada-Melo AC, Chao C, Reid MS, Jiang C-Z. Overexpression of an ABA biosynthesis gene using a stress-inducible promoter enhances drought resistance in petunia. *Hortic Res*. 2015;2.

262. Blatt MR. Cellular signaling and volume control in stomatal movements in plants. *Annu Rev Cell Dev Biol.* 2000; 16:221–41.

263. Cohen AC, Bottini R, Pontin M, Berli FJ, Moreno D, Boccanlandro H, *et al. Azospirillum brasilense* ameliorates the response of *Arabidopsis thaliana* to drought mainly via enhancement of ABA levels. *Physiol Plant*. 2015; 153:79–90.

264. Cheng L, Wang Y, He Q, Li H, Zhang X, Zhang F. Comparative proteomics illustrates the complexity of drought resistance mechanisms in two wheat (*Triticum aestivum* L.) cultivars under dehydration and rehydration. *BMC Plant Biol*. 2016;16.

265. Abeles FB, Morgan PW, Saltveit Jr ME, Aertsen A, Braitenberg V, JE A, *et al.* Booklist No. 112. *FEBS Lett*. 1993.

266. Lin Z, Zhong S, Grierson D. Recent advances in ethylene research. *J Exp Bot*. 2009; 60:3311–36.

267. Wang KL-C, Li H, Ecker JR. Ethylene biosynthesis and signaling networks. *Plant Cell*. 2002;14 suppl_1: S131–51.

268. Kaur G, Asthir B. Proline: a key player in plant abiotic stress tolerance. *Biol Plant*. 2015; 59:609–19.

269. Sadak MS. Physiological role of trehalose on enhancing salinity tolerance of wheat plant. *Bull Natl Res Cent.* 2019; 43:1–10.

270. Ghosh D, Sen S, Mohapatra S. Modulation of proline metabolic gene expression in *Arabidopsis thaliana* under water-stressed conditions by a drought-mitigating *Pseudomonas putida* strain. *Ann Microbiol*. 2017; 67:655–68.

271. Kerepesi I, Galiba G. Osmotic and salt stress-induced alteration in soluble carbohydrate content in wheat seedlings. *Crop Sci*. 2000; 40:482–7.

272. Kohler J, Hernández JA, Caravaca F, Roldán A. Plant-growth-promoting rhizobacteria and arbuscular mycorrhizal fungi modify alleviation biochemical mechanisms in water-stressed plants. *Functional Plant Biology*. 2008; 35:141–51.

273. Fernandez O, Vandesteene L, Feil R, Baillieul F, Lunn JE, Clément C. Trehalose metabolism is activated upon chilling in grapevine and might participate in *Burkholderia phytofirmans* induced chilling tolerance. *Planta*. 2012; 236:355–69.

274. Kosová K, Holková L, Prášil IT, Prášilová P, Bradáčová M, Vítámvás P, *et al.* Expression of dehydrin 5 during the development of frost tolerance in barley (*Hordeum vulgare*). *J Plant Physiol*. 2008; 165:1142–51.

275. Mehrabad Pour-Benab S, Fabriki-Ourang S, Mehrabi A-A. Expression of dehydrin and antioxidant genes and enzymatic antioxidant defense under drought stress in wild relatives of wheat. *Biotechnology & Biotechnological Equipment*. 2019; 33:1063–73.

276. Xiong L, Schumaker KS, Zhu J-K. Cell signaling during cold, drought, and salt stress. *Plant Cell*. 2002;14 suppl_1: S165–83.

277. Battaglia M, Covarrubias AA. Late Embryogenesis Abundant (LEA) proteins in legumes. *Front Plant Sci*. 2013; 4:190.

278. Fahad S, Bajwa AA, Nazir U, Anjum SA, Farooq A, Zohaib A, *et al.* Crop production under drought and heat stress: plant responses and management options. *Front Plant Sci*. 2017;1147.

279. Cruz de Carvalho MH. Drought stress and reactive oxygen species: production, scavenging and signaling. *Plant Signal Behav*. 2008; 3:156–65.

280. Xun F, Xie B, Liu S, Guo C. Effect of plant growth-promoting bacteria (PGPR) and arbuscular mycorrhizal fungi (AMF) inoculation on oats in saline-alkali soil contaminated by petroleum to enhance phytoremediation. *Environmental Science and Pollution Research*. 2015; 22:598–608.

281. Pandey GK, Sanyal SK, Pandey GK, Sanyal SK. Plant ion channels without molecular identity and Two-Pore Channel 1. *Functional Dissection of Calcium Homeostasis and Transport Machinery in Plants*. 2021;43–52.

282. Hanin M, Ebel C, Ngom M, Laplaze L, Masmoudi K. New insights on plant salt tolerance mechanisms and their potential use for breeding. *Front Plant Sci*. 2016; 7:1787.

283. Wang Y-J, Yu J-N, Chen T, Zhang Z-G, Hao Y-J, Zhang J-S, *et al.* Functional analysis of a putative Ca^{2+} channel gene TaTPC1 from wheat. *J Exp Bot*. 2005; 56:3051–60.

284. Liu J, Niu Y, Zhang J, Zhou Y, Ma Z, Huang X. Ca^{2+} channels and Ca^{2+} signals involved in abiotic stress responses in plant cells: Recent advances. *Plant Cell, Tissue and Organ Culture (PCTOC)*. 2018; 132:413–24.

285. Zhang Y, Mao B, Tang X, Liu X, Zhao J, Zhang H, *et al.* Integrative genome and metabolome analysis reveal the potential mechanism of osmotic stress tolerance in *Bifidobacterium bifidum*. *LWT*. 2022; 159:113199.

286. Hildebrandt TM, Nesi AN, Araújo WL, Braun H-P. Amino acid catabolism in plants. *Mol Plant*. 2015; 8:1563–79.

287. Parthasarathy A, Cross PJ, Dobson RCJ, Adams LE, Savka MA, Hudson AO. A three-ring circus: metabolism of the three proteogenic aromatic amino acids and their role in the health of plants and animals. *Front Mol Biosci*. 2018; 5:29.

288. Mareya CR, Tugizimana F, Piater LA, Madala NE, Steenkamp PA, Dubery IA. Untargeted metabolomics reveal defensome-related metabolic reprogramming in *Sorghum bicolor* against infection by *Burkholderia andropogonis*. *Metabolites*. 2019; 9:8.

289. Ivanov BN. Role of ascorbic acid in photosynthesis. *Biochemistry (Moscow)*. 2014; 79:282–9.

290. Akram NA, Shafiq F, Ashraf M. Ascorbic acid-a potential oxidant scavenger and its role in plant development and abiotic stress tolerance. *Front Plant Sci*. 2017;613.

291. Ahmed A, Hasnain S. Auxins as one of the factors of plant growth improvement by plant growth promoting rhizobacteria. *Pol J Microbiol*. 2014; 63:261.

292. Suguiyama VF, Silva EA, Meirelles ST, Centeno DC, Braga MR. Leaf metabolite profile of the Brazilian resurrection plant *Barbacenia purpurea* Hook. (Velloziaceae) shows two time-dependent responses during desiccation and recovering. *Front Plant Sci*. 2014; 5:96.

293. Rzepka A, Rut G, Krupa J. Effect of abiotic stress factors on fluctuations in contents of malate and citrate and on malic enzyme activity in moss gametophores. *Photosynthetica*. 2009; 47:141–5.

294. Wang H, Tang X, Wang H, Shao H-B. Proline accumulation and metabolism-related genes expression profiles in *Kosteletzkya virginica* seedlings under salt stress. *Front Plant Sci*. 2015; 6:792.

295. Kavi Kishor PB, Hima Kumari P, Sunita MSL, Sreenivasulu N. Role of proline in cell wall synthesis and plant development and its implications in plant ontogeny. *Front Plant Sci*. 2015; 6:544.

296. Gharibi S, Tabatabaei BES, Saeidi G, Talebi M, Matkowski A. The effect of drought stress on polyphenolic compounds and expression of flavonoid biosynthesis related genes in *Achillea pachycephala. Rech. f. Phytochemistry*. 2019; 162:90–8.

297. Zhu M, Assmann SM. Metabolic signatures in response to abscisic acid (ABA) treatment in *Brassica napus* guard cells revealed by metabolomics. *Sci Rep*. 2017; 7(1): 12875.

298. Pál M, Ivanovska B, Oláh T, Tajti J, Hamow KÁ, Szalai G, *et al.* Role of polyamines in plant growth regulation of Rht wheat mutants. *Plant physiology and biochemistry*. 2019; 137:189–202.

299. Agurla S, Gayatri G, Raghavendra AS. Polyamines increase nitric oxide and reactive oxygen species in guard cells of *Arabidopsis thaliana* during stomatal closure. *Protoplasm*. 2018; 255:153–62.

300. Ghosh R, Barman S, Mukherjee R, Mandal NC. Role of phosphate solubilizing *Burkholderia* sp. for successful colonization and growth promotion of *Lycopodium cernuum* L. (Lycopodiaceae) in lateritic belt of Birbhum district of West Bengal, India. *Microbiol Res*. 2016; 183:80–91.

301. Li W, Raoult D, Fournier P-E. Bacterial strain typing in the genomic era. *FEMS Microbiol Rev*. 2009; 33:892–916.

302. Gupta G, Panwar J, Jha PN. Natural occurrence of *Pseudomonas aeruginosa*, a dominant cultivable diazotrophic endophytic bacterium colonizing *Pennisetum glaucum* (L.) R. Br. *Applied Soil Ecology*. 2013; 64:252–61.

303. Ramirez D, Giron M (2022) Enterobacter Infections (Jan 2023). [Updated 2022 Jun 27]. In: StatPearls [Internet]. Treasure Island (FL): StatPearls Publishing.

304. Pati NB, Doijad SP, Schultze T, Mannala GK, Yao Y, Jaiswal S, *et al. Enterobacter bugandensis*: a novel enterobacterial species associated with severe clinical infection. *Sci Rep*. 2018; 8:5392.

305. Ghatak A, Chaturvedi P, Weckwerth W. Cereal crop proteomics: Systemic analysis of crop drought stress responses towards marker-assisted selection breeding. *Frontiers in Plant Science*. 2017;8.

306. Liu H, Sultan MARF, Liu XL, Zhang J, Yu F, Zhao HX. Physiological and comparative proteomic analysis reveals different drought responses in roots and leaves of drought-tolerant wild wheat (*Triticum boeoticum*). *PLoS One*. 2015;10.

307. Zhao Y, Zhang F, Mickan B, Wang D, Wang W. Physiological, proteomic, and metabolomic analysis provide insights into *Bacillus* sp.-mediated salt tolerance in wheat. *Plant Cell Rep*. 2022; 41:95–118.

308. Halder T, Choudhary M, Liu H, Chen Y, Yan G, Siddique KHM. Wheat proteomics for abiotic stress tolerance and root system architecture: current status and future prospects. *Proteomes*. 2022;10.

309. Li L, Xu Y, Ren Y, Guo Z, Li J, Tong Y, *et al.* Comparative proteomic analysis provides insights into the regulatory mechanisms of wheat primary root growth. *Sci Rep*. 2019;9.

310. Mathesius U. Comparative proteomic studies of root–microbe interactions. *J Proteomics*. 2009; 72:353–66.

311. Kandasamy S, Loganathan K, Muthuraj R, Duraisamy S, Seetharaman S, Thiruvengadam R, *et al.* Understanding the molecular basis of plant growth promotional effect of *Pseudomonas fluorescens* on rice through protein profiling. *Proteome Sci*. 2009;7.

312. Oskuei BK, Bandehagh A, Sarikhani MR, Komatsu S. Protein profiles underlying the effect of plant growth-promoting rhizobacteria on canola under osmotic stress. *J Plant Growth Regul*. 2018; 37:560–74.

313. Ashburner M, Ball CA, Blake JA, Botstein D, Butler H, Cherry JM, *et al.* Gene ontology: tool for the unification of biology. *Nat Genet*. 2000; 25:25–9.

314. Hajheidari M, Abdollahian-Noghabi M, Askari H, Heidari M, Sadeghian SY, Ober ES, *et al.* Proteome analysis of sugar beet leaves under drought stress. *Proteomics*. 2005; 5:950–60.

315. Zadražnik T, Moen A, Šuštar-Vozlič J. Chloroplast proteins involved in drought stress response in selected cultivars of common bean (*Phaseolus vulgaris* L.). 3 Biotech. 2019; 9:1–15.

316. Demirevska K, Simova-Stoilova L, Vassileva V, Feller U. Rubisco and some chaperone protein responses to water stress and rewatering at early seedling growth of drought sensitive and tolerant wheat varieties. *Plant Growth Regul*. 2008; 56:97–106.

317. Kandasamy S, Loganathan K, Muthuraj R, Duraisamy S, Seetharaman S, Thiruvengadam R, *et al.* Understanding the molecular basis of plant growth promotional effect of *Pseudomonas fluorescens* on rice through protein profiling. *Proteome Sci*. 2009; 7:47.

318. Lu C, Zhang J. Effects of water stress on photosystem II photochemistry and its thermostability in wheat plants. *J Exp Bot*. 1999; 50:1199–206.

319. Xu X, Ji J, Ma X, Xu Q, Qi X, Chen X. Comparative proteomic analysis provides insight into the key proteins involved in cucumber (*Cucumis sativus* L.) adventitious root emergence under waterlogging stress. *Front Plant Sci*. 2016;7.

320. Wang L, Wei J, Shi X, Qian W, Mehmood J, Yin Y, *et al.* Identification of the light-harvesting chlorophyll a/b binding protein gene family in peach (*Prunus persica* L.) and their expression under drought stress. *Genes (Basel)*. 2023; 14:1475.

321. Lehtimäki N, Lintala M, Allahverdiyeva Y, Aro E-M, Mulo P. Drought stress-induced upregulation of components involved in ferredoxin-dependent cyclic electron transfer. *J Plant Physiol*. 2010; 167:1018–22.

322. Yang H, Liu J, Wen X, Lu C. Molecular mechanism of photosystem I assembly in oxygenic organisms. *Biochimica et Biophysica Acta (BBA)-Bioenergetics*. 2015; 1847:838–48.

323. Cornic G, Massacci A. Leaf photosynthesis under drought stress. *In: Photosynthesis and the Environment. Springer*; 1996. p. 347–66.

324. Wang X, Cai X, Xu C, Wang Q, Dai S. Drought-responsive mechanisms in plant leaves revealed by proteomics. *Int J Mol Sci*. 2016; 17:1706.

325. Pan J, Li Z, Wang Q, Garrell AK, Liu M, Guan Y, *et al.* Comparative proteomic investigation of drought responses in foxtail millet. *BMC Plant Biol*. 2018; 18:1–19.

326. Zeng W, Peng Y, Zhao X, Wu B, Chen F, Ren B, *et al.* Comparative proteomics analysis of the seedling root response of drought-sensitive and drought-tolerant maize varieties to drought stress. *Int J Mol Sci*. 2019; 20:2793.

327. Li W, Wei Z, Qiao Z, Wu Z, Cheng L, Wang Y. Proteomics analysis of alfalfa response to heat stress. *PLoS One*. 2013;8: e82725.

328. Du C-X, Fan H-F, Guo S-R, Tezuka T, Li J. Proteomic analysis of cucumber seedling roots subjected to salt stress. *Phytochemistry*. 2010; 71:1450–9.

329. Timperio AM, Egidi MG, Zolla L. Proteomics applied on plant abiotic stresses: role of heat shock proteins (HSP). *J Proteomics*. 2008; 71:391–411.

330. Swindell WR, Huebner M, Weber AP. Transcriptional profiling of *Arabidopsis* heat shock proteins and transcription factors reveals extensive overlap between heat and non-heat stress response pathways. *BMC Genomics*. 2007; 8:1–15.

331. Masand S, Yadav SK. Overexpression of MuHSP70 gene from *Macrotyloma uniflorum* confers multiple abiotic stress tolerance in transgenic *Arabidopsis thaliana*. *Mol Biol Rep*. 2016; 43:53–64.

332. Pang Q, Chen S, Dai S, Chen Y, Wang Y, Yan X. Comparative proteomics of salt tolerance in *Arabidopsis thaliana* and *Thellungiella halophila*. *J Proteome Res*. 2010; 9:2584–99.

333. Simova-Stoilova L, Vaseva I, Grigorova B, Demirevska K, Feller U. Proteolytic activity and cysteine protease expression in wheat leaves under severe soil drought and recovery. *Plant Physiology and Biochemistry*. 2010; 48:200–6.

334. Ford KL, Cassin A, Bacic A. Quantitative proteomic analysis of wheat cultivars with differing drought stress tolerance. *Front Plant Sci*. 2011; 2:44.

335. Levesque-Tremblay G, Havaux M, Ouellet F. The chloroplastic lipocalin AtCHL prevents lipid peroxidation and protects *Arabidopsis* against oxidative stress. *The Plant Journal*. 2009; 60:691–702.

336. Ashoub A, Beckhaus T, Berberich T, Karas M, Brüggemann W. Comparative analysis of barley leaf proteome as affected by drought stress. *Planta*. 2013; 237:771–81.

337. Ashoub A, Baeumlisberger M, Neupaertl M, Karas M, Brüggemann W. Characterization of common and distinctive adjustments of wild barley leaf proteome under drought acclimation, heat stress and their combination. *Plant Mol Biol*. 2015; 87:459–71.

338. Cho SK, Kim JE, Park J-A, Eom TJ, Kim WT. Constitutive expression of abiotic stress-inducible hot pepper CaXTH3, which encodes a xyloglucan endotransglucosylase/hydrolase homolog, improves drought and salt tolerance in transgenic *Arabidopsis* plants. *FEBS Lett*. 2006; 580:3136–44.

339. Wang X, Cai X, Xu C, Wang Q, Dai S. Drought-responsive mechanisms in plant leaves revealed by proteomics. *Int J Mol Sci*. 2016; 17:1706.

340. Borghi L, Kang J, Ko D, Lee Y, Martinoia E. The role of ABCG-type ABC transporters in phytohormone transport. *Biochem Soc Trans*. 2015; 43:924–30.

341. Dhara A, Raichaudhuri A. ABCG transporter proteins with beneficial activity on plants. *Phytochemistry.* 2021; 184:112663.

342. Chen L, Yu D. ABA regulation of plant response to biotic stresses. *Abscisic acid: metabolism, transport and signaling*. 2014;409–29.

343. Shivaraj SM, Sharma Y, Chaudhary J, Rajora N, Sharma S, Thakral V, *et al.* Dynamic role of aquaporin transport system under drought stress in plants. *Environ Exp Bot*. 2021; 184:104367.

344. Benešová M, Hola D, Fischer L, Jedelský PL, Hnilička F, Wilhelmová N, *et al.* The physiology and proteomics of drought tolerance in maize: early stomatal closure as a cause of lower tolerance to short-term dehydration? *PLoS One*. 2012;7: e38017.

345. Zhou S, Hu W, Deng X, Ma Z, Chen L, Huang C, *et al.* Overexpression of the wheat aquaporin gene, TaAQP7, enhances drought tolerance in transgenic tobacco. *PLoS One*. 2012;7: e52439.

346. Sánchez-McSweeney A, González-Gordo S, Aranda-Sicilia MN, Rodríguez-Rosales MP, Venema K, Palma JM, *et al.* Loss of function of the chloroplast membrane K+/H+ antiporters AtKEA1 and AtKEA2 alters the ROS and NO metabolism but promotes drought stress resilience. *Plant Physiology and Biochemistry*. 2021; 160:106–19.

347. Osakabe Y, Arinaga N, Umezawa T, Katsura S, Nagamachi K, Tanaka H, *et al.* Osmotic stress responses and plant growth controlled by potassium transporters in *Arabidopsis*. *Plant Cell*. 2013; 25:609–24.

348. Sheng P, Tan J, Jin M, Wu F, Zhou K, Ma W, *et al.* Albino midrib 1, encoding a putative potassium efflux antiporter, affects chloroplast development and drought tolerance in rice. *Plant Cell Rep*. 2014; 33:1581–94.

349. Muhammad Aslam M, Waseem M, Jakada BH, Okal EJ, Lei Z, Saqib HSA, *et al.* Mechanisms of abscisic acid-mediated drought stress responses in plants. *Int J Mol Sci*. 2022; 23:1084.

350. Ali S, Hayat K, Iqbal A, Xie L. Implications of abscisic acid in the drought stress tolerance of plants. *Agronomy*. 2020; 10:1323.

351. Lefebvre V, North H, Frey A, Sotta B, Seo M, Okamoto M, *et al.* Functional analysis of *Arabidopsis* NCED6 and NCED9 genes indicates that ABA synthesized in the endosperm is involved in the induction of seed dormancy. *The Plant Journal*. 2006; 45:309–19.

352. Iuchi S, Kobayashi M, Taji T, Naramoto M, Seki M, Kato T, *et al.* Regulation of drought tolerance by gene manipulation of 9-cis-epoxycarotenoid dioxygenase, a key enzyme in abscisic acid biosynthesis in *Arabidopsis*. *The Plant Journal*. 2001; 27:325–33.

353. Xie N, Li B, Yu J, Shi R, Zeng Q, Jiang Y, *et al.* Transcriptomic and proteomic analyses uncover the drought adaption landscape of *Phoebe zhennan*. *BMC Plant Biol*. 2022; 22:1–16.

354. Wang X, Oh MW, Komatsu S. Characterization of S-adenosylmethionine synthetases in soybean under flooding and drought stresses. *Biol Plant*. 2016; 60:269–78.

355. Yan J, Wang D, Kang S, He Z, Li X, Tang W, *et al.* Ethylene regulates combined drought and low nitrogen tolerance in wheat: proteomic analysis. *Agronomy*. 2023; 13:1950.

356. Llanes AS, Andrade AM, Alemano SG, Luna MV. Alterations of endogenous hormonal levels in plants under drought and salinity. *American Journal of Plant Sciences*. 2016, 7, 1357-1371

357. Dong TX, Cai KZ, Zhang JX, Rong H, Xie G, Zeng RS. The physiological roles of methyl jasmonate (MeJA) in drought resistance of rice seedlings. *Ecol Environ*. 2007; 16:1261–5.

358. XU B, GAO X, GAO J, Jing LI, Pu Y, FENG B. Transcriptome profiling using RNA-seq to provide insights into foxtail millet seedling tolerance to short-term water deficit stress induced by PEG-6000. *J Integr Agric*. 2019; 18:2457–71.

359. Nagy Z, Németh E, Guóth A, Bona L, Wodala B, Pécsváradi A. Metabolic indicators of drought stress tolerance in wheat: Glutamine synthetase isoenzymes and Rubisco. *Plant Physiology and Biochemistry*. 2013; 67:48–54.

360. Michaletti A, Naghavi MR, Toorchi M, Zolla L, Rinalducci S. Metabolomics and proteomics reveal drought-stress responses of leaf tissues from spring-wheat. *Sci Rep*. 2018; 8:5710.

361. Baek W, Lim CW, Lee SC. A DEAD-box RNA helicase, RH8, is critical for regulation of ABA signalling and the drought stress response via inhibition of PP2CA activity. *Plant Cell Environ*. 2018; 41:1593–604.

Appendix–I

Research Publications

Research Articles

1. **Arora, S**., & Jha, P. N. (2023). Drought-tolerant *Enterobacter bugandensis* WRS7 induces systemic tolerance in *Triticum aestivum* L.(wheat) under drought conditions. *Journal of Plant Growth Regulation*, 1-16.
2. **Arora, S**., Babele, P. K., & Jha, P. N. (2023). Biochemical and metabolic signatures are fundamental to drought adaptation in PGPR *Enterobacter bugandensis* WRS7. *Molecular Omics*, *19*(8), 640-652.

Book Chapters

1. **Arora, S**., & Jha, P. N. (2019). Impact of plant-associated microbial communities on host plants under abiotic stresses. *Microbial Interventions in Agriculture and Environment: Volume 2: Rhizosphere, Microbiome and Agro-ecology*, 303-340.

Abstracts at Conference

1. **Arora, S.**, & Jha, P. N. (2021). Amelioration of Drought Stress Tolerance by PGPR *Enterobacter* sp. WRS7 in wheat plant. International Virtual Conference on Recent Trends and Innovations in Microbiology held at Department of Microbiology, Mohanlal Sukhadia University, Udaipur, Rajasthan, India. July 15. Abstract no. PP-15, Pg. No. 42. (Secured 3rd Position)

Appendix–II

Biography of Prof. Prabhat Nath Jha

Dr. P.N. Jha is working as a Professor in the Department of Biological Sciences, Birla Institute of Technology and Science Pilani, Pilani campus, Rajasthan. He obtained his master's degree in biotechnology from Lalit Narayan Mithila University, Darbhanga (Bihar), and completed his PhD in Microbial Biotechnology from Banaras Hindu University, Varanasi (U.P.). He did his postdoctoral research in plant molecular biology at the National Botanical Research Institute, Lucknow, and microbial ecology at Michigan State University, USA. He has been engaged in teaching and research since 2007. His broad research interests are Host-Microbe interaction, Plant Microbiology, and Applied Microbiology. Dr. Jha has completed research projects funded by DST, DBT, and ICAR, and Industries (ABG, Tablet India) and mentored research students for Govt-funded projects such as DST-WoS. He has published 68 research articles in journals of international repute, seven chapters in edited books, and edited two books. He also has filed patent two jointly. He has successfully guided five students to PhD and guided more than thirty undergraduate and post-graduate students for their research studies. He is currently guiding three students for Ph.D.

He is a recipient of Raman postdoctoral fellowship under India-US knowledge initiative 2013 programme (University Grant Commission, New Delhi), DST travel grant to attend international conference at Czeck-Republic, DBT- Postdoctoral fellowship, CSIR-SRF and K.C. Bose Young Scientist award (Gold medal). He was a Visiting Fellow in Department of Botany and Zoology, Institute of Life Sciences, Rajiv Gandhi University, Rono Hills, Doimukh, Itanagar, Arunachal Pradesh, India to teach Molecular Biology and Plant Biotechnology to post-graduate student. He has delivered motivational talk to students of Navodaya Vidhyalaya, and NTSE scholars and scientific talks at research and academic institutes. In addition to academics, Dr. Jha has served as Head of the Department of Biological Sciences, BITS Pilani (2016-2020); Co-coordinator of Sophisticated Instrument Facility, BITS Pilani (2020-2022); Member Secretary of the Institute Biosafety Committee, BITS Pilani; Convenor, Departmental Research Committee convener of the Dept.; PI, DBT-BUILDER, BITS Pilani; Member of library committee, Member, Member of Human Ethics Committee, and nucleus member of research and consultancy division; DBT nominee, IBSC, IIT-Jodhpur; Member of National Steering committee of NetSCoFAN (Biological group), FSSAI, India; Member of Board of Studies, Choudhary Banshi Lal University, Bhiwani, Haryana etc.

Biography of Saumya Arora

Ms. Saumya Arora has completed her M.Sc. (Biotechnology) from Banasthali Vidyapith, (Rajasthan, India). She enrolled in the Ph.D. program of BITS Pilani, Pilani campus, Rajasthan in January 2018. During his PhD program, she received financial assistance from DST- INSPIRE, Govt. of India. She has qualified the National Eligibility Test (NET-2017) conducted by ICAR/ASRB, India in Agricultural Biotechnology and Gratitude Aptitude Test in Engineering (GATE 2016) organized by the Indian Institute of Sciences on behalf of the National Coordination Board (NCB) for the Department of Higher Education, MHRD in Biotechnology. She had been ranked 1st in M.Sc. Biotechnology (Batch 2013-2015) at Banasthali Vidyapeeth. During her research, she was involved in teaching various courses at the Department of Biological Sciences, BITS Pilani. She was awarded the best poster award (3^{rd} position) in national conferences organized by Department of Microbiology, Mohanlal Sukhadia University, Udaipur, Rajasthan, India. She has published research articles in renowned international journals.

Journal of Plant Growth Regulation
https://doi.org/10.1007/s00344-023-11044-6

Drought-Tolerant *Enterobacter bugandensis* WRS7 Induces Systemic Tolerance in *Triticum aestivum* L. (Wheat) Under Drought Conditions

Saumya Arora[1] · **Prabhat Nath Jha**[1]

Received: 12 September 2022 / Accepted: 23 May 2023

Abstract

Some plant growth-promoting bacteria (PGPR) can ameliorate abiotic stressors like drought stress and promote plant growth. The present study investigated various drought-tolerant mechanisms of *Enterobacter bugandensis* WRS7, a rhizospheric isolate, by which it alleviates the deleterious effects of drought stress in wheat plants (*Triticum aestivum* L). The isolate WRS7 showed different plant growth-promoting properties, including nitrogen fixation, phosphate solubilization, siderophore production, phytohormone (indole acetic acid and gibberellic acid) production, exopolysaccharide secretion, and ACC deaminase activity. Its inoculation to wheat plants improved plant growth in terms of root/shoot growth and chlorophyll content. Its inoculation also exhibited drought stress ameliorating properties, including increased osmolyte content (proline and total soluble sugar), relative water content, catalase and superoxide dismutase activity, and decreased lipid peroxidation compared to non-inoculated plants. Our biochemical data were coherent with gene expression analysis of WRS7-treated plants, which showed altered expression of genes encoding antioxidant enzymes (*CAT*, *APX*, and *GPX*), osmolyte synthesis (*P5CS*, *P5CR*, and *TPS1*), biosynthesis of stress hormone genes (*NCED, WZE, SAMS, ACS1*, and *ACO* encoding proteins for the biosynthesis of abscisic acid and ethylene), and calcium transporter (*TPC1*) in the wheat plant. The regulation of the ethylene biosynthesis gene and modulation of TPC1 gene expression by PGPR *E. bugandensis* WRS7 in wheat plants highlights its additional role in alleviating drought stress. The colonization study demonstrated the successful colonization of *E. bugandensis* WRS7 in wheat plants. Overall, the present study indicates that *E. bugandensis* WRS7 alleviates drought stress in wheat plants by differentially regulating various metabolic genes in treated plants.

Keywords *Triticum aestivum* · *Enterobacter bugandensis* WRS7 · Drought stress · Gene expression · Induced systemic tolerance

Introduction

Wheat (*Triticum aestivum* L) is an important cereal and staple crop globally, contributing around 20% of total dietary calories consumed (Clarke et al. 2021). According to the FAO, the global annual wheat production is about 680 million tons and is likely to increase by 60% by 2050. Still, the production amount is not enough to meet the ever-growing demand of the growing population (FAO 2017). Moreover, World agriculture faces severe challenges in meeting the demands of the increasing population and health safety concerns due to adverse environmental conditions, including drought. Since wheat is a water-intensive crop, drought stress negatively impacts yield and grain quality (Caverzan et al. 2016; Clarke et al. 2021; Gontia-Mishra et al. 2016). It interrupts many physio-biochemical processes, including photosynthesis, carbon assimilation, nutrient uptake, plant growth, and development. According to FAO, over 34% of crop and livestock production loss in least-developed countries (LDCs) and low to middle-income countries (LMICs) is due to drought between 2008 and 2018. Therefore, measures to overcome abiotic stressors, including drought stress, must be addressed. Applying chemical fertilizers can promote plant growth under such environmental conditions (Aslam et al. 2021). However, chemical fertilizers have several health and environmental concerns. Generating genetically

Handling Editor: Chetan Keswani.

✉ Prabhat Nath Jha
prabhatjha@pilani.bits-pilani.ac

[1] Department of Biological Sciences, Birla Institute of Technology and Science, Pilani, Rajasthan 333031, India

modified drought stress-resistant crops can be an appropriate solution to enhance agricultural productivity. However, its health and environmental impacts are not fully known. Also, there are ethical concerns with the use of genetically modified crops. Therefore, taking account of the present scenario, role of the Plant Growth-Promoting Rhizobacteria (PGPR), capable of drought stress amelioration, could be crucial for sustainable agriculture.

PGPR are beneficial soil microorganisms that promote plant growth directly by increasing the availability and uptake of nutrients and indirectly by ameliorating abiotic and biotic stressors (Vessey 2003). Exploiting these beneficial microorganisms for plant stress alleviation is an eco-friendly and cost-effective approach to sustainable agriculture (Niu et al. 2018). Certain PGPR can withstand drought and helps plants to tolerate drought stress by several symbiotic mechanisms, including decreased production of stress ethylene due to bacterial ACC deaminase enzymes, elevated osmolyte production, nutrient uptake, and antioxidant mechanism and altered phytohormone signaling (Singh et al. 2015a, b; Vaishnav et al. 2020). In the past few decades, several researchers have isolated and characterized PGPR to alleviate the deleterious effects of drought stress in different plants. Rashid et al. isolated *Bacillus megaterium* MU2 from the semi-arid condition and reported it as a potential candidate to promote wheat plant growth under drought conditions (Rashid et al. 2021).

Similarly, Khan and Bano reported that exopolysaccharide secreting PGPR and applying plant growth hormone salicylic acid improve wheat plant growth under drought stress (Khan and Bano 2019). Gontia-Mishra et al. (2016) and their group investigated the effect of PGPR *Enterobacter ludwigii* and *Flavobacterium* sp. in wheat at physiological and biochemical parameters and studied gene expression of stress-responsive genes under drought stress. These PGPR can improve plant growth under drought stress by attributing plant growth directly and by influencing plant physiology and regulating the expression of genes required to protect plants from abiotic stress-mediated alteration of plant functions. For instance, Gontia-Mishra et al. (2016) reported upregulation of some stress-related genes such as *CAT1* and *DREB2A* in uninoculated wheat plants under drought stress, whereas attenuated transcript levels were observed in PGPR-inoculated plants, indicating improved tolerance due to PGPR interaction (Gontia-Mishra et al. 2016). Similarly, Barnawal et al. suggested that PGPR inoculation confers abiotic stress tolerance by modulating the expression of the *CTR1* gene, a regulatory component of the ethylene signaling pathway and *DREB2* in wheat (Barnawal et al. 2017). These works suggest that the plant–microbe interaction can be a promising approach to improving plant growth and productivity in a drought environment through multiple mechanisms. Therefore, understanding plant–PGPR interaction at the biochemical and molecular level will be highly helpful in exploiting PGPR for sustainable agriculture.

Though there are studies reporting the PGPR-mediated drought stress amelioration in wheat plants, exploration of more efficient PGPR is still required, which can be used for improved and sustainable agriculture. Moreover, mechanisms by which PGPR modulates host plant physiology at biochemical and molecular levels are important for better exploitation of PGPR-plant interactions. Therefore, the present study aimed to isolate drought-tolerant plant growth-promoting bacteria and characterize their abilities to ameliorate drought stress in wheat plants by employing biochemical and molecular approaches. To date, only a few studies have highlighted the combinational impact of rhizobacteria and drought stress through gene expression analysis in different plants, including wheat. In the present study, we isolated and characterized *Enterobacter bugandensis* WRS7 for detailed characterization based on drought stress tolerance and plant growth-promoting features. This study elaborates our understanding of bacteria-mediated Induced Systemic Tolerance (IST) in plants. Also, to the best of our knowledge, the role of *Enterobacter bugandensis* as PGPR has not been characterized in detail.

Materials and Methods

Isolation and Molecular Characterization of Water Stress-Tolerant Rhizobacteria from Wheat Rhizosphere

Healthy wheat plants (*Triticum aestiv*um L.) were carefully uprooted from cultivated fields of Pilani (28.37° N 75.6° E), Rajasthan, India, in January 2019. To isolate rhizospheric bacteria, 10 g of rhizospheric soil adhered to roots was weighed and added to 50 mL of 0.85% sodium saline and kept on a shaker for mixing. The soil was allowed to settle, and 1 mL aliquot was inoculated to nutrient broth (NB) media containing 10% of polyethylene glycol (PEG) to induce drought stress (Busse and Bottomley 1989) and incubated at 30 °C for 24 h on a shaker at 200 rpm to enrich water stress-tolerant bacteria. One ml of the above culture was re-inoculated in NB media containing 10% PEG and incubated as above-stated culture conditions. The culture suspension was serial diluted up to 10^{-6} dilution and 100 µl of the final dilution was plated onto a solid NB agar medium containing 10% PEG. The inoculated plates were incubated at 30 °C for 72 h. Bacterial colonies growing on the above selective medium were aseptically picked, sub-cultured, and maintained for further use. Total 12 different isolates were selected initially, out of which 9 morphotypes were finally selected based on shape, size, and morphology to test plant growth-promoting properties. Based on the result of plant

growth-promoting properties, isolate WRS7 was selected for further studies.

For molecular identification, the genomic DNA of the bacterial isolate was extracted using a genomic DNA extraction kit (Qiagen, USA) as per the manufacturer's instructions. 16S rRNA gene was amplified by PCR using a standard method (Singh et al. 2015a, b). The rRNA gene was sequenced by Sanger Sequencing at Delhi University, South Campus, India. The nucleotide sequence was compared against the GenBank database using the NCBI-BLAST algorithm and deposited in the NCBI database (http://www.ncbi.nlm.nih.gov/BLAST). A phylogenetic tree was constructed using the Neighbor-Joining (NJ) method with a bootstrap value of 500 in MEGA 6.0 (Tamura et al. 2013).

Biochemical Characterization of *E. bugandensis* WRS7

Biochemical assays, including Gram staining, IMViC test, and enzyme assays, such as catalase, chitinase, lipase, and amylase, were performed following standard protocols (Prescott and Harley 2002). The carbohydrate utilization ability of the isolate was tested using a commercial kit (KB 009, Hi-media, India). Further, antibiotic sensitivity against standard antibiotics such as streptomycin (10 µg), tetracycline (10 µg), kanamycin (30 µg), ampicillin (10 µg), chloramphenicol (10 µg), and gentamycin (30 µg) were tested using antibiotic discs (HTM 002, Hi-media). All the experiments were performed in triplicate.

Test of Plant Growth-Promoting (PGP) Activities of *E. bugandensis* WRS7

E. bugandensis WRS7 was screened for plant growth-promoting (PGP) activity like the production of indole-3-acetic acid (IAA), phosphate solubilization, siderophore production, a preliminary test for nitrogen fixation, and ACC deaminase activity using standard methods (Singh et al. 2015a, b). Quantification of exopolysaccharides secreted by bacteria was done following the standard protocol (Ghosh et al. 2019). Considering that motility is required for colonization, different types of motility, such as swimming, swarming, and twitching of the isolate, were also tested using a standard protocol (Singh et al. 2015a, b). Production of HCN and ammonia was determined using a standard method (Bakker and Schippers 1987; Dye 1962), as these traits show the ability of bacteria to suppress the proliferation of fungi in the soil. Hydrolytic enzyme activity such as endoglucanase, cellobiohydrolase, and glucosidase was assayed following the standard protocols of (Kosová et al. 2008) and (Reinhold-Hurek et al. 1993), respectively.

For IAA and GA_3 detection, the protocol of Ghosh et al. (2019) was followed with slight modifications (Ghosh et al. 2019). Phytohormones secreted by bacterial isolate were extracted using an equal volume of ethyl acetate and kept for 48-h incubation at 150 rpm at 4 °C. The organic layer was separated and evaporated using a rotary evaporator under a vacuum. The residue was re-dissolved in methanol, filtered through a 0.22µ filter, and then subjected to HPLC analysis (HPLC 1260, Agilent Technology, USA) using a C18 column (4.6 × 150 mm, 4 µm). The column was washed with 80% methanol and equilibrated with an isocratic flow of acetonitrile and 10-mM ammonium acetate buffer (pH 4.2) in a 70:30 (v/v) ratio at a flow rate of 2.0 mL/min. (Ghosh et al. 2019; Górka and Wieczorek 2017). The same solvent system was used to separate phytohormones, and 20 µl of the sample was injected at a flow rate of 1 mL/min. Detection of peaks respective to phytohormones was done using a UV–visible detector (VWD detector) at a wavelength of 254 nm and 280 nm for GA_3 and IAA, respectively. For quantification or to know the concentration of IAA and GA_3, a standard curve (area under the curve vs. concentration) was prepared and extrapolated using different concentrations of commercially available phytohormones. Later, the samples were subjected to HRMS (Agilent Technologies 6545 Q-TOF LC/MS) to confirm the presence of IAA. The sample was prepared as stated above. The Solvent system used for HRMS analysis was a mixture of acetonitrile and water in a 40:60 (v/v) ratio at a flow rate of 3.0 mL/min.

Effect of *E. bugandensis* WRS7 on Growth of Wheat Crop Under Drought Stress

For the experimental studies, healthy and uniform size seeds of wheat variety WH1142, procured from the Indian Institute of Wheat and Barley Research, Karnal, were selected. For the plant growth-promoting test, the inoculum of the bacterium isolate WRS7 was prepared. The bacterial culture was grown in a Luria broth (LB) medium and optical density (OD) at 600 nm was maintained at 0.15 using 1X PBS. Wheat seeds were surface sterilized by treating with 0.1% $HgCl_2$ for 1 min, followed by 70% ethanol for 1 min. The sterile seeds were washed five times with distilled water. Surface-sterilized seeds were treated with 2.5×10^3 CFU (colony-forming unit) of bacterial inoculum at room temperature (RT) for 2 h and dried under aseptic conditions. Five seeds were sown in each plastic pot filled with sterile soil in triplicates in a growth chamber (LabTech, South Korea) with a 16:8 photoperiod at 28 ± 2 °C with a humidity of 70% and 140 µmol m^{-2} s^{-1}. Control seeds were incubated with PBS. Murashige and Skoog (MS) macronutrient solution was applied to soil as a nutrient solution on alternate days. To impose drought stress, plants were not watered after 15 days of germination (plants grown up to the three-leaf stage). After 15 days of stress, plants were harvested and their growth was measured based on various parameters,

such as percent germination, root, and shoot length, fresh and dry weight of five randomly collected seedlings, and chlorophyll content. For measurement of photosynthetic pigments chlorophyll a/b, 1-g fresh leaf samples were homogenized in 80% acetone, and pigment was extracted and quantified as per the method of Duxbury and Yentch (1956) (Duxbury and Yentsch 1956). The relative water content (RWC) of wheat plant leaves was determined by following the standard protocol (Vaishnav and Choudhary 2019).

For evaluation of different biochemicals in control and bacteria-treated plants, osmolyte content (proline and total soluble sugars) and lipid peroxidation assays were performed under drought stress. Proline content in the leaves was determined by the standard protocol of Bates et al. 1973 (Bates et al. 1973). Total Soluble Sugar (TSS) was estimated by following the standard protocol of Irigoyen et al. 1992 using anthrone reagent (Irigoyen et al. 1992). Lipid peroxidation was determined by estimating the malondialdehyde (MDA) content produced by the thiobarbituric acid reaction (Hodges et al. 1999).

Effect of *E. bugandensis* WRS7 on Antioxidant Enzyme Activities of Wheat Crop

Antioxidant enzymes or stress markers such as catalase (CAT) and superoxide dismutase (SOD) were determined using a standard protocol (Aebi 1984; Giannopolitis and Ries 1977). To measure the enzyme activity, 0.5 g of leaf from bacteria-treated plants grown under drought stress and their respective control plants were homogenized with 50-mM phosphate buffer (pH 7.0) and centrifuged at 15,000 g for 20 min at 4 °C. The supernatant was used for the estimation of protein content and antioxidant enzyme activity. Catalase activity was measured based on the decomposition of hydrogen peroxide (H_2O_2) by recording the decrease in absorbance at 240 nm at 30 °C (Aebi 1984). The activity of SOD was determined by the photoreduction of nitro blue tetrazolium (NBT). The reaction mixture contained phosphate buffer along with NBT, riboflavin, and enzyme extract. Riboflavin was the last component to be added and then the reaction was initiated by placing the tubes in fluorescent lamps. The reaction was terminated after 10 min by removing the light source. Absorption of the reaction products was recorded at 560 nm (Giannopolitis and Ries 1977).

Gene Expression Analysis of Stress-Responsive Genes in Wheat Plant

To understand the plant response to PGPR inoculation, the expression of different genes contributing to drought stress amelioration was investigated. Wheat plants were grown and treated as described above. The leaves of experimental plants were used for total RNA extraction using the CTAB method (White et al. 2008). Three biological replicates were employed for each treatment. The extracted RNA was checked for its quality and quantity using the Biospectrometer (Eppendorf, Germany). The cDNA was synthesized using a verso cDNA synthesis kit (Thermo Fisher Scientific, USA) for gene expression profiling. Real-Time qPCR (BioRad, USA) was performed using a SsoFast EvaGreen Supermix (BioRad, USA) and a gene-specific set of primers as listed in Table 1. Primers were designed using Sequence Manipulator Suit (https://www.bioinformatics.org/sms2/) and NCBI primer blast. Tubulin 1 (tubb1) was used as an internal control. Gene expression analysis was done using relative quantification by the $2^{-\Delta\Delta CT}$ method (Livak and Schmittgen 2001). The selection of stress-responsive genes for expression studies was based on available literature (Dudziak et al. 2019; Wang et al. 2021).

Table 1 List and sequence of primers used in real-time gene expression

Primer	Primer (5′ → 3’) forward sequence	Primer (5′ → 3’) reverse sequence
CAT1	AAGTGCTCCCACCACAACAA	CTGGCCGAGAGACTTGTCAG
APX	TCAGTTTGTCCCCGTGAAGG	ACCTTTCAGGATGCGCCTTT
GPX	GTTCAGTTTGCCTGCACTCG	CAACGTGACCCTCCTTGTCA
NCED	CACTCTGTCGACTGCGCC	AAGTCGTGGATCATGGTGGG
WZE	AAGCAAACCAGATCCGAGCA	CATCGGAAGGGTGGAAACGA
SAMS	GCTGACCACTGCAAGGTACT	TGGTCACTGTCTCATCGTG
ACS1	CAGCCTCTCCAAAGACCTC	AATGCCGATCTCCTTGAGC
ACO	ATGAAGGAATTCGCGTCCGA	GGTAGCTGCTGACCTTGGTG
PC5S	TGATGGGACTCGCTTTGGTC	CACAACTCCCTTGTCACCGT
PC5R	AATGCCAAACACCCCCTCTG	TCAAGCCAGTAACCGCATCA
TPS1	TCTATGTGTTCTTCGACCCT	ACGAGTTGAGCAGGTAACGG
LEA1	CAGTACACCAAGGAGTCCGC	GCCAACACATGCGTCTAGTG
TPC1	CACTTCCGCTCGTAGCTT	CTTCTGGTAACGGTCGCCAT
Tubulin (tubb1)	CCGTCAACCTGATCCCCTTC	GTCAACCTCCTTGGTGCTCA

Bacterial Colonization Assay Under Normal and Drought Stress Conditions

Bacterial colonization to plant root surface was determined by the previously described method (Simons et al. 1996) with slight modifications. To confirm bacterial root colonization, the plants were uprooted carefully and washed twice with sterile DDW to remove loosely adhered bacterial cells from the root surface. Then, 1 g of root sample was weighed and crushed, added to saline solution, and kept at 120 rpm for 2 h, serially diluted and plated on LB media (Hi-media). The colony-forming unit (CFU g^{-1}) in the root sample was determined. To ascertain that the recovered colonies were of WRS-7, some of the recovered colonies were randomly selected for DNA fingerprinting using enterobacterial repetitive intergenic consensus (ERIC) PCR as described by (Singh et al. 2015a, b).

For further confirmation, 1–2 cm of root segment was fixed using 2.5% glutaraldehyde overnight and dehydrated with gradient ethanol of 30, 50, 70, 80, 90, and 100%. The fixed roots were sputter-coated with gold, and further imaging was performed using Field Emission Scanning Electron Microscope (FEI-APREO SEM, Thermo Fisher Scientific, USA).

Statistical Analysis

All the experiments were conducted in triplicates, and results were expressed as mean ± Standard Error Mean (SEM) ($n = 3$). Data were analyzed by analysis of variance (ANOVA) and subsequently by Duncan's multiple range test at $p < 0.05$.

Results

Isolation and Characterization of Water Stress-Tolerant Rhizobacteria from Wheat Rhizosphere

Bacterial colonies growing actively on NB media supplemented with 10% PEG were selected and sub-cultured several times to enrich water stress-tolerant bacteria. Based on continuous growth after subculturing, isolate WRS7 was selected for further characterization. The isolate WRS7 was found positive for catalase, amylase, nitrate reductase, and Voges–Proskauer's (VP) and negative for the test of chitinase, lipase, urease, indole, and Methyl Red (MR). Also, isolate WRS7 showed resistance to the antibiotic ampicillin but was sensitive to streptomycin, tetracycline, kanamycin, chloramphenicol, and gentamycin. Since bacterial motility is required for the initial colonization of the partnering bacteria to host plants, the isolate was tested for different types of motilities. Isolate WRS7 showed swimming, swarming, and twitching motility. Further, the results of hydrolytic activity required for bacterial colonization demonstrated the presence of endoglucanase activity. However, it showed a negative result for cellobiohydrolase and β-glucosidase activity.

For identification, a 1.5 kb of 16S rRNA gene of the isolate was amplified by PCR and sequenced. The sequence of the resulting amplicon was submitted to the NCBI GenBank under the accession number MW453057. Based on the sequence similarity, the isolate was identified as *E. bugandensis* with a close match to *E. bugandensis* strain XM29, with 99.16% similarity. Phylogenetic analysis showed that the sequence of 16S rRNA of the same genus clustered together (Supplementary Fig. 1).

Plant Growth-Promoting (PGP) Activities of *E. bugandensis* WRS7

Isolate WRS7 was screened qualitatively or quantitatively for various PGP properties. It showed positive results for phosphate solubilization (12.26 ± 1.72 µg/ml) and siderophore and showed potential to fix atmospheric nitrogen based on its growth on nitrogen-free $JNFb^{-}$ media. It also showed a positive test for ammonia production but a negative for HCN production. Both spectrometric and HPLC methods confirmed the production of IAA and gibberellic acid by the given isolate. The water stress caused a significant increase of 23.11% and 119.31% in the level of the phytohormones IAA and GA, respectively (Fig. 1), compared to non-stressed conditions. Further, the presence of IAA was confirmed by HRMS analysis. A mass peak of 175.066 was detected in mass spectra at 0.126-min retention time, which may correspond to IAA (Supplementary Fig. S2).

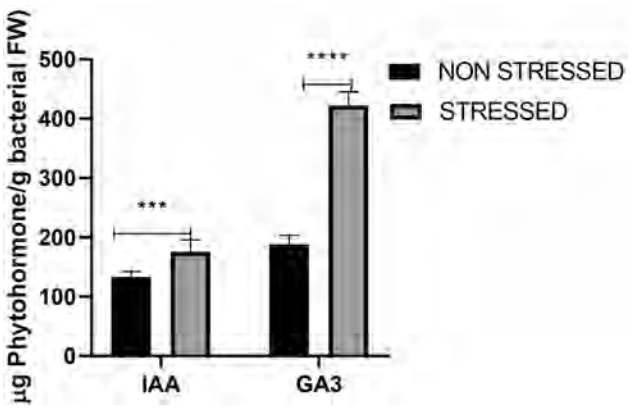

Fig. 1 Quantification of secreted Indole Acetic Acid (IAA) and Gibberellic Acid (GA) of bacterial isolate WRS7 both under osmotic-stressed conditions. The concentration of the secreted phytohormones is expressed in µg/g bacterial fresh weight (FW). Each bar represents the mean ± SE of 5 biological replicates. Symbol '*' represents a significant difference between test samples

Since the ACC deaminase activity of PGPR appears to be important in inducing systemic tolerance in plants against drought stress, the efficiency of WRS7 to utilize ACC as a nitrogen source was determined quantitatively. It showed the ACCD activity of 0.46 ± 0.01 µmol/mg protein/h. In addition to ACC deaminase, isolate WRS7 also showed production of 179.25 ± 1.25-µg/ml exopolysaccharides (EPS) which can protect the plant roots from desiccation under drought stress by maintaining soil moisture, thereby enhancing plant growth.

Effect of *E. bugandensis* WRS7 on Growth of Wheat Crop Under Drought Stress

To study the effect of *E. bugandensis* WRS7 on drought stress amelioration in the wheat plant, pot-based plant growth studies were conducted. As compared to uninoculated control plants, treatment of wheat seeds with WRS7 showed an enhanced increase in all the growth parameters, such as root length (53.62%), shoot height (13.64%), fresh weight (16.67%), dry weight (16.66%), chlorophyll a (33.53%), and chlorophyll b (29.89%) content, when tested under drought stress (Table 2). Inoculation of bacteria also significantly increased relative water content (RWC) in plants as compared to uninoculated control plants (Fig. 2a) under both non-stressed (90.15%) and stressed conditions (210.53%). Seed germination was not affected by bacterial inoculation as there is no significant change with respect to control (Fig. 2b). Stunted growth along with less chlorophyll content was observed in uninoculated plants under drought stress. These results show the efficiency of bacterial isolate WRS7 in ameliorating drought stress and promoting growth in wheat crops.

To analyze the accumulation of osmoprotectants under drought stress, the proline content and total soluble sugar (TSS) of the plants were measured (Figs. 3a and 4b). Osmoprotectants maintain osmotic potential inside the plants under water stress conditions. As noticed in Fig. 3, there was a significant increase in proline content under stressed conditions (53.51%), whereas this increase was

Table 2 Effect of bacterial isolate WRS7 on plant growth under drought stress employing different parameters

Isolates	Shoot length (cm)	Root length (cm)	Total length (cm)	Fresh wt. (g)	Dry wt. (g)	Chl. a (mg g^{-1} FW)	Chl. b (mg g^{-1} FW)
Control	23.66 ± 0.55	21.83 ± 0.67	45.70 ± 0.07	2.49 ± 0.44	0.24 ± 0.03	11.39 ± 0.52	6.63 ± 0.27
Stressed	19.46 ± 0.48**	12.16 ± 0.28***	31.55 ± 0.66****	1.80 ± 0.49****	0.18 ± 0.01****	8.75 ± 0.49*	3.15 ± 0.27*
NS + WRS7	25.97 ± 0.09*	25.31 ± 0.19*	50.96 ± 0.17**	2.90 ± 0.02****	0.29 ± 0.02****	16.13 ± 0.16**	5.82 ± 0.31^{ns}
S + WRS7	21.68 ± 1.44*	23.87 ± 0.47^{ns}	42.04 ± 0.83**	2.10 ± 0.09***	0.21 ± 0.01****	14.09 ± 0.57*	6.04 ± 0.07^{ns}

Value represents the mean ± SD, $n = 3$. Symbol '*' indicates significant difference ($p < 0.05$) between uninoculated and WRS7-inoculated plants under both non-stressed and stressed conditions w.r.t control (well-watered non-inoculated plants)

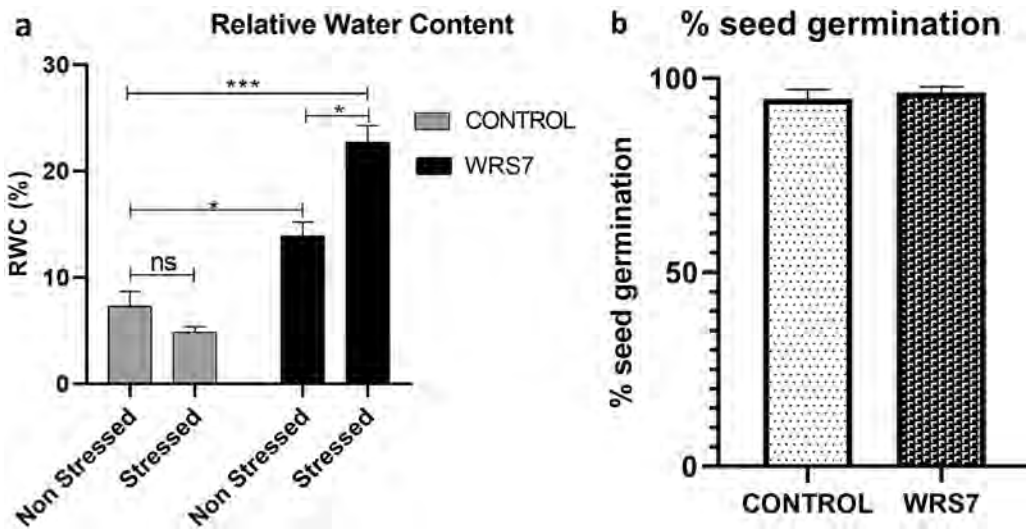

Fig. 2 The impact of *E. bugandensis* WRS7 on drought stress amelioration in wheat. **a** Relative water content (RWC) of the whole plant after 15 days of the drought treatment. Each bar represents mean ± SE ($n = 30$). **b** Seed germination percentage of 100 seeds with and without bacterial inoculation under standard conditions. Symbol '*' represents significant differences among different treatments ($p < 0.05$)

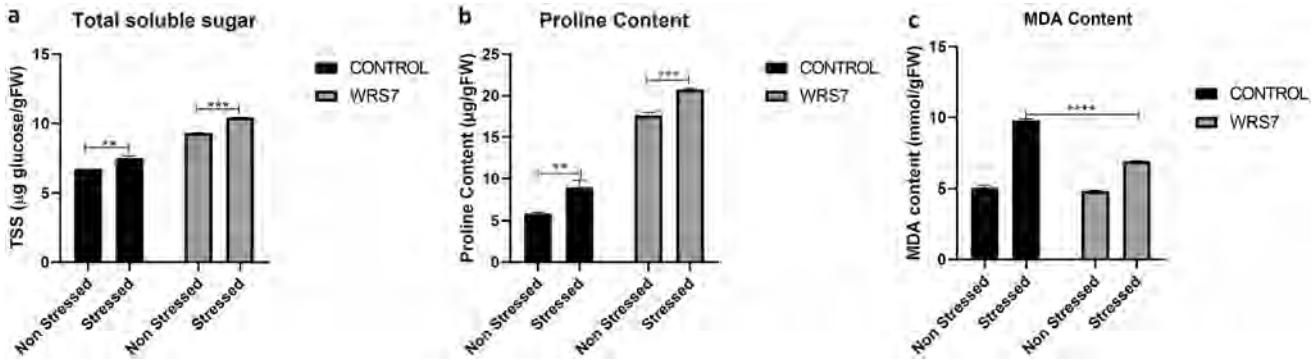

Fig. 3 Osmolyte contents and cell membrane integrity indexes in wheat under osmotic stress. **a** soluble sugar content; **b** proline content; and **c** malondialdehyde (MDA) content. Values represent the mean ± SE, $n = 3$. Symbol '*' indicates significant differences among different treatments ($p < 0.05$)

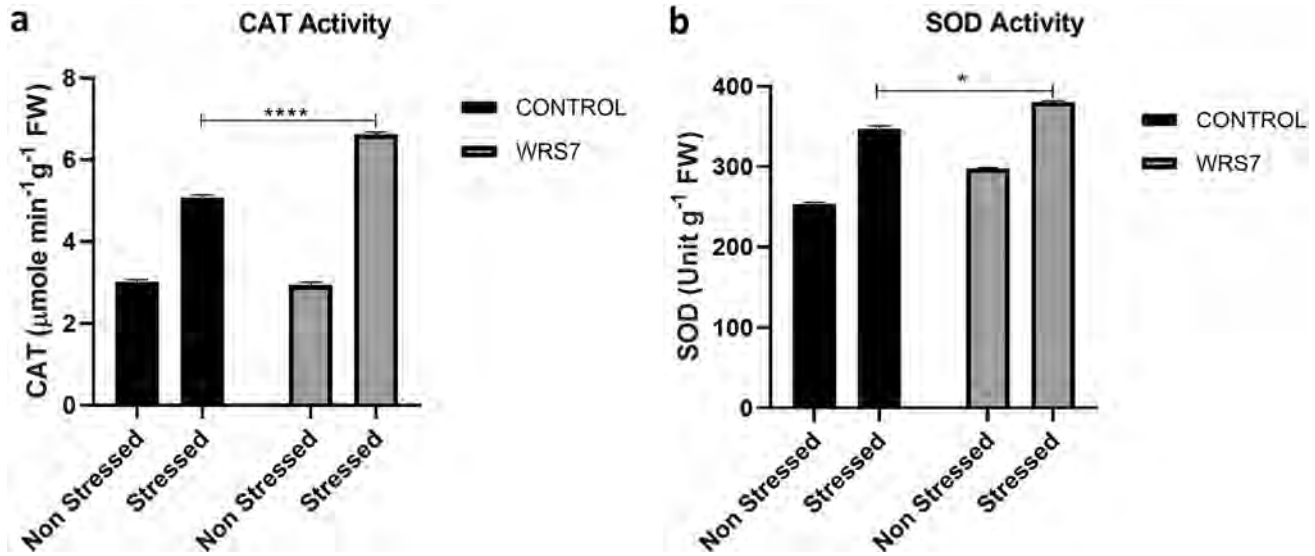

Fig. 4 Effect of bacterial (WRS7) inoculation on **a** Catalase (CAT) activity and **b** Superoxide Dismutase (SOD) activity in wheat plants under drought stress. Values represent the mean ± SD, $n = 3$. Symbol '*' indicates significant differences among different treatments ($p < 0.05$)

enhanced in bacteria-inoculated plants under both non-stressed (199.06%) and stressed (252.86) conditions when compared to uninoculated non-stressed plants. Similar results were also obtained for TSS content. The TSS content increased by 10.98% in uninoculated plants under drought stress, whereas the inoculated plants showed an increase of 38.01% and 55.02% under non-stressed and stressed conditions, respectively. Further, the extent of lipid peroxidation was evaluated by measuring malondialdehyde (MDA), a marker for stress-induced damage (Gontia-Mishra et al. 2016). No significant difference in MDA content was observed in WRS7-treated plants under non-stressed conditions compared to uninoculated controls. However, WRS7 inoculation significantly decreased MDA content by 29.59% in plants grown under drought stress (Fig. 3c).

The physiological changes in plants under drought stress and their amelioration by WRS7 were also evaluated by measuring the level of different oxidative enzymes known to overcome damages induced by oxidative bursts under stress conditions. Catalase activity was significantly increased in stressed conditions in both uninoculated (67.79%) and bacteria-inoculated (119.44%) plants, but no significant increase was noticed in bacteria-inoculated plants under non-stressed conditions. Similarly, SOD activity increased in plants under stress in both bacteria-uninoculated (36.84%) and bacteria-inoculated (50.15%) plants, although a slight increase of 17.37% was also observed in bacteria-inoculated plants under non-stressed conditions (Fig. 4).

Expression of Genes Encoding Antioxidant Enzymes

The molecular basis of plant–microbe interaction was determined through expression analysis of some of the stress-responsive genes in wheat plants (Fig. 5). All the experiments were calibrated with the control plants with regular watering. We analyzed WRS7-mediated gene expression of catalase (*CAT*), ascorbate peroxidase (*APX*), and glutathione peroxidase (*GPX*) in response to drought stress in the wheat plant. In the case of *CAT* gene expression, we did not observe a significant difference in bacteria-inoculated plants under non-stressed conditions (1.5-fold increase), w.r.t to control plants. However, the level of *CAT* gene expression significantly increased in uninoculated plants (threefold) and WRS7-treated plants (threefold) grown under drought stress (Fig. 5a). For the *APX* gene, we found around a fourfold change in expression in uninoculated plants under stressed conditions. The bacterial inoculation also increased *APX* gene expression under non-stressed conditions by 4.5 folds. However, the level of APX gene expression was lower in WRS7-treated under drought stress than in plants treated with only stress or only PGPR (Fig. 5a). The analysis of *GPX* gene expression indicated a different pattern as compared to the above two genes. Its expression decreased in bacterial inoculation under non-stressed and stressed conditions, whereas it increased in uninoculated plants under stress conditions (Fig. 5a).

Expression of Genes Encoding ABA and Ethylene Biosynthesis

ABA and ethylene are key stress hormones in plants under drought stress. We studied the expression of genes encoding the key enzymes, 9-*cis*-epoxy-carotenoid dioxygenase (*NCED*) and zeaxanthin epoxidase (*WZE*), involved in ABA biosynthesis. The basal level expression of *NCED* was observed in both control and WRS7-treated plants, where the expression was lower in inoculated plants than in the control plants. The *NCED* expression increased under drought stress conditions. The combination of WRS7 and drought treated further increased its expression by 2.2-fold, but there is no significant difference between drought-stressed and bacteria-treated stressed plants, suggesting that bacteria do not affect ABA gene expression directly. Similar results were obtained for *WZE* except for the equivalent level of gene expression in both control and WRS7 (non-stressed) plants (Fig. 5b).

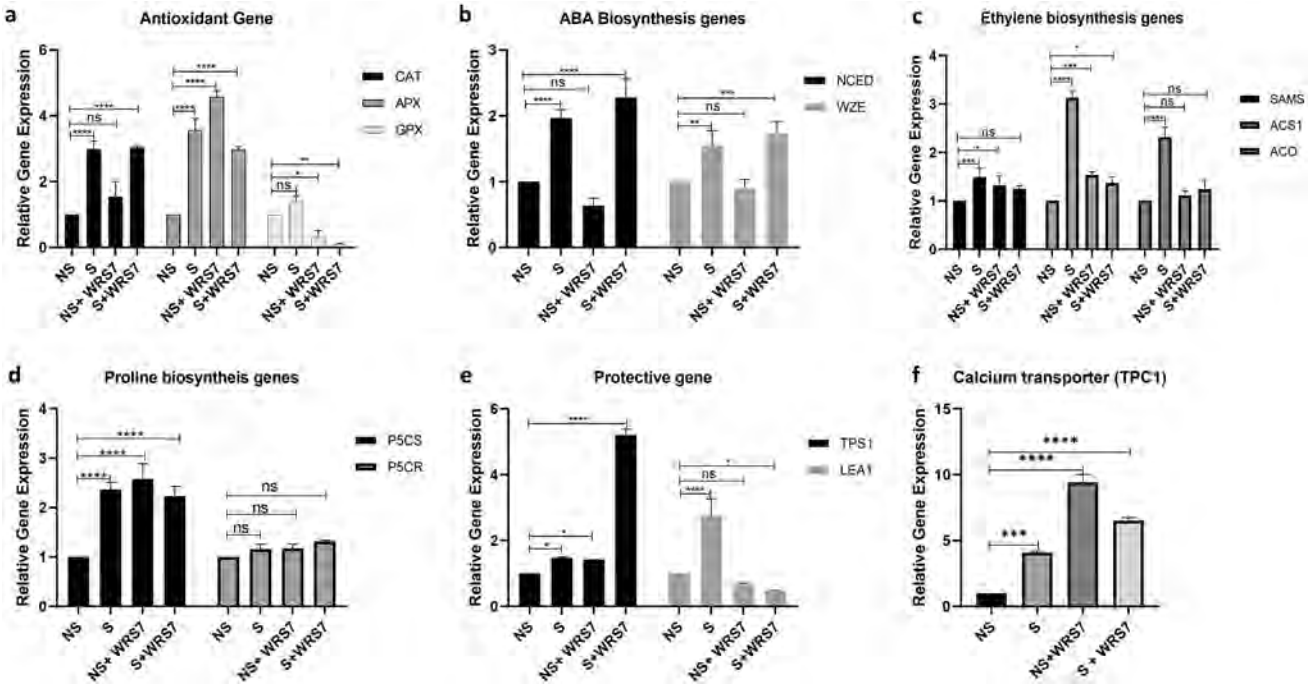

Fig. 5 Effect of inoculation of bacterial isolate *E. bugandensis* WRS7 on the expression of stress-associated genes in wheat plants. **a** Antioxidant Genes (CAT, PX, and GPX). **b** ABA Biosynthesis Gene. **c** Ethylene Biosynthesis Gene. **d** Proline Biosynthesis Gene. **e** Trehalose and Late Embryogenic Abundant (LEA) Gene. **f** Calcium Transporter *TPC1* gene under drought stress. Values represent the mean ± SD, $n = 3$. Symbol '*' indicates significant differences among different treatments ($p < 0.05$). Abbreviations: CAT = catalase; APX = Ascorbate peroxidase; GPX = Glutathione peroxidase; NCED = 9-*cis*-epoxy-carotenoid dioxygenase; WZE = wheat zeaxanthin epoxidase; SAMS = *S*-adenosyl-methionine synthetase; ACS1 = ACC synthase; ACO = ACC oxidase; P5CS = pyrroline-5-carboxylate synthetase; P5CR = pyrroline-5-carboxylate reductase; TPS1 = Trehalose Phosphate Synthase 1; TPC1 = Two-pore calcium channel protein 1

Since ethylene production is rapidly stimulated under abiotic stress, we looked for genes involved in its biosynthesis of *S*-adenosyl-methionine synthetase (*SAMS*), ACC synthase (*ACS 1*), and ACC oxidase (*ACO*). All three genes were highly upregulated under drought stress showing their induction to 1.5-, three, and 2.3-fold induction for *SAMS*, *ACS 1*, and *ACO* genes, respectively. However, inoculation of WRS7 decreased their expression level, bringing it to the basal level as observed in non-stressed control plants. (Fig. 5c).

Expression of Various Osmolyte Synthesis Genes

Knowing the role of osmolytes in ameliorating drought stress, the expression of genes associated with the synthesis of osmolytes, such as proline, trehalose, and LEA protein, was analyzed. Though the expression level of *P5CR* was not affected under drought stress, bacterial inoculation or their combination (both drought stress and WRS7 inoculation) upregulated *P5CS* by 2.5- and 2.2-fold, respectively. (Fig. 5d). For trehalose biosynthesis, the expression of the trehalose phosphate synthase encoding gene (*TPS1*) was evaluated. There was slight induction of *TPS1* gene expression in drought- and WRS7-treated plants separately. Strangely, the combinatorial treatment of drought and WRS7 inoculation showed fivefold higher expression of *TPS1* than the other treatments (Fig. 5e). We also examined the expression of the *LEA1* gene encoding Late Embryogenesis Abundant (LEA) proteins which also protect plants from osmotic stress. Drought stress significantly induced the expression of *LEA1* by 2.7-fold as compared to control plants. On the other hand, WRS7-treated plants grown either in the presence or absence of drought showed a lower level of gene expression than the control plants (Fig. 5e).

Expression of Calcium Transporter TPC1

Two-pore calcium channel protein 1 (TPC1), a voltage-gated Ca^{2+} channel in plant vacuolar membrane, plays an important role in various signaling responses under abiotic stress (Choi et al. 2014; Larisch et al. 2016). The drought stress-induced expression of TPC1 by fourfold compared to the control plants, whereas steep induction (9.4-fold) in the expression was observed in WRS7-inoculated plants. However, the level of the expression of TPC1 decreased in plants treated both with WRS7 and drought stress, yet it was higher than only drought stress-treated plants (Fig. 5f).

Root Colonization of Bacteria

The colonization ability of bacterial isolate WRS7 in the treated and control plants' roots was determined by CFU count, ERIC-PCR, and scanning electron microscopy after the experimental period. After 15 days of the drought period, root-associated bacteria were detected in the range of 2.5×10^6 CFU/g of the root (Supplementary fig. S3a). Bacterial establishment and colonization were also supported by visualization of dense adherence of bacteria on the root surface seen under a scanning electron microscope (Fig. 6). No bacterial colonization was observed in the case of the uninoculated plant's root surface. For confirmation of identified bacteria, ERIC-PCR was performed with genomic DNA of colonies obtained on LB plates and pure culture of WRS7. The banding pattern of the isolated colonies from the root surface were similar to that of pure culture (Supplementary fig. S3b), confirming its colonization ability.

Discussion

Some PGPR is known to cause induced systemic tolerance (IST) by various mechanisms, including increased nutrient uptake, phytohormones production, and ACC deaminase activity. These PGPR can interact with plants and modulate host functions by inducing gene expression required to alleviate the deleterious effects of abiotic stressors, including drought stress. Some studies have shown the potential of various *Enterobacter* species as PGPR and its role in ameliorating different abiotic stresses in plants (Bhatt et al. 2015; Singh et al. 2015a, b). The present study elucidates the role of water stress-tolerant PGPR *E. bugandensis* WRS7, a wheat rhizospheric isolate, in mitigating drought stress of the wheat plant by affecting several genes, including those required for stress-related phytohormones (abscisic acid and ethylene biosynthesis), antioxidant, osmolytes, and Ca^{2+} transporter TPC. To the best of our knowledge, this is the first study highlighting the potential of *E. bugandensis* WRS7 as PGPR protecting the wheat plant from drought stress.

E. bugandensis WRS7 showed various PGP, including phytohormone production, P-solubilization, and Siderophore production. The properties such as phosphate solubilization, siderophore production, and nitrogen fixation help in nutrient uptake by plants. Out of different PGPs, phytohormones secreted as secondary metabolites by bacteria can act as phytostimulants and prominently impact plant growth and metabolism both under stress and non-stress conditions (Ghosh et al. 2019). Bacteria-secreted phytohormones modulate plant hormones level in a similar way as exogenous phytohormone application does. As previously reported, bacterial IAA stimulates primary root elongation and helps form lateral roots, thereby affecting the root architecture and helping plants to survive under stressful conditions (Gupta et al. 2016; Vaishnav and Choudhary 2019). Gibberellic acid is a growth hormone involved in cell elongation and division and responds to abiotic stress. Also, GAs produced by

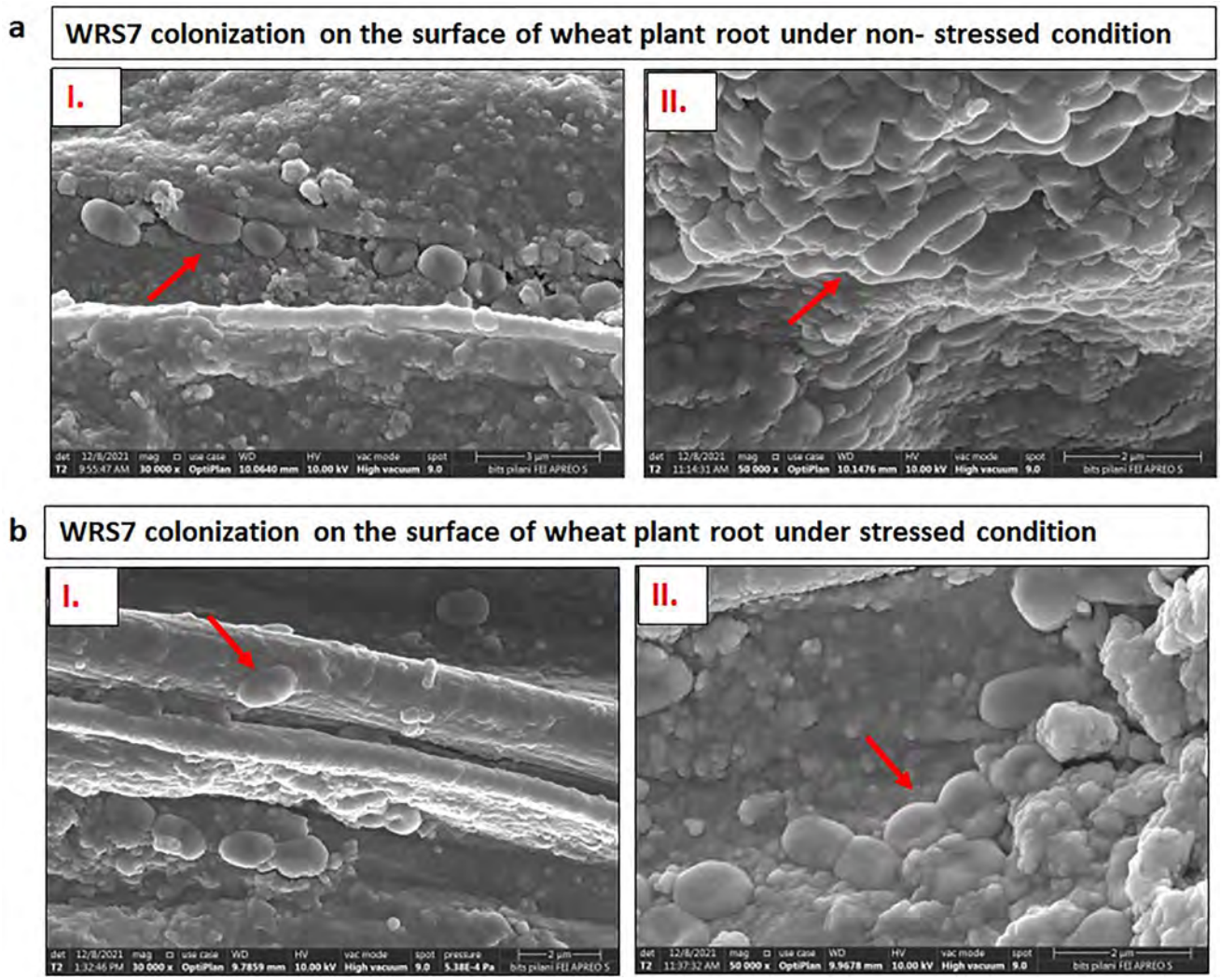

Fig. 6 Evaluation of colonization efficiency of bacterial isolate WRS7 on wheat root surface employing FESEM **a** under non-stressed conditions and **b** under drought stress conditions. Column (i) and (ii) represent magnification 30,000X and 50,000X, respectively. The arrow indicates bacterial colonization on the root surface

PGPR improves plant growth and yield (Bottini et al. 2004). Similar to our observations regarding increased IAA and GA_3 production under drought stress, some research groups also reported increased production of phytohormones by PGPR under drought stress. Ghosh et al. reported enhanced production of auxin and GA_3 by *Bacillus* and *Pseudomonas* strains under osmotic stress (Ghosh et al. 2019), whereas Bhatt et al. reported the same for *Enterobacter* strain P-39 under osmotic stress (Bhatt et al. 2015).

Certain PGPR can mitigate the adverse effects of abiotic stressors and promote crop production through one or more mechanisms. As the ACC deaminase activity of PGPR is one of the important PGPs for inducing systemic tolerance to the plants (Singh et al. 2015a, b; Singh et al. 2015a, b), we quantitatively analyzed the ACC deaminase activity of WRS7. Bacteria with ACC deaminase activity can lower the level of stress ethylene in plants by cleaving its precursor ACC into α-ketobutyrate and ammonia (Singh et al. 2015a, b). The ability of *Enterobacter* sp. to produce ACCD has been previously reported (Gontia-Mishra et al. 2017; Singh et al. 2015a, b). The ACCD activity of WRS7 (460 ± 0.01 nmol/mg protein/h) is much higher than the minimum threshold value of 20 nmol of α-KB mg^{-1} h^{-1}, which can influence plant growth by reducing the level of stress ethylene in plants (Singh et al. 2015a, b). Another important property of IST is the production of exopolysaccharides by PGPR. Exopolysaccharides produced by PGPR not only protect bacteria from the detrimental effect of osmotic stress but also improve plant growth through improved nutrient uptake as it increases root permeability to the soil and maintains high water potential around the

roots (Ghosh et al. 2019; Gontia-Mishra et al. 2017; Gontia-Mishra et al. 2016; Khan and Bano 2019).

Drought stress disturbs the water use efficiency of a plant, reducing plant growth and rate of photosynthesis, causing membrane damage, and affecting the activity of various enzymes (Noman et al. 2018). The role of PGPR in mitigating the adverse effects of drought stress has been exclusively studied (Abd El-Daim et al. 2019; Chandra et al. 2021; Egamberdieva et al. 2019). To test the efficacy of *Enterobacter* sp. WRS7 as biofertilizer, we conducted plant growth studies under drought stress conditions and its amelioration by *E. bugandensis* WRS7 under laboratory conditions. It was evident that WRS7-inoculated plants showed better root and shoot length and increased RWC, FW, and DW under water-stressed conditions (Table 2), suggesting the ability of WRS7 to mitigate the negative effects of drought. Our results are also supported by previous studies on PGPR-mediated drought stress mitigation (Ansari et al. 2021; Gontia-Mishra et al. 2016; Singh et al. 2015a, b). Increased root length increases root surface area, which in turn helps in more water absorption from the soil under drought stress. The bacterial auxin and GA might have a role in increased root length in plants (Sarma and Saikia 2014; Yuwono et al. 2005). Our study found increased chlorophyll content in PGPR-primed plants, which indirectly improved plant photosynthetic efficiency and energy metabolism. Earlier studies have also established increased photosynthetic efficiency and chlorophyll content in PGPR-inoculated plants (Martins et al. 2018; Murali et al. 2021).

To establish the role of *E. bugandensis* WRS7 in drought stress amelioration through the modulation of abiotic stress-related phytohormones, we evaluated the level of genes associated with the synthesis of ABA and ethylene. ABA plays a major role in regulating water balance and drought stress tolerance in plants by inducing stomatal closure (Zhu 2002). Other than stomatal closure, osmotic-responsive genes are activated due to increased ABA concentration in plants. Proteins encoded by these genes help plants maintain water balance by accumulating organic solutes, thus, lowering water potential and reducing water loss under drought stress (Estrada-Melo et al. 2015). Accumulation of ABA in host plants upon PGPR inoculation under osmotic stress is a well-established fact (Blatt 2000; Cohen et al. 2015; Estrada-Melo et al. 2015). Therefore, in this study, we measured ABA accumulation by studying the expression of genes encoding ABA biosynthesis enzymes. Zeaxanthin epoxidase (known as *WZE* in wheat) and 9-cis-epoxy-carotenoid dioxygenase (*NCED*) are the major ABA biosynthesis gene, which later catalyzes the rate-limiting step. Upregulation of ABA biosynthesis genes (*NCED* and *WZE*) under drought stress in crop plants has been reported in earlier studies (Chen et al. 2016; Wang et al. 2021), which supports our findings. We found expression of genes encoding ABA biosynthesis enzymes was not significant in bacteria-inoculated plants under watered and drought stress conditions. This outcome suggests that WRS7 can assist plant growth under drought stress, independent of the ABA.

Ethylene, a gaseous hormone, is involved in the regulation of plant growth and development, but its concentration increases in response to various abiotic stressors, referred to as 'Stress ethylene' (Abeles et al. 1992), which inhibits plants' growth and yield. There are three major enzymes involved in ethylene biosynthetic pathways, including *S*-AdoMet Synthetase (*SAMS*), ACC synthase (*ACS*), and ACC oxidase (*ACO*) (Lin et al. 2009), where *ACS* is a rate-limiting step and a major target for regulating ethylene production under stress (Wang et al. 2002). Our results show that *E. bugandensis* regulates the level of stress ethylene not only through ACC deaminase activity but also by regulating the expression of genes required for the biosynthesis of ethylene. To our knowledge, this is the first study that reports the regulation of ethylene biosynthesis genes in host plants by PGPR. Future studies can be conducted to identify bacterial factors affecting the expression of the genes mentioned above.

Plants mitigate the effects of drought stress by producing osmolytes, which is triggered by a change in turgor, a key signal for the activation of osmolyte biosynthesis genes (Zhu 2002). Osmolytes such as proline and TSS can be important biochemical indicators of stress tolerance in plants. Osmolytes accumulation maintains optimum turgor pressure within the cell and stabilizes the structure of various macromolecules against drought stress (Kaur and Asthir 2015). In the current study, WRS7-inoculated plants showed a higher accumulation of proline than the uninoculated stressed plants, as shown in the biochemical test (Fig. 3). However, the gene expression (*P5CS* and *P5CR*) studies did not show an equivalent increase in WRS7-treated plants. This slight discrepancy may be attributed to a higher translation rate of corresponding proteins or high enzyme activity leading to increased proline production (Sadak 2019). Expression studies of proline biosynthesis genes were also done by various research groups under abiotic stress (Ghosh et al. 2017). Ghosh et al. found increased expression of both *P5CS* and *P5CR* genes under drought stress in uninoculated and bacteria-inoculated *Arabidopsis* plants. We observed an increase in TSS, another osmolyte, was also observed in bacteria-inoculated wheat plants under stressed conditions. A high amount of TSS might result from increased hydrolysis of starch, resulting in more sugar availability for osmotic adjustment to minimize the adverse effects of drought stress (Kerepesi and Galiba 2000). Accumulation of osmolytes in PGPR-inoculated plants under abiotic stress in various plant species has been reported (Ansari et al. 2021; Kohler et al. 2008; Vaishnav and Choudhary 2019). The biochemical data of TSS correlated with the increased expression

of the *TPS1* gene transcript, which suggests elevated trehalose biosynthesis in PGPR-primed plants under drought stress. *TPS1* encodes the trehalose phosphate synthase (TPS) enzyme involved in trehalose biosynthesis. Trehalose is a non-reducing disaccharide involved in stress resistance and protects not only plants but also bacteria and fungi (Fernandez et al. 2012; Sadak 2019). Fernandez and the group have observed an accumulation of *TPS1* gene transcript upon chilling in PGPR-inoculated grapevine plants (Fernandez et al. 2012). Along with osmolyte production, plants also comprise osmotically active compounds, including hydrophilic proteins such as Late Embryogenic Abundant (LEA) proteins as a cellular response (Kosová et al. 2008; Mehrabad Pour-Benab et al. 2019). ABA acts as a key signal for activating these genes, protecting cells from stress and regulating genes involved in water transport and detoxifying enzymes (Estrada-Melo et al. 2015). LEA-type gene activation represents a damage repair pathway (Xiong et al. 2002). Our observation found increased expression of the *LEA1* gene in drought-affected plants, but decreased expression was noticed in bacteria-inoculated plants. The decreased expression of LEA might result from other cross-talked pathways, like the antioxidant defense system for damage repair in these plants. Our observation tallied with the report of Battaglia and Covarrubias, who highlighted that inoculation of rhizobia in legumes plants did not show LEA transcript in these plants (Battaglia and Covarrubias 2013).

Further, to protect plants and their organelles from the adverse effect of drought stress, plants have antioxidant defense systems, including enzymes like catalase, superoxide dismutase, and peroxidases (Gowtham et al. 2020). Increased activity of these enzymes to overcome the oxidative damage caused by environmental stressors has been demonstrated in PGPR-treated plants (Fahad et al. 2017; Kohler et al. 2008). In our study, biochemical assays showed enhanced catalase and superoxide dismutase activity in bacteria-inoculated plants under drought stress conditions, suggesting an active and improved role of defense machinery in the plant for ROS detoxification (Cruz de Carvalho 2008). We also found increased expression of *CAT* genes in uninoculated and bacteria-inoculated drought-treated plants but with no significant difference, suggesting WRS7 might not be directly regulating the catalase gene expression. However, the *APX* gene showed a significant fold increase in bacteria-inoculated plants under non-stressed conditions, whereas GPX genes was downregulated in bacteria-inoculated plants. Since peroxidase has many isoenzymes encoded by multigene families and their gene expression is regulated at different times and places by various abiotic stressors, the gene expression of various isoenzymes of these peroxidases can be tested in future for better understanding. Also, these enzymes have different affinities for H_2O_2 and different functions in scavenging. Upregulation of *CAT* and *APX* genes can efficiently scavenge H_2O_2, preventing the accumulation of toxic reactive oxygen species. Our data suggest that a complex enzymatic system is responsible for scavenging excess ROS production due to drought stress. Bacterial isolate WRS7 modulates this response positively, protects plants from oxidative damage caused due to water deficit conditions, and helps maintain the plant's structural integrity. As malondialdehyde (MDA) content is one of the stress markers (Gontia-Mishra et al. 2016; Hossain et al. 2015), we evaluated its content in treated plant leaves. The inoculation of WRS7 caused a decrease of up to 40% in MDA content in plants as compared to its control plants grown under stress conditions. It indicates that PGPR helps plants combat the negative effects of stress. Our results support the previous investigations stating that PGRP-inoculated plants combat oxidative damage induced by abiotic stress (Gontia-Mishra et al. 2016; Xun et al. 2015).

One of the prime reactions to abiotic and biotic stress is an alleviation in the cytosolic Ca^{2+} concentration and subsequent Ca^{2+} signal transduction leads to cellular responses to mitigate potential damages caused due to the stress (Xiong et al. 2002; Zhu 2002). Therefore, we looked for the expression of two-pore channels (TPCs) in response to PGPR and drought stress. TPCs are voltage-gated, nicotinic acid adenine dinucleotide phosphate (NAADP)-regulated, and slow activating (SV) Ca^{2+} channels located in the vacuole membrane of plants (Pandey and Sanyal 2021). These channels make the tonoplast and plasma membrane permeable to Ca^{2+}, accumulating Ca^{2+} in the cytosol. TPC1 is involved in cation homeostasis as well as in vacuolar storage function (Hanin et al. 2016). *TaTPC1* is reportedly induced by drought, high salinity, ABA, or cold in wheat (Liu et al. 2018; Wang et al. 2005). By quantitative PCR analysis, we found increased expression of the *TPC1* gene under drought stress. Since the role of PGPR in modulating the level of TPC1 during drought stress has not been reported earlier, detailed characterization is required in future studies. Previously in our lab, through quantitative proteomics analysis, Singh et al. (2017) reported enhanced expression of Two-pore calcium channel proteins in wheat plants inoculated with *Enterobacter cloacae* under salt stress (Singh et al. 2017). From our results, it appears that PGPR mediates Ca^{2+} signaling through TPC1 to alleviate the effect of abiotic stressors.

Finally, we investigated the colonization potential of *E. bugandensis* WRS7 as root colonization by PGPR is an important trait for plant growth stimulation and for survival of bacteria under stress conditions (Singh et al. 2015a, b). All form of motility was shown by the isolate required for chemotaxis response and root colonization (Singh et al. 2015a, b). Further colonization efficiency of the bacterial isolate to the root surface was determined by FESEM (Ghosh et al. 2016) and ERIC-PCR (Li et al.

2009). DNA fingerprinting through ERIC-PCR has been established by earlier reports also (Gupta et al. 2013; Singh et al. 2015a, b).

Overall, the present study demonstrates that *Enterobacter bugandensis* WRS7 is a plant growth-promoting bacteria that can ameliorate drought stress in wheat plants indicating its potential to be used as a biofertilizer for enhanced growth of host plants. Enterobacter sp. is primarily associated with healthcare-related infections, although not all species are known to cause infection in humans (Ramirez and Giron, 2022). *Enterobacter bugandensis*, an emerging human pathogen, can cause nosocomial infections in neonates (Pati et al. 2018). However, the pathogenic potential of environmental isolates has not been reported and must be investigated before its use as a biofertilizer.

Conclusion

The present study investigated the potential of a PGPR *E. bugandensis* WRS7, a drought-tolerant wheat rhizospheric isolate, in ameliorating drought stress in the wheat plant. Our results suggest that *E. bugandensis* WRS7 having multiple PGP protects plants from adverse effects of drought stress by modulating host physiology and expression of stress-related genes and improves plant growth (Fig. 7). The inoculation of WRS7 stimulates the accumulation of osmolytes and enhances the level of antioxidative enzymes as compared to uninoculated plants. Further, the gene expression analysis suggests that *E. bugandensis* WRS7 differentially regulates the expression of stress-associated genes, including those required for the synthesis of trehalose and prolines (osmolytes), antioxidative enzymes, phytohormone biosynthesis, and Ca^{2+} transporter TPC1. To our knowledge, PGPR-mediated inhibition of ethylene biosynthesis by regulating the expression of *SAMS*, *ACS1*, and *ACO*, and modulation of TPC1 transporter is being reported for the first time in the present study. These findings contribute to our understanding of PGPR-mediated drought tolerance in wheat plants and provide future scope to understand the underlying molecular mechanism. Since the isolate used in the present study belongs to the genus *Enterobacter*, which encompasses several human pathogens, its biosafety and environmental considerations before mass application needs to be evaluated and scientifically validated (Keswani et al. 2019).

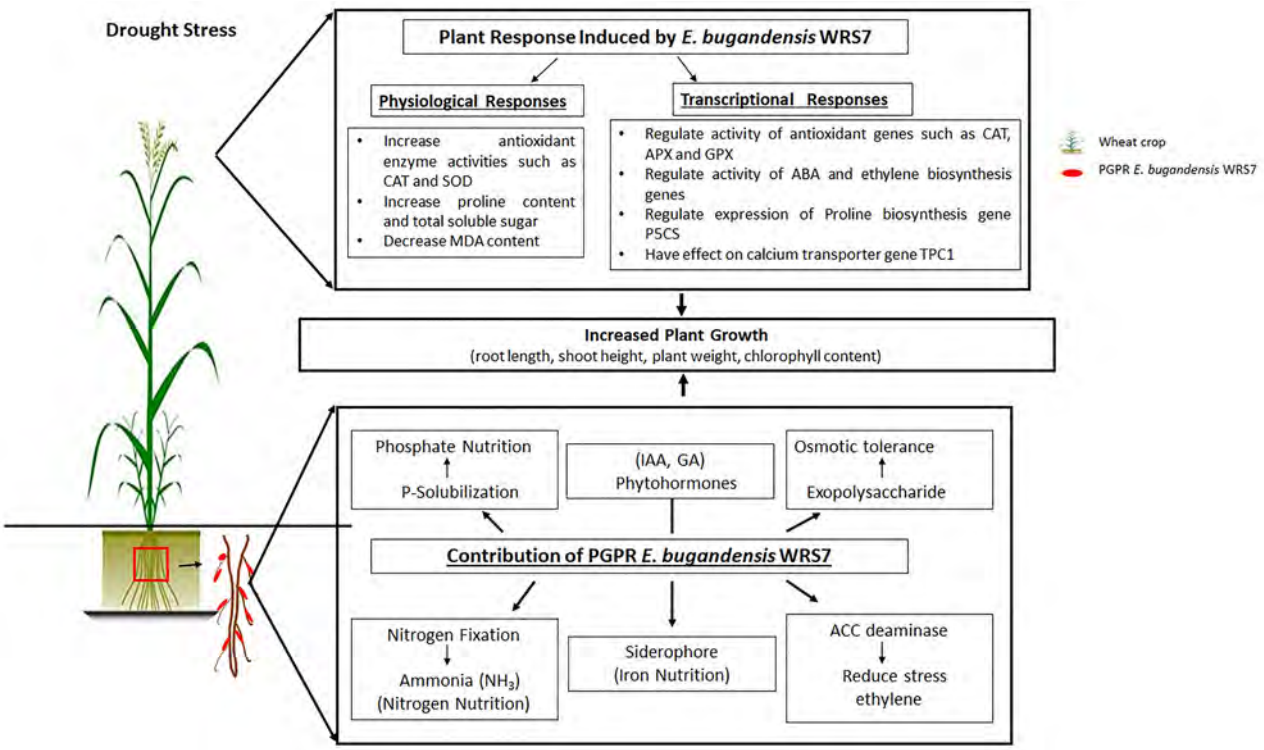

Fig. 7 A model representing the mechanistic insights of *E. bugandensis* WRS7 to mitigate the effects of drought stress in wheat plants

Supplementary Information The online version contains supplementary material available at https://doi.org/10.1007/s00344-023-11044-6.

Acknowledgements SA is thankful to DST-INSPIRE, government of India, for providing a research fellowship. We acknowledge Department of Biological Sciences, BITS Pilani, Pilani campus for logistic support, Sophisticated Instrument Facility, BITS Pilani, Pilani for FESEM facility, and Indian Institute of Wheat and Barley Research, Karnal for providing wheat variety WH1142. We would like to thank Department of Chemistry, BITS Pilani for HRMS facility.

Author Contributions All authors contributed to the study conception and design. PJ has supervised the theme of work. All experiments were performed by SA. The first draft of the manuscript was written by SA. PJ wrote and edited the manuscript. Both authors read and approved the final manuscript.

Funding The authors declare that no funds, grants, or other support were received during the preparation of this manuscript.

Declarations

Conflict of interest We declare that we have no conflicts of interest related to this work; this paper has not been published previously.

References

Abd El-Daim IA, Bejai S, Meijer J (2019) *Bacillus velezensis* 5113 induced metabolic and molecular reprogramming during abiotic stress tolerance in wheat. Sci Rep 9:16282

Abeles F, Morgan P, Saltveit M (1992) Ethylene in plant biology. Academic press, Cambridge

Aebi H (1984) [13] Catalase in vitro. Methods in enzymology. Elsevier, Amsterdam, pp 121–126

Ansari F, Jabeen M, Ahmad I (2021) *Pseudomonas azotoformans* FAP5, a novel biofilm-forming PGPR strain, alleviates drought stress in wheat plant. Int J Environ Sci Te 18:3855–3870

Aslam MM, Farhat F, Siddiqui MA, Yasmeen S, Khan MT, Sial MA, Khan IA (2021) Exploration of physiological and biochemical processes of canola with exogenously applied fertilizers and plant growth regulators under drought stress. PLoS ONE 16:e0260960

Bakker AW, Schippers B (1987) Microbial cyanide production in the rhizosphere in relation to potato yield reduction and *Pseudomonas* spp-mediated plant growth-stimulation. Soil Biol Biochem 19:451–457

Barnawal D, Bharti N, Pandey SS, Pandey A, Chanotiya CS, Kalra A (2017) Plant growth-promoting rhizobacteria enhance wheat salt and drought stress tolerance by altering endogenous phytohormone levels and TaCTR1/TaDREB2 expression. Physiol Plant 161:502–514

Bates LS, Waldren RP, Teare I (1973) Rapid determination of free proline for water-stress studies. Plant Soil 39:205–207

Battaglia M, Covarrubias AA (2013) Late embryogenesis abundant (LEA) proteins in legumes. Front Plant Sci 4:190

Bhatt RM, Selvakumar G, Upreti KK, Boregowda PC (2015) Effect of biopriming with *Enterobacter* strains on seed germination and seedling growth of tomato (*Solanum lycopersicum* L.) under osmotic stress. Proc Natl Acad Sci, India Sect. b: Biol Sci 85:63–69

Blatt MR (2000) Cellular signaling and volume control in stomatal movements in plants. Annu Rev Cell Dev Bio 16:221–241

Bottini R, Cassán F, Piccoli P (2004) Gibberellin production by bacteria and its involvement in plant growth promotion and yield increase. Appl Microbiol Biotechnol 65:497–503

Busse MD, Bottomley PJ (1989) Growth and nodulation responses of *Rhizobium meliloti* to water stress induced by permeating and nonpermeating solutes. Appl Environ Microbiol 55:2431–2436

Caverzan A, Casassola A, Brammer SP (2016) Antioxidant responses of wheat plants under stress. Genet Mol Biol 39:1–6

Chandra P, Wunnava A, Verma P, Chandra A, Sharma RK (2021) Strategies to mitigate the adverse effect of drought stress on crop plants—influences of soil bacteria: a review. Pedosphere 31:496–509

Chen L, Liu Y, Wu G, VeronicanNjeri K, Shen Q, Zhang N, Zhang R (2016) Induced maize salt tolerance by rhizosphere inoculation of *Bacillus amyloliquefaciens* SQR9. Physiol Plant 158:34–44

Choi W-G, Toyota M, Kim S-H, Hilleary R, Gilroy S (2014) Salt stress-induced Ca^{2+} waves are associated with rapid, long-distance root-to-shoot signaling in plants. Proc Natl Acad Sci 111:6497–6502

Clarke D, Hess TM, Haro-Monteagudo D, Semenov M, Knox JW (2021) Assessing future drought risks and wheat yield losses in England. Agric Meteorol 297:108248

Cohen AC, Bottini R, Pontin M, Berli FJ, Moreno D, Boccanlandro H, Travaglia CN, Piccoli PN (2015) Azospirillum brasilense ameliorates the response of *Arabidopsis thaliana* to drought mainly via enhancement of ABA levels. Physiol Plant 153:79–90

Cruz de Carvalho MH (2008) Drought stress and reactive oxygen species: production, scavenging and signaling. Plant Signal Behav 3:156–165

Dudziak K, Zapalska M, Börner A, Szczerba H, Kowalczyk K, Nowak M (2019) Analysis of wheat gene expression related to the oxidative stress response and signal transduction under short-term osmotic stress. Sci Rep 9:2743

Duxbury AC, Yentsch CS (1956) Plankton pigment nomographs. J Mar Res 15(1). https://elischolar.library.yale.edu/journal_of_marine_research/866

Dye D (1962) The inadequacy of the usual determinative tests for the identification of *Xanthomonas* spp. N Z J Sci 5:393–416

Egamberdieva D, Wirth S, Bellingrath-Kimura SD, Mishra J, Arora NK (2019) Salt-tolerant plant growth promoting rhizobacteria for enhancing crop productivity of saline soils. Front Microbiol. https://doi.org/10.3389/fmicb.2019.02791

Estrada-Melo AC, Chao C, Reid MS, Jiang C-Z (2015) Overexpression of an ABA biosynthesis gene using a stress-inducible promoter enhances drought resistance in petunia. Hortic Res 2:15013

Fahad S, Bajwa AA, Nazir U, Anjum SA, Farooq A, Zohaib A, Sadia S, Nasim W, Adkins S, Saud S (2017) Crop production under drought and heat stress: plant responses and management options. Front Plant Sci. https://doi.org/10.3389/fpls.2017.01147

FAO (2017) The future of food and agriculture—Trends and challenges. Rome

Fernandez O, Vandesteene L, Feil R, Baillieul F, Lunn JE, Clément C (2012) Trehalose metabolism is activated upon chilling in grapevine and might participate in *Burkholderia phytofirmans* induced chilling tolerance. Planta 236:355–369

Ghosh R, Barman S, Mukherjee R, Mandal NC (2016) Role of phosphate solubilizing *Burkholderia* spp. for successful colonization and growth promotion of *Lycopodium cernuum* L. (*Lycopodiaceae*) in lateritic belt of Birbhum district of West Bengal. India Microbiol Res 183:80–91

Ghosh D, Sen S, Mohapatra S (2017) Modulation of proline metabolic gene expression in *Arabidopsis thaliana* under water-stressed conditions by a drought-mitigating *Pseudomonas putida* strain. Annals Microbiol 67:655–668

Ghosh D, Gupta A, Mohapatra S (2019) A comparative analysis of exopolysaccharide and phytohormone secretions by four drought-tolerant rhizobacterial strains and their impact on osmotic-stress

mitigation in *Arabidopsis thaliana*. World J Microbiol Biotechnol 35:1–15
Giannopolitis CN, Ries SK (1977) Superoxide dismutases: II. Purification and quantitative relationship with water-soluble protein in seedlings. Plant Physiol 59:315–318
Gontia-Mishra I, Sapre S, Sharma A, Tiwari S (2016) Amelioration of drought tolerance in wheat by the interaction of plant growth-promoting rhizobacteria. Plant Biol 18:992–1000
Gontia-Mishra I, Sapre S, Kachare S, Tiwari S (2017) Molecular diversity of 1-aminocyclopropane-1-carboxylate (ACC) deaminase producing PGPR from wheat (*Triticum aestivum* L.) rhizosphere. Plant Soil 414:213–227
Górka B, Wieczorek PP (2017) Simultaneous determination of nine phytohormones in seaweed and algae extracts by HPLC-PDA. J Chromatogr B 1057:32–39
Gowtham H, Singh B, Murali M, Shilpa N, Prasad M, Aiyaz M, Amruthesh K, Niranjana S (2020) Induction of drought tolerance in tomato upon the application of ACC deaminase producing plant growth promoting rhizobacterium *Bacillus subtilis* Rhizo SF 48. Microbiol Res 234:126422
Gupta G, Panwar J, Jha PN (2013) Natural occurrence of *Pseudomonas aeruginosa*, a dominant cultivable diazotrophic endophytic bacterium colonizing *Pennisetum glaucum* (L.) R. Br Appl Soil Ecol 64:252–261
Gupta S, Seth R, Sharma A (2016) Plant growth-promoting rhizobacteria play a role as phytostimulators for sustainable agriculture. Plant-microbe interaction: an approach to sustainable agriculture. Springer, Singapore, pp 475–493
Hanin M, Ebel C, Ngom M, Laplaze L, Masmoudi K (2016) New insights on plant salt tolerance mechanisms and their potential use for breeding. Front Plant Sci 7:1787
Hodges DM, DeLong JM, Forney CF, Prange RK (1999) Improving the thiobarbituric acid-reactive-substances assay for estimating lipid peroxidation in plant tissues containing anthocyanin and other interfering compounds. Planta 207:604–611
Hossain MA, Bhattacharjee S, Armin S-M, Qian P, Xin W, Li H-Y, Burritt DJ, Fujita M, Tran L-SP (2015) Hydrogen peroxide priming modulates abiotic oxidative stress tolerance: insights from ROS detoxification and scavenging. Front Plant Sci 6:420
Irigoyen J, Einerich D, Sánchez-Díaz M (1992) Water stress induced changes in concentrations of proline and total soluble sugars in nodulated alfalfa (*Medicago sativd*) plants. Physiol Plant 84:55–60
Kaur G, Asthir B (2015) Proline: a key player in plant abiotic stress tolerance. Biol Plant 59:609–619
Kerepesi I, Galiba G (2000) Osmotic and salt stress-induced alteration in soluble carbohydrate content in wheat seedlings. Crop Sci 40:482–487
Keswani C, Prakash O, Bharti N, Vílchez JI, Sansinenea E, Lally RD, Borriss R, Singh SP, Gupta VK, Fraceto LF (2019) Re-addressing the biosafety issues of plant growth promoting rhizobacteria. Sci Total Environ 690:841–852
Khan N, Bano A (2019) Exopolysaccharide producing rhizobacteria and their impact on growth and drought tolerance of wheat grown under rainfed conditions. PLoS ONE 14:e0222302
Kohler J, Hernández JA, Caravaca F, Roldán A (2008) Plant-growth-promoting rhizobacteria and arbuscular mycorrhizal fungi modify alleviation biochemical mechanisms in water-stressed plants. Funct Plant Biol 35:141–151
Kosová K, Holková L, Prášil IT, Prášilová P, Bradáčová M, Vítámvás P, Čapková V (2008) Expression of dehydrin 5 during the development of frost tolerance in barley (*Hordeum vulgare*). J Plant Physiol 165:1142–1151
Larisch N, Kirsch SA, Schambony A, Studtrucker T, Böckmann RA, Dietrich P (2016) The function of the two-pore channel TPC1 depends on dimerization of its carboxy-terminal helix. Cell Mol Life Sci 73:2565–2581
Li W, Raoult D, Fournier P-E (2009) Bacterial strain typing in the genomic era. FEMS Microbiol Rev 33:892–916
Lin Z, Zhong S, Grierson D (2009) Recent advances in ethylene research. J Exp Bot 60:3311–3336
Liu J, Niu Y, Zhang J, Zhou Y, Ma Z, Huang X (2018) Ca^{2+} channels and Ca^{2+} signals involved in abiotic stress responses in plant cells: recent advances. Plant Cell Tiss Organ Cult (PCTOC) 132:413–424
Livak KJ, Schmittgen TD (2001) Analysis of relative gene expression data using real-time quantitative PCR and the $2^{-\Delta\Delta CT}$ method. Methods 25:402–408
Martins SJ, Rocha GA, de Melo HC, de Castro GR, Ulhôa CJ, de Campos DÉ, Oshiquiri LH, da Cunha MG, da Rocha MR, de Araújo LG (2018) Plant-associated bacteria mitigate drought stress in soybean. Environ Sci Pollut Res 25:13676–13686
Mehrabad Pour-Benab S, Fabriki-Ourang S, Mehrabi A-A (2019) Expression of dehydrin and antioxidant genes and enzymatic antioxidant defense under drought stress in wild relatives of wheat. Biotechnol Biotechnol Equip 33:1063–1073
Murali M, Singh SB, Gowtham H, Shilpa N, Prasad M, Aiyaz M, Amruthesh K (2021) Induction of drought tolerance in *Pennisetum glaucum* by ACC deaminase producing PGPR-*Bacillus amyloliquefaciens* through antioxidant defense system. Microbiol Res 253:126891
Niu X, Song L, Xiao Y, Ge W (2018) Drought-tolerant plant growth-promoting rhizobacteria associated with foxtail millet in a semi-arid agroecosystem and their potential in alleviating drought stress. Front Microbiol 8:2580
Noman A, Ali Q, Maqsood J, Iqbal N, Javed MT, Rasool N, Naseem J (2018) Deciphering physio-biochemical, yield, and nutritional quality attributes of water-stressed radish (*Raphanus sativus* L.) plants grown from Zn-Lys primed seeds. Chemosphere 195:175–189
Pandey GK, Sanyal SK (2021) Plant ion channels without molecular identity and two-pore channel 1. Functional dissection of calcium homeostasis and transport machinery in plants. Springer International Publishing, Cham, pp 43–52
Pati NB, Doijad SP, Schultze T, Mannala GK, Yao Y, Jaiswal S, Ryan D, Suar M, Gwozdzinski K, Bunk B, Mraheil MA, Marahiel MA, Hegemann JD, Spröer C, Goesmann A, Falgenhauer L, Hain T, Imirzalioglu C, Mshana SE, Overmann J, Chakraborty T (2018) Enterobacter bugandensis: a novel enterobacterial species associated with severe clinical infection. Sci Rep 8(1):5392
Prescott LM, Harley JP (2002) Harley prescott: laboratory exercises in microbiology, 5th edn. McGraw-Hill, New York
Ramirez D, Giron M (2022) Enterobacter Infections (Jan 2023). [Updated 2022 Jun 27]. In: StatPearls [Internet]. Treasure Island (FL): StatPearls Publishing. Available from https://www.ncbi.nlm.nih.gov/books/NBK559296/
Rashid U, Yasmin H, Hassan MN, Naz R, Nosheen A, Sajjad M, Ilyas N, Keyani R, Jabeen Z, Mumtaz S (2021) Drought-tolerant *Bacillus megaterium* isolated from semi-arid conditions induces systemic tolerance of wheat under drought conditions. Plant Cell Rep 41:549–569
Reinhold-Hurek B, Hurek T, Claeyssens M, Van Montagu M (1993) Cloning, expression in *Escherichia coli*, and characterization of cellulolytic enzymes of *Azoarcus* sp., a root-invading diazotroph. J Bacteriol 175:7056–7065
Sadak MS (2019) Physiological role of trehalose on enhancing salinity tolerance of wheat plant. Bull Natl Res Cent 43:1–10
Sarma RK, Saikia R (2014) Alleviation of drought stress in mung bean by strain *Pseudomonas aeruginosa* GGRJ21. Plant Soil 377:111–126

Simons M, Van Der Bij A, Brand I, De Weger L, Wijffelman C, Lugtenberg B (1996) Gnotobiotic system for studying rhizosphere colonization by plant growth-promoting *Pseudomonas* bacteria. Mol Plant-Microbe Interact: MPMI 9:600–607

Singh RP, Jha P, Jha PN (2015a) The plant-growth-promoting bacterium *Klebsiella* sp. SBP-8 confers induced systemic tolerance in wheat (*Triticum aestivum*) under salt stress. J Plant Physiol 184:57–67

Singh RP, Shelke GM, Kumar A, Jha PN (2015b) Biochemistry and genetics of ACC deaminase: a weapon to "stress ethylene" produced in plants. Front Microbiol 6:937

Singh RP, Runthala A, Khan S, Jha PN (2017) Quantitative proteomics analysis reveals the tolerance of wheat to salt stress in response to *Enterobacter cloacae* SBP-8. PLoS ONE 12:e0183513

Tamura K, Stecher G, Peterson D, Filipski A, Kumar S (2013) MEGA6: molecular evolutionary genetics analysis version 6.0. Mol Biol Evol 30:2725–2729

Vaishnav A, Choudhary DK (2019) Regulation of drought-responsive gene expression in *Glycine max* l. Merrill is mediated through *Pseudomonas simiae* strain AU. J Plant Growth Regul 38:333–342

Vaishnav A, Singh J, Singh P, Rajput RS, Singh HB, Sarma BK (2020) Sphingobacterium sp BHU-AV3 induces salt tolerance in tomato by enhancing antioxidant activities and energy metabolism. Front Microbiol 11:443

Vessey JK (2003) Plant growth promoting rhizobacteria as biofertilizers. Plant Soil 255:571–586

Wang KL-C, Li H, Ecker JR (2002) Ethylene biosynthesis and signaling networks. Plant Cell 14:S131–S151

Wang Y-J, Yu J-N, Chen T, Zhang Z-G, Hao Y-J, Zhang J-S, Chen S-Y (2005) Functional analysis of a putative Ca^{2+} channel gene TaTPC1 from wheat. J Exp Bot 56:3051–3060

Wang X, Li Q, Xie J, Huang M, Cai J, Zhou Q, Dai T, Jiang D (2021) Abscisic acid and jasmonic acid are involved in drought priming-induced tolerance to drought in wheat. Crop J 9:120–132

White EJ, Venter M, Hiten NF, Burger JT (2008) Modified Cetyltrimethylammonium bromide method improves robustness and versatility: the benchmark for plant RNA extraction. Wiley Online Library, New York

Xiong L, Schumaker KS, Zhu J-K (2002) Cell signaling during cold, drought, and salt stress. Plant Cell 14:S165–S183

Xun F, Xie B, Liu S, Guo C (2015) Effect of plant growth-promoting bacteria (PGPR) and arbuscular mycorrhizal fungi (AMF) inoculation on oats in saline-alkali soil contaminated by petroleum to enhance phytoremediation. Environ Sci Pollut Res 22:598–608

Yuwono T, Handayani D, Soedarsono J (2005) The role of osmotolerant rhizobacteria in rice growth under different drought conditions. Aust J Agric Res 56:715–721

Zhu J-K (2002) Salt and drought stress signal transduction in plants. Annu Rev Plant Biol 53:247–273

Molecular Omics

ROYAL SOCIETY OF CHEMISTRY

RESEARCH ARTICLE

View Article Online
View Journal

Cite this: DOI: 10.1039/d3mo00051f

Biochemical and metabolic signatures are fundamental to drought adaptation in PGPR *Enterobacter bugandensis* WRS7†

Saumya Arora,‡[a] Piyoosh K Babele ‡[b] and Prabhat Nath Jha *[a]

Drought alone causes more annual loss in crop yield than the sum of all other environmental stresses. There is growing interest in harnessing the potential of stress-resilient PGPR in conferring plant resistance and enhancing crop productivity in drought-affected agroecosystems. A detailed understanding of the complex physiological and biochemical responses will open up the avenues to stress adaptation mechanisms of PGPR communities under drought. It will pave the way for rhizosphere engineering through metabolically engineered PGPR. Therefore, to reveal the physiological and metabolic networks in response to drought-mediated osmotic stress, we performed biochemical analyses and applied untargeted metabolomics to investigate the stress adaptation mechanisms of a PGPR *Enterobacter bugendensis* WRS7 (*Eb* WRS7). Drought caused oxidative stress and resulted in slower growth rates in *Eb* WRS7. However, *Eb* WRS7 could tolerate drought stress and did not show changes in cell morphology under stress conditions. Overproduction of ROS caused lipid peroxidation (increment in MDA) and eventually activated antioxidant systems and cell signalling cascades, which led to the accumulation of ions (Na^+, K^+, and Ca^{2+}), osmolytes (proline, exopolysaccharides, betaine, and trehalose), and modulated lipid dynamics of the plasma membranes for osmosensing and osmoregulation, suggesting an osmotic stress adaption mechanism in PGPR *Eb* WRS7. Finally, GC–MS-based metabolite profiling and deregulated metabolic responses highlighted the role of osmolytes, ions, and intracellular metabolites in regulating *Eb* WRS7 metabolism. Our results suggest that understanding the role of metabolites and metabolic pathways can be exploited for future metabolic engineering of PGPR and developing bio inoculants for plant growth promotion under drought-affected agroecosystems.

Received 10th March 2023,
Accepted 28th May 2023

DOI: 10.1039/d3mo00051f

rsc.li/molomics

Introduction

Drought is a major abiotic stress that undermines crop productivity and quality and may lead to plant death under prolonged conditions. Drought induces osmotic stress in plants and modulates several physiological and biochemical processes, including stomatal closure, decreased photosynthesis and respiration, altered root system architecture and root exudation, and the onset of oxidative stress.[1] Drought also substantially affects soil biota, as it increases soil heterogeneity, restricts nutrient mobility and accessibility, and increases soil oxygen, frequently resulting in a drastic decrease in microbial biomass.[2] During drought, plant systems actively trigger specific signalling and metabolic responses to maintain osmotic balance by promoting root elongation for water uptake from the soil, stomata closure to reduce water loss, adjusting osmotic and biochemical processes within tissues, activating phytohormone (*e.g.*, abscisic acid) signalling, and producing and mobilizing antioxidant and metabolites.[3] Traditional breeding and genetic engineering approaches have continuously been applied to design drought-tolerant transgenic plants. Unfortunately, these methods are time-consuming, expensive, and difficult to apply in the field.[2]

In an agroecosystem, plants are inhabited by a large microbiota. Interaction between plant roots, soil, and microbes forms a most complex zone known as the rhizosphere.[4] Plant root exudates mediate the interactions and selection of beneficial soil microbial communities or plant growth-promoting rhizobacteria (PGPR), thus, playing a key role in plant-microbial communication, which is crucial for both these counterparts.[5,6] PGPR colonize the rhizosphere/endo-rhizosphere and confer specific functions to their hosts, such as ameliorating abiotic stress tolerance (*e.g.*, drought) and triggering systemic resistance against biotic stress factors.[7] PGPR support plant growth, health, and productivity through various direct and indirect mechanisms, such

[a] *Department of Biological Sciences, Birla Institute of Technology and Science, Pilani 333031, Rajasthan, India. E-mail: prabhatjha@pilani.bits-pilani.ac; Tel: +91-1596-515755, +91-9983629726*

[b] *College of Agriculture, Rani Lakshmi Bai Central Agricultural University, Jhansi 284003, Uttar Pradesh, India*

† Electronic supplementary information (ESI) available. See DOI: https://doi.org/10.1039/d3mo00051f

‡ Equally contributed.

as facilitating the nutrient acquisition, producing phytohormones and lytic enzymes, and accumulating osmolytes, antioxidants, and secondary metabolites.[8,9] Climate change-driven environmental stresses alter the rhizosphere properties and functioning, and thus have a direct impact on the plant-microbe interactions and eventually on crop growth and yield.[2] Sustainable and efficient crop production to feed a growing world population in the era of global climate change requires alternate and eco-friendly approaches. Rhizosphere engineering by harnessing the potential of PGPR is one of the alternatives to increase crop resilience against drought.[10,11] Certain PGPR have unique metabolic capabilities and exhibit various tolerance and adaptation mechanisms to drought stress. It includes thickening of the cell wall, maintaining the dormant stage (spore formation), accumulation of osmolyte/compatible solutes (proline, trehalose, glycine betaine), ions (Na^+, K^+), and exopolysaccharide (EPS) production to overcome reduced water potential for maintaining normal cell physiology.[12,13] The drought-tolerant PGPR maintains the biologically active state of the plasma membrane in response to drought/osmotic stress by modifying the fatty acid composition and maintaining the ratio of unsaturated to saturated fatty acid, thereby ensuring the fluidity and rigidity of the plasma membrane.[14]

There is growing interest in harnessing the potential of stress-resilient PGPR and its subsequent application to induce stress tolerance mechanisms in plants.[2] Rhizosphere engineering based on genetically/metabolically engineered PGPR with improved performance under stress is one of the most important critical strategies to achieve sustainable crop production in drylands. Developing genetically modified PGPR is simpler and less time-consuming than plants with a higher level of genetic complexity.[10,11] Hence, developing more effective PGPR strains with longer shelf lives and improved stress adaptation requires identifying and investigating useful metabolic pathways associated with producing secondary metabolites and complex stress-responsive pathways modulated in response to specific stress environments.[8,15] We hypothesize that plant-associated-PGPR undergoes morphological and physiological reprogramming under abiotic stress and produces metabolites that protect bacteria and the associated plants from the harmful effects of given stress. To date, little is known about the drought tolerance mechanisms of PGPR and how their biochemical and metabolic characteristics can influence plant performance under drought/osmotic stress. Therefore, it is necessary to comprehend the physiology and metabolism of stress-resistant PGPR and their interaction with plants before implementing them in intensive farming practices to enhance plant performance under drought stress.

Metabolomics has the potential to identify and characterize metabolites and biochemical pathways and their dynamic responses to changes in the environment, *e.g.*, stress.[16,17] This information is utilized to manipulate novel metabolic pathways involved in drought/osmotic tolerance in PGPR. Therefore, to investigate the physiological and biochemical capabilities of stress-resilient PGPR, we studied the physicochemical parameters of *Enterobacter bugandensis* WRS7 (hereafter *Eb* WRS7). This bacterium, isolated from the wheat rhizosphere, showed its ability to grow under drought/osmotic stress and improved wheat plant growth under drought stress (accepted manuscript). Furthermore, to discover the underlying metabolic signatures and their role in stress tolerance mechanisms, we employed untargeted gas chromatography–mass spectrometry (GC–MS) based metabolomics to profile the deregulated metabolite (central and secondary) pool and identify core metabolic pathways under stress. Our results provide a detailed understanding of the stress-responsive mechanism(s) in *Eb* WRS7 at a metabolic level under drought/osmotic stress conditions. Stress-tolerant abilities of PGPR strains and their detailed understanding of the osmo-adaptation mechanism could be translated into the engineering of efficient PGPR inocula (biofertilizer) with wide adaptability to the different agroecosystems with varying soil types and eventually can be harnessed for the betterment of dryland agriculture.

Materials and methods

Eb WRS7 culture conditions and drought exposure

Eb WRS7, a PGPR isolated from wheat rhizospheric soil under drought stress conditions, was used in the present study. *Eb* WRS7 showed different plant growth-promoting properties, including nitrogen fixation, phosphate solubilisation, siderophore production, phytohormones (indole-acetic acid and gibberellic acid) production, exopolysaccharide secretion, and ACC deaminase activity (accepted manuscript). For all the experiments, *Eb* WRS7 was grown in LB media. To test the ability of *Eb* WRS7 to grow under a hyperosmotic environment, LB media was supplemented with different concentrations (0 to 25%) of polyethylene glycol (PEG-6000). The cultures were grown at 30 °C with constant shaking at 150 rpm in an incubator shaker. Bacterial growth was measured by reading the optical density (OD) at 600 nm using a UV-visible spectrophotometer (BioSpectrometer, Eppendorf, Germany). OD_{600} was measured every hour, and then the growth curve was plotted to study its growth pattern.

Morphophysiological and biochemical analyses

Field emission scanning electron microscopy. To check the osmotic efficiency of *Eb* WRS7, the cellular morphology of non-stressed and osmotic-stressed cells (10% PEG) was studied through Field Emission Scanning Electron Microscopy (FESEM) following a standard protocol. 1 ml of 24 h grown bacterial cells was pelleted down and washed with phosphate buffer saline (PBS) twice. Cells were then suspended in 2.5% of glutaraldehyde solution and kept overnight incubated in the dark at 4 °C. The cell pellet was collected through centrifugation (5000 g for 5 min) and washed three times with PBS. The sample was then dehydrated with 30%, 50%, 70%, 80%, and 90% ethanol with 10 min incubation each. The cell pellet was dehydrated with 100% ethanol. Finally, SEM stubs were prepared by applying adhesive tape and adding bacterial samples. The fixed bacterial cells were sputter coated with gold and subjected to FE-SEM (FEI-APREO SEM, Thermo Fisher Scientific, USA) to investigate the morphological changes in bacterial cells under drought stress.

Reactive oxygen species (ROS) detection. To measure the level of intracellular ROS, a stress marker, in control and stressed

bacterial cells of *Eb* WRS7, the cell-permeable free radical sensor 2′,7′-dichlorodihydrofluorescein diacetate (H_2DCFDA) was used.[18] Briefly, 1 ml of bacterial culture grown in LB media supplemented with (control) and without 10% PEG (stressed) was collected at 6, 12, and 24 h. Bacterial cells were harvested through centrifugation, washed with 1X PBS, and resuspended in PBS. H_2DCFDA (10 μM) was added to the cells and incubated in the dark for 30 min at room temperature (RT). The ROS generation was detected using Fluorimeter (Fluoroskan Ascent, Thermo Scientific) at excitation/emission at 485 nm/535 nm, respectively.

Malondialdehyde (MDA) assay. MDA is one of the final products of the peroxidation of polyunsaturated fatty acids in cells. An increase in free radicals causes the overproduction of MDA and is commonly known as a marker of oxidative stress and the antioxidant status of the cell. Lipid peroxidation was determined by observing the formation of a thiobarbituric acid-reactive substance (TBARS). Bacterial cells from non-stressed and stressed conditions were harvested at 6, 12, and 24 h, washed with 0.85% NaCl once, and then suspended in 0.25% SDS by gentle swirling, then TBA buffer reagent was added, followed by 60 min incubation at 95 °C. Tubes were then allowed to cool to RT by incubating on ice for 10 min. Then, the reaction mixture was centrifuged at 3000 g, and the supernatant was collected. The adduct formation of MDA–thiobarbituric acid (TBA) was measured at 532 nm by using a spectrophotometer (BioSpectrometer Eppendorf, Germany). The concentration of MDA formed was calculated by comparing the absorbance obtained from experimental samples to the standard curve obtained using the malondialdehyde (MDA). The extent of lipid peroxidation was expressed in nanomoles of MDA.

Estimation of intracellular ion concentration. The inductively coupled plasma–optical emission spectroscopy (ICP–OES) method was performed to know the concentrations of intracellular potassium (K^+), sodium (Na^+), and calcium (Ca^{2+}) ions in the bacterial cell under control and stress conditions as described previously.[19] Briefly, 10 ml bacterial culture was collected at 6, 12, and 24 h of growth under control and stressed conditions, and centrifuged at 3000 g for 15 min. The supernatant was decanted, and the residual media was completely removed. The cell pellet was dried at RT for 24 h, followed by its digestion with 1 ml of 30% nitric acid, and incubated at RT for 48 h. Later, the solution was sonicated using a probe sonicator (ultrasonic cell disruptor, Microson, USA) at 10 Hz with 10 sec pulses for 5 cycles. Samples were then centrifuged at 20 000 g for 20 min. The supernatant was filtered through 0.2 μm syringe filters, and the filtrate was diluted five times with sterilized, deionized water. Samples were then analyzed by ICP–OES (Optima 8000 PerkinElmer, USA). Standard curves for K^+, Na^+, and Ca^{2+} were prepared for quantitative estimation. Ion concentration was normalized using bacterial optical density at 600 nm.

Quantification of exopolysaccharide production. *Eb* WRS7 was analyzed for its ability to produce EPS under no stress and osmotic stress according to the method of Sandhya *et al.* (2010) with slight modifications.[20] Briefly, 3-day-old culture grown in LB (with and without 10% PEG) was centrifuged at high speed (13 000 g) for 30 min at 4 °C, and the supernatant was collected. To the supernatant, two-volumes of chilled absolute alcohol was added and kept overnight at 4 °C. The precipitated EPS was harvested by centrifugation at 10 000 g for 20 min and suspended in water. Precipitated EPS was estimated for total carbohydrate content following the method of Dubois *et al.*[21] The glucose standard of different concentrations was used for the standard curve preparation and carbohydrate quantification in EPS.

Protein content estimation. Total cellular protein in the bacterial cell was determined by lysing the cell pellet obtained from the 3 day-old culture under normal and osmotic-stress conditions with 5 ml of lysis buffer.[20] The cell suspension was sonicated, cell lysate was collected through centrifugation at 13 000 g for 10 min, and total protein was estimated using the standard Bradford method.[22]

Proline content estimation. The estimation of free proline accumulated in bacterial cells under normal and osmotic-stress conditions was estimated as per a previously described method.[23] Cell pellets obtained from 72 h grown cultures were lysed. The supernatant (1 ml) obtained was treated with 2 ml of 3% aqueous sulphosalicylic acid, followed by incubation for 30 min. After incubation, the solution was centrifuged at 8000 g for 20 min at 4 °C, and the supernatant was collected. The obtained supernatant was treated with 2 ml glacial acetic acid and 2 ml acid ninhydrin and incubated at 100 °C in a water bath for 1 h. The reaction was terminated by keeping the tubes in ice. 4 ml of toluene was added to each reaction mixture and mixed well. The chromophore containing the toluene layer was collected, and the absorbance was measured spectrophotometrically at 520 nm against toluene as the blank. The concentration of free proline was calculated from the standard curve prepared using different concentrations of L-proline.

Fatty acid methyl ester analysis

In order to comprehend the fatty acid profile under osmotic stress, the fatty acid composition of PGPR *Eb* WRS7 was analysed following a standard protocol.[24] The bacterial cells were grown in only LB media (control) and LB media containing 10% PEG (stressed) for 24 h. Cells were harvested by centrifugation at 1000 g for 5 min and sonicated in lysis buffer containing 50 mM tris–Cl (pH 7.6), 1.1 mM dithiothreitol, 1 mM PMSF, and 0.2% lysozyme. The resulting supernatant was extracted using a mixture of methanol and chloroform in a 1 : 2 ratio followed by centrifugation at 6000 g for 10 min. The supernatant was diluted with the same solvent system ten times and kept on a shaker at 160 rpm for 3 hr for phase separation. The lower organic phase was collected and concentrated using a rotary evaporator, dissolved in toluene, and converted to fatty acid methyl ester (FAME) by the trans-esterification reaction. Later, samples were subjected to GC–MS analysis (GCMS-TQ8040, Shimadzu Corporation, Japan). GC was operated in split-less injector mode with the following conditions: initial oven temperature of 50 °C held for 2 min and temperature ramping from 50 to 250 °C at a rate of 10 °C per min. MetaBoAnalyst 5.0 was used for the Hierarchical heat map construction.

Metabolite extraction, derivatization, and GC–MS analysis

Polar and non-polar metabolites were extracted from the bacterial cells grown in only LB media (control) and LB media containing 10% PEG (stressed) for 24 h for GC–MS Analysis. Cell pellets were sonicated in lysis buffer using a sonicator probe using three cycles of 10 s pulses at 40 Hz on ice. Cells were centrifuged at 20 000 g for 5 min. Metabolites from the supernatant were extracted using a 2 : 1 ratio of chloroform and methanol. Then, 100 µl of each solvent layer was collected and evaporated to dryness using a rotary vacuum concentrator. The dried supernatant was suspended in 1 ml methanol. As mentioned below, 200 µl was aliquoted into a fresh microcentrifuge tube, followed by evaporation to dryness and derivatization. To each 200 µl of the dried sample, 30 µl of methoxyamine hydrochloride was added, heated at 70 °C for 45 min, and then cooled at room temperature to derivatize the samples. After that, 50 µl of MSTFA was added and heated at 40 °C for 90 min. Later, derivatized samples were transferred to auto-sampler vials for analysis. 1 µl of the derivatized sample was loaded on Shimadzu capillary column SH-RXi-5SilMS (30 m × 0.32 mm × 0.25 µm) through autosampler in split-less mode at 250 °C. The constant flow rate of 1 ml min^{-1} of helium gas was maintained. Initially, the GC program was started at 60 °C for 1 min, followed by temperature ramping of 10 °C min^{-1} to 180 °C with a temperature hold of 2 min, followed by a second ramping of 4 °C min^{-1} until the final temperature reached 300 °C and remained constant for 10 minutes. Data acquisition involved a mass range of 50 to 650 *m*/*z*. Peaks were identified using the NIST 14 library. The metabolomics data were obtained in .qgd file format for analysis. MetaBoAnalyst 5.0 was used for the statistical analysis.

Statistical analysis

All the experiments were carried out in triplicates, unless otherwise stated, repeated in three different experimental sets, and plotted as mean ± SD using Prism 8 (Graph Pad software). Statistical analysis was performed using an unpaired student's *t* test. Statistical significance: $^{*}P \leq 0.05$, $^{**}P \leq 0.01$, $^{***}P \leq 0.001$, and $^{****}P < 0.0001$, ns = not significant. For GC–MS analysis, four replicates of each control and stressed sample were used in the experiment. After data normalization, all significant metabolites were analyzed using unsupervised principal component analysis (PCA) to observe the overall distribution trend among samples. Differential metabolites were screened according to VIP >1 and $p < 0.05$. Univariate analysis and metabolic pathway enrichment analyses were performed using the online tool MetaboAnalyst 5.0 (**https://www.metaboanalyst.ca**).

Results

Cell growth and morphological responses under osmotic stress

First, we asked whether and to what extent the cells of *Eb* WRS7 could tolerate and survive the osmotic stress. To test this, we exposed cells to a range of PEG (5 to 25%) concentrations and measured the optical density (600 nm). The growth curve showed maximum cell growth under control (no PEG exposure) conditions, while significant growth retardation was observed with increasing concentrations of PEG (Fig. S1, ESI†). Although cells can sustain up to 25% PEG, there was a significant loss in cell growth. In all the tested doses of PEG, *Eb* WRS7 could withstand 10% PEG concentration without significant growth defects and showed about 50% of survival of *Eb* WRS7 as compared to the control. Therefore, 10% PEG was selected to induce drought/osmotic stress in all the subsequent experiments to analyze the physiological, biochemical, and molecular responses. After testing the growth defect in *Eb* WRS7 in response to osmotic stress, we observed the changes in cellular morphology directly related to the osmotic tolerance efficiency. Small (100 nm to 250 nm in size) vesicle-like structures were

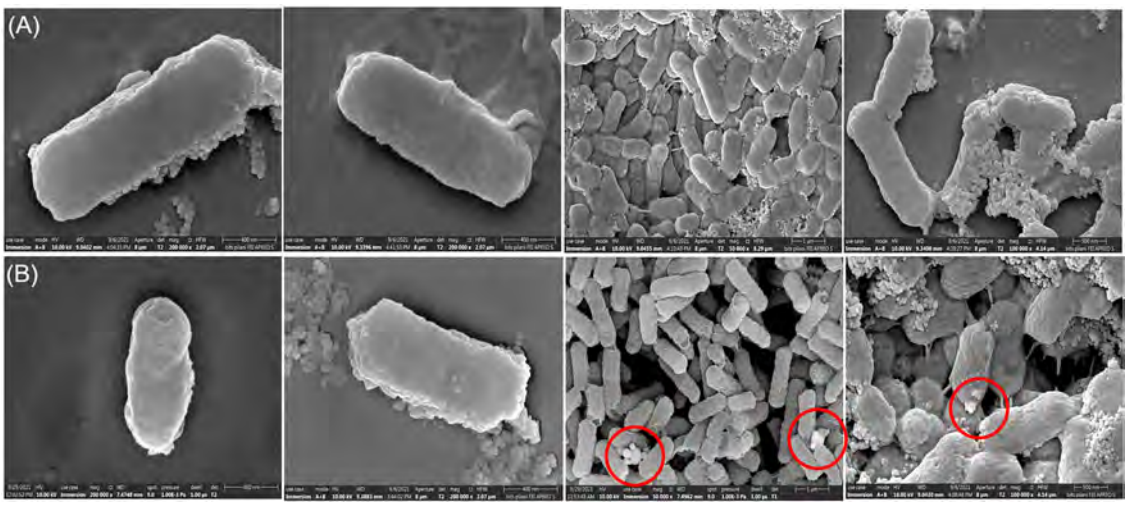

Fig. 1 Scanning electron microscopic images of *Eb* WRS7 cells under (A) non-stressed and (B) osmotic (10% polyethylene glycol) stressed conditions. Osmotic stress-exposed cells do not show significant morphological changes; small vesicle-like structures (inside red circles) were seen. Similar appearances were found in separate experiments. Two left panel images (with single cell) were captured at 200 000× magnification (Bar-400 nm). Two right panel images (with multiple cells) were captured at 50 000× (Bar-1 µm) and 100 000× magnification (Bar-500 nm).

also observed in PEG-exposed cells. FE-SEM analysis showed that *Eb* WRS7 maintained cellular integrity upon exposure to 10% PEG (Fig. 1).

Physiological and biochemical responses under osmotic stress

Cell growth and morphology analysis indicated that PEG-induced osmotic stress slowed down the growth of *Eb* WRS7. However, we did not observe significant morphological alterations in cells grown with 10% PEG. To determine whether decreased cell growth resulted from oxidative stress and membrane damage, we measured the accumulation of intracellular reactive oxygen species (ROS) and conducted lipid peroxidation assays in control and osmotically stressed cultures. At 6 h of growth of PEG-treated cells, there was a significantly high level of both ROS (81.33%) and MDA (179.59%) as compared to non-stressed cells (Fig. 2). Thereafter, a gradual decline in both ROS and MDA contents was observed at 12 and 24 h suggesting the stress adaptation and tolerance of *Eb* WRS7 under osmotic stress.

ROS and MDA analysis pointed out that osmotic stress triggers oxidative stress in the cells. We expected that stress exposure would activate the ROS-mediated signaling cascades and eventually promote stress-responsive pathways for cell survival in response to stress events. Since the uptake and release of ions, especially K^+, Na^+, and Ca^{2+}, are involved in osmoregulation, we measured the intracellular concentration of K^+, Na^+, and Ca^{2+} to understand the mechanism of osmotic stress tolerance in *Eb* WRS7. The content of these ions significantly increased at 6 h but decreased gradually at 12 and 24 h under osmotic stress. At 24 h, a significant difference in ionic concentration under stress and non-stress conditions was found only for Ca^{2+} (Fig. 3). The Na^+ concentrations were significantly different at 6, 12, and 24 h showing 182.33 ± 4.426, 154.465 ± 5.933, and 27.22 ± 0.938 mM respectively under osmotic stress. In contrast, K^+ was relatively low and measured to be 91.325 ± 0.148, 40.393 ± 0.061, and 4.557 ± 0.054 mM, respectively. Similarly, the level of Ca^{2+} decreased with an increase in time duration of stress, with a maximum of 14.825 ± 0.594 mM after 6 h of osmotic stress. We observed an increase of 75% in Na^+ until reaching 12 h of stress compared to the control conditions, whereas the K^+ content first increased to 185.12% at the initial hour of stress, which further decreased to 47% after 24 h compared to the control conditions. Interestingly, we observed a very high concentration (~15 mM) of Ca^{2+} during the initial hour of stress, which further decreased to ~5 mM after 24 h of stress conditions (Fig. 3(C)). We tested EPS production, along with the ability of *Eb* WRS7 to modulate endogenous proline and cellular protein under osmotic stress. In response to PEG-induced osmotic stress conditions, there was about a 3-fold increase in EPS concentration. We also observed 1.8-fold higher free proline levels in stressed cells than in control cells. Finally, there was an increment in the total cellular protein content after 72 h under stress conditions (Fig. 4).

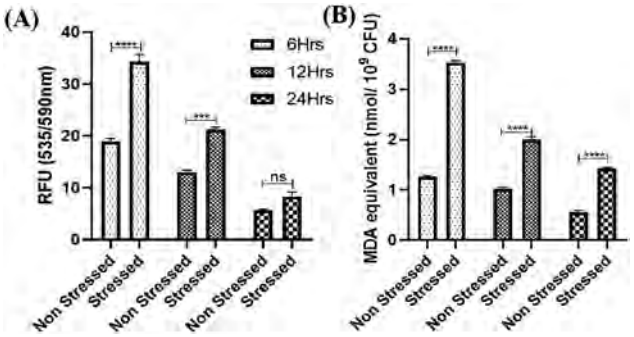

Fig. 2 *Eb* WRS7 responses under osmotic-stressed conditions. (A) Reactive oxygen species (ROS) detection by H_2DCFDA and expressed as relative fluorescence unit (RFU) at 535/590 nm, (B) membrane lipid peroxidation products were determined as TBARS (MDA-TBA adduct) and are reported as nmol MDA equivalents/10^9 cells. The error bars indicate standard deviations from three independent cultures assayed in triplicate. The error bar refers to the mean ± SD of three independent measurements. Horizontal bars with asterisks (*) indicate statistical significances between two values based on a Student's *t* test. Statistical significance: *$P \leq 0.05$, **$P \leq 0.01$, ***$P \leq 0.001$, and ****$P < 0.0001$, ns = not significant. Abbreviations: MDA – malondialdehyde; TBA – thiobarbituric acid.

Plasma membrane lipid dynamics under osmotic stress

Since membrane lipids are crucial in protecting an organism from the adverse effect of osmotic stress, we analyzed the fatty acid profile of *Eb* WRS7 by GC–MS analysis. Saturated hydrocarbons such as triacontane, pentacosane, and tetradecane were detected at 0% PEG (non-stressed condition) along with unsaturated hydrocarbons such as Heptadecene and Nonadecene. At 10% PEG (osmotic stress), the hydrocarbon composition of the extract changed, showing the presence of hexadecane, heptadecane, triacontane, docosane, tetradecane, 9-eicosene, 1-dodecene, 1-heptadecene, 1-nonadecene, and 1-pentadecene (Fig. 5(A) and Table S1, ESI†). Some short-change fatty acids like valeric acid were also detected under stressed conditions. Fatty alcohols like 1-dodecanol, 1-heptacosanol, and *n*-tetracosanol-1 were observed in both stressed and non-stressed conditions. The saturated fatty acids C16:0 and C18:0 and the monounsaturated fatty acid C18:1 were the predominant lipid components in non-stressed bacterial cells. A hierarchical heatmap was drawn using Metaboanalyst 5.0 software to represent the change in the fatty acid profile (Fig. 5(B)), which showed the qualitative distribution of fatty acids under control and stress conditions. Heatmap clustering showed that saturated fatty acids like myristic acid and palmitic acid were less in stressed bacterial cells. In contrast, branched-chain fatty acids like isopalmitic acid were dominant in stressed bacterial cells.

Metabolic responses under osmotic stress

To study the role of metabolites and identify the metabolic pathways participating in osmotic stress tolerance, we extracted intracellular metabolites and performed GC–MS-based untargeted metabolomics of *Eb* WRS7 grown under normal and osmotic stress conditions (PEG-10%). We identified 33 significantly deregulated metabolites (fold change ≥ 1.9) in control *vs.* stress-exposed cells. Based on their chemical structure, functions, and associated metabolic pathways, annotated metabolites were categorized into different classes such as organic acids (TCA cycle metabolites), sugar/carbohydrates, amino acids, polyamines, phytohormones, and osmolytes (Fig. 6(A)). Metabolites of glycolysis, TCA cycle pathways, and sugar/carbohydrates are significantly higher in stress exposed cells as compared to control cells.

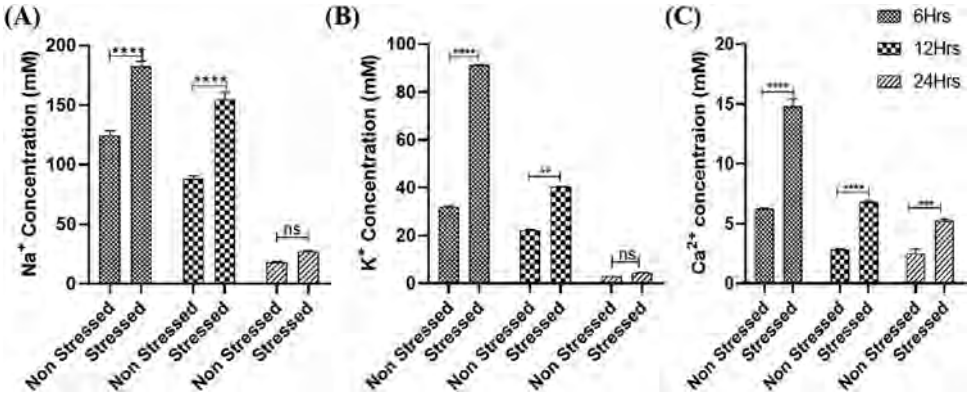

Fig. 3 Intracellular ion concentration in *Eb* WRS7 (A) sodium ion, (B) potassium ion, and (C) calcium ion. The error bar refers to the mean ± SD of three independent measurements. Horizontal bars with asterisks (*) indicate statistical significances between two values based on a Student's *t* test. Statistical significance: $*P \leq 0.05$, $**P \leq 0.01$, $***P \leq 0.001$, and $****P < 0.0001$, ns = not significant.

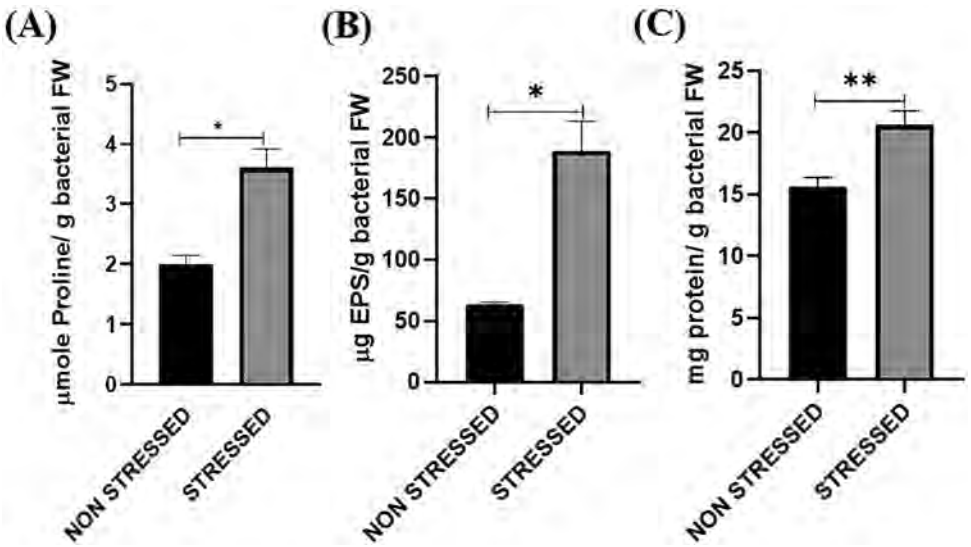

Fig. 4 Quantification of (A) cell-free proline, (B) exopolysaccharide (EPS) production, and (C) total cellular protein in *Eb* WRS7 under non-stressed and osmotic-stressed (10% PEG) conditions. Each bar represents the mean ± SE of three replicate samples. '*' represents the significant difference between osmotic-stressed *versus* non-stressed conditions, based on a Student's *t* test. Statistical significance: $*P \leq 0.05$, $**P \leq 0.01$, $***P \leq 0.001$, and $****P < 0.0001$, ns = not significant.

Similarly, polyamines (putrescine and cadaverine), phytohormones (indole acetic acid and gibberellic acid), and osmolytes (trehalose, proline, glycine betaine, and ethanolamine) were also over-accumulated in stress exposed cells. Osmotic stress also resulted in a higher level of some amino acids such as aspartate, proline, glutamate, and tryptophan, whereas amino acids like leucine, tyrosine, and lysine were significantly reduced (Fig. 6(A)).

The biological replicates clustered together, whereas metabolites under normal and stressed conditions clustered differently. Principle component analysis (PCA) was used to visualize variance between the two conditions, which showed a similar clustering pattern. A total variance of 85.1% (PC 1 = 78.6% and PC 2 = 6.5%) was observed (Fig. 6(B)). Considering the control (non-stressed) condition as in ref. 26, metabolites were significantly upregulated (shown in red), whereas 7 were significantly down-regulated (shown in blue) in stress exposed cells as shown in the volcano plot (Table 1 and Fig. 6(C)). Annotated metabolites were further processed by hierarchical clustering to provide an intuitive visualization of metabolite changes under the tested conditions (Fig. 6(D)). The heat map obtained from the selected metabolites indicates that some metabolites are upregulated while others are down-regulated under osmotic stress (Fig. 6(D)). Finally, metabolite enrichment analysis revealed the functions and involvement of these metabolites in various metabolic pathways. Based on this observation, we conclude that the TCA cycle, glyoxylate, dicarboxylate metabolism, alanine, aspartate and glutamate metabolism, and fatty acid biosynthesis metabolic pathways are significantly more active in response to osmotic stress in *Eb* WRS7 (Fig. 7(A) and (B)).

Discussion

The rhizosphere microbiome is considered one of the effective and better alternative approaches for sustainable agriculture

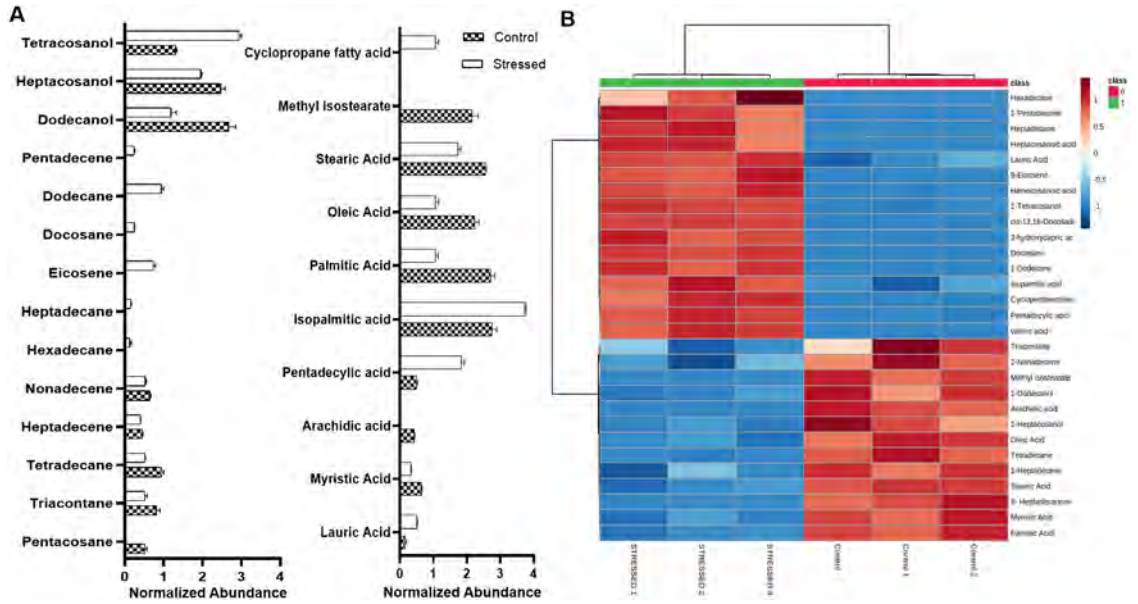

Fig. 5 Change in fatty acids composition of *Eb* WRS7 cells exposed to osmotic stress. (A) Normalized abundance of saturated and unsaturated fatty acids and (B) heatmap hierarchical clustering of detected fatty acids. A hierarchical tree was performed for detected fatty acids in control (non-stressed) and osmotic stress treatment using Metaboanalyst 5.0 software. Each colored cell on the map represents the peak intensity. Columns correspond to two conditions in replicates (n = 3), while rows represent different metabolites detected. On the top of the heatmap, control samples are represented in red while stressed samples are in green. Dark blue to dark red color gradient denotes lower to higher expression.

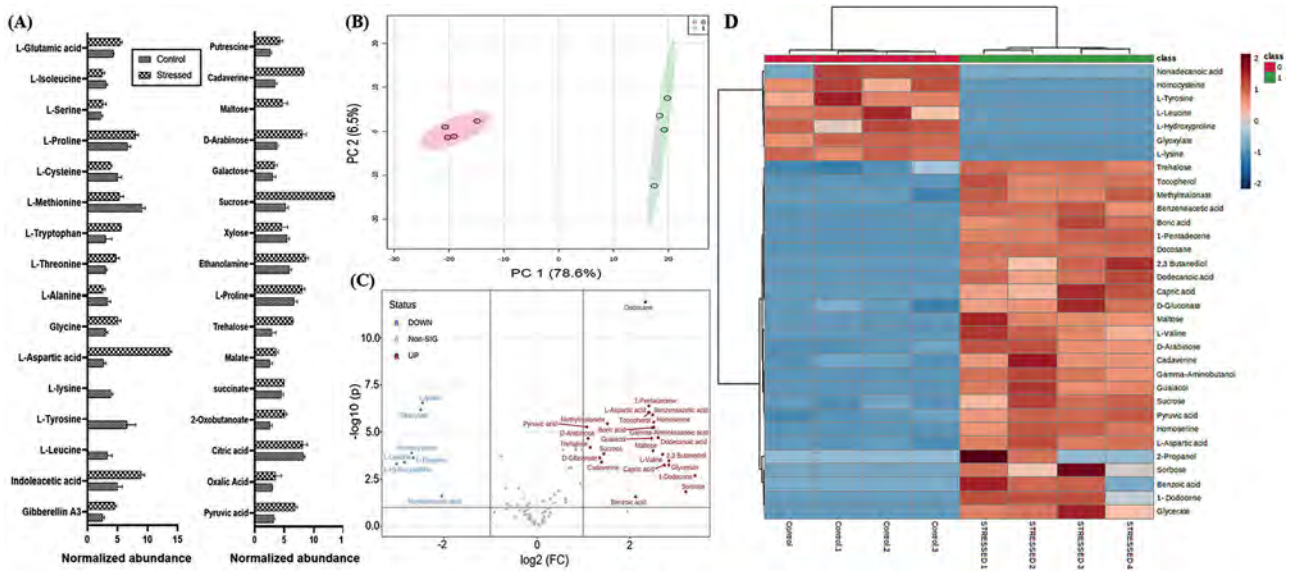

Fig. 6 Change in intracellular metabolites of *E. bugandensis* WRS7 cells exposed to osmotic stress (PEG-10%). (A) Normalized abundance of different metabolites. (B) Scores Plot (PC1 *vs.* PC2) of partial least-squares–discriminant analysis (PLS–DA) of metabolites. Each ring represents the distribution of biological replicates. The pink color donates control samples, whereas the green color represents stressed samples. (C) Volcano map depicting contributory metabolites to the differences in two conditions, with fold change threshold (X-axis) = 2 and t tests threshold (Y-axis) = 0.1. (D) Heatmap hierarchical clustering of detected intracellular metabolite pools. Hierarchical trees were drawn based on the detected metabolites in control (non-stressed) and osmotic stress treatment. Columns correspond to two conditions in replicates, while rows represent different metabolites detected.

and a reasonable solution to meet the twin challenges of food security and environmental stability. This approach offers several advantages, including the capability of PGPR to confer abiotic stress tolerance through modulating plant physiological and biochemical traits.[2] Developing drought-tolerant PGPR (bio-inocula) seems a promising solution to improve crop productivity under drought-prone agroecosystems. However, despite an increased application of PGPR, our understanding

of the stress adaptation mechanisms of PGPR communities under drought is still incomplete. In this paper, we contend that a comprehensive understanding of the complex physiological and biochemical responses to drought will pave the way for rhizosphere engineering through PGPR and, ultimately, the exploitation of these responses to increase the drought resistance of crop production. Our lab previously isolated and characterized PGPR *Eb* WRS7 (accession number MW453057) from wheat rhizosphere and reported its growth-promoting and abiotic stress tolerance ability under drought stress (accepted manuscript). Being isolated from a drought-prone agroecosystem and considering its role in ameliorating plant growth under drought stress, we have hypothesized that this PGPR might have unique stress adaptation abilities.

To prove our hypothesis, we initially assessed the growth and morphology of this bacterium upon drought exposure. Since dehydrating agents like PEG can reduce bacterial growth, *Eb* WRS7 growth was studied at different concentrations of PEG. It is evident from Fig. S1 (ESI†) that *Eb* WRS7 showed better growth and survival under osmotic stress conditions than *E. coli*, used as a control (Fig. S2, ESI†). However, slower growth was observed than its non-stressed counterparts. Under stress conditions, bacterial cells might have directed their energy flow towards activating the protection mechanisms, which might have affected their growth.[13,25] Previous reports have also described the tolerance of PGPR *Pseudomonas* sp. and *Bacillus* sp. under osmotic stress.[13,25] There were no significant morphological changes, but we observed the formation of vesicle-like structures in response to osmotic stress. Vesicle formation is influenced by the bacterial growth stage and stress insults. These vesicles might serve some specialized function, such as nutrient acquisition or biofilm formation, and play an important role in host–microbe interactions, hence, offering stress tolerance under stressful environmental conditions.[26,27] McMillian *et al.*, 2021 reported that outer membrane vesicles from *Pseudomonas syringae* and *Pseudomonas fluorescens* activate plant immune response in *Arabidopsis thaliana* against pathogenic bacteria.[28] Membrane vesicles play an essential defense function in mitigating osmotic and oxidative stress.[29] The latest study described the role of vesicles in mitigating the osmotic stress in *E. coli* when exposed to titanium dioxide nanoparticles showing that osmotic stress and cell vesiculation are associated with nanoparticle resistance.[30] However, factors stimulating vesicle generation and their specialized functions in PGPR are not well studied. Therefore, specific experiments are required to know the exact function of this vesicle-like structure in future studies.

Table 1 Significantly altered intracellular metabolites of *Eb* WRS7. Compared to the non-stressed conditions, the fold change shows metabolite levels from Eb WRS7 with osmotic stress (by PEG 10%)

S. no.	Metabolites	Log 2 (fold change)
1	1-Dodecene	3.406
2	Sorbose	3.2082
3	L-Hydroxyproline	−3.0187
4	L-Leucine	−2.8512
5	2,3 Butanediol	2.844
6	Glycerate	2.8413
7	Capric acid	2.7461
8	L-Valine	2.7076
9	Homocysteine	−2.697
10	L-Tyrosine	−2.6581
11	Dodecanoic acid	2.6116
12	Homoserine	2.5187
13	Gamma-aminobutanoic acid	2.517
14	Maltose	2.5027
15	Glyoxylate	−2.4979
16	Benzeneacetic acid	2.4945
17	Boric acid	2.4891
18	Guaiacol	2.467
19	L-Lysine	−2.4569
20	Tocopherol	2.4213
21	1-Pentadecene	2.4108
22	L-Aspartic acid	2.4041
23	Docosane	2.3378
24	Benzoic acid	2.1249
25	Nonadecanoic acid	−2.0448
26	2-Propanol	1.9509
27	Methylmalonate	1.5216
28	Sucrose	1.4431
29	Cadaverine	1.3913
30	D-Gluconate	1.3558
31	Trehalose	1.1505
32	D-Arabinose	1.1025
33	Pyruvic acid	1.0769

The primary signal caused by drought is hyperosmotic stress, which often induces complex secondary effects such as oxidative stress, damage to cellular macromolecules, and consequently metabolic dysfunction. Oxidative stress triggers overaccumulation of the cells' reactive oxygen species (ROS). Excess ROS production induces lipid (polyunsaturated fatty acids) peroxidation in the cells, as evidenced by a high content of malondialdehyde (MDA), a common biomarker of oxidative stress, and determines the antioxidant status of the cell.[31] Lipid peroxidation results in alterations of the membrane structure, affecting its fluidity and damaging its integrity.[32] We observed an initial increase in ROS and MDA followed by a decline at 24 h, indicating adaptive responses of this bacteria against stress. ROS production is a normal physiological process and plays a vital role in cell signaling and homeostasis.[33] Overaccumulation of ROS is, however, kept under tight control by a versatile and cooperative antioxidant system. ROS functions as a secondary messenger that triggers adaptive responses by activating signal transduction pathways which in turn limits intracellular ROS concentration and hence maintains the redox homeostasis of the cell.[33]

The common osmoadaptation mechanisms of bacteria include accumulating or releasing solutes such as inorganic ions (often K^+, Na^+, and Cl^-) and organic osmolytes to attenuate water fluxes (efflux/influx) to counter the variations in external osmotic pressure.[34,35] In bacteria, K^+ is the most abundant inorganic ion in the cell cytosol and, therefore, is the most suitable candidate for osmotic adjustment purposes under stress conditions. The electrochemical gradients favor K^+ loss and accumulation of Na^+ into the cell *via* specific ion transport systems, hence, play a significant role in maintaining normal cell turgor. The imbalance in the cytosolic K^+/Na^+ ratio dramatically impacts cell metabolism and may trigger programmed cell death.[36] In *E. coli*, it has been reported that osmotic shock

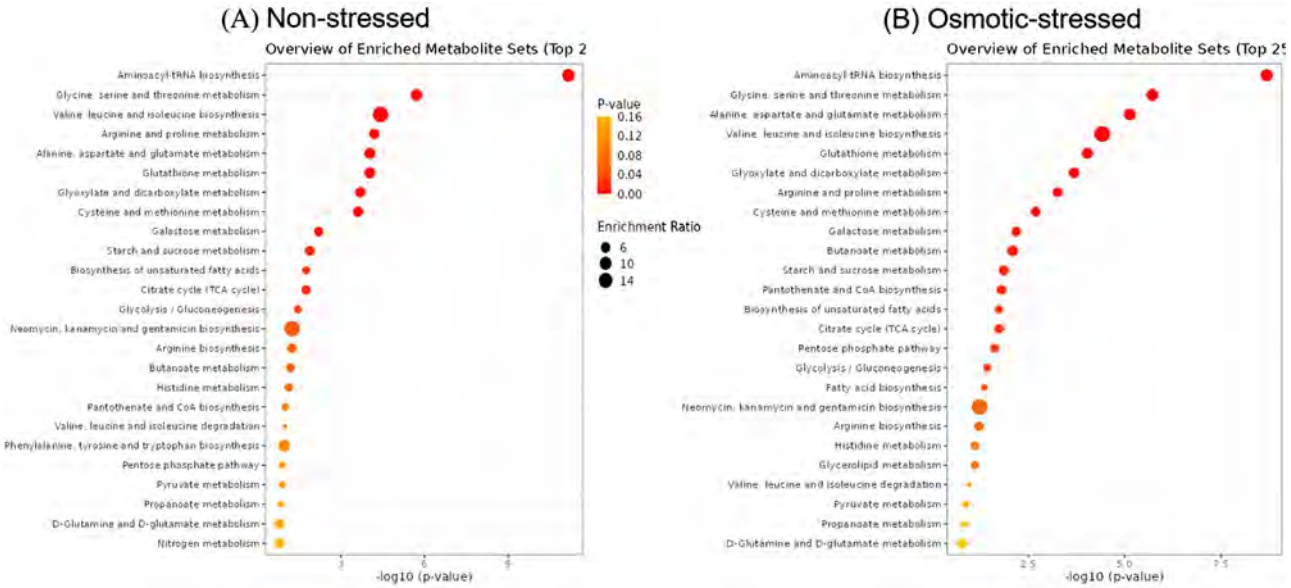

Fig. 7 Dot plot of KEGG pathway enrichment of metabolites corresponding to (A) Non-stressed and (B) Osmotic-stressed in *Eb* WRS7. The top 25 enriched pathway terms are displayed. The *P* value indicates the enrichment level of the pathway term and ranges from 0 to 1.

causes an increase in intracellular Na^+ over K^+ concentration.[37] We also observed higher Na^+ concentrations than K^+ in stressed cultures, suggesting inorganic ions' role in maintaining osmotic balance in *Eb* WRS7. However, more experimental data are needed to support our hypothesis. It is well established that hyperosmotic stress induces a rapid rise in intracellular Ca^{2+} concentration in plants and may reflect the activities of biochemical and metabolic components to counter osmotic stress.[38] Interestingly, we also observed a higher Ca^{2+} concentration suggesting the role of this secondary messenger in activating the osmo-adaptation mechanism in this PGPR. A previous report shows that Ca^{2+} affects several bacterial physiological processes, including chemotaxis, cell differentiation (spore development and heterocyst formation), and membrane transport.[39] We also recorded high Ca^{2+} under stress conditions, which might be involved in an osmotic stress signalling pathway.

Microorganisms preferentially accumulate organic solutes like glutamate, glycine betaine, proline, and trehalose, decreasing water potential without interfering with cellular metabolism. These osmolytes maintain osmotic potential and scavenge ROS, thus preventing cellular damage from oxidative stress without any adverse effects on cellular macromolecules.[20,34] We observed around a two-fold increase in proline content under stress. Microorganisms can increase their function and survival in hostile environments by improving their local habitat. Since drought limits substrate availability and reduces nutrient diffusion, bacteria preferably start synthesizing extracellular polymeric substance (EPS) as an effective drought adaptation method. EPS functions like a sponge, slowing the drying process and thus retaining water by allowing action at a low water potential.[40] Our results also indicate increased EPS (predominantly containing polysaccharides, protein, and DNA) production and a significant increase in protein content after 72 h in stressed cells. This might be because of the enhanced production of bacterial extracellular protein for the production of EPS, which protects them against desiccation.[40] Bacterial cellular protein contributes to exopolysaccharide (EPS) production under stress conditions,[13] which in turn forms a sheath around the bacterial colonies and protects them from osmotic stress by decreasing water loss.[20] EPS is known to exhibit high antioxidant properties, which protect bacteria from ROS-dependent cell death.[41] EPS produced by bacteria not only help them tolerate osmotic stress but also improve the quality and fertility of the soil, act as a nutrient facilitator, reduce ion toxicity, and maintain plant health under abiotic stress.[42]

Microbes tune their membrane lipid composition to maintain membrane fluidity and properties in response to environmental changes. Global patterns of lipid remodeling can provide insights into fundamental principles of membrane adaptation.[43,44] Lipid determination by FAME analysis is an accurate reflection and can be used to quantify total lipids. Using FAME-based lipidomics, we examined the total lipid fraction of this PGPR to understand the role of fatty acids in regulating membrane dynamics. The change in fatty acid composition, especially carbon length and degree of saturation under stressed conditions, indicates the adaption of bacteria to tolerate osmotic stress, increasing the cytoplasmic membrane's fluidity. They also play an important role in membrane stability and permeability.[45] Under stressed conditions, there was an increase in cyclopropane fatty acids. The bacterial production of the cyclopropane ring is related to changes in the membrane fatty acids composition. It represents one of the most important adaptive microbial responses that favor the stress tolerance of several bacteria.[46] Cyclopropanate membrane lipids have been associated with resistance to oxidative stress in *Mycobacterium tuberculosis*, organic solvent stress in *E. coli*, and acid stress in *E. coli* and *Salmonella*.[47] It has been reported that in the membrane of *Lactococcus lactis*, osmotic stress induces high levels of cyclopropane fatty acid (ΔC19:0).[48] Although the mechanism is not yet known, researchers believe that a change in the fatty acid composition of

the lipid membrane may regulate glycine betaine transporter activity.[12] Earlier studies showed a different profile of fatty acids under stress conditions, which might help bacterial cells to survive the changing environment by maintaining the cell membrane as an iso-osmotic barrier.[24] Therefore, the present study highlighted that bacteria change their membrane composition in changing environments for survival.

To obtain a deeper insight into the stress adaption mechanism, we evaluated the metabolic responses of this PGPR (*Eb* WRS7) under drought. To better understand the mechanism of osmolality and adaptability, we employed GC–MS-based untargeted metabolomics to determine the change in primary and secondary metabolites under drought stress. Deregulation in these intracellular metabolites indicated the operation of central carbon and nitrogen metabolism in response to osmotic stress and provided deeper insights into the osmoadaptation mechanism of PGPR. Deregulated metabolites were subdivided into several classes based on their biochemical structure, functions, and involvement in different metabolic pathways. We recorded higher organic osmolyte content, including amino acids, polyamines, quaternary ammonium compounds, and sugars. The role of these metabolites in osmoprotection has been very well-established in many bacteria.[34] We observed higher content of ethanolamine and polyamines. It has been reported that ethanolamine is a precursor of betaine and proline, and its supplementation promotes glycine biosynthesis.[49] Polyamines possess antioxidant properties and protect bacteria exposed to oxidative stress by decreasing ROS, binding and shielding negatively charged macromolecules, and modulating the expression of adaptive genes.[50] For instance, cadaverine can bind to porin proteins and lipopolysaccharides of the cell envelope, regulate transport through the outer membrane, and is involved in the adaptive responses to acid stress, redox-active compounds, and antibiotics. Putrescine primarily binds to nucleic acids, regulates gene expression by modulating transcription, protein stability, mRNA secondary structure, and functioning of the ribosome, stabilizes and protects DNA, and is involved in the adaptive responses to oxidative stress, osmotic shock, heat shock, *etc.*[49]

In addition to the aforementioned organic molecules, volatile organic compounds (VOCs) were over-accumulated in stress-exposed cultures. Under stress exposure, PGPR produces volatile organic compounds (VOCs) to regulate osmolyte and phytohormones biosynthesis. These compounds also play a crucial role in plant–microbe interactions.[41] The ability of 2,3-butanediol, and acetoin in plant growth promotion and induced systemic

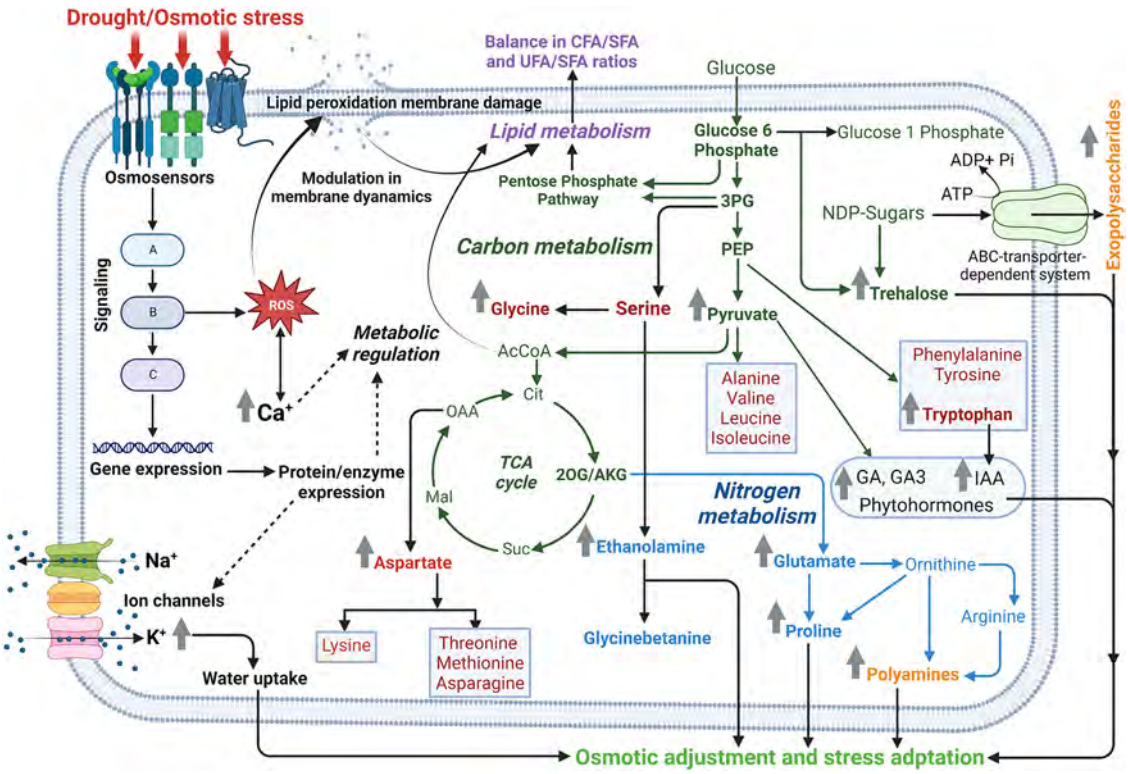

Fig. 8 *Eb* WRS7 response to osmotic stress and tolerance mechanism. Drought/osmotic stress triggers osmosensors and induces oxidative stress through ROS accumulation. ROS causes lipid peroxidation and damage to the plasma membrane. ROS over accumulation activates cell signaling cascades and induces gene expression. Osmotic stress tolerance mechanisms are governed by maintaining the lipid dynamics (balance in membrane fatty acids) and ion transport systems. PGPR regulate their carbon and nitrogen metabolism to fulfill the energy demands and biosynthesis of osmolytes and other secondary metabolites. Abbreviations: 2OG – 2-oxoglutarate3PG-3-phosphoglycerate, AcCoA – acetyl coenzyme A, AKG – α-ketoglutarate, Cit – Citrate, CFA – cyclo fatty acid, GA – gibberellic acid, IAA – indole acetic acid, Mal – malate, NDP – nucleotide diphosphates, OAA – oxaloacetic acid, PEP- phosphoenolpyruvate, ROS – reactive oxygen species, SFA – saturated fatty acid, Suc – succinate, UFA – unsaturated fatty acid.

resistance against pathogenic fungi, bacteria, and viruses in plants has been reported in previous studies.[51,52] In our study, 2,3-butanediol was detected under osmotic stress known to be produced by various root-associated bacteria such as *Bacillus* spp., *Aerobacter* spp., and *Klebsiella* spp.[52] Although VOCs regulate growth hormones and ion acquisition, a lot more can be explored regarding their direct role in the bacteria defense system and ameliorating abiotic stress in plants. Metabolomics data also highlighted increased levels of sugar molecules such as sucrose, maltose, and arabinose in *Eb* WRS7 under osmotic stress. It has been reported that the production of EPS required a higher amount of glucose, trehalose, mannose, and rhamnose for better water retention ability.[13] Therefore, higher sugar content might contribute to EPS production, enhance water retention within the bacteria, and protect them from fluctuating water potential.[53] Higher sugars may also act as a carbon pool to fulfill the carbon demands of this PGPR under drought.

Finally, we observed a higher accumulation of the glycolytic pathway and TCA cycle metabolites such as pyruvate, α-ketoglutarate, succinate, malate, and oxaloacetate. Moreover, several amino acids, such as aspartate and glutamate, are over-accumulated in contrast to leucine, lysine, and tyrosine, showing lower concentrations under stress exposure. Since survival in high osmotic stress is an energy-demanding process, and the production of osmolytes demands high energy and carbon, the activation of glycolytic and TCA cycle might be involved in fulfilling these demands.[54] Under osmotic stress, the glycolytic pathway may have contributed to the production of trehalose in plants and bacteria.[53] Also, increased levels of glycolysis and TCA cycle metabolites might provide energy in the form of ATP to the bacterial cell under stressed conditions.[55,56] Glutamate is an important metabolite that plays a role in various metabolic processes and is involved in protein synthesis and other fundamental processes such as glycolysis, gluconeogenesis, and the TCA cycle. Glutamate metabolism plays a vital role in resistance to acid stress and multiple other stresses in *E. coli*.[57] Since the synthesis of glutamate and aspartate are energetically economical for the bacteria and act as a counter partner for K^+, which increases during the osmotic stress, this can be an adaptive strategy of bacteria to deal with hyperosmotic stress.[55] Similar to our findings, a previous study reported a decrease in aromatic (tyrosine) and branched-chain (leucine and isoleucine) amino acids, which may result from increased energy demands for maintaining cell integrity and homeostasis under stress.[55] Moreover, the increased production of essential amino acids like threonine and serine during stress can play a role in producing the defense molecule glutathione.[56] Furthermore, there was an increase in intracellular tryptophan, IAA, and GA levels under osmotic stress conditions. These observations support the PGPR capability of *Eb* WRS7. However, to understand the specific role of phytohormones in bacterial physiology, further experiments are needed using mutant bacterial strains, compromising their ability to produce these phytohormones. The deregulation in metabolites indicates that *Eb* WRS7 can modulate their physiological and metabolic processes to combat stress. These metabolic responses and alterations in cellular metabolism might be related to certain stress signaling and adaptation mechanisms and provides a roadmap for the commercialization of bacterial metabolites for the development of bio-inoculants, which can combat abiotic stress and improve plant growth and yield in drought-prone agroecosystems in a sustainable manner.

Conclusion

This study highlights the stress tolerance mechanism of a PGPR, *Eb* WRS7, to mitigate osmotic stress by utilizing morphological, biochemical, and metabolic capabilities (Fig. 8). The formation of a vesicle-like structure seems to play a crucial role in stress tolerance by facilitating the nutrient acquisition and activation of the immune response. Osmotic stress induces ROS production leading to oxidative stress. In response, the bacteria modulate their membrane fatty acid composition leading to changed membrane fluidity for their survival under osmotic stress. Higher concentrations of Na^+ and Ca^{2+} over K^+ under stress suggest the role of these ions in maintaining osmotic balance and activation of Ca^{2+} dependent osmotic stress signalling pathways in *Eb* WRS7. Activation of the signaling cascade under stress conditions suggests its role in osmoadaptation through physiological and metabolic modulations. Metabolomics profiling showed metabolic capabilities such as the production of osmolytes, polyamines, 2,3-butanediol, quaternary ammonium compounds, sugars, and higher accumulation of the glycolytic pathway, and TCA cycle metabolites, used for survival under drought/osmotic stress. Overall, the metabolite fingerprint reveals the mechanisms adapted by PGPR and highlights the importance of stress-responsive metabolites and their metabolic pathways, which in the future may be targeted for the metabolic engineering of this PGPR for rhizosphere engineering. Considering the ability to tolerate osmotic stress and PGP properties, *Eb* WRS7 can be used as a biofertilizer candidate to promote plant growth under drought-stress conditions, which can be tested in future studies.

Data availability

All data generated or analyzed during this study are included in this published article (and its ESI†).

Ethical declaration

This article does not contain any studies involving human participants or animals performed by any of the authors.

Author contributions

All authors contributed to the study's conception and design. PNJ and PKB supervised the theme of the work. Experiments were performed by SA and PKB; data were analyzed by SA and PKB. SA wrote the first draft of the manuscript, and PKB and PNJ wrote and edited the manuscript. All authors read and approved the final manuscript.

Conflicts of interest

The authors declare no conflict of interest.

Acknowledgements

SA is thankful to DST-INSPIRE, the government of India, for providing a research fellowship. PKB is thankful to SERB-DST, New Delhi, India, for the financial support of a Ramanujan fellowship. We acknowledge the Department of Biological Sciences, BITS Pilani, Pilani campus for logistic support, Sophisticated Instrument Facility, BITS Pilani, Pilani for FESEM and GC–MS facility. This work was supported by a prestigious Ramanujan fellowship (File no. RJF/2020/000043) by the Science and Engineering Research Board, Department of Science and Technology (SERB-DST) New Delhi, India.

References

1 P. K. Babele, H. Kudapa, Y. Singh, R. K. Varshney and A. Kumar, *Front. Plant Sci.*, 2022, 2806.
2 F. T. De Vries, R. I. Griffiths, C. G. Knight, O. Nicolitch and A. Williams, *Science*, 2020, **368**, 270–274.
3 A. Gupta, A. Rico-Medina and A. I. Caño-Delgado, *Science*, 2020, **368**, 266–269.
4 K. Hartman and S. G. Tringe, *Biochem. J.*, 2019, **476**, 2705–2724.
5 A. Williams and F. T. de Vries, *New Phytol.*, 2019, **225**, 1899–1905.
6 Y. N. Chai and D. P. Schachtman, *Trends Plant Sci.*, 2022, **27**, 80–91.
7 E. Korenblum, Y. Dong, J. Szymanski, S. Panda, A. Jozwiak, H. Massalha, S. Meir, I. Rogachev and A. Aharoni, *Proc. Natl. Acad. Sci. U. S. A.*, 2020, **117**, 3874–3883.
8 E. Ngumbi and J. Kloepper, *Appl. Soil Ecol.*, 2016, **105**, 109–125, DOI: **10.1016/j.apsoil.2016.04.009**.
9 J.-S. Jeon, D. Rybka, N. Carreno-Quintero, R. de Vos, J. Raaijmakers and D. Etalo, *Authorea Prepr.*, 2022, **45**, 3086–3099.
10 A. H. Ahkami, R. Allen White, P. P. Handakumbura and C. Jansson, *Rhizosphere*, 2017, **3**, 233–243.
11 J. Ke, B. Wang and Y. Yoshikuni, *Trends Biotechnol.*, 2021, **39**, 244–261.
12 D. Paul, *J. Basic Microbiol.*, 2013, **53**, 101–110.
13 D. Ghosh, A. Gupta and S. Mohapatra, *World J. Microbiol. Biotechnol.*, 2019, **35**, 1–15.
14 Y. Yoon, H. Lee, S. Lee, S. Kim and K. H. Choi, *Food Res. Int.*, 2015, **72**, 25–36.
15 H. Zhang and M. Dai, *Plant Commun.*, 2021, 100228.
16 A. R. Fernie and N. Schauer, *Trends Genet.*, 2009, **25**, 39–48.
17 P. C. P. Bueno and N. P. Lopes, *ACS Omega*, 2020, **5**, 1752–1763.
18 R. Magerand, P. Rey, L. Blanchard and A. de Groot, *Sci. Rep.*, 2021, **11**, 1–12.
19 J. Tu, Q. Zhao, L. Wei and Q. Yang, *Environ. Monit. Assess.*, 2012, **184**, 1645–1655.
20 V. Sandhya, S. Z. Ali, B. Venkateswarlu, G. Reddy and M. Grover, *Arch. Microbiol.*, 2010, **192**, 867–876.
21 M. Dubois, K. A. Gilles, J. K. Hamilton, P. A. Rebers and F. Smith, *Anal. Chem.*, 1956, **28**, 350–356.
22 M. M. Bradford, *Anal. Biochem.*, 1976, **72**, 248–254.
23 L. S. Bates, R. P. Waldren and I. D. Teare, *Plant Soil*, 1973, **39**, 205–207.
24 R. P. Singh and P. N. Jha, *Symbiosis*, 2017, **73**, 213–222.
25 M. Kumar, S. Mishra, V. Dixit, M. Kumar, L. Agarwal, P. S. Chauhan and C. S. Nautiyal, *Plant Signal Behav.*, 2016, **11**(1), e1071004, DOI: **10.1080/15592324.2015.1071004**.
26 J. C. Caruana and S. A. Walper, *Front. Microbiol.*, 2020, **11**, 432.
27 M. Potter, C. Hanson, A. J. Anderson, E. Vargis and D. W. Britt, *Sci. Rep.*, 2020, **10**, 1–14.
28 H. M. McMillan, S. G. Zebell, J. B. Ristaino, X. Dong and M. J. Kuehn, *Cell Rep.*, 2021, **34**, 108645, DOI: **10.1016/J.CELREP.2020.108645**.
29 C. Schwechheimer and M. J. Kuehn, *Nat. Rev. Microbiol.*, 2015, **13**, 605–619.
30 C. Pagnout, A. Razafitianamaharavo, B. Sohm, C. Caillet, A. Beaussart, E. Delatour, I. Bihannic, M. Offroy and J. F. L. Duval, *Commun. Biol.*, 2021, **4**, 1–15.
31 P. K. Babele, G. Singh, A. Singh, A. Kumar, M. B. Tyagi and R. P. Sinha, *Acta Physiol. Plant.*, 2017, **39**, 248, DOI: **10.1007/s11738-017-2540-4**.
32 R. Hong, T. Y. Kang, C. A. Michels and N. Gadura, *Appl. Environ. Microbiol.*, 2012, **78**, 1776–1784.
33 P. K. Babele, J. Kumar and V. Chaturvedi, *Front. Microbiol.*, 2019, **10**, 1315, DOI: **10.3389/fmicb.2019.01315**.
34 R. D. Sleator and C. Hill, *FEMS Microbiol. Rev.*, 2002, **26**, 49–71.
35 J. M. Wood, *J. Gen. Physiol.*, 2015, **145**, 381–388.
36 S. Shabala and L. Shabala, *Biomol. Concepts*, 2011, **2**, 407–419.
37 D. Szatmári, P. Sárkány, B. Kocsis, T. Nagy, A. Miseta, S. Barkó, B. Longauer, R. C. Robinson and M. Nyitrai, *Sci. Rep.*, 2020, **10**, 1–13.
38 A. B. Stephan, H. H. Kunz, E. Yang and J. I. Schroeder, *Proc. Natl. Acad. Sci. U. S. A.*, 2016, **113**, E5242–E5249.
39 D. C. Dominguez, *Mol. Microbiol.*, 2004, **54**, 291–297.
40 N. S. N. A. Rahman, N. W. A. Hamid and K. Nadarajah, *Int. J. Mol. Sci.*, 2021, **22**, 9036.
41 K. Sunita, I. Mishra, J. Mishra, J. Prakash and N. K. Arora, *Front. Microbiol.*, 2020, **11**, 2619.
42 N. Bhagat, M. Raghav, S. Dubey and N. Bedi, *J. Microbiol. Biotechnol.*, 2021, **31**, 1045–1059.
43 G. Chwastek, M. A. Surma, S. Rizk, D. Grosser, O. Lavrynenko, M. Rucińska, H. Jambor and J. Sáenz, *Cell Rep.*, 2020, **32**, 108165.
44 J. R. Willdigg and J. D. Helmann, *Front. Mol. Biosci.*, 2021, **8**, 634438, DOI: **10.3389/FMOLB.2021.634438**.
45 X. Gong, H. Yu, J. Chen and B. Han, *Eur. Food Res. Technol.*, 2012, **4**, 671–678.
46 L. Shabala and T. Ross, *Res. Microbiol.*, 2008, **159**, 458–461.
47 J. E. Karlinsey, A. M. Fung, N. Johnston, H. Goldfine, S. J. Libby and F. C. Fang, *Infect. Immun.*, 2022, **90**, e0047921, DOI: **10.1128/IAI.00479-21**.
48 A. Guillot, D. Obis and M. Y. Mistou, *Int. J. Food Microbiol.*, 2000, **55**, 47–51.

49 S. Rajaeian, A. A. Ehsanpour, M. Javadi and B. Shojaee, *Biol. Plant.*, 2017, **61**, 797–800.
50 A. V. Akhova and A. G. Tkachenko, *Microbiol. Soc. Korea*, 2020, **56**, 103–110.
51 H. S. Yi, Y. R. Ahn, G. C. Song, S. Y. Ghim, S. Lee, G. Lee and C. M. Ryu, *Front. Microbiol.*, 2016, **7**, 993, DOI: **10.3389/FMICB.2016.00993**.
52 H. G. Kong, T. S. Shin, T. H. Kim and C. M. Ryu, *Front. Plant Sci.*, 2018, **9**, 90.
53 R. J. L. Morcillo, J. I. Vílchez, S. Zhang, R. Kaushal, D. He, H. Zi, R. Liu, K. Niehaus, A. K. Handa and H. Zhang, *Metabolites*, 2021, **11**, 369.
54 Y. Zhang, B. Mao, X. Tang, X. Liu, J. Zhao, H. Zhang, S. Cui and W. Chen, *LWT*, 2022, **159**, 113199.
55 N. N. Joghee and G. Jayaraman, *Biochimie*, 2014, **102**, 102–111.
56 M. Wang, S. Zhao, L. Wang, S. Chen, S. Li, X. Lei, X. Sun and L. Qin, *Sci. Total Environ.*, 2021, **782**, 147125.
57 C. Feehily and K. A. G. Karatzas, *J. Appl. Microbiol.*, 2013, **114**, 11–24.